Summer 7-27-2018

Localization and Scrambling of Quantum Information with Applications to Quantum Computation and Thermodynamics

Adrian Kristian Chapman
University of New Mexico

Adrian Chapman

Candidate

Physics and Astronomy

Department, The University of New Mexico

This dissertation is approved, and it is acceptable in quality and form for publication:

Approved by the Dissertation Committee:

Dr. Akimasa Miyake, Chair

Dr. Carlton M. Caves

Dr. Ivan H. Deutsch

Dr. Steven T. Flammia

Defended July 25th, 2018.

Localization and Scrambling of Quantum Information with Applications to Quantum Computation and Thermodynamics

by

Adrian Chapman

B.S., California Institute of Technology, 2012
M.S., University of New Mexico, 2014

DISSERTATION

Submitted in Partial Fulfillment of the
Requirements for the Degree of

Doctor of Philosophy
Physics

The University of New Mexico

Albuquerque, New Mexico

December 2018

Dedication

To my family.

Acknowledgments

This thesis could not have been written without the support, hard work, and sacrifice of many people in my life. Foremost, I owe all of my accomplishments to the support of my family, to whom this thesis is dedicated. My parents, Darrel and Susan Chapman, have been extremely supportive and loving my entire life and sparked my interest in science from a young age. My siblings, Keir, Theo, and Siobhan Chapman, despite being younger, are my role models in many ways. I am also extremely thankful for the love of my girlfriend, Van Tran, who has been supportive throughout my entire career in graduate school. Everything I've accomplished, I owe in-part to her, for I could not have completed this journey without her in my life, and I consider her to be a part of my family as well. I would also like to thank Eli and Joseph Schenkel, my lifelong friends, whom I similarly consider to be my family, and whose accomplishments continue to inspire me.

I would also like to thank my academic family, Jacob Miller, and my advisor, Akimasa Miyake. As an academic brother, Jacob has also been a role model to me, and his incredible accomplishments continue to challenge me to push myself. Akimasa is the kind of scientist every student should hope to have as an advisor. He is always pushing for you to go that little extra step beyond what you expect of yourself, and by the time you look back, you've accomplished something you didn't think was possible. He strikes a good balance of being part of the research conversation while also leaving you to work out the details for yourself. He gives you the space to shape your own interests as well as to make your own mistakes. I expect he'll continue to shape young minds in the field of quantum information science for years to come.

Next, I thank my friends through the graduate program at the Physics and Astronomy department of the University of New Mexico (UNM). Foremost, I thank James Hendrie, Matthew Curry, and Eric Bahr. These are some of my closest friends, whose support has been invaluable to me over the years. I also thank the graduate students I have met through the Center for Quantum Information and Control (CQuIC), namely Jonathan Gross, Xiaodong Qi, Ninnat "Tom" Dangniam, Anirban Chowdhury, Gopikrishnan Muraleedharan, Ezad Shojaee, Mari Gachechiladze, Davide Orsucci, Travis Scholten, Andrew Ferdinand, Charles Baldwin, and Ciarán Ryan-Anderson. It has been an amazing experience to get to know all of you as well as the past — and future — students of CQuIC. Of the CQuIC alumni, I particularly thank Ben Baragiola, Zhang Jiang, Leigh Norris, Matthias Lang, Tyler "Bob" Keating, and Rob Cook for their role in encouraging me as a young graduate student. I would also like to thank the postdoctoral researchers of CQuIC, Christopher Jackson, Rafael Alexander, Sayonee Ray, Pablo Poggi, Christopher Ferrie, Joshua Combes, and Amir Kalev, who have all been a great source of support and guidance. I thank the CQuIC faculty at Sandia and Los Alamos national laboratories, Andrew Landahl, Robin Blume-Kohout, and Rolando Somma. I would further like to thank Satomi Sugaya, Matthew Chase, Farzin Farzam, Jacek Osinski, Megan Lewis, Kathy DeBlasio, Mark Gorski, Lewis Chiang, Neil McFadden, Stephen "Keith" Sanders,

Paul Gieri, Karishma Bansal, Kaleb Campbell, Mitchell Brickson, Jaimie Stephens, Akram Etemadi Amin, Mohamadreza Fazel, Christopher DiLullo, Peter Sinclair, and Nathaniel Ristoff, as well as all of the other graduate students of the Physics and Astronomy department at UNM. I especially thank Matthew DiMario and Rachel James for their support and encouragement as I was completing this thesis. I would also like to thank the supporting staff of the Physics and Astronomy department, and especially Gloria Cordova, Alisa Gibson, Gary Harrison, Tom Hess, Michael Sammy Martinez, and Steve Portillo. I am sure this remains an incomplete list of the people to whom I owe my gratitude, but nevertheless please know how thankful I am to have been a part of this wonderful community.

Finally, I would like to thank my dissertation committee, Akimasa Miyake (my advisor), Carlton Caves, Ivan Deutsch, and Steven Flammia. Steve was my mentor in my first exposure to quantum information science research as an undergraduate at Caltech, and I love the art of the field today as much as I did back then. Not every graduate student is able to say that their dissertation committee is made up of their heroes. I am fortunate enough to be able to do so.

Localization and Scrambling of Quantum Information with Applications to Quantum Computation and Thermodynamics

by

Adrian Chapman

B.S., California Institute of Technology, 2012
M.S., University of New Mexico, 2014

Ph.D., Physics, University of New Mexico, 2018

Abstract

As our demand for computational power grows, we encounter the question: "What are the physical limits to computation?" An answer is necessarily incomplete unless it can incorporate physics at the smallest scales, where we expect our near-term high-performance computing to occur. Microscopic physics – namely, quantum mechanics – behaves counterintuitively to our everyday experience, however. Quantum matter can occupy superpositions of states and build stronger correlations than are possible classically. This affects how quantum computers and quantum thermodynamic engines will behave.

Though these properties may seem to overwhelmingly defeat our attempts to build a quantum computer at-first-glance, what is remarkable is that they can also be immensely helpful to computation. Quantum mechanics hinders and helps computation, and the nuanced details of how we perform computations are important. In this dissertation, we examine the transition between these two behaviors and

connect it to a well-studied behavior in condensed matter physics, known as the many-body-localization transition.

Our idea utilizes the fact that quantum many-body systems have an intrinsic fastest speed at which signals can travel. When this speed is maximal, we expect arbitrary universal quantum computation to be achievable, since strong quantum correlations, or entanglement, can be built quickly. When it is limited, however, the difficulty of the computation is classically simulatable. We demonstrate a similar transition in the amount of thermodynamic work that can be performed by a quantum system when entanglement is present.

We first consider computations consisting of the evolution of a single particle or many noninteracting particles. When the number of such noninteracting particles is comparable to the total size of the system, we do not know of any way to simulate such computations classically. However, we find that we can still determine the fastest signal speed in such systems. We extend our result to interacting particles, which are universal for quantum computation, and observe a many-body-localization transition in a simple computational model using our algorithm. Finally, we apply ideas from quantum information to simulate the thermodynamic performance of a simple quantum system, showing that quantum effects can enable it to outperform its classical counterpart.

Contents

List of Symbols xiii

1 Introduction 1

1.1 List of Publications 5

2 Matchgates 6

2.1 Introduction 6

2.2 Basic Formalism 8

2.3 Mapping to Free-Fermions 10

2.4 Relationship to Representations of SO(2n) 17

2.4.1 Lie Closure of Quadratic and Linear Terms 20

2.4.2 Majorana Configuration Operators and "Matchgate Symmetry" 23

2.5 Computational Complexity of Matchgate Circuits 29

3 Out-of-Time-Ordered Correlators 34

3.1 Introduction 34

3.2 Formalism 36

3.2.1 Definitions 36

3.2.2 Covariant Behavior under Unitary Transformation 38

3.2.3 Relation to the Lieb-Robinson Bound 39

3.3 Relation to the Frame Potential 41

3.4 Relation to the Rényi Entropy 48

3.5 Localizing Systems 52

4 Classical simulation of quantum circuits by dynamical localization 55

4.1 Introduction 55

4.2 Background 57

4.3 Analytic results 59

4.4 Numerical example 61

4.5 Discussion 63

5 Many-body-localization transition in universal quantum circuits 67

5.1 Introduction 67

5.2 Background 70

5.2.1 Out-of-Time-Ordered Correlator 70

5.2.2 Gaussian Fermionic Evolution 73

5.3 Results 76

5.3.1 A. Universal Circuit Model 76

5.3.2 Exact Formula 79

5.3.3 Approximative method 82

5.3.4 Variational Optimization of the Free Parameter 88

5.4 Many-body location transition 89

5.5 Discussion 92

6 Autonomous quantum-correlated Maxwell demon 93

6.1 Introduction 93

6.2 Overview of the Model 95

6.3 Main Results 102

6.3.1 Global Clausius Inequality 102

6.3.2 Matrix Product Density Operator Solution 103

6.3.3 Simultaneous Refrigeration and Erasure 108

6.3.4 Quantum Thermodynamic Advantage 113

6.4 Conclusion 116

7 Summary and Outlook 118

Appendices 119

Appendices 119

A "Classical simulation of quantum circuits by dynamical localization" 120

A.1 Proof of Theorem 4.1 120

A.2 Modified Cauchy-Binet Formula 123

A.3 Fixed-Parity Sum 126

A.4 Exact Calculation of the OTO Correlator 128

A.5 Proof of Theorem 4.2 131

A.6 Numerical Analysis 135

B "Many-body-localization transition in universal quantum circuits" 137

B.1 Modified Cauchy-Binet Formula with Different Background Sets – Diagrammatic Proof 137

B.2 Modified Cauchy-Binet Formula with Different Background Sets – Determinental Proof 141

B.3 Exact Formula for the OTO Commutator 143

B.4 Exact formula for Lightcone Boundary 150

C "Autonomous quantum Maxwell demon" 152

C.1 Exposition of the Interaction Lindbladian 152

C.2 Generalized Clausius Inequality 154

C.3 Matrix Product Density Operator Update Method 156

References 160

List of Symbols

i	Imaginary unit
δ_{jk}	Kronecker delta
$A^\dagger$	Hermitian conjugate of A
A^*	Complex conjugate of A
A^T	Transpose of A
$\det(A)$	Determinant of A
$\mathrm{tr}(A)$	Trace of A
$\langle A \rangle$	Expectation value of A
$[A, B]$	Commutator of A and B
$\{A, B\}$	Anticommutator of A and B
$\|\|A\|\|_F$	Frobenius norm of A
$\mathrm{Re}(z)$	Real part of z
$\mathrm{Im}(z)$	Imaginary part of z
I, X, Y, Z	The identity operator and qubit Pauli operators, respectively
c_μ	Majorana fermion mode operator
c.c.	Complex conjugate
H.c.	Hermitian conjugate
$\vec{\alpha}$	$\equiv (\alpha_1, \alpha_2, \ldots, \alpha_k)$, where $\alpha_j < \alpha_{j+1}\ \forall\ 1 \leq \alpha_j \leq N$.
$\|\vec{\alpha}\|$	$\equiv k$, the number of elements in the tuple $\vec{\alpha} = (\alpha_1, \alpha_2, \ldots, \alpha_k)$.
$[k]$	$\equiv (1, 2, \ldots, k)$, the tuple of consecutive integers from 1 to k.
$\overline{\alpha}$	$\equiv$ Ordered tuple of indices in the set-complement of $\vec{\alpha}$ in $[N]$.
$()$	$\equiv$ The empty tuple, for which $\|()\| = 0$.
$\vec{\alpha} \cup \vec{\beta}$	$\equiv$ Ordered tuple of all indices in either $\vec{\alpha}$ or $\vec{\beta}$.

$\vec{\alpha} \subset \vec{\beta}$ $\equiv \vec{\alpha}$ is an ordered tuple of indices $\alpha_j \in \vec{\beta}$ for all $j \in \{1, 2, \ldots, |\vec{\alpha}| < |\vec{\beta}|\}$.

$\vec{\alpha} \backslash \alpha_j$ $\equiv$ Tuple of indices from $\vec{\alpha}$ with α_j removed.

$(\vec{\alpha}, \vec{\beta})$ $\equiv (\alpha_1, \alpha_2, \ldots, \alpha_k, \beta_1, \beta_2, \ldots)$; the unordered concatenation of $\vec{\alpha}$ and $\vec{\beta}$.

$C_{\vec{\alpha}}$ $\equiv \prod_{j=1}^{|\vec{\alpha}|} c_{\alpha_j}$ ascending, called a *Majorana configuration operator*.

$\mathbf{u}_{\vec{\alpha}\vec{\beta}}$ $\equiv$ Submatrix $\mathbf{u}_{\vec{\alpha}\vec{\beta}}$ of $\mathbf{u}$; i.e. $\left(\mathbf{u}_{\vec{\alpha}\vec{\beta}}\right)_{jk} = u_{\alpha_j \beta_k}$.

Chapter 1

Introduction

One of the most important revelations in modern physics is the idea that *information* is physical. This is to say that the observer and the observed cannot be treated separately in any proper description of a physical system. The state of knowledge of the observer is as relevant as the state of the system itself to predicting the outcomes of experiments.

This idea was famously first demonstrated in 1867 (before the discovery of quantum mechanics, in fact) with the gedanken experiment of James Clerk Maxwell, known as "Maxwell's demon." In the thought experiment, an intelligent agent, the demon, sits at the insulating partition between two halves of a container filled with fluid, initially at equal temperatures. The demon has perfect knowledge of the *microscopic* state of the fluid and so is able to track the motion of every one of its molecules to arbitrary precision. It also has the ability to raise and lower the partition arbitrarily fast and with negligible effort. In this ideal situation, the demon can exploit its knowledge and control to allow only particles traveling faster than a certain speed to pass through to only one side of the partition, raising the temperature of the fluid on that side and lowering the temperature of the fluid on the opposing side, particle-by-particle.

This behavior is apparently in direct conflict with the Second Law of Thermodynamics, which, in the Kelvin-Planck formulation, states:

> It is impossible for any device that operates on a cycle to receive heat from a single reservoir and produce a net amount of work.

This law is empirically observed to be ubiquitously true, and is often given as the statement that the net amount of disorder, or entropy, in the universe must always increase. Nevertheless, it would seem the demon in this example is storing a net amount of work in the temperature gradient it builds between the two halves of the container at the expense of the negligible work required to move the partition. It is apparently lowering the entropy of the universe by ordering the molecules of the fluid according to their speed, without increasing entropy anywhere else. The resolution ultimately came in 1961, when Rolf Landauer noted that the demon does not actually operate cyclically when its state of knowledge of the fluid is accounted for. Rather, any demon with a *finite* amount of memory must continuously erase the memory in-order to update its knowledge of the fluid, and such erasure is guaranteed to require work as well as dissipate heat. This led Landauer to his famous bound relating work to information [Lan61], the Second Law was saved, and information and physics were irrevocably and forever unified.

Concomitant with these developments was the discovery of quantum mechanics, pioneered in the early 20th century. Quantum mechanics, remarkably effective at describing the behavior of small-scale systems, similarly incorporates the observer within its framework. Namely, a quantum system cannot be said to be in any definite *classical* state at a given time, but is rather described in-general by a superposition of such states. Only when the observer makes a measurement does the state of the quantum system collapse into one of its classical components. Quantum mechanics says that there is no way to determine *a priori* which way this collapse will happen: only the statistics of repeated such measurements can be predicted. A great deal of effort has gone into interpreting this so-called "measurement postulate," and in-particular, this phenomenon forces one to re-examine the role of information in physical systems at the quantum level.

It wasn't until nearly a century later that Richard Feynman suggested that

quantum information may be fundamentally different from classical information in a way that may be exploited for the purpose of performing computation. Such a computation would entail preparing a quantum system in a definite state, allowing it to evolve into a superposition whose statistics encode the solution to some problem of interest, and performing a measurement, repeating the process many times to obtain the computation's result. Shortly thereafter, Peter Shor introduced a quantum algorithm for factoring integers exponentially faster than any known classical algorithm [Sho97], and a palpable distinction between classical and quantum computation was demonstrated. This algorithm functions by forcing undesired computational paths to destructively interfere, or "cancel each other out," a phenomenon which has no classical counterpart, and as-such, there is no comparable equivalent for factoring by a classical algorithm to this day.

These discoveries reinforce the idea that an information theoretic treatment is necessary for any complete description of a physical system, and they motivate the question, "what are the physical limits to the ability to process information, or perform computation?" In the thermodyamic framework, we see that this ability is limited by our capacity to perform work, and in the quantum setting, we see that it is limited by quantum uncertainty and interference, though such effects can also be leveraged to enhance our computational power as well. In this thesis, we examine the relationships between thermodynamics, quantum information, and computation with the aid of several illuminating problems. We first extend the concept of Anderson localization, the confinement of quantum information in a spatially irregular potential in the absence of interactions, to quantum circuits. Considering matchgate circuits, generated by time-dependent spin-1/2 XY Hamiltonians, we give an analytic formula for the out-of-time-ordered (OTO) correlator of a local observable, and show that it can be efficiently evaluated by a classical computer even when the explicit Heisenberg time evolution cannot. Because this quantity bounds the average error incurred by truncating the evolution to a spatially limited region, we demonstrate dynamical localization as a means for classically simulating quantum computation and give examples of localized phases under certain spatiotemporal disordered Hamiltonians.

We extend our method to study a transition to many-body-localizing behavior, which has limited dynamical complexity and is often classically simulatable. To detect the the transition from scrambling to many-body localization, we develop both exact and approximate methods to compute OTO correlators for arbitrary universal quantum circuits. We take advantage of the mapping of quantum circuits to the dynamics of interacting fermions in one dimension, as Gaussian time evolution supplemented by quartic interaction gates. In this framework, the OTO correlator can be calculated exactly as a superposition of exponentially many Gaussian-fermionic trajectories in the number of interaction gates. We approximate this formula using a restriction to the fastest-traveling fermionic modes alone and guarantee the correctness of our approach by variationally optimizing this restriction relative to the exact, brute-force calculation for small system size.

Finally, we study a particular autonomous quantum system, which exhibits refrigeration under an information-work tradeoff like a Maxwell demon. The system becomes correlated as a single "demon" qubit interacts sequentially with memory qubits while in contact with two heat reservoirs of different temperatures. Using strong subadditivity of the von Neumann entropy, we derive a global Clausius inequality to show thermodynamic advantages from access to correlated information. It is demonstrated, in a matrix product density operator formalism, that our demon can simultaneously realize refrigeration against a thermal gradient and erasure of information from its memory, which is impossible without correlations. We proceed to demonstrate that the phenomenon can be enhanced by the presence of quantum coherence.

The work in this thesis is based on that of several publications, listed below in Section 1.1. It further includes some necessary background over several chapters. Chapter 2 introduces the matchgate formalism and gives a summary of classical simulatability results. Chapter 3 gives some pedagogy for the out-of-time-ordered correlator, introducing its original motivation as a tool for studying quantum chaotic systems, giving some formal examples to relate it to other, more conventionally-studied quantities, and finally a brief summary of its application for the study of

localizing systems. From there, we proceed to provide our original results in Chapters 4, 5, and 6. The introductory material of these chapters will be redundant with some of that in Chapters 2 and 3, so as to be self-contained. Finally, we conclude with future directions and interesting open problems in Chapter 7.

1.1 List of Publications

- A. Chapman and A. Miyake, "How an autonomous quantum Maxwell demon can harness correlated information," Phys. Rev. E **92**, 062125 (2015). (Appears in Chapter 6)

- A. Chapman and A. Miyake, "Classical simulation of quantum circuits by dynamical localization: Analytic results for Pauli-observable scrambling in time-dependent disorder," Phys. Rev. A **98**, 012309 (2018). (Appears in Chapter 4)

- A. Chapman and A. Miyake, "Many-body-localization transition in a universal quantum circuit model," ArXiv:1807.09261 [quant-ph] (2018). (Appears in Chapter 5)

Chapter 2

Matchgates

2.1 Introduction

Matchgates are an especially interesting example of exactly solvable quantum dynamics. Introduced by Leslie Valiant in 2002 as an example of a class of quantum computations that could be simulated classically in polynomial time [Val02], matchgate circuits seem to defy our conventional notion of solvability, as their simulatability arises from an inherently algebraic origin. Such circuits can be built out of 2-input 2-output, nearest-neighbor gates satisfying 10 quadratic identities in their elements [JMS15]. These arise in the context of solving for the total weight of all perfect matchings of a planar graph. A perfect matching of a graph is a subset of its edges such that every vertex is included by exactly one edge in the subset. Surprisingly, for a weighted, planar graph, the total weight of such subsets can be computed efficiently by the Fisher-Kasteleyn-Temperley (FKT) [Kas61, TF61] algorithm. This algorithm defines an associated antisymmetric covariance matrix A to the graph, for which the number of perfect matchings is given by $\sqrt{\det(A)}$ (called the Pfaffian of A for antisymmetric A). Matchgate circuits can be described as planar graphs composed of elementary "graph gadgets," corresponding to the elementary nearest-neighbor matchgates, for which amplitudes of the circuit are computed as perfect matching sums. As planarity is a necessary criterion for classical simulatability, we see that the

topology of the circuit is intimately related to its complexity [Bra].

It was later demonstrated by Knill [Kni01] and Terhal and DiVincenzo [TD02] that such circuits are related to the dynamics of free-fermions hopping on a one-dimensional lattice with arbitrary single-particle Hamiltonian by the Jordan-Wigner transformation, providing further physical basis to matchgate simulatability. In this picture, a non-planar topology can surprisingly be seen as a type of fermionic interaction. Furthermore, upon inclusion of such operations (i.e. either an interaction of a $SWAP$), these circuits are extended to be universal for quantum computation [JM08, BC14, BGa11]. Similar extensions include nondemolition charge measurements on the fermions [BDEK04] and the inclusion of four-qubit "magic states" [Bra06].

In this chapter, we will review the formalism of matchgates from their basic connection to free-fermion dynamics. In Sec. 2.3, we give an explicit correspondence between the SWAP gate in the qubit picture and an interaction gate in the fermionic construction. In Sec. 2.4, we will show that matchgate circuits on n qubits generate the group $\mathrm{Spin}(2n)$, which restricts to a representation of the special orthogonal group $\mathrm{SO}(2n)$ when acting by conjugation. In this section, we will also reconcile the notions of "linear" versus "algebraic" symmetry by giving a set of observables which commute with quadratic tensor powers of matchgate circuits. Finally, we close with a brief review of the matchgate-circuit complexity class and an explicit construction of its extension to universal quantum computation upon the inclusion of SWAP gates in Sec. 2.5.

2.2 Basic Formalism

We define a 2-input 2-output matchgate as

$$G(V,W) = \begin{pmatrix} V_{00} & 0 & 0 & V_{01} \\ 0 & W_{00} & W_{01} & 0 \\ 0 & W_{10} & W_{11} & 0 \\ V_{10} & 0 & 0 & V_{11} \end{pmatrix}, \tag{2.1}$$

where

$$V = \begin{pmatrix} V_{00} & V_{01} \\ V_{10} & V_{11} \end{pmatrix} \qquad W = \begin{pmatrix} W_{00} & W_{01} \\ W_{10} & W_{11} \end{pmatrix} \tag{2.2}$$

with

$$\det V = \det W. \tag{2.3}$$

Without loss of generality, we can take $\det V = \det W = 1$, since this quantity simply contributes to an overall phase on $G(V,W)$. We see that matchgates are block diagonal on the even- and odd-parity subspaces of a 2-qubit Hilbert space with (ordered) basis $\{|00\rangle, |01\rangle, |10\rangle, |11\rangle\}$. However, it is truly the determinantal constraint, Eq. (2.3) that restricts the computational power of matchgate circuits[1]. To see this, let

$$G(V,W) = \exp\left[i\left(\mathbf{n}\cdot\boldsymbol{\sigma}_{\text{even}} + \mathbf{m}\cdot\boldsymbol{\sigma}_{\text{odd}}\right)\right], \tag{2.4}$$

[1]We will refer to a general parity-preserving 2-qubit gate as $G(U,V)$, even if it violates Eq. (2.3).

where $\boldsymbol{\sigma}_{\{\text{even,odd}\}}$ are vectors of operators preserving their respective fixed-parity subspaces, given by

$$\begin{cases} X_{\text{even}} \equiv \sigma^x_{\text{even}} & = \frac{1}{2}\left(X \otimes X - Y \otimes Y\right) \\ Y_{\text{even}} \equiv \sigma^y_{\text{even}} & = \frac{1}{2}\left(Y \otimes X + X \otimes Y\right), \\ Z_{\text{even}} \equiv \sigma^z_{\text{even}} & = \frac{1}{2}\left(Z \otimes I + I \otimes Z\right) \end{cases} \tag{2.5}$$

and

$$\begin{cases} X_{\text{odd}} \equiv \sigma^x_{\text{odd}} & = \frac{1}{2}\left(X \otimes X + Y \otimes Y\right) \\ Y_{\text{odd}} \equiv \sigma^y_{\text{odd}} & = \frac{1}{2}\left(Y \otimes X - X \otimes Y\right). \\ Z_{\text{odd}} \equiv \sigma^z_{\text{odd}} & = \frac{1}{2}\left(Z \otimes I - I \otimes Z\right) \end{cases} \tag{2.6}$$

Since they preserve the fixed-parity subspaces, operators acting on opposite-parity subspaces commute with one another (e.g., $[X_{\text{even}}, Y_{\text{odd}}] = 0$), and operators acting on a fixed-parity subspace form a Pauli algebra

$$\begin{aligned} [\sigma^j_{\text{even}}, \sigma^k_{\text{even}}] &= 2i\varepsilon_{jkl}\sigma^l_{\text{even}} \\ [\sigma^j_{\text{odd}}, \sigma^k_{\text{odd}}] &= 2i\varepsilon_{jkl}\sigma^l_{\text{odd}} \end{aligned} \tag{2.7}$$

for ε_{jkl} the totally antisymmetric 3-index Levi-Civita tensor, for which $\varepsilon_{xyz} = 1$, and there is a summation implied over repeated indices in Eq. (2.7) above.

From Eq. (2.4), we have the correspondence

$$\begin{cases} V & = \exp\left[i\left(\mathbf{n} \cdot \sigma\right)\right] \\ W & = \exp\left[i\left(\mathbf{m} \cdot \sigma\right)\right] \end{cases}. \tag{2.8}$$

The identity $\det\left(e^{iH}\right) = e^{i\,\mathrm{tr}\,(H)}$ implies that the condition Eq. (2.3) is automatically satisfied by the parameterization given by Eq.s (2.4) and (2.8) ($\det V = \det W = 1$, since $\mathrm{tr}\,(\mathbf{n}\cdot\sigma) = \mathrm{tr}\,(\mathbf{m}\cdot\sigma) = 0$). Furthermore, every $G(V,W)$ for which $V, W \in \mathrm{SU}(2)$ can be written according to this parameterization. We can include a relative phase between the two fixed-parity subspaces by defining

$$\begin{cases} I_{\text{even}} & \equiv \frac{1}{2}\left(I\otimes I + Z\otimes Z\right) \\ I_{\text{odd}} & \equiv \frac{1}{2}\left(I\otimes I - Z\otimes Z\right) \end{cases} \tag{2.9}$$

and including these operators in the exponential Eq. (2.4) with arbitrary real coefficients will allow us to vary the determinants of V and W as arbitrary phases. It is clear that $G(V,W)$ will still preserve fixed-parity subspaces even with a relative phase between V and W. However, including this phase has an important and surprising consequence for the complexity of circuits composed of 2-input, 2-output, nearest-neighbor matchgates, as we will see in the coming section.

2.3 Mapping to Free-Fermions

To elucidate the complexity of nearest-neighbor 2-qubit matchgate *circuits*, it is necessary to define the $2n$ Majorana operators $\{c_\mu\}$, for $\mu \in \{1,\ldots,2n\}$ as particular Pauli strings acting on n qubits by the Jordan-Wigner transformation

$$\begin{cases} c_{2j-1} & = \bigotimes_{k=1}^{j-1} Z_k \otimes X_j \\ c_{2j} & = \bigotimes_{k=1}^{j-1} Z_k \otimes Y_j \end{cases} \tag{2.10}$$

These operators satisfy the fermionic canonical anticommutation relations

$$\{c_\mu, c_\nu\} = 2I\delta_{\mu,\nu}, \tag{2.11}$$

where $\delta_{\mu,\nu}$ is the Kronecker delta. That is, two Majorana operators anticommute unless they are identical, for which we have $c_\mu^2 = I$. It is straightforward to verify that the Pauli strings in the right-hand side of Eq. (4.3) satisfy Eq. (2.11), since the Pauli operators square to the identity, and distinct such strings will commute on every qubit except for one (either both Paulis are Z or one is the identity on the commuting qubits), where one of the Paulis will be an X or Y and the other will be a Z. Distinct Majorana operators therefore anticommute.

Rewriting the parity-preserving Pauli operators Eq.s (2.5) and (2.6) in-terms of the four Majorana modes $\{c_1, c_2, c_3, c_4\}$ gives

$$\begin{cases} X_{\text{even}} &= -\frac{i}{2}\left(c_1 c_4 + c_2 c_3\right) \\ Y_{\text{even}} &= \frac{i}{2}\left(c_1 c_3 - c_2 c_4\right) \\ Z_{\text{even}} &= -\frac{i}{2}\left(c_1 c_2 + c_3 c_4\right) \end{cases}, \tag{2.12}$$

and

$$\begin{cases} X_{\text{odd}} &= \frac{i}{2}\left(c_1 c_4 - c_2 c_3\right) \\ Y_{\text{odd}} &= \frac{i}{2}\left(c_1 c_3 + c_2 c_4\right) \\ Z_{\text{odd}} &= -\frac{i}{2}\left(c_1 c_2 - c_3 c_4\right) \end{cases}. \tag{2.13}$$

We see that, between the two sets of operators, we have all symmetric and antisymmetric linear combinations of the $\binom{4}{2} = 6$ quadratics in the four Majorana operators, and so any linear combination of these quadratics can be written as some linear combination of these parity-preserving Paulis. We therefore conveniently rewrite our parameterization in Eq. (2.4) as

$$G(U, V) = \exp\left(\sum_{\mu,\nu=1}^{4} h_{\mu\nu} c_\mu c_\nu\right) \equiv \exp\left(\mathbf{c}^{\mathrm{T}} \cdot \mathbf{h} \cdot \mathbf{c}\right), \tag{2.14}$$

where $\mathbf{c}$ is a column vector of the Majorana operators, and the coefficients $\{h_{\mu\nu}\}$, for $\mu, \nu \in \{1, \ldots, 4\}$, define a real, antisymmetric matrix $\mathbf{h}$, given by

$$\mathbf{h} = \frac{1}{4} \begin{pmatrix} 0 & n_z + m_z & n_y + m_y & n_x - m_x \\ -(n_z + m_z) & 0 & n_x + m_x & n_y - m_y \\ -(n_y + m_y) & -(n_x + m_x) & 0 & n_z - m_z \\ -(n_x - m_x) & -(n_y - m_y) & -(n_z - m_z) & 0 \end{pmatrix}. \tag{2.15}$$

Antisymmetry follows from the canonical anticommutation relations, Eq. (2.11), which imply that any symmetric part of $\mathbf{h}$ will vanish, and since we have taken the operator in the exponential to be traceless in Eq. (2.4).

General quadratics in the Majorana operators are closed under commutation:

$$\left[\left(\mathbf{c}^{\mathrm{T}} \cdot \mathbf{h} \cdot \mathbf{c}\right), \left(\mathbf{c}^{\mathrm{T}} \cdot \mathbf{g} \cdot \mathbf{c}\right)\right] = \sum_{\mu,\nu,\lambda,\eta} h_{\mu\nu} g_{\lambda\eta} [c_\mu c_\nu, c_\lambda c_\eta] \tag{2.16}$$

$$= 2 \sum_{\mu,\nu,\lambda,\eta} h_{\mu\nu} g_{\lambda\eta} \left[\delta_{\mu\lambda}(1 - \delta_{\nu\eta}) c_\eta c_\nu + \delta_{\mu\eta}(1 - \delta_{\nu\lambda}) c_\nu c_\lambda \right.$$
$$\left. + \delta_{\nu\lambda}(1 - \delta_{\mu\eta}) c_\mu c_\eta + \delta_{\nu\eta}(1 - \delta_{\mu\lambda}) c_\lambda c_\mu \right] \tag{2.17}$$

$$= 2 \left[\sum_{\nu,\eta} \left(\sum_{\mu} h_{\mu\nu} g_{\mu\eta} \right) (1 - \delta_{\nu\eta}) c_\eta c_\nu \right.$$
$$+ \sum_{\nu,\lambda} \left(\sum_{\mu} h_{\mu\nu} g_{\lambda\mu} \right) (1 - \delta_{\nu\lambda}) c_\nu c_\lambda$$
$$+ \sum_{\mu,\eta} \left(\sum_{\nu} h_{\mu\nu} g_{\nu\eta} \right) (1 - \delta_{\mu\eta}) c_\mu c_\eta$$
$$\left. + \sum_{\lambda,\mu} \left(\sum_{\nu} h_{\mu\nu} g_{\lambda\nu} \right) (1 - \delta_{\mu\lambda}) c_\lambda c_\mu \right] \tag{2.18}$$

$$= 4 \sum_{\nu,\lambda} (\mathbf{hg} - \mathbf{gh})_{\nu\lambda} (1 - \delta_{\nu\lambda}) c_\nu c_\lambda \tag{2.19}$$

$$\left[\left(\mathbf{c}^{\mathrm{T}} \cdot \mathbf{h} \cdot \mathbf{c}\right), \left(\mathbf{c}^{\mathrm{T}} \cdot \mathbf{g} \cdot \mathbf{c}\right)\right] = 4\, \mathbf{c}^{\mathrm{T}} \cdot [\mathbf{h}, \mathbf{g}] \cdot \mathbf{c} \tag{2.20}$$

From Eq. (2.16) to Eq. (2.17), we restricted to the four mutually exclusive cases for

which the term does not vanish, wherein two of the indices μ, ν, λ, η are equal and the other two are not. We cannot have $\mu = \nu$ or $\lambda = \eta$ by the antisymmetry of $\mathbf{h}$ and $\mathbf{g}$, and if two pairs of indices are equal (e.g. $\mu = \lambda$ and $\nu = \eta$) or all of the indices are different, then the commutator vanishes for that term. From Eq. (2.17) to Eq. (2.18), we summed over one of the indices appearing in a Kronecker delta on each term and rearranged sums to separate those over Majorana operators from contractions on matrix indices. From Eq. (2.18) to Eq. (2.19), we relabeled dummy indices, collected terms, and relabeled an index contraction as matrix multiplication. Finally, from Eq. (2.19) to Eq. (2.20), we again relabeled index contraction as matrix multiplication with the vector $\mathbf{c}$, using the fact that $[\mathbf{h}, \mathbf{g}]$ is also antisymmetric, and so its diagonal elements are zero.

We therefore see that the commutator of two quadratics in the Majorana operators is itself quadratic in the Majorana operators. The Baker-Campbell-Hausdorff (BCH) formula expresses the product of two operator exponentials in terms of the exponential of a series of the operators and their commutators

$$\exp(X)\exp(Y) = \exp\left[\sum_{n=1}^{\infty} \frac{(-1)^{n-1}}{n} \sum_{\substack{r_1+s_1>0 \\ \vdots \\ r_n+s_n>0}} \frac{\mathrm{ad}_X^{r_1}\mathrm{ad}_Y^{s_1}\mathrm{ad}_X^{r_2}\mathrm{ad}_Y^{s_2}\ldots\widetilde{\mathrm{ad}}_X^{r_n}\widetilde{\mathrm{ad}}_Y^{s_n}}{\sum_{i=1}^{n}(r_i+s_i)\cdot\prod_{i=1}^{n} r_i! s_i!}\right] \tag{2.21}$$

$$\exp(X)\exp(Y) = \exp\left\{X + Y + \frac{1}{2}[X,Y] + \frac{1}{12}([X,[X,Y]] + \ldots) + \ldots\right\}, \tag{2.22}$$

where $\mathrm{ad}_X(\,\cdot\,) \equiv [X, \cdot\,]$, and

$$\widetilde{\mathrm{ad}}_X = \begin{cases} X & \text{if appearing as last factor} \\ \mathrm{ad}_X & \text{otherwise} \end{cases}. \tag{2.23}$$

The sum is over all nonnegative $s_i, r_i \geq 0$ such that $r_i + s_i > 0$ (so at least one of these values must be greater than zero). Since $[X, X] = 0$, we see that the term is zero if $s_n > 1$ or if $s_n = 0$ and $r_n > 1$. This general expression of the BCH formula was actually introduced by Eugene Dynkin in 1947 [Jac66]. We thus have

$$\begin{aligned}
&\exp\left(\mathbf{c}^{\mathrm{T}} \cdot \mathbf{h} \cdot \mathbf{c}\right) \exp\left(\mathbf{c}^{\mathrm{T}} \cdot \mathbf{g} \cdot \mathbf{c}\right) \\
&= \exp\left[\mathbf{c}^{\mathrm{T}} \cdot \sum_{n=1}^{\infty} \frac{(-1)^{n-1}}{n} \sum_{\substack{r_1+s_1>0 \\ \vdots \\ r_n+s_n>0}} \frac{4^{\sum_{i=1}^{n}(r_i+s_i)} \mathrm{ad}_{\mathbf{h}}^{r_1} \mathrm{ad}_{\mathbf{g}}^{s_1} \mathrm{ad}_{\mathbf{h}}^{r_2} \mathrm{ad}_{\mathbf{g}}^{s_2} \ldots \widetilde{\mathrm{ad}}_{\mathbf{h}}^{r_n} \widetilde{\mathrm{ad}}_{\mathbf{g}}^{s_n}}{4 \sum_{i=1}^{n} (r_i + s_i) \prod_{i=1}^{n} r_i! s_i!} \cdot \mathbf{c}\right],
\end{aligned} \tag{2.24}$$

Since again, the commutator of antisymmetric matrices is antisymmetric, the coefficients in the exponential on the right-hand-side form an antisymmetric matrix. The factor of four in the denominator here is due to the fact that each commutator comes with a factor of four due to Eq. (2.20), but there is one fewer factor of four than the number of matrices $\mathbf{h}$ or $\mathbf{g}$ due to the fact that $\widetilde{\mathrm{ad}}_X = X$ (and not $4X$) if it is the last factor. We can therefore rewrite Eq. (2.24) in such a way that it is clear that unitaries of the form $\exp\left(\mathbf{c}^{\mathrm{T}} \cdot \mathbf{h} \cdot \mathbf{c}\right)$ form a group, as

$$\begin{aligned}
&\exp\left[\frac{\mathbf{c}^{\mathrm{T}}}{2} \cdot (4\mathbf{h}) \cdot \frac{\mathbf{c}}{2}\right] \exp\left[\frac{\mathbf{c}^{\mathrm{T}}}{2} \cdot (4\mathbf{g}) \cdot \frac{\mathbf{c}}{2}\right] \\
&= \exp\left[\frac{\mathbf{c}^{\mathrm{T}}}{2} \cdot \sum_{n=1}^{\infty} \frac{(-1)^{n-1}}{n} \sum_{\substack{r_1+s_1>0 \\ \vdots \\ r_n+s_n>0}} \frac{\mathrm{ad}_{4\mathbf{h}}^{r_1} \mathrm{ad}_{4\mathbf{g}}^{s_1} \mathrm{ad}_{4\mathbf{h}}^{r_2} \mathrm{ad}_{4\mathbf{g}}^{s_2} \ldots \widetilde{\mathrm{ad}}_{4\mathbf{h}}^{r_n} \widetilde{\mathrm{ad}}_{4\mathbf{g}}^{s_n}}{\sum_{i=1}^{n} (r_i + s_i) \prod_{i=1}^{n} r_i! s_i!} \cdot \frac{\mathbf{c}}{2}\right],
\end{aligned} \tag{2.25}$$

This group, for two operators of the form (2.14), is in-fact Spin(4), which shares a Lie algebra with SO(4), but forms a double-covering [Vla01] due to the factor of $\frac{1}{2}$ on each of the vectors $\mathbf{c}$ in the exponential, since these guarantee, e.g., $\exp\left(2\pi \cdot \frac{c_i c_j - c_j c_i}{4}\right) = -I$.

More generally, any exponential of a sum of quadratics in the Majorana operators, which may act non-locally on n qubits, will satisfy Eq. (2.25), where it forms the group $\mathrm{Spin}(2n)$. We will generally refer to such exponential operators as *Gaussian fermionic operations* synonymously with the phrase "matchgate circuits". General Gaussian fermionic operators can always be written as products of (polynomially-many) operators of the form (2.1) acting on nearest-neighbor qubits using the generalized Euler angle decomposition [JM08]. This nearest-neighbor property is crucial, as non-nearest-neighbor parity-preserving Pauli operators will not be quadratic in the Majorana operators. For example,

$$X_{\text{even}}^{(1,3)} \equiv \frac{1}{2}\left(X \otimes I \otimes X - Y \otimes I \otimes Y\right) \tag{2.26}$$

$$X_{\text{even}}^{(1,3)} \equiv -\frac{1}{2}\left(c_2 c_3 c_4 c_5 + c_1 c_3 c_4 c_6\right) \tag{2.27}$$

It is straightforward to verify that this property holds for non-nearest-neighbor parity-preserving Paulis in-general, since a string of identities between either X or Y Paulis will be a completely filled string of Majorana operators on those qubits under the Jordan-Wigner transformation.

Additionally, Eq.s (2.9) will also involve quartics in the Majorana operators under the Jordan-Wigner transformation, despite being nearest-neighbor, as

$$\begin{cases} I_{\text{even}} & \equiv \frac{1}{2}\left(I - c_1 c_2 c_3 c_4\right) \\ I_{\text{odd}} & \equiv \frac{1}{2}\left(I + c_1 c_2 c_3 c_4\right) \end{cases} \tag{2.28}$$

As we state below Eq. (2.9), we can vary the determinants of V and W by including these operators in the exponential parameterization Eq. (2.4) with arbitrary real coefficients, as

$$G(V,W) = \exp\left\{i\left[\left(\mathbf{n}\cdot\boldsymbol{\sigma}_{\text{even}} + aI_{\text{even}}\right) + \left(\mathbf{m}\cdot\boldsymbol{\sigma}_{\text{odd}} + bI_{\text{odd}}\right)\right]\right\} \tag{2.29}$$

$$G(V,W) = \exp\left[\left(\mathbf{c}^{\mathrm{T}} \cdot \mathbf{h} \cdot \mathbf{c}\right) + \frac{i}{2}(b+a)\, I + \frac{i}{2}(b-a)\, c_1 c_2 c_3 c_4\right], \tag{2.30}$$

where, $\mathbf{h}$ is again defined by Eq. (2.15). Unless $b = a$, the exponent in Eq. (2.30) will include a quartic term, which will not preserve quadratics in the Majorana operators. For example,

$$[c_1 c_2 c_3 c_4, c_4 c_5] = 2 c_1 c_2 c_3 c_5 \tag{2.31}$$

Though such exponentials of quartic terms are still nearest-neighbor, they can be used to extend the range of nearest-neighbor matchgates, since they are related to the SWAP operation by matchgate multiplication, as

$$\mathrm{SWAP} = G(I,X) = G(I,iI)G(I,-iX), \tag{2.32}$$

and

$$G(I,iI) = \exp\left(\frac{i\pi}{2} I_{\mathrm{odd}}\right) \tag{2.33}$$

$$= \exp\left[\frac{i\pi}{4}(I \otimes I - Z \otimes Z)\right] \tag{2.34}$$

$$G(I,iI) = \exp\left[\frac{i\pi}{4}(I + c_1 c_2 c_3 c_4)\right] \tag{2.35}$$

Clearly $G(I,-iX)$ satisfies the determinental constraint, Eq. (2.3), whereas $G(I,iI)$ (and $G(I,X)$) does not. It was shown, surprisingly, in Ref. [JM08] that non-nearest-neighbor matchgate circuits, composed of nearest-neighbor matchgates and SWAP, are universal for quantum computation. The above relations demonstrate that such circuits are equivalent to those composed of nearest-neighbor matchgates and nearest-neighbor 2-qubit parity-preserving unitaries generated by quartic products of Majorana operators. Therefore, it is sufficient to only violate the determinental

constraint Eq. (2.3) in circuits composed of nearest-neighbor parity-preserving unitaries to achieve universal quantum computation. We will return to the nuanced computational complexity of matchgate circuits in an upcoming section. In the next section however, we examine the relationship between matchgate circuits and the group action of $\mathrm{SO}(2n) \cong \mathrm{Spin}(2n)/\mathbb{Z}_2$.

2.4 Relationship to Representations of SO(2n)

We begin by proving the relation

$$U^\dagger c_\mu U = \sum_{\nu=1}^{2n} \left(e^{4\mathbf{h}}\right)_{\mu\nu} c_\nu, \tag{2.36}$$

where $U \equiv \exp\left(\mathbf{c}^{\mathrm{T}} \cdot \mathbf{h} \cdot \mathbf{c}\right)$ is a Gaussian fermionic operation, and the *single-particle transition matrix* $\mathbf{u} = e^{4\mathbf{h}}$ is an element of $\mathrm{SO}(2n)$, since it is the exponential of an antisymmetric matrix, as

$$\begin{cases} \mathbf{u}\mathbf{u}^{\mathrm{T}} = e^{4\mathbf{h}} e^{4\mathbf{h}^{\mathrm{T}}} = e^{4\mathbf{h}} e^{-4\mathbf{h}} = \mathbf{I} \\ \mathbf{u}^{\mathrm{T}}\mathbf{u} = e^{4\mathbf{h}^{\mathrm{T}}} e^{4\mathbf{h}} = e^{-4\mathbf{h}} e^{4\mathbf{h}} = \mathbf{I} \end{cases}. \tag{2.37}$$

This relation is proved in Ref. [JM08] by showing that

$$c_\mu(t) = \sum_{\nu=1}^{2n} \left(e^{4\mathbf{h}t}\right)_{\mu\nu} c_\nu \tag{2.38}$$

satisfies the Schrödinger equation

$$\frac{\partial}{\partial t} c_\mu(t) = -\left[\left(\mathbf{c}^{\mathrm{T}} \cdot \mathbf{h} \cdot \mathbf{c}\right), c_\mu(t)\right], \tag{2.39}$$

and then choosing $t = 1$. Here however, we prove the relation in a related yet slightly different way. We first show that such conjugation on a linear combination in the Majorana operators can be related to that on a quadratic in the Majoranas by introducing a mode which does not participate in the evolution. We then evolve the quadratic by the adjoint action of the group $\mathrm{Spin}(2n) \subseteq \mathrm{Spin}(2n+1)$ of Gaussian fermionic operators. We will find that this adjoint action is the same as that of $\mathrm{SO}(2n)$ in accordance with Eq. (2.36), since the two groups share a Lie algebra.

Following Ref. [JMS15], we introduce the Majorana operator c_0 and basis vectors $\{\mathbf{e}_0, \mathbf{e}_\mu\}$ for $\mu \in \{1, \ldots, 2n\}$ (in general, we will refer to an index in the set $\{1, \ldots, 2n\}$ by a Greek letter). Let $\widetilde{\mathbf{h}}$ be an antisymmetric matrix, related to the antisymmetric matrix $\mathbf{h}$ by $\widetilde{h}_{0\mu} = \widetilde{h}_{\mu 0} = 0$ and $\widetilde{h}_{\mu\nu} = h_{\mu\nu}$. Additionally, let $\mathbf{g}^{(0,\mu)} \equiv \frac{1}{2}\left(\mathbf{e}_0\mathbf{e}_\mu^{\mathrm{T}} - \mathbf{e}_\mu\mathbf{e}_0^{\mathrm{T}}\right)$ be the antisymmetric matrix coupling indices μ and 0 We have

$$\left[\left(\mathbf{c}^{\mathrm{T}} \cdot \widetilde{\mathbf{h}} \cdot \mathbf{c}\right), c_0 c_\mu\right] = 4\mathbf{c}^{\mathrm{T}} \cdot \left[\widetilde{\mathbf{h}}, \mathbf{g}^{(0,\mu)}\right] \cdot \mathbf{c} \tag{2.40}$$

$$= -2\left\{\mathbf{c}^{\mathrm{T}} \cdot \left[\left(\widetilde{\mathbf{h}} \cdot \mathbf{e}_\mu\right)\mathbf{e}_0^{\mathrm{T}} + \mathbf{e}_0\left(\mathbf{e}_\mu^{\mathrm{T}} \cdot \widetilde{\mathbf{h}}\right)\right] \cdot \mathbf{c}\right\} \tag{2.41}$$

$$= -2\left\{\left[\mathbf{c}^{\mathrm{T}} \cdot \left(\widetilde{\mathbf{h}} \cdot \mathbf{e}_\mu\right)\right] c_0 + c_0\left[\left(\mathbf{e}_\mu^{\mathrm{T}} \cdot \widetilde{\mathbf{h}}\right) \cdot \mathbf{c}\right]\right\} \tag{2.42}$$

$$= -4c_0\left[\left(\mathbf{e}_\mu^{\mathrm{T}} \cdot \widetilde{\mathbf{h}}\right) \cdot \mathbf{c}\right] \tag{2.43}$$

$$\left[\left(\mathbf{c}^{\mathrm{T}} \cdot \widetilde{\mathbf{h}} \cdot \mathbf{c}\right), c_0 c_\mu\right] = -4c_0\left(\mathbf{h} \cdot \mathbf{c}\right)_\mu \tag{2.44}$$

In Eq. (2.40), we applied Eq. (2.20). From Eq. (2.40) to Eq. (2.41), we expanded the commutator and the definition of $\mathbf{g}^{(0,\mu)}$ and used the fact that $\widetilde{\mathbf{h}} \cdot \mathbf{e}_0 = \left(\mathbf{e}_0^{\mathrm{T}} \cdot \widetilde{\mathbf{h}}\right)^{\mathrm{T}} = \mathbf{0}$. From Eq. (2.41) to Eq. (2.42), we used the fact that $\mathbf{e}_0^{\mathrm{T}} \cdot \mathbf{c} = \mathbf{c}^{\mathrm{T}} \cdot \mathbf{e}_0 = c_0$. From Eq. (2.42) to Eq. (2.43), we used the fact that, since $\mathbf{e}_0^{\mathrm{T}} \cdot \widetilde{\mathbf{h}} \cdot \mathbf{e}_\mu = 0$,

$$\left[\mathbf{c}^{\mathrm{T}} \cdot \left(\widetilde{\mathbf{h}} \cdot \mathbf{e}_\mu\right)\right] c_0 = -c_0\left[\mathbf{c}^{\mathrm{T}} \cdot \left(\widetilde{\mathbf{h}} \cdot \mathbf{e}_\mu\right)\right], \tag{2.45}$$

and

$$\mathbf{c}^{\mathrm{T}} \cdot \left(\widetilde{\mathbf{h}} \cdot \mathbf{e}_\mu\right) = \left[\mathbf{c}^{\mathrm{T}} \cdot \left(\widetilde{\mathbf{h}} \cdot \mathbf{e}_\mu\right)\right]^{\mathrm{T}} \tag{2.46}$$

$$= \left(\mathbf{e}_\mu^{\mathrm{T}} \cdot \widetilde{\mathbf{h}}^{\mathrm{T}}\right) \cdot \mathbf{c} \tag{2.47}$$

$$\mathbf{c}^{\mathrm{T}} \cdot \left(\widetilde{\mathbf{h}} \cdot \mathbf{e}_\mu\right) = -\left(\mathbf{e}_\mu^{\mathrm{T}} \cdot \widetilde{\mathbf{h}}\right) \cdot \mathbf{c} \tag{2.48}$$

Finally, we used the fact that $\left[\left(\mathbf{e}_\mu^{\mathrm{T}} \cdot \widetilde{\mathbf{h}}\right) \cdot \mathbf{c}\right] = (\mathbf{h} \cdot \mathbf{c})_\mu$ to arrive at Eq. (2.44). We expand the commutator using the product rule

$$\left[\left(\mathbf{c}^{\mathrm{T}} \cdot \widetilde{\mathbf{h}} \cdot \mathbf{c}\right), c_0 c_\mu\right] = c_0 \left[\left(\mathbf{c}^{\mathrm{T}} \cdot \widetilde{\mathbf{h}} \cdot \mathbf{c}\right), c_\mu\right] + \left[\left(\mathbf{c}^{\mathrm{T}} \cdot \widetilde{\mathbf{h}} \cdot \mathbf{c}\right), c_0\right] c_\mu, \tag{2.49}$$

for which $\left[\left(\mathbf{c}^{\mathrm{T}} \cdot \widetilde{\mathbf{h}} \cdot \mathbf{c}\right), c_0\right] = 0$. This gives

$$c_0 \left[\left(\mathbf{c}^{\mathrm{T}} \cdot \widetilde{\mathbf{h}} \cdot \mathbf{c}\right), c_\mu\right] = -4 c_0 \left(\mathbf{h} \cdot \mathbf{c}\right)_\mu \tag{2.50}$$

and multiplying both sides by c_0 on the right, using the fact that $c_0^2 = I$, gives

$$\left[\left(\mathbf{c}^{\mathrm{T}} \cdot \widetilde{\mathbf{h}} \cdot \mathbf{c}\right), c_\mu\right] = \left(-4\mathbf{h} \cdot \mathbf{c}\right)_\mu . \tag{2.51}$$

We apply a similar trick to demonstrate Eq. (2.36), using the adjoint representation of the group $\mathrm{Spin}(2n) \subseteq \mathrm{Spin}(2n)$

$$\exp\left[-\left(\mathbf{c}^{\mathrm{T}} \cdot \widetilde{\mathbf{h}} \cdot \mathbf{c}\right)\right] c_0 c_\mu \exp\left(\mathbf{c}^{\mathrm{T}} \cdot \widetilde{\mathbf{h}} \cdot \mathbf{c}\right) = \exp\left[-\mathrm{ad}_{\left(\mathbf{c}^{\mathrm{T}} \cdot \widetilde{\mathbf{h}} \cdot \mathbf{c}\right)}\right](c_0 c_\mu) \tag{2.52}$$

$$c_0 \exp\left[-\left(\mathbf{c}^{\mathrm{T}} \cdot \widetilde{\mathbf{h}} \cdot \mathbf{c}\right)\right] c_\mu \exp\left(\mathbf{c}^{\mathrm{T}} \cdot \widetilde{\mathbf{h}} \cdot \mathbf{c}\right) = c_0 \left(e^{4\mathbf{h}} \cdot \mathbf{c}\right)_\mu \tag{2.53}$$

Once again, we multiply both sides by c_0 on the right, using the fact that, restricted to the modes $\{c_\mu\}_{\mu=1}^{2n}$, we can make the replacement $\widetilde{\mathbf{h}} \to \mathbf{h}$ to obtain the relation

$$\exp\left[-\left(\mathbf{c}^{\mathrm{T}}\cdot\mathbf{h}\cdot\mathbf{c}\right)\right]c_\mu\exp\left(\mathbf{c}^{\mathrm{T}}\cdot\mathbf{h}\cdot\mathbf{c}\right)=\sum_{\nu=1}^{2n}\left(e^{4\mathbf{h}}\right)_{\mu\nu}c_\nu, \tag{2.54}$$

as desired. In Eq. (2.52), we simply applied the action of the adjoint representation of $\mathrm{Spin}(2n)\subseteq\mathrm{Spin}(2n+1)$. In Eq. (2.53) on the left, we used the fact that c_0 and $\left(\mathbf{c}^{\mathrm{T}}\cdot\widetilde{\mathbf{h}}\cdot\mathbf{c}\right)$ commute. On the right, we applied Eq. (2.44) iteratively within the exponent, noting that the relation (2.44) holds for all $\mu\in\{1,\ldots,2n\}$, and so repeated application of the adjoint map corresponds to repeated matrix multiplication by $-4\mathbf{h}$.

2.4.1 Lie Closure of Quadratic and Linear Terms

The introduction of this extra operator c_0 may seem overly complicated, but it is useful for proving that operators which are linear and quadratic in the $\{c_\mu\}_{\mu=1}^{2n}$ also form a closed Lie algebra. To see this, let $\mathbf{h}'$ be an antisymmetric matrix over all modes $\{c_0\}\cup\{c_\mu\}_{\mu=1}^{2n}$, such that $\mathbf{e}_0^{\mathrm{T}}\cdot\mathbf{h}'\cdot\mathbf{c}\equiv\sum_{\mu=1}^{2n}v_\mu c_\mu\equiv\mathbf{v}^{\mathrm{T}}\cdot\mathbf{c}$. That is,

$$\mathbf{h}'=\widetilde{\mathbf{h}}+\mathbf{e}_0\mathbf{v}^{\mathrm{T}}-\mathbf{v}\mathbf{e}_0^{\mathrm{T}}, \tag{2.55}$$

where $\widetilde{\mathbf{h}}$ is as defined above. We have

$$\left[\left(\mathbf{c}^{\mathrm{T}}\cdot\mathbf{h}'\cdot\mathbf{c}\right),c_0c_\mu\right]=\left[\mathbf{c}^{\mathrm{T}}\cdot\left(\widetilde{\mathbf{h}}+\mathbf{e}_0\mathbf{v}^{\mathrm{T}}-\mathbf{v}\mathbf{e}_0^{\mathrm{T}}\right)\cdot\mathbf{c},c_0c_\mu\right]. \tag{2.56}$$

We already know $\left[\left(\mathbf{c}^{\mathrm{T}}\cdot\widetilde{\mathbf{h}}\cdot\mathbf{c}\right),c_0c_\mu\right]$ from Eq. (2.44). We thus only need calculate

$$\begin{aligned}\left[\mathbf{c}^{\mathrm{T}}\cdot\left(\mathbf{e}_0\mathbf{v}^{\mathrm{T}}-\mathbf{v}\mathbf{e}_0^{\mathrm{T}}\right)\cdot\mathbf{c},c_0c_\mu\right]&=4\mathbf{c}^{\mathrm{T}}\cdot\left[\left(\mathbf{e}_0\mathbf{v}^{\mathrm{T}}-\mathbf{v}\mathbf{e}_0^{\mathrm{T}}\right),\mathbf{g}^{(0,\mu)}\right]\cdot\mathbf{c} &(2.57)\\&=2\mathbf{c}^{\mathrm{T}}\cdot\left(-v_\mu\mathbf{e}_0\mathbf{e}_0^{\mathrm{T}}-\mathbf{v}\mathbf{e}_\mu^{\mathrm{T}}+v_\mu\mathbf{e}_0\mathbf{e}_0^{\mathrm{T}}+\mathbf{e}_\mu\mathbf{v}^{\mathrm{T}}\right)\cdot\mathbf{c} &(2.58)\end{aligned}$$

$$= 2\left[-\left(\mathbf{c}^{\mathrm{T}}\cdot\mathbf{v}\right)c_\mu + c_\mu\left(\mathbf{v}^{\mathrm{T}}\cdot\mathbf{c}\right)\right] \tag{2.59}$$

$$\left[\mathbf{c}^{\mathrm{T}}\cdot\left(\mathbf{e}_0\mathbf{v}^{\mathrm{T}} - \mathbf{v}\mathbf{e}_0^{\mathrm{T}}\right)\cdot\mathbf{c}, c_0c_\mu\right] = 4c_\mu\left(\mathbf{v}^{\mathrm{T}}\cdot\mathbf{P}_{\overline{\mu}}\cdot\mathbf{c}\right) \tag{2.60}$$

where $\mathbf{P}_{\overline{\mu}}$ is the diagonal matrix for which $\left(\mathbf{P}_{\overline{\mu}}\right)_{\nu\eta} = \delta_{\nu\eta}\left(1-\delta_{\nu\mu}\right)$. Eq (2.57) follows straightforwardly from Eq. (2.20), with $\mathbf{g}^{(0,\mu)} \equiv \frac{1}{2}\left(\mathbf{e}_0\mathbf{e}_\mu^{\mathrm{T}} - \mathbf{e}_\mu\mathbf{e}_0^{\mathrm{T}}\right)$ as defined above. From Eq. (2.57) to Eq. (2.58), we expanded the commutator, using

$$\begin{cases} \mathbf{e}_0^{\mathrm{T}}\cdot\mathbf{e}_0 = 1 & \mathbf{e}_\mu^{\mathrm{T}}\cdot\mathbf{e}_0 = 0 \\ \mathbf{e}_0^{\mathrm{T}}\cdot\mathbf{v} = 0 & \mathbf{e}_\mu^{\mathrm{T}}\cdot\mathbf{v} = v_\mu \end{cases} \tag{2.61}$$

From Eq. (2.58) to Eq. (2.59), we performed cancellations and used the fact that $\mathbf{e}_\mu^{\mathrm{T}}\cdot\mathbf{c} = c_\mu$. Finally, we used the fact that c_μ anticommutes with $\mathbf{v}^{\mathrm{T}}\cdot\mathbf{c}$, except for the c_μ term in the linear combination, yielding the projector $\mathbf{P}_{\overline{\mu}}$ in Eq. (2.60). We next expand the right-hand side of this equation, as

$$\left[\mathbf{c}^{\mathrm{T}}\cdot\left(\mathbf{e}_0\mathbf{v}^{\mathrm{T}} - \mathbf{v}\mathbf{e}_0^{\mathrm{T}}\right)\cdot\mathbf{c}, c_0c_\mu\right] = \left[c_0\left(\mathbf{v}^{\mathrm{T}}\cdot\mathbf{c}\right) - \left(\mathbf{c}^{\mathrm{T}}\cdot\mathbf{v}\right)c_0, c_0c_\mu\right] \tag{2.62}$$

$$= 2\left[c_0\left(\mathbf{v}^{\mathrm{T}}\cdot\mathbf{c}\right), c_0c_\mu\right] \tag{2.63}$$

$$= 2\Big\{\left[\left(\mathbf{v}^{\mathrm{T}}\cdot\mathbf{c}\right), c_\mu\right] + c_0\left[\left(\mathbf{v}^{\mathrm{T}}\cdot\mathbf{c}\right), c_0\right]c_\mu + c_0\left[c_0, c_\mu\right]\left(\mathbf{v}^{\mathrm{T}}\cdot\mathbf{c}\right) + \left[c_0, c_0\right]c_\mu\left(\mathbf{v}^{\mathrm{T}}\cdot\mathbf{c}\right)\Big\} \tag{2.64}$$

$$= 2\Big\{\left[\left(\mathbf{v}^{\mathrm{T}}\cdot\mathbf{c}\right), c_\mu\right] - 2\left(\mathbf{v}^{\mathrm{T}}\cdot\mathbf{c}\right)c_\mu + 2c_\mu\left(\mathbf{v}^{\mathrm{T}}\cdot\mathbf{c}\right)\Big\} \tag{2.65}$$

$$= 2\Big\{\left[\left(\mathbf{v}^{\mathrm{T}}\cdot\mathbf{c}\right), c_\mu\right] - 2\left[\left(\mathbf{v}^{\mathrm{T}}\cdot\mathbf{c}\right), c_\mu\right]\Big\} \tag{2.66}$$

$$\left[\mathbf{c}^{\mathrm{T}}\cdot\left(\mathbf{e}_0\mathbf{v}^{\mathrm{T}} - \mathbf{v}\mathbf{e}_0^{\mathrm{T}}\right)\cdot\mathbf{c}, c_0c_\mu\right] = -2\left[\left(\mathbf{v}^{\mathrm{T}}\cdot\mathbf{c}\right), c_\mu\right] \tag{2.67}$$

and so combining Eq.s (2.67) and (2.60) gives

$$\left[\left(\mathbf{v}^{\mathrm{T}}\cdot\mathbf{c}\right), c_\mu\right] = -2c_\mu\left(\mathbf{v}^{\mathrm{T}}\cdot\mathbf{P}_{\overline{\mu}}\cdot\mathbf{c}\right) \tag{2.68}$$

We may therefore write the commutator of quadratic-plus-linear combinations of Majorana operators succinctly as

$$\begin{aligned}&[\left(\mathbf{c}^{\mathrm{T}}\cdot\mathbf{h}\cdot\mathbf{c}\right)+\left(\mathbf{v}^{\mathrm{T}}\cdot\mathbf{c}\right),\left(\mathbf{c}^{\mathrm{T}}\cdot\mathbf{g}\cdot\mathbf{c}\right)+\left(\mathbf{w}^{\mathrm{T}}\cdot\mathbf{c}\right)]\\&=\mathbf{c}^{\mathrm{T}}\cdot\left\{4\left[\mathbf{h},\mathbf{g}\right]+\left(\mathbf{v}\mathbf{w}^{\mathrm{T}}-\mathbf{w}\mathbf{v}^{\mathrm{T}}\right)\right\}\cdot\mathbf{c}+4\left(\mathbf{v}^{\mathrm{T}}\cdot\mathbf{g}-\mathbf{w}^{\mathrm{T}}\cdot\mathbf{h}\right)\cdot\mathbf{c}\end{aligned}\tag{2.69}$$

We can check Eq. (2.69) against the smallest nontrivial case of Pauli operators on a single qubit

$$\begin{cases}\mathbf{n}\cdot\boldsymbol{\sigma}\equiv n_z Z+\mathbf{n}_\perp\cdot\boldsymbol{\sigma}_\perp & =\frac{n_z}{2}\left(\mathbf{c}^{\mathrm{T}}\cdot\mathbf{Y}\cdot\mathbf{c}\right)+\mathbf{n}_\perp^{\mathrm{T}}\cdot\mathbf{c}\\\mathbf{m}\cdot\boldsymbol{\sigma}\equiv m_z Z+\mathbf{m}_\perp\cdot\boldsymbol{\sigma}_\perp & =\frac{m_z}{2}\left(\mathbf{c}^{\mathrm{T}}\cdot\mathbf{Y}\cdot\mathbf{c}\right)+\mathbf{m}_\perp^{\mathrm{T}}\cdot\mathbf{c}\end{cases}\tag{2.70}$$

where $\mathbf{Y}$ is the Pauli-Y operator acting on the Majorana operator space, and $\mathbf{n}_\perp$ and $\mathbf{m}_\perp$ are the components of the Bloch vector along the equatorial plane of the Bloch sphere. We have

$$\begin{aligned}[(\mathbf{n}\cdot\boldsymbol{\sigma}),(\mathbf{m}\cdot\boldsymbol{\sigma})]=\mathbf{c}^{\mathrm{T}}\cdot&\left\{4n_z m_z\left[\mathbf{Y},\mathbf{Y}\right]+\left(\mathbf{n}_\perp\mathbf{m}_\perp^{\mathrm{T}}-\mathbf{m}_\perp\mathbf{n}_\perp^{\mathrm{T}}\right)\right\}\cdot\mathbf{c}\\&+2\left[m_z\mathbf{n}_\perp^{\mathrm{T}}-n_z\mathbf{m}_\perp^{\mathrm{T}}\right]\cdot\mathbf{Y}\cdot\mathbf{c}\end{aligned}\tag{2.71}$$

Expanding

$$\begin{cases}\mathbf{n}_\perp=n_x\mathbf{e}_x+n_y\mathbf{e}_y\\\mathbf{m}_\perp=m_x\mathbf{e}_x+m_y\mathbf{e}_y\end{cases},\tag{2.72}$$

and performing some simplification gives

$$[(\mathbf{n}\cdot\boldsymbol{\sigma}),(\mathbf{m}\cdot\boldsymbol{\sigma})]=\mathbf{c}^{\mathrm{T}}\cdot\left(n_x m_y-m_x n_y\right)\left(\mathbf{e}_x\mathbf{e}_y^{\mathrm{T}}-\mathbf{e}_y\mathbf{e}_x^{\mathrm{T}}\right)\cdot\mathbf{c}$$

$$+ 2i \left[\left(n_y m_z - m_y n_z \right) \mathbf{e}_x^{\mathrm{T}} + \left(n_z m_x - m_z n_x \right) \mathbf{e}_y^{\mathrm{T}} \right] \cdot \mathbf{c} \tag{2.73}$$

$$= 2i \left(\mathbf{n} \times \mathbf{m} \right)_z \left(-ic_1 c_2 \right) \cdot \mathbf{c} + 2i \left[\left(\mathbf{n} \times \mathbf{m} \right)_x c_1 + \left(\mathbf{n} \times \mathbf{m} \right)_y c_2 \right] \tag{2.74}$$

$$\left[\left(\mathbf{n} \cdot \boldsymbol{\sigma} \right), \left(\mathbf{m} \cdot \boldsymbol{\sigma} \right) \right] = 2i (\mathbf{n} \times \mathbf{m}) \cdot \boldsymbol{\sigma} \tag{2.75}$$

Just as we expect.

2.4.2 Majorana Configuration Operators and "Matchgate Symmetry"

Let us introduce a *Majorana configuration* as

$$C_{\vec{\alpha}} = c_{\alpha_1} c_{\alpha_2} \ldots c_{\alpha_k} \tag{2.76}$$

for $\vec{\alpha}$ a k-tuple of indices, where the ordering $\alpha_1 < \alpha_2 < \cdots < \alpha_k$ in the product is taken. We will often denote set-theoretic operations on these tuples using conventional notation (see, "List of Symbols"). In this section, we prove the formula

$$U^\dagger C_{\vec{\alpha}} U = \sum_{\{\vec{\beta} || \vec{\beta}| = |\vec{\alpha}|\}} \det \left(\mathbf{u}_{\vec{\alpha}\vec{\beta}} \right) C_{\vec{\beta}}, \tag{2.77}$$

for some matchgate unitary U, indexed by single particle transition matrix $\mathbf{u} \in \mathrm{SO}(2n)$, by induction on the number of Majorana factors $k \equiv |\vec{\alpha}|$. Here, $\mathbf{u}_{\vec{\alpha}\vec{\beta}}$ is the $\vec{\alpha}$, $\vec{\beta}$ submatrix of the single-particle transition matrix (i.e. $\left(\mathbf{u}_{\vec{\alpha}\vec{\beta}} \right)_{jk} = u_{\alpha_j, \beta_k}$). First consider the case where $k = 2$, and let $\alpha_1 < \alpha_2$. We have

$$U^\dagger c_{\alpha_1} c_{\alpha_2} U = \left(U^\dagger c_{\alpha_1} U \right) \left(U^\dagger c_{\alpha_2} U \right) \tag{2.78}$$

$$= \left(\sum_{\beta_1} u_{\alpha_1\beta_1} c_{\beta_1} \right) \left(\sum_{\beta_2} u_{\alpha_2\beta_2} c_{\beta_2} \right) \tag{2.79}$$

$$= \left(\sum_{\{(\beta_1,\beta_2)|\beta_1=\beta_2\}} + \sum_{\{(\beta_1,\beta_2)|\beta_1<\beta_2\}} + \sum_{\{(\beta_1,\beta_2)|\beta_1>\beta_2\}} \right) u_{\alpha_1\beta_1} u_{\alpha_2\beta_2} c_{\beta_1} c_{\beta_2} \tag{2.80}$$

$$= \left(\sum_{\beta_1} u_{\alpha_1\beta_1} u_{\alpha_2\beta_1} \right) I + \sum_{\{(\beta_1,\beta_2)|\beta_1<\beta_2\}} \left(u_{\alpha_1\beta_1} u_{\alpha_2\beta_2} - u_{\alpha_1\beta_2} u_{\alpha_2\beta_1} \right) c_{\beta_1} c_{\beta_2} \tag{2.81}$$

$$U^\dagger c_{\alpha_1} c_{\alpha_2} U = \sum_{\{(\beta_1,\beta_2)|\beta_1<\beta_2\}} \det \left[\mathbf{u}_{(\alpha_1,\alpha_2)(\beta_1,\beta_2)} \right] c_{\beta_1} c_{\beta_2}, \tag{2.82}$$

where, from Eq. (2.80) to Eq. (2.81), we used the canonical anticommutation relations, Eq. (2.11), relabeling dummy indices $\beta_1 \leftrightarrow \beta_2$ on the third sum in Eq. (2.80). From Eq. (2.81) to Eq. (2.82), we see that the identity term vanishes as its coefficient is the inner product between two distinct row vectors of an orthogonal matrix. This proves the statement for $k = 2$. Next, we assume the statement holds for general k and use this assumption to prove the statement for $k + 1$. Without loss of generality, assume $\alpha_j < \alpha_{k+1}$ for all $j \leq k$. We now have

$$U^\dagger C_{\vec{\alpha}} c_{\alpha_{k+1}} U = \left(U^\dagger C_{\vec{\alpha}} U \right) \left(U^\dagger c_{\alpha_{k+1}} U \right) \tag{2.83}$$

$$= \left[\sum_{\{\vec{\beta}||\vec{\beta}|=|\vec{\alpha}|\}} \det \left(\mathbf{u}_{\vec{\alpha}\vec{\beta}} \right) C_{\vec{\beta}} \right] \left(\sum_{\beta_{k+1}} u_{\alpha_{k+1}\beta_{k+1}} c_{\beta_{k+1}} \right) \tag{2.84}$$

$$U^\dagger C_{\vec{\alpha}} c_{\alpha_{k+1}} U = \sum_{\{(\vec{\beta},\beta_{k+1})||\vec{\beta}|=|\vec{\alpha}|\}} u_{\alpha_{k+1}\beta_{k+1}} \det \left(\mathbf{u}_{\vec{\alpha}\vec{\beta}} \right) C_{\vec{\beta}} c_{\beta_{k+1}} \tag{2.85}$$

Each of the terms in the sum above falls into one of two categories. Either (i) $\beta_{k+1} \in \vec{\beta}$, and $C_{\vec{\beta}} c_{\beta_{k+1}} = \pm C_{\vec{\beta}\setminus\beta_{k+1}}$, or (ii) $\beta_{k+1} \notin \vec{\beta}$, and $C_{\vec{\beta}} c_{\beta_{k+1}} = \pm C_{\vec{\beta}\cup\beta_{k+1}}$, with sign given in both cases by $(-1)^{|\{j\leq k|\beta_j>\beta_{k+1}\}|}$. We first proceed to demonstrate that all of the terms in category (i) vanish. Fix a particular configuration operator $C_{\vec{\beta}\setminus\beta_{k+1}}$. The

coefficient on this operator in the right-hand side of Eq. (2.85) is given by a sum over all indices γ which could have been removed from $\vec{\beta}$ to yield $\vec{\beta}\backslash\beta_{k+1}$

$$\sum_{\gamma\notin\vec{\beta}\backslash\beta_{k+1}} u_{\alpha_{k+1}\gamma}\det\left[\mathbf{u}_{\vec{\alpha}(\vec{\beta}\backslash\beta_{k+1},\gamma)}\right] = \sum_{\gamma} u_{\alpha_{k+1}\gamma}\det\left[\mathbf{u}_{\vec{\alpha}(\vec{\beta}\backslash\beta_{k+1},\gamma)}\right], \tag{2.86}$$

where we were able to cancel any sign factors on the terms inside the sum by reordering columns in $\mathbf{u}$ so that the γ column appears at the rightmost position, using the alternating sign property of the determinant. The equality is due to the fact that if $\gamma \in \vec{\beta}\backslash\beta_{k+1}$, then the determinant in that term evaluates to zero. Finally, we use the multilinearity property of the determinant to bring the sum on to the last column, as

$$\sum_{\gamma} u_{\alpha_{k+1}\gamma}\det\left[\mathbf{u}_{\vec{\alpha}(\vec{\beta}\backslash\beta_{k+1},\gamma)}\right] = \det\left[\begin{pmatrix} \mathbf{u}_{\vec{\alpha},\vec{\beta}\backslash\beta_{k+1}} & \sum_{\gamma} u_{\alpha_{k+1}\gamma}\mathbf{u}_{\vec{\alpha}\gamma} \end{pmatrix}\right], \tag{2.87}$$

i.e. the determinant of a matrix whose last column vector is $\sum_{\gamma} u_{\alpha_{k+1}\gamma}\mathbf{u}_{\vec{\alpha}\gamma}$. The lth element of this column is given by

$$\sum_{\gamma} u_{\alpha_{k+1}\gamma}u_{\alpha_l\gamma} = \delta_{\alpha_{k+1}\alpha_l} \tag{2.88}$$

again following from the fact that this sum is the inner product between two column vectors of an orthogonal matrix. However, $\alpha_{k+1} > \alpha_l$ by assumption, so this sum is actually always zero and the determinant in (2.87) vanishes. Each of the terms in category (i) therefore vanishes, and the only terms in the r.h.s of Eq. (2.85) that survive are in category (ii). We examine these terms by next fixing a particular configuration operator $C_{\vec{\beta}\cup\beta_{k+1}}$. The coefficient on this operator in the right-hand side of (2.85) is given by a sum over all indices γ that could have been added to $\vec{\beta}$ to yield $\vec{\beta}\cup\beta_{k+1}$ (we cannot cancel sign factors this time)

$$\sum_{\gamma\in\vec{\beta}\cup\beta_{k+1}} (-1)^{|\{j\leq k+1|\beta_j>\gamma\}|} u_{\alpha_{k+1}\gamma} \det\left[\mathbf{u}_{\vec{\alpha},\left(\vec{\beta}\cup\beta_{k+1}\right)\setminus\gamma}\right] = \det\left[\mathbf{u}_{(\vec{\alpha},\alpha_{k+1}),\vec{\beta}\cup\beta_{k+1}}\right]. \tag{2.89}$$

To see that this equality indeed holds, relabel indices in $\vec{\beta}\cup\beta_{k+1}$ such that $\beta_i<\beta_{i+1}$ for all $i\leq k$, and suppose $\gamma=\beta_s$ in this labeling. Then we have

$$(-1)^{|\{j\leq k+1|\beta_j>\gamma\}|} = (-1)^{(k+1)-s} = (-1)^{(k+1)+s} \tag{2.90}$$

As $\alpha_j<\alpha_{k+1}$ for all $j\leq k$, this is exactly the sign factor that would appear had we expanded along the last [$(k+1)$st] row of the matrix in the r.h.s. above, since β_s appears as the sth column of this matrix. We therefore have

$$U^\dagger C_{\vec{\alpha}} c_{\alpha_{k+1}} U \;\; = \sum_{\{\vec{\beta}||\vec{\beta}|=k+1\}} \det\left[\mathbf{u}_{(\vec{\alpha},\alpha_{k+1})\vec{\beta}}\right] C_{\vec{\beta}}, \tag{2.91}$$

which proves the statement for $k+1$, given that it holds for k. This completes our inductive proof of Eq. (2.77).

We therefore see that, not only do matchgate circuits preserve the linear space of single Majorana operators under conjugation, but they also preserve each vector space of degree-k Majorana configuration operators. This is not obvious, since it was not immediately clear that such action would not *decrease* the number of Majorana operators in a configuration by the relation $c_\mu^2=I$. As we saw above however, this is essentially guaranteed by matchgate circuits preserving the linear space of single Majorana operators and their unitarity, which guarantees they will preserve the canonical anticommutation relations

$$\{U^\dagger c_\mu U, U^\dagger c_\nu U\} = \sum_{\eta,\lambda} u_{\mu\eta} u_{\nu\lambda} \{c_\eta, c_\lambda\} \tag{2.92}$$

$$= 2 \sum_{\eta,\lambda} u_{\mu\eta} u_{\nu\lambda} \delta_{\eta\lambda} I \tag{2.93}$$

$$= 2 \left(\mathbf{u}\mathbf{u}^{\mathrm{T}}\right)_{\mu\nu} I \tag{2.94}$$

$$\{U^\dagger c_\mu U, U^\dagger c_\nu U\} = 2\delta_{\mu\nu} I. \tag{2.95}$$

These two properties together therefore imply that $\mathbf{u}$ will be orthogonal, and this was the essential property for the coefficients on terms like $c_\mu^2 = I$ to vanish.

We are now in a position to reconcile the notion of what we will refer to as an *algebraic* symmetry, obeyed by matchgate circuits, with the more conventional notion of what we will refer to as a *linear* symmetry. The latter corresponds to conserved quantities, which are identified in quantum mechanics with observables that commute with the Hamiltonian. For example, suppose we have an operator L for which

$$[H, L] = 0 \tag{2.96}$$

then it is straightforward to show that H preserves the degenerate eigenspaces of L and vice-versa. That is, if $|l\rangle$ is an eigenstate of L with eigenvalue l, then so is $H|l\rangle$, and a similar statement holds for eigenstates of H. The unitary time evolution operator e^{-iHt} is therefore block-diagonal in the degenerate eigenspaces of L, and so the quantum number l remains conserved over time.

However, for general Gaussian fermionic time-evolution U (which may even be generated by a time-dependent Hamiltonian $-iH(t) = \mathbf{c}^{\mathrm{T}} \cdot \mathbf{h}(t) \cdot \mathbf{c}$), there does not seem to be a corresponding conserved observable L. The parity operator $Z^{\otimes n}$ does commute with all matchgate circuits with quadratic generators in the Majorana operators, but it only has two degenerate eigenspaces, corresponding to eigenvalues ± 1, which is not enough to account for the $n+1$ preserved linear spaces of Majorana

configuration operators. Indeed, matchgate circuits are constrained by a symmetry in the Heisenberg picture, over linear spaces of *operators* in $\mathcal{H} \otimes \mathcal{H}^*$ rather than vectors in the Hilbert space $\mathcal{H}$. The corresponding conserved "observable" here is actually

$$\Lambda = \sum_{\mu=1}^{2n} c_\mu \otimes c_\mu \tag{2.97}$$

since

$$(U \otimes U)^\dagger \Lambda (U \otimes U) = \sum_{\mu=1}^{2n} \left(U^\dagger c_\mu U\right) \otimes \left(U^\dagger c_\mu U\right) \tag{2.98}$$

$$= \sum_{\lambda,\eta=1}^{2n} \left(\sum_{\mu=1}^{2n} u_{\mu\lambda} u_{\mu\eta} \right) c_\lambda \otimes c_\eta \tag{2.99}$$

$$= \sum_{\lambda,\eta=1}^{2n} \delta_{\lambda\eta} c_\lambda \otimes c_\eta \tag{2.100}$$

$$(U \otimes U)^\dagger \Lambda (U \otimes U) = \sum_{\lambda=1}^{2n} c_\lambda \otimes c_\lambda = \Lambda \tag{2.101}$$

That is, $U \otimes U$ preserves eigenspaces of Λ. Furthermore, any general unitary tensor power $(U \otimes U)$ which preserves this operator must be a matchgate circuit, as

$$(U \otimes U)^\dagger \Lambda (U \otimes U) = \sum_{\vec{\alpha}\vec{\beta}} \left(\sum_{\mu=1}^{2n} u_{\mu\vec{\alpha}} u_{\mu\vec{\beta}} \right) C_{\vec{\alpha}} \otimes C_{\vec{\beta}} \tag{2.102}$$

due to linear independence of the operators $C_{\vec{\alpha}} \otimes C_{\vec{\beta}}$, we must have that the sum in parentheses is equal to $\delta_{\vec{\alpha}\vec{\beta}} \delta_{|\vec{\alpha}|1}$. This will only be the case if the action of U is to preserve the number of Majorana operators in the configuration (due to $\delta_{|\vec{\alpha}|1}$) and map single Majorana operators to orthogonal linear combinations (due to $\delta_{\vec{\alpha}\vec{\beta}}$). Since any such orthogonal single particle transition matrix can be generated by a matchgate circuit, Λ will only be preserved if U is a matchgate circuit.

The action of matchgate evolution is therefore block diagonal over the linear space of operators $\mathcal{H} \otimes \mathcal{H}^*$, and the requirement that unitary evolution preserve algebraic relations between operators, in addition to linearity, constrains the evolution to give the relation between blocks by Eq. (2.77). This has implications for the computational complexity of simulating some matchgate circuits classically, since the determinant can be evaluated efficiently by a classical computer, as we show in Chapter 4. In the next section, we review some basic results about the weak and strong simulation of classically simulating matchgate circuits.

2.5 Computational Complexity of Matchgate Circuits

In this section, we summarize some results to give a picture of how matchgate circuits fit into the framework of computational complexity. We begin by giving an explicit construction for universal quantum computation by matchgate circuits on nearest- and next-nearest-neighboring qubits, with computational basis preparation and measurement, originally introduced by Jozsa and Miyake [JM08]. We go on to summarize several results in the literature classifying the delicate computational power of matchgate circuits.

To simulate universal quantum computation, it is sufficient to simulate arbitrary product rotations and any 2-qubit entangling gate, such as the CZ gate, written in the computational basis as

$$\mathrm{CZ} = G(Z, I) = \begin{pmatrix} 1 & 0 & 0 & 0 \\ 0 & 1 & 0 & 0 \\ 0 & 0 & 1 & 0 \\ 0 & 0 & 0 & -1 \end{pmatrix} \tag{2.103}$$

To achieve this, Jozsa and Miyake consider a logical encoding of a qubit by four

physical qubits, as

$$\begin{cases} |0_L\rangle = |0000\rangle \\ |1_L\rangle = |1001\rangle \end{cases} \tag{2.104}$$

In such an encoding, it is clear that logical CZ between nearest-neighboring logical qubits can be simulated as a physical CZ between the last physical of the first logical and the first physical of the second logical qubit, as

$$\mathrm{CZ}_L|00_L\rangle = |000\rangle \otimes (\mathrm{CZ}|00\rangle) \otimes |000\rangle = |00_L\rangle \tag{2.105}$$
$$\mathrm{CZ}_L|01_L\rangle = |000\rangle \otimes (\mathrm{CZ}|01\rangle) \otimes |001\rangle = |01_L\rangle \tag{2.106}$$
$$\mathrm{CZ}_L|10_L\rangle = |100\rangle \otimes (\mathrm{CZ}|10\rangle) \otimes |000\rangle = |10_L\rangle \tag{2.107}$$
$$\mathrm{CZ}_L|11_L\rangle = |100\rangle \otimes (\mathrm{CZ}|11\rangle) \otimes |001\rangle = -|11_L\rangle \tag{2.108}$$

as desired. This CZ can be simulated by a SWAP gate, since

$$\mathrm{CZ} \equiv G(Z, I) \tag{2.109}$$
$$= G(HXH, I) \tag{2.110}$$
$$= G(H, H)G(I, X)G(X, X)G(H, H) \tag{2.111}$$
$$\mathrm{CZ} = G(H, H)\mathrm{SWAP}G(X, X)G(H, H) \tag{2.112}$$

and we see that the determinental constraint Eq. (2.3) is satisfied for every parity-preserving gate in this factorization except for SWAP. A single-qubit logical gate is applied as

$$A_L = G(Z, X)_{1,2}G(Z, X)_{3,4}G(A, A)_{2,3}G(Z, X)_{1,2}G(Z, X)_{3,4}, \tag{2.113}$$

since

$$G(Z, X) = G(Z, I)G(I, X) = CZ \cdot \text{SWAP}. \tag{2.114}$$

In this encoding, the first round of CZ does nothing (since it either acts on $|00\rangle$, $|10\rangle$, or $|01\rangle$). The SWAP brings the $|1\rangle$, if it is present, from the outer (qubit 1 or 4) to the inner two qubits, encoding the logical qubit in the $\{|00\rangle, |11\rangle\}$ subspace of qubits 2 and 3. $G(A, A)$ simply applies A to this subspace, and the next round of $G(Z, X)$ brings the logical qubit back to its original encoding. Clearly, we can measure any logical qubit in the computational basis by measuring in the computational basis either qubit 1 or 4 for this logical qubit. By preparing an arbitrary computational basis state (in the logical encoding), applying a next-nearest-neighbor matchgate circuit, and measuring in the computational basis, we can therefore simulate an arbitrary universal quantum computation.

This result highlights the computational fragility of matchgate circuits acting on computational-basis input with computational-basis measurements, since the simple inclusion of SWAP gates to this class will extend it to quantum computational universality. It begs the question, then, of how other seemingly innocuous adjustments to this framework might affect its computational complexity. In Ref. [Bro16], it was shown that the output probabilities of matchgate circuits can be efficiently calculated by a classical computer when (i) the input is given in the computational basis and multiple qubits of the output are measured in the computational basis (even if these measurements are adaptive), and (ii) the input is given in an arbitrary product state and a single qubit of the output is measured in the computational basis. In the latter setting, when single qubits are measured in an arbitrary basis, the output probabilities can be sampled efficiently by a classical computer, known as weak classical simulation. This last setting will be our focus in Chapter 4, where we will show that localization will allow us to compute expectation values and output probabilities for certain families of matchgate circuits to exponential precision, even for arbitrary product basis input and measurements.

We therefore summarize some of the of Ref. [Bro16] in this section.

An important related result by Brod [BC14] shows that matchgate interactions on any graph topologies which are not equivalent to either a ring or a line are sufficient to simulate a universal quantum computation. Furthermore, it was shown by Brod and Galvão in 2011 that *any* parity preserving non-matchgate (including SWAP) is sufficient to endow matchgates with the power of universal quantum computation [BGa11]. Matchgates are therefore quite delicate as a computational complexity class. In particular, Van den Nest showed in 2010 that the class of matchgates to compute a given function with some probability of success is equivalent to that of linear threshold gates [VdN11a]. When this success probability is greater than $\frac{3}{4}$, the only functions that can be computed are those that depend on only a single bit of the input. In [VDN11b], it was shown that, for success probability $\geq \frac{2}{3}$, the complexity class of functions efficiently computable by matchgate circuits must lie strictly within P. Namely, there are poly-time classically computable functions which cannot be efficiently evaluated with matchgate circuits (on computational input with computational basis measurements) with success probability $\geq \frac{2}{3}$. Surprisingly, if this were not the case, then the quantum algorithm performing Simon's algorithm – one of a handful of quantum algorithms known to demonstrate an exponential speedup over any known classical algorithm – would admit a classically efficient simulation.

Finally, in Ref. [Bro16], it was shown that matchgate circuits with computational basis input and arbitrary single-qubit measurements can be *weakly* simulated efficiently by a classical computer. That is, a classical computer can efficiently sample from the probability distribution generated by such processes. Though this is arguably a more natural notion of classical simulatability for quantum computation, it is only guaranteed to achieve polynomial accuracy with probability exponentially close to one due to the Chernoff-Hoeffding bound [VdN11a]. One of our main results, demonstrated in Chap. 4, concerns the complexity separation in calculating $\langle U^\dagger X_{\lfloor n/2 \rfloor} U \rangle$ (i.e. an X observable in the middle of the qubit chain) and $\langle U^\dagger Z_k U \rangle$, for any qubit k. From Eq. (2.77), we see that the former has a number of terms which scales exponentially in the system size, whereas the latter has a constant number of terms. This is reflected

in the fact that the latter has constant operator bond dimension [XS18a], yet the optimal operator bond dimension of the former is likely exponential [SRF+13]. In the next chapter, we utilize a quantum phenomenon known as Anderson localization, introduced in Chap. 3 and further developed in Chap. 4, to show that simulating the former quantity can be achieved with exponential accuracy and similarly exponential confidence in certain systems.

Chapter 3

Out-of-Time-Ordered Correlators

3.1 Introduction

When considering classical chaos in the framework of quantum mechanics, an apparent paradox emerges. Quantum evolution, being inherently reversible, seems ill-equipped to incorporate the exponentially rapid divergence between nearby phase-space trajectories observed in classically chaotic systems. The two descriptions are reconciled when nonlocal, highly entangled, degrees of freedom are incorporated into the description of the classical system. From this perspective, the distinction of "quantum chaotic" can be made for systems for which the local variables quickly mix, or "scramble" into these nonlocally entangled degrees of freedom.

In a series of lectures in 2014 [Kit14, Kit15a], Alexei Kitaev, in examining the role of holography in the famous black hole information paradox [AMPS13], drew an analogy between two seemingly disparate, highly chaotic systems. The first of these is a black hole in anti-de Sitter spacetime, with metric

$$ds^2 = -f(r)dt^2 + \frac{1}{f(r)}dr^2 + rd\Omega^2 \qquad \text{where} \qquad f(r) \equiv \frac{r(r-a)}{R^2}, \tag{3.1}$$

for scale parameters R and a. The second is the so-called Sachdev-Ye-Kitaev (SYK)

model, with Hamiltonian

$$H_{\text{SYK}} = \frac{1}{4 \cdot 4!} \sum_{j,k,l,m=1}^{N} \mathcal{J}_{jklm} c_j c_k c_l c_m. \tag{3.2}$$

Here, the $\{c_j\}$ are Majorana fermions, as defined in Chapter 2. The quartic interactions between fermion modes in this Hamiltonian are defined on an all-to-all hypergraph, with interaction strengths randomly drawn from an ensemble such that

$$\begin{cases} \overline{\mathcal{J}_{jklm}} = 0 & \forall j,\ k,\ l,\ m \\ \frac{1}{3!} \sum_{k,l,m} \overline{\mathcal{J}_{jklm}^2} = 0 & \forall j \end{cases}. \tag{3.3}$$

Like black holes, which are believed to be the fastest scramblers in nature [SS14], the SYK model has been found to demonstrate quantum chaotic evolution and holographic behavior in the limit of many spins $N \gg 1$ and strong coupling $\beta\mathcal{J} \gg 1$, where β is the inverse temperature of an ambient thermal bath to which the system is weakly-coupled. The fast-scrambling behavior manifests as an early-time, exponential divergence in the value of a particular four-point correlator between observables taken at distinct times 0 and t

$$\langle D(t)C(0)B(t)A(0)\rangle_\beta - \langle C(0)A(0)\rangle_\beta \langle D(t)B(t)\rangle_\beta \sim \frac{1}{N} e^{\kappa t} \tag{3.4}$$

where $\kappa = \frac{2\pi}{\beta}$ is analogous to the Lyapunov exponent in classically chaotic systems. This quantity is known as the out-of-time-ordered correlator (OTO correlator), and Eq. (3.4) is referred to as the "quantum butterfly effect." This behavior is expected to persist until $\kappa t \sim O(1)$, after which quantum corrections become relevant [CDP17]. After a longer timescale $t_{\text{scr}} \sim \kappa^{-1} \ln N$, known as the scrambling time, this quantity once again decays to zero. It was conjectured that κ^{-1} can in fact be no greater than $\frac{2\pi}{\beta}$ in Ref. [MSS16], and it was shown how this exponent increases from zero

to its limiting value in Ref. [CZZ17] as the coupling strength to the thermal bath is increased.

Since its re-introduction, the OTO correlator has found wide application in contexts beyond chaotic systems, and in-particular, it has been useful in characterizing the absence of thermalization, known as Anderson and many-body localization in quantum many-body spin systems. Localization is a uniquely quantum phenomenon, whereby destructive interference between wavepackets scattering in a disordered potential confines an initially localized disturbance to a bounded region near its initial position for all time. As such, these systems display behavior at the opposite extreme to chaos, and thus fail to thermalize. This is the regime we will consider for the remainder of this thesis. In the coming sections, we will try to build some intuition for how this quantity captures quantum chaotic behavior by showing its relation to other, more conventional measures of chaos. In the final section, we will show how this quantity has been used to demonstrate localizing behavior, thereby laying the foundation for our coming results in the next chapters.

3.2 Formalism

3.2.1 Definitions

For our purposes, we will restrict to defining the infinite-temperature OTO correlator between Hermitian observables A and B after some unitary evolution U for a time t as

$$\mathcal{F}_{AB}(t) \equiv d^{-1} \operatorname{tr}\{AB(t)AB(t)\} \tag{3.5}$$

where d is the dimension of the Hilbert space and $B(t) = U^\dagger BU$. It is clear that this quantity is related to the four-point correlator defined in Eq. (3.4) by taking the special case where $D(t) = B(t)$ and $C(0) = A(0)$ and the expectation value is taken

with respect to the infinite-temperature Gibbs state, or maximally mixed state $\frac{I}{d}$.

This quantity is related to the so-called infinite-temperature out-of-time-ordered *commutator*, which we define as

$$\mathcal{C}_{AB}(t) \equiv \frac{1}{2\sqrt{d}} ||[A, B(t)]||_F \equiv \frac{1}{2\sqrt{d}} \operatorname{tr}\{[A, B(t)]^\dagger [A, B(t)]\}^{1/2}, \tag{3.6}$$

where $||\cdot||_F$ is the Frobenius norm. It is straightforward to verify that, when A and B are also unitary observables (i.e. $A^2 = B^2 = I$, such as in the case of n-qubit Pauli observables), then we have

$$\mathcal{C}_{AB}(t)^2 = \frac{1}{2}[1 - \mathcal{F}_{AB}(t)] \tag{3.7}$$

We have chosen our normalizations such that $\mathcal{C}_{AB}(t) \in [0, 1]$ and $\mathcal{F}_{AB}(t) \in [-1, 1]$. In general, when a unique Hamiltonian H is naturally defined, a dependence on nonzero inverse temperature β can be included, as

$$\mathcal{F}_{AB}(t, \beta) \equiv Z^{-1} \operatorname{tr}\{e^{-\beta H} AB(t)AB(t)\}, \tag{3.8}$$

where $Z \equiv \operatorname{tr}\left(e^{-\beta H}\right)$ is the partition function at inverse-temperature β. In our main results, we will generally consider time-dependent Hamiltonians, and so it is more natural for us to restrict to the infinite-temperature case. We will discuss several results at finite-temperature in this section, however. When discussing infinite-temperature quantities, we will generally drop the dependence on β for notational convenience, and only refer to β when we wish to draw attention to finite-temperature dependence.

3.2.2 Covariant Behavior under Unitary Transformation

Returning to the infinite-temperature case, we see that Eq. (3.6) can be related to the following matrix

$$(\varrho_B(t))_{jk} = \frac{1}{4d} \operatorname{tr}\left\{[P_j^\dagger, B(t)^\dagger][B(t), P_k]\right\} \tag{3.9}$$

where $\{P_j\}_j$ is a complete basis of operators for the Hilbert space (such as the basis of d-dimensional Pauli matrices). We see $\mathcal{C}_{AB}(t)^2 = (\varrho_B(t))_{AA}$, and letting

$$UP_jU^\dagger = \sum_k \mathcal{U}_{kj} P_k, \tag{3.10}$$

for unitary evolution U we furthermore see that ϱ_B transforms covariantly under such evolution on B, as

$$\begin{aligned}
(\varrho_B(t))_{jk} &= \frac{1}{4d} \operatorname{tr}\left\{\left[P_j^\dagger, \left(U^\dagger B^\dagger U\right)\right]\left[\left(U^\dagger B U\right), P_k\right]\right\} && (3.11)\\
&= \frac{1}{4d} \operatorname{tr}\left\{\left[UP_j^\dagger U^\dagger, B\right]\left[B, UP_kU^\dagger\right]\right\} && (3.12)\\
&= \frac{1}{4d} \sum_{m,n} \mathcal{U}_{mj}^* \mathcal{U}_{nk} \operatorname{tr}\left\{\left[UP_m^\dagger U^\dagger, B\right]\left[B, UP_n^\dagger U^\dagger\right]\right\} && (3.13)\\
(\varrho_B(t))_{jk} &= \left(\mathcal{U}^\dagger \varrho_B(0) \mathcal{U}\right)_{jk} && (3.14)
\end{aligned}$$

This clearly implies that ϱ_B is trace-normalized. Taking the $\{P_j\}_j$ to be the d-dimensional Pauli matrices, we have

$$\begin{aligned}
\operatorname{tr}\left[\varrho_B(t)\right] &= \frac{1}{4d} \sum_j \operatorname{tr}\left\{\left[P_j^\dagger, B(t)^\dagger\right]\left[B(t), P_j\right]\right\} && (3.15)\\
&= \frac{1}{2d} \sum_j \left(\operatorname{tr}\left[B(t)^\dagger B(t)\right] - \operatorname{Re}\left\{\operatorname{tr}\left[B(t)^\dagger P_j^\dagger B(t) P_j\right]\right\}\right) && (3.16)
\end{aligned}$$

$$= \frac{1}{2d}\left\{d^2||B(t)||_F - d|\operatorname{tr}\left[B(t)\right]|^2\right\} \tag{3.17}$$

$$\operatorname{tr}\left[\varrho_B(t)\right] = \frac{1}{2d}\left\{d^2||B||_F - d|\operatorname{tr}\left(B\right)|^2\right\}, \tag{3.18}$$

where, from Eq. (3.15) to Eq. (3.16), we expanded the commutators and used unitarity of the Pauli matrices $P_j^\dagger P_j = I$. From Eq. (3.16) to Eq. (3.17), we used the identity

$$\frac{1}{d}\sum_j \left(P_j^\dagger\right)_{mn}\left(P_j\right)_{pq} = \delta_{mq}\delta_{np} \tag{3.19}$$

for the d-dimensional Pauli operators. We will return to this identity in Section 3.3. Finally, we used unitary invariance to remove the time-dependence from $B(t)$, showing that the trace of ϱ_B is constant in time. We also have that ϱ_B is positive since $\left(\varrho_B(t)\right)_{AA} = \mathcal{C}_{AB}(t)^2 > 0$ for all operators A, as it is the Frobenius norm of the commutator. These three properties—positivity, trace-normalization, and covariant evolution—therefore lead us to expect that $\mathcal{C}_{AB}(t)$ will evolve analogously to the (square root of the) population of a certain basis state in the density matrix under the Schrödinger evolution of global quantum state. This results from our use of the Frobenius norm, which is the 2-norm for a vectorized operator, and we can even tighten the analogy further by choosing B to be the Bloch operator of a density matrix. This lets us see how quantum chaotic evolution "hides" population in the nonlocal degrees of freedom, which make up exponentially many of the other populations in this matrix.

3.2.3 Relation to the Lieb-Robinson Bound

Now let us consider A and B to be initially local operators in a quantum many-body system, such as a spin chain. Here, $\mathcal{C}_{AB}(t)$ can be intuitively understood as the degree to which a "disturbance," B, effects a response in the observable, A, at a time t later. We can apply the bound relating the Frobenius norm to the induced vector 2-norm

$$||A||_F \leq \sqrt{r}||A||_2, \tag{3.20}$$

where

$$||A||_2 \equiv \sup_{|\psi\rangle\neq 0} \frac{||A|\psi\rangle||_2}{|||\psi\rangle||_2} = \lambda_{\max}(A), \tag{3.21}$$

i.e. the maximum singular value of A. Here, r is the rank of A. As $r \leq d$, we have

$$\mathcal{C}_{AB}(t) \leq \frac{1}{2}|||[A, B(t)]||_2 \tag{3.22}$$

The right-hand side is bounded by the conventional Lieb-Robinson bound on quantum lattice systems

$$|||[A, B(t)]||_2 \leq K||A||_2||B||_2 e^{-\eta[d(A,B)-vt]}, \tag{3.23}$$

This inequality states that the degree of noncommutativity between the local observable A and time-evolved observable $B(t) \equiv U^\dagger BU$ initially separated by lattice distance $d(A, B) > 0$, such that $[A, B] = 0$, is exponentially decaying with decay constant $\eta > 0$. It gives an effective speed at which disturbances propagate [LR72, NS06, HK06, NS10].

Despite $\mathcal{C}_{AB}(t)$ only lower bounding the Lieb-Robinson commutator in Eq. (3.22), it is argued that $\mathcal{C}_{AB}(t)$ is a good heuristic for this quantity. In particular, Ref.s [HZC17, FZSZ17a] argue that $\mathcal{C}_{AB}(t)$ can distinguish between propagation in the Anderson localized and the many-body localized phases, in which more stringent bounds than (3.23) are known to hold. In the former, we have the so-called *zero-velocity Lieb-Robinson bound*

$$||[A, B(t)]||_2 \lesssim \min(|t|, 1) e^{-\eta d(A,B)}, \tag{3.24}$$

and in the latter, propagation is confined to within the *logarithmic lightcone*, which is bounded by

$$||[A, B(t)]||_2 \lesssim e^{-\eta[d(A,B) - v \log |t|]}. \tag{3.25}$$

We have neglected the overall normalization prefactors from Eq. (3.23) in these last two bounds. We will discuss the precise physical setting in which the bounds apply in a subsequent section. For now, we consider the relationship between the OTO correlator and more conventional heuristic quantities in the next section, which is often seen through various kinds of averaging.

3.3 Relation to the Frame Potential

It was shown by Roberts and Yoshida in 2016 that OTO correlators can be thought of as a good measure for quantifying the "randomness" of an ensemble of unitary time evolutions [RY17a]. To see this, we first define the Haar measure dU over the group $\mathrm{SU}(d)$ as the unique (up to positive multiplicative constant) measure over the group which is invariant under both left and right translations of the group action

$$\int_{\text{Haar}} d(VU) = \int_{\text{Haar}} d(UV) = \int_{\text{Haar}} dU \equiv 1, \tag{3.26}$$

where we have chosen the normalization to be one in the last equality. We will assess the randomness of ensembles of unitary operators $\mathcal{E} \equiv \{p_j, U_j\}_j$, where p_j is the probability of enacting the unitary U_j, by comparing them to the Haar measure, which can be thought of as completely uniform over the group. This comparison is done through the *frame potential*, given by

$$F_{\mathcal{E}}^{(k)} = \int_{\mathcal{E}} dU \int_{\mathcal{E}} dV |\operatorname{tr}\{U^\dagger V\}|^{2k}, \tag{3.27}$$

where $\int_{\mathcal{E}} dU \equiv 1$ as well. The quantity $F_{\mathcal{E}}^{(k)}$ can be thought of as quantifying the distance to the Haar ensemble at the "kth level" in a way that we will now make precise. Let

$$S = \int_{\mathcal{E}} dU \left(U^{\otimes k}\right)^\dagger \otimes U^{\otimes k} - \int_{\text{Haar}} dU \left(U^{\otimes k}\right)^\dagger \otimes U^{\otimes k} \tag{3.28}$$

be the difference in the kth *moments* between the Haar ensemble and the ensemble $\mathcal{E}$. The Frobenius norm of this operator is given by

$$\begin{aligned}
||S||_F^2 \equiv \operatorname{tr}\left(S^\dagger S\right) &= \operatorname{tr}\left\{\left[\int_{\mathcal{E}} dU U^{\otimes k} \otimes \left(U^{\otimes k}\right)^\dagger - \int_{\text{Haar}} dU U^{\otimes k} \otimes \left(U^{\otimes k}\right)^\dagger\right]\right. \\
&\qquad \left.\times \left[\int_{\mathcal{E}} dU \left(U^{\otimes k}\right)^\dagger \otimes U^{\otimes k} - \int_{\text{Haar}} dU \left(U^{\otimes k}\right)^\dagger \otimes U^{\otimes k}\right]\right\} \qquad (3.29) \\
&= \operatorname{tr}\left[\int_{\mathcal{E}} dU \int_{\mathcal{E}} dV \left(UV^\dagger\right)^{\otimes k} \otimes \left(U^\dagger V\right)^{\otimes k}\right. \\
&\qquad - \int_{\mathcal{E}} dU \int_{\text{Haar}} dV \left(UV^\dagger\right)^{\otimes k} \otimes \left(U^\dagger V\right)^{\otimes k} \\
&\qquad - \int_{\text{Haar}} dU \int_{\mathcal{E}} dV \left(UV^\dagger\right)^{\otimes k} \otimes \left(U^\dagger V\right)^{\otimes k} \\
&\qquad \left. + \int_{\text{Haar}} dU \int_{\text{Haar}} dV \left(UV^\dagger\right)^{\otimes k} \otimes \left(U^\dagger V\right)^{\otimes k}\right] \qquad (3.30) \\
&= \operatorname{tr}\left\{\int_{\mathcal{E}} dU \int_{\mathcal{E}} dV \left(UV^\dagger\right)^{\otimes k} \otimes \left(U^\dagger V\right)^{\otimes k}\right. \\
&\qquad - 2\int_{\mathcal{E}} dU \left[\int_{\text{Haar}} dV \left(V^{\otimes k}\right)^\dagger \otimes V^{\otimes k}\right] \\
&\qquad \left. + \int_{\text{Haar}} dU \left[\int_{\text{Haar}} dV \left(V^{\otimes k}\right)^\dagger \otimes V^{\otimes k}\right]\right\} \qquad (3.31) \\
&= \int_{\mathcal{E}} dU \int_{\mathcal{E}} dV |\operatorname{tr}\left(U^\dagger V\right)|^{2k} - \int_{\text{Haar}} dU \int_{\text{Haar}} dV |\operatorname{tr}\left(U^\dagger V\right)|^{2k} \qquad (3.32) \\
||S||_F &= F_{\mathcal{E}}^{(k)} - F_{\text{Haar}}^{(k)} \qquad (3.33)
\end{aligned}$$

That is, the distance between moments of these ensembles (in Frobenius norm) is the difference between frame potentials. From Eq. (3.30) to Eq. (3.31), we used the translation-invariance of the Haar measure to perform the change-of-variables $UV^\dagger \to V$ for all $U \in \mathcal{E}$ in the double-integrals over $\mathcal{E}$ and the Haar ensemble (the variable-labels U and V are switched in the second of these), and then collected terms by switching the ordering of one of the pairs of integrals. From Eq. (3.31) to Eq. (3.32), we used the fact that $\int_{\mathcal{E}} dU = \int_{\text{Haar}} dU = 1$ to identify the last two terms in Eq. (3.31) as being equal and used the fact that $\text{tr}\left[\left(U^\dagger\right)^{\otimes k} \otimes U^{\otimes k}\right] = |\,\text{tr}\,(U)\,|^{2k}$. Finally, we recognized the terms in Eq. (3.32) as frame potentials to arrive at Eq. (3.33).

$||S||_F$ is zero if and only if the kth moments of $\mathcal{E}$ and the Haar ensemble are equal by the definition of S, and we see from Eq. (3.33) that this is true if and only if the frame potentials of the two ensembles are equal. Since only the difference between frame potentials appears on the right-hand-side of Eq. (3.33), and yet knowing that the left-hand-side must be positive, we see that $F_{\mathcal{E}}^{(k)}$ is actually *minimized* at the value of $F_{\text{Haar}}^{(k)}$. It known that $F_{\text{Haar}}^{(k)} = k!$.

Ensembles $\mathcal{E}$ with the property that their kth moments are equal to that of the Haar ensemble are known as *k-designs*. k-designs have the property that

$$\int_{\mathcal{E}} dU \left(U^{\otimes k}\right)^\dagger \rho U^{\otimes k} = \int_{\text{Haar}} dU \left(U^{\otimes k}\right)^\dagger \rho U^{\otimes k}, \tag{3.34}$$

for all $\rho \in \mathcal{H}^{\otimes k}$ in the k-fold tensor product Hilbert space. Defining

$$\Phi_{\mathcal{E}}^{(k)}(\rho) = \int_{\mathcal{E}} dU \left(U^{\otimes k}\right)^\dagger \rho U^{\otimes k}, \tag{3.35}$$

as the k-fold $\mathcal{E}$-channel, we see that Eq. (3.34) is the statement that

$$\Phi_{\mathcal{E}}^{(k)} = \Phi_{\text{Haar}}^{(k)}, \tag{3.36}$$

or, put another way, a k-design is such that averaging any polynomial in k elements of U and k elements of $U^\dagger$ over the design gives the Haar average. A k-design is automatically a $(k-1)$-design, since we can choose $\rho \equiv \sigma \otimes I$ in Eq. (3.34), for any $\sigma \in \mathcal{H}^{\otimes(k-1)}$, and trace over the identity on both sides to obtain the property satisfied by a $(k-1)$-design.

Eq. (3.19) is actually the statement that the Pauli operators form a 1-design up to normalization. To see this, first note that

$$\int_{\text{Haar}} dU U^\dagger \rho U = \frac{1}{d} \operatorname{tr}(\rho) I \tag{3.37}$$

since

$$\rho = \frac{1}{d} \sum_j P_j \operatorname{tr}\{P_j^\dagger A\}, \tag{3.38}$$

by the property that the Pauli operators form a basis, and thus

$$\int_{\text{Haar}} dU U^\dagger \rho U = \frac{1}{d} \sum_j \operatorname{tr}\{P_j^\dagger \rho\} \int_{\text{Haar}} dU U^\dagger P_j U. \tag{3.39}$$

Therefore, it suffices to show that this integral is zero unless P_j is the identity. To do this, we make use of the d-dimensional Pauli algebra, which is generated by operators X and Z, for which

$$ZX = \omega XZ, \tag{3.40}$$

where $\omega = e^{\frac{2\pi i}{d}}$. Letting $P_j \equiv X^{a_j} Z^{b_j}$ for a_j, $b_j \in \mathbb{Z}_d$ (as $X^d = Z^d = I$), we make the change-of-variables $U \to X^m Z^n U$, which will not change the value of the integral by the Haar property, Eq. (3.26), as

$$\int_{\text{Haar}} dU U^\dagger P_j U = \int_{\text{Haar}} dU \left(X^m Z^n U\right)^\dagger X^{a_j} Z^{b_j} \left(X^m Z^n U\right) \tag{3.41}$$

$$= \int_{\text{Haar}} dU U^\dagger \left(Z^{n\dagger} X^{a_j} Z^n\right) \left(X^{m\dagger} Z^{b_j} X^m\right) U \tag{3.42}$$

$$= \omega^{na_j + mb_j} \int_{\text{Haar}} dU U^\dagger X^{a_j} Z^{b_j} U \tag{3.43}$$

$$\int_{\text{Haar}} dU U^\dagger P_j U = \omega^{na_j + mb_j} \int_{\text{Haar}} dU U^\dagger P_j U \tag{3.44}$$

We can average this last line over all m and $n \in \mathbb{Z}_d$, using

$$\begin{cases} \frac{1}{d} \sum_{n=1}^{d} \omega^{na_j} = \delta_{a_j,0} \\ \frac{1}{d} \sum_{m=1}^{d} \omega^{mb_j} = \delta_{b_j,0} \end{cases} \tag{3.45}$$

to obtain

$$\int_{\text{Haar}} dU U^\dagger P_j U = \delta_{a_j,0} \delta_{b_j,0} \int_{\text{Haar}} dU U^\dagger P_j U. \tag{3.46}$$

Therefore, this integral will only be nonzero if $P_j = I$, which, from Eq. (3.38), proves the identity Eq. (3.37). Next, we show that Eq. (3.19) implies that Pauli operators satisfy the 1-design property, as

$$\frac{1}{d^2} \sum_j \left(P_j^\dagger \rho P_j\right)_{mq} = \frac{1}{d^2} \sum_{j,n,p} \left(P_j^\dagger\right)_{mn} \rho_{np} \left(P_j\right)_{pq} \tag{3.47}$$

$$= \frac{1}{d} \sum_{n,p} \delta_{mq} \delta_{np} \rho_{np} \tag{3.48}$$

$$\frac{1}{d^2} \sum_j \left(P_j^\dagger \rho P_j\right)_{mq} = \frac{1}{d} \operatorname{tr}(\rho) \delta_{mq} \tag{3.49}$$

Thus,

$$\frac{1}{d^2}\sum_j \left(P_j^\dagger \rho P_j\right)_{mq} = \frac{1}{d}\,\mathrm{tr}\,(\rho)\, I \tag{3.50}$$

as desired.

With this formalism in-hand, we are ready to see how the frame potential is related to the OTO correlator. In Ref. [RY17a], it was shown that

$$\frac{1}{d^{4k+2}}\sum_{\{A_i,B_i|i\in\{1,\ldots,k\}\}} |\int_{\mathcal{E}} dU\,\mathrm{tr}\left[A_1\left(U^\dagger B_1 U\right)\ldots A_k\left(U^\dagger B_k U\right)\right]|^2 = \frac{1}{d^{2(k+1)}}F_{\mathcal{E}}^{(k)} \tag{3.51}$$

where the sum over each A_i and B_i is taken over all Pauli operators. The left-hand-side is an average over quantities like the four-point-correlator in Eq. (3.4). This theorem is therefore the statement that, as the ensemble approaches a k-design, the OTO correlator is decreased on-average. The proof simply follows from the 1-design property of Pauli operators, Eq. (3.50). We begin by expanding the left-hand-side of Eq. (3.51) as

$$\begin{aligned}
&\frac{1}{d^{4k+2}}\sum_{\{A_i,B_i|i\in\{1,\ldots,k\}\}} |\int_{\mathcal{E}} dU\,\mathrm{tr}\left[A_1\left(U^\dagger B_1 U\right)\ldots A_k\left(U^\dagger B_k U\right)\right]|^2 \\
&\quad= \frac{1}{d^{4k+2}}\sum_{\{A_i,B_i|i\in\{1,\ldots,k\}\}}\int_{\mathcal{E}} dU\int_{\mathcal{E}} dV\,\mathrm{tr}\left[\left(V^\dagger B_k^\dagger V\right)A_k^\dagger\ldots\left(V^\dagger B_1^\dagger V\right)A_1^\dagger\right] \\
&\qquad\times\mathrm{tr}\left[A_1\left(U^\dagger B_1 U\right)\ldots A_k\left(U^\dagger B_k U\right)\right] \qquad (3.52)\\
&\quad= \frac{1}{d^{4k+2}}\sum_{\{A_i,B_i|i\in\{1,\ldots,k\}\}}\sum_{m,n}\int_{\mathcal{E}} dU\int_{\mathcal{E}} dV\,\langle m|\left(V^\dagger B_k^\dagger V\right)A_k^\dagger\ldots\left(V^\dagger B_1^\dagger V\right)A_1^\dagger|m\rangle \\
&\qquad\times\langle n|A_1\left(U^\dagger B_1 U\right)\ldots A_k\left(U^\dagger B_k U\right)|n\rangle \qquad (3.53)
\end{aligned}$$

We next apply Eq. (3.50) to this expression iteratively, as

$$\frac{1}{d^2}\sum_{A_1} A_1^\dagger |m\rangle\langle n| A_1 = \frac{1}{d}\,\mathrm{tr}\left(|m\rangle\langle n|\right) I = \frac{1}{d}\delta_{mn} I \tag{3.54}$$

$$\frac{1}{d^2}\sum_{B_1} B_1^\dagger V U^\dagger B_1 = \frac{1}{d}\,\mathrm{tr}\left(VU^\dagger\right) I \tag{3.55}$$

$$\frac{1}{d^2}\sum_{A_2} A_2^\dagger V^\dagger U A_2 = \frac{1}{d}\,\mathrm{tr}\left(V^\dagger U\right) I \tag{3.56}$$

$$\vdots$$

With each application of Eq. (3.50), we replace the sum by the scalar shown above times the identity, allowing us to apply Eq. (3.50) for the next iteration. Each sum over A_i for $i \geq 2$ contributes a factor of $\mathrm{tr}\left(V^\dagger U\right)$, and each sum of B_i for $i \geq 1$ contributes a factor of $\mathrm{tr}\left(VU^\dagger\right)$. The final factor of $\mathrm{tr}\left(V^\dagger U\right)$ comes from taking

$$\sum_{m,n}\langle m|V^\dagger U|n\rangle\delta_{mn} = \mathrm{tr}\left(V^\dagger U\right) \tag{3.57}$$

where the Kronecker delta came from Eq. (3.54). Keeping track of factors of d (we replaced $d^{-2} \to d^{-1}$, $2k$ times), we have

$$\begin{aligned}
&\frac{1}{d^{4k+2}}\sum_{\{A_i,B_i|i\in\{1,\ldots,k\}\}} \left|\int_{\mathcal{E}} dU\,\mathrm{tr}\left[A_1\left(U^\dagger B_1 U\right)\ldots A_k\left(U^\dagger B_k U\right)\right]\right|^2 \\
&= \frac{1}{d^{2k+2}}\int_{\mathcal{E}} dU \int_{\mathcal{E}} dV\,\mathrm{tr}\left(VU^\dagger\right)^k \mathrm{tr}\left(V^\dagger U\right)^k &(3.58)\\
&= \frac{1}{d^{2(k+1)}}\int_{\mathcal{E}} dU \int_{\mathcal{E}} dV \left|\,\mathrm{tr}\left(U^\dagger V\right)\right|^{2k} &(3.59)\\
&= \frac{1}{d^{2(k+1)}} F_{\mathcal{E}}^{(k)} &(3.60)
\end{aligned}$$

Lastly, we simply summarize a result of Ref. [RY17a], which may of be relevance to quantum information, and deals with the complexity of a quantum circuit ensemble. We define a member of such an ensemble as an n-qubit quantum circuit whose gates are drawn randomly from a finite gate set $\mathcal{G}$ of g possible 2-qubit gates. The theorem

states that the minimum number of such gates that need to be chosen, called the circuit complexity $\mathcal{K}(\mathcal{E})$, to generate a given ensemble $\mathcal{E}$ with kth frame potential $F_{\mathcal{E}}^{(k)}$ is lower-bounded, as

$$\mathcal{K}(\mathcal{E}) \geq \frac{2kn\log(2) - \log F_{\mathcal{E}}^{(k)}}{\log(\text{choices})}, \tag{3.61}$$

where "choices" is the number of choices that can be made at each step (which of g gates to apply as well as where to apply it). Note that changing the base of the logarithm in this equation will not change the bound, since common conversion factors will cancel. This bound shows that, as the ensemble becomes closer to Haar random (decreasing $F_{\mathcal{E}}^{(k)}$), the complexity required to generate it increases. It follows from a counting argument in a simple lower bound on $F_{\mathcal{E}}^{(k)}$ (for details, see Ref [RY17a]). We continue to the next section by connecting the OTO correlator to a more information-theoretic quantity, the Rényi entropy.

3.4 Relation to the Rényi Entropy

The α-Rényi entanglement entropy across a partition $\mathcal{H} = \mathcal{H}_A \otimes \mathcal{H}_B$ into subsystems A and B for a state ρ is defined as

$$S_A^{(\alpha)} \equiv \frac{1}{1-\alpha}\log \operatorname{tr}\left(\rho_A^{\alpha}\right), \tag{3.62}$$

where $\rho_A \equiv \operatorname{tr}_B(\rho)$. This quantity reduces to the conventional von Neumann entanglement entropy as $\alpha \to 1$, as

$$\lim_{\alpha\to 1} S_A^{(\alpha)} = \lim_{\alpha\to 1}\frac{1}{1-\alpha}\log\left(\sum_{\{j|p_j\neq 0\}} p_j^{\alpha}\right) \tag{3.63}$$

$$= -\lim_{\alpha\to 1}\left(\sum_{\{j|p_j\neq 0\}} p_j^\alpha\right)^{-1}\left(\sum_{\{j|p_j\neq 0\}} p_j^\alpha \log p_j\right) \tag{3.64}$$

$$= -\sum_{\{j|p_j\neq 0\}} p_j \log p_j \tag{3.65}$$

$$\lim_{\alpha\to 1} S_A^{(\alpha)} = -\operatorname{tr}\left(\rho_A \log \rho_A\right) \equiv S_A^{(\mathrm{vn})}. \tag{3.66}$$

Here, p_j, for which $\sum_j p_j = 1$, are the eigenvalues of ρ_A, and we used the basis-invariance of $S_A^{(\alpha)}$ in Eq. (3.63). From Eq. (3.64) to Eq. (3.65), we used L'Hôpital's rule with numerator $\log\left(\sum_{\{j|p_j\neq 0\}} p_j^\alpha\right)$ and denominator $1-\alpha$ to evaluate the limit. In Eq. (3.65), we again used basis-invariance to recognize the quantity on the right-hand-side as the von Neumann entropy. From Eq. (3.63), we see that for pure states, for which $p_j = 1$ for some j and $p_j = 0$ otherwise, $S_A^{(\alpha)} = 0$, as we would like. For maximally mixed states, for which $p_j = \frac{1}{d}$ for all j, we have $S_A^{(\alpha)} = \log d$ as we would expect. For $\alpha > 1$, $S_A^{(\alpha)}$ is otherwise monotonically decreasing in α for fixed ρ_A neither pure nor maximally mixed.

We can apply the 1-design property, Eq. (3.19), locally, as the authors in [FZSZ17b] did, to connect our form of the OTO correlator, $\mathcal{F}(t)$, as defined in Eq. (3.8) for $\beta = 0$, to the second Rényi entanglement entropy at time t of an initial Gibbs state locally quenched by an observable O, as

$$\exp\left(-S_A^{(2)}\right) = \frac{1}{d_B}\sum_B \operatorname{tr}\left[B(t)^\dagger\left(OO^\dagger\right)B(t)\left(OO^\dagger\right)\right], \tag{3.67}$$

where the sum is taken over all Pauli observables on subsystem B. Here, the system is taken to be initially maximally mixed prior to the quench $\rho = \frac{I}{d}$. After the quench, the system is in the state $OO^\dagger$ (with normalization such that $\operatorname{tr}\left(OO^\dagger\right) = 1$), from which it is evolved by the unitary dynamics U for a time t. This gives

$$\frac{1}{d_B}\sum_B \operatorname{tr}\left[B(t)^\dagger\left(OO^\dagger\right)B(t)\left(OO^\dagger\right)\right]$$

$$= \frac{1}{d_B} \sum_B \mathrm{tr}\left[\left(U^\dagger B^\dagger U\right)\left(OO^\dagger\right)\left(U^\dagger B U\right)\left(OO^\dagger\right)\right] \tag{3.68}$$

$$= \frac{1}{d_B} \sum_B \mathrm{tr}\left\{U^\dagger\left[\mathrm{tr}_B\left(UOO^\dagger U^\dagger\right)\otimes I_B\right] U\left(OO^\dagger\right)\right] \tag{3.69}$$

$$= \mathrm{tr}\left\{\mathrm{tr}_B\left[U\left(OO^\dagger\right)U^\dagger\right]^2\right\} \tag{3.70}$$

$$\frac{1}{d_B}\sum_B \mathrm{tr}\left[B(t)^\dagger\left(OO^\dagger\right)B(t)\left(OO^\dagger\right)\right] = \exp\left(-S_A^{(2)}\right) \tag{3.71}$$

Letting $\rho_O \equiv OO^\dagger$, this can similarly be generalized to arbitrary $\alpha \geq 2 \in \mathbb{Z}$, as

$$\begin{aligned}
&\frac{1}{d_B^{\alpha-1}} \sum_{\{B_i | i\in\{1,\ldots,\alpha-1\}\}} \mathrm{tr}\left[B_1(t)\rho_O B_2(t)\rho_O \ldots B_{\alpha-1}(t)\rho_O U^\dagger\left(\prod_{j=1}^{\alpha-1} B_j\right)^\dagger U\rho_O\right] \\
&= \frac{1}{d_B^{\alpha-2}} \sum_{\{B_i | i\in\{1,\ldots,\alpha-2\}\}} \mathrm{tr}\left\{\left[\mathrm{tr}\left(U\rho_O U^\dagger\right)\otimes I_B\right] U\rho_O B_2(t)\rho_O\ldots B_{\alpha-1}(t)\right. \\
&\qquad \left.\times\rho_O U^\dagger\left(\prod_{j=1}^{\alpha-2} B_j\right)^\dagger\right\} \qquad (3.72) \\
&= \mathrm{tr}\left\{\left[\mathrm{tr}\left(U\rho_O U^\dagger\right)\otimes I_B\right]^{\alpha-1}\left(U\rho_O U^\dagger\right)\right\} \qquad (3.73) \\
&= \mathrm{tr}\left[\mathrm{tr}_B\left(U\rho_O U^\dagger\right)^\alpha\right] \qquad (3.74) \\
&= \exp\left[(1-\alpha)S_A^{(\alpha)}\right] \qquad (3.75)
\end{aligned}$$

Clearly, this reduces to Eq. (3.67) for $\alpha = 2$. Here, the product over $\{B_j\}$ is taken in ascending order in j, so that the Hermitian conjugate of this product has $B_1^\dagger$ as its final factor, and this product over $\{B_j^\dagger\}$ is taken in descending order. Finally, this formula may be generalized to the finite temperature β^{-1} case by taking $\rho_O = Z^{-1}Oe^{-\beta H}O^\dagger$ for some naturally-defined Hamiltonian H and partition function $Z \equiv \mathrm{tr}\left(e^{-\beta H}\right)$.

The OTOC can also be linked to the entanglement entropy of operators, as in [HQRY16, XS18a]. Here, it is common to consider the *thermofield double state* with inverse-temperature β on two copies of the system with energy eigenstates $\{|n\rangle\}$, as

$$|\Phi\rangle = Z^{-1/2} \sum_n e^{-\beta E_n/2} |n, n\rangle \tag{3.76}$$

Applying unitary time-evolution U to one of these two copies (say, the first) gives

$$U_1|\Phi\rangle = Z^{-1/2} \sum_{m,n} e^{-\beta E_n/2} u_{mn} |m, n\rangle \tag{3.77}$$

where $u_{mn} \equiv \langle m|U|n\rangle$. Contracting U on the thermofield double therefore corresponds to an application of the Choi-Jamilkowski isomorphism, which maps an operator to a state in a basis-dependent way for which the preferred basis is set as the energy eigenstates of a particular Hamiltonian, with an additional weight given by the Gibbs factor (though this is $d^{-1/2}$ for $\beta = 0$). If $U = e^{-iHt}$ for the same Hamiltonian as in the thermofield double, then we have

$$U_1|\Phi\rangle = Z^{-1/2} \sum_{n,n} e^{-\beta E_n/2} e^{-iE_n t} |n, n\rangle \tag{3.78}$$

The operator entanglement of, say, $X(t)$ at a time t is thus the entanglement of the state $X_1(t)|\Phi\rangle$ across a partition into subsystems A_1A_2 and B_1B_2 (e.g. the input and output degrees of freedom for one half of a qubit chain). In Ref. [HQRY16], a similar result to Eq. (3.67) was shown, as

$$\exp\left(-S^{(2)}_{A_1A_2}\right) = \frac{1}{4^n} \sum_{A,B} \frac{1}{2^n} \operatorname{tr}\left[AX(t)^\dagger BX(t)AX(t)^\dagger BX(t)\right] \tag{3.79}$$

where, again, the sum is over all Pauli strings in regions A and B of an n-qubit spin chain. The authors of Ref. [XS18a] utilize this to prove the bound

$$S^{(2)}_{B_1B_2} \leq -\log\left(1 - \frac{1}{2} \sum_{r \in B, P_r} ||[X(t), P_r]||^2\right) \tag{3.80}$$

where the sum is over all sites r in region B and all single-site Pauli operators at the r. Though a small second Rényi entropy does not immediately guarantee a good matrix product operator approximation to $X(t)$, the authors argue that it should serve as a good heuristic to bound the bond dimension of such an approximation in physical systems of interest. In the next section, we will examine some investigations into this assumption in the context of Anderson and many-body localized systems. This will provide a segue into our next chapter, where we will demonstrate our first main result.

3.5 Localizing Systems

Localization is the quantum phenomenon whereby destructive interference between wavepackets propagating in a disordered potential confines a particle to its initial position for all time. Localizing systems therefore exhibit behavior at the opposite extreme to that of chaotic systems. To provide a concrete example, consider the disordered Heisenberg model on a 1-d lattice of n qubits

$$H = \sum_{j=1}^{n-1} \left(X_j X_{j+1} + Y_j Y_{j+1}\right) + \sum_{j=1}^{n} \nu_j Z_j + J \sum_{j=1}^{n-1} Z_j Z_{j+1} \tag{3.81}$$

$$\begin{aligned} H = &\sum_{j=1}^{n-1} \left(-ic_{2j}c_{2j+1} + ic_{2j-1}c_{2(j+1)}\right) - i \sum_{j=1}^{n} \nu_j c_{2j-1}c_{2j} \\ &- J \sum_{j=1}^{n-1} c_{2j-1}c_{2j}c_{2j+1}c_{2(j+1)} \end{aligned} \tag{3.82}$$

where the ν_j are drawn randomly from a uniform distribution $[-\nu, \nu]$, where ν is the disorder strength. Eq. (3.82) is the Jordan-Wigner transform of this model. It is well-known that for $J = 0$ and any nonzero value of the disorder strength ν, this system exhibits Anderson-localized behavior. This implies that we have the so-called *zero-velocity* Lieb-Robinson bound Eq. (3.24). We will elaborate on this bound in the next chapter. Additionally, even for nonzero J and disorder strength below a critical

value ν_c, the system is *many-body localized*. In this phase, propagation is limited to the logarithmic lightcone, and Eq. (3.25) holds.

In general, many-body localized systems admit a phenomenological description in terms of local, commuting integrals of motion $\{\tau_j^z\}$, conventionally called, "l-bits" [SPacA13, HNO14]

$$H = \sum_i \xi_i \tau_i^z + \sum_{ij} V_{ij} \tau_i^z \tau_j^z + \sum_{ijk} V_{ijk} \tau_i^z \tau_j^z \tau_k^z + \dots . \tag{3.83}$$

The "l-bits" τ^z can be thought of as locally dressed Pauli-z operators, which all commute ($[\tau_i^z, \tau_j^z] = 0$ for all i, j). The coupling coefficients $\{\xi_i\}$, $\{V_{ij}\}$, $\{V_{ijk}\}$ decay exponentially as the distance between the spins i, j, k increase. From the Majorana description of the system, Eq. (3.82), it is clear that when $J = 0$, we cannot have higher order terms than quadratic in the Majorana modes, so the $\{V_{ij}\}$, $\{V_{ijk}\}$ vanish here, and we are left with a set of decoupled, locally dressed spins. In either the many-body-localized or Anderson-localized phases, the Hamiltonian can be fully diagonalized in the mutual eigenbasis of the $\{\tau_j^z\}$. Thus, in Ref. [FZSZ17b], it is shown that the infinite-temperature OTOC is given by

$$\mathcal{F}_{ij}(t) = \frac{1}{2^n} \sum_k \langle k | \tau_i^x(t) \tau_j^x \tau_i(t) \tau_j | k \rangle \tag{3.84}$$

$$\mathcal{F}_{ij}(t) = \cos\left(4 V_{ij} t\right) \tag{3.85}$$

Letting

$$V_{ij} = \tilde{V}_{ij} e^{-\eta |i-j|}, \tag{3.86}$$

where the $\tilde{V}_{ij}$ are uniformly distributed in $[-V, V]$, and η is the localization length, the disorder average over $\tilde{V}_{ij}$ gives

	Rényi Entropy	Lightcone envelope
Thermal	Linear increase	Linear
Diffusive	Sub-linear	Sub-linear
MBL	Logarithmic increase	Logarithmic
AL	Constant	Constant

Table 3.1: Classification of dynamical-phase behavior by the Rényi Entropy and lightcone envelope behavior of the OTO Correlator. See Ref. [FZSZ17b], and references therein, for further details.

$$\overline{\mathcal{F}}_{ij}(t) = \frac{\sin\left[4V\exp\left(-\eta|i-j|\right)t\right]}{4V\exp\left(-\eta|i-j|\right)t} \tag{3.87}$$

A similar result was shown in Ref. [Che16]. A key implication of these analytic results is that the OTO correlator $\overline{\mathcal{F}}_{ij}(t)$ for many-body-localized systems decays polynomially, rather than exponentially, as we would expect for chaotic systems. A similar behavior is observed in Ref. [HL17]. The OTO correlator approaches a constant as $V \to 0$ in Eq. (3.87), which demonstrates that the OTOC can distinguish the many-body-localized from the Anderson-localized phase. In fact, in Ref. [HZC17], the authors numerically demonstrate that the OTO correlator can detect the logarithmic light cone to distinguish between these phases, where time-ordered lower-order correlators (i.e. $AB(t)$) cannot, when $J = 1$ in Eq. (3.81) above. In Ref. [FZSZ17b], the authors numerically demonstrate the correctness of Eq. (3.87). Furthermore, they show that the Rényi entropy behaves similarly to the von Neumann entropy in both the Anderson and Many-Body localized phases, justifying the approximation made in Ref. [XS18a]. In Table 3.1, we give a classification summarizing the behavior of the second Rényi entropy and lightcone-envelope behavior of the OTO correlator in different dynamical phases.

In the next chapter, we will provide our first main result: a method for calculating the OTO correlator analytically for observables undergoing matchgate evolution whose direct, strong simulation is not known to be classically efficient. This will allow us to determine when Anderson, and in the following chapter, many-body localization has occurred, even though the direct simulation cannot be performed nominally.

Chapter 4

Classical simulation of quantum circuits by dynamical localization

4.1 Introduction

A peculiar phenomenon exhibited uniquely by quantum lattice systems is the suppression of conductance in the presence of disorder. This effect, known as *Anderson localization* [And58, LBCS10, Abr10, COR$^+$13] in the single-particle setting and *many-body localization* [GMP05, BAA06, OH07, PH10, VA14, BLCR15, BSHMB15] in the interacting-multi-particle regime, is a result of interference, which confines a local disturbance to a bounded region near its initial position for a very long time. As a result, these systems do not act as thermal reservoirs for their own subsystems [Deu91, Pal12, NH15, HNO$^+$13, KBP14], since local subsystems retain information about their initial conditions forever.

An important consequence of the fact that local quantum information does not mix, or scramble, among nonlocal degrees of freedom in localizing systems is that many properties of these systems can be efficiently simulated classically. Such properties include local integrals of motion [KCA14, YQX16], Hamiltonians' eigenbases [BN13, YQX16, FWB$^+$15, Hua15, YPC17, PKCS16], unitary time-evolution operators [BO07,

icvcvPPcv08], and samples from their output distributions [DFT$^+$18]. In light of these many results, we ask the question of whether localization could manifest in time-dependent quantum systems, such as those performing a quantum computation. If this is possible, then it would allow for the efficient simulation of an otherwise apparently complex quantum algorithm by classical means.

However, there are currently very few prior investigations into localization in the time-dependent regime. Initial explorations into fluctuating disorder [BEO09, SD16] and Floquet circuit ensembles [CL15] suggest that a form of localization persists in these time-dependent cases, yet few analytic results are known in general. In this work, we consider the setting of nearest-neighbor matchgate circuits, which are generated by time-dependent spin-1/2 XY Hamiltonians, and can be mapped onto the dynamics of free-fermions with arbitrarily time-dependent single-particle Hamiltonians by the Jordan-Wigner transformation [Kni01, TD02, BK02, Bra06, JM08, dMT13, BC14]. These circuits therefore constitute the natural framework in which to study the generalization of Anderson localization to quantum circuits.

Despite the encoding by free-fermion dynamics, some properties of these circuits are not known to be classically simulatable. The example we consider is the Pauli-expectation value $\langle U^\dagger X_j U\rangle$ on an arbitrary qubit j in the output of a matchgate circuit U from an initial arbitrary product state. Despite being local in the qubit picture, this observable takes the form of a long-range correlation function in the fermion picture and requires exponential resources to simulate by brute-force. We solve this problem for circuits U describing localizing dynamics by exploiting the confinement of their measurement observables in the Heisenberg picture. For time-independent Hamiltonians, this confinement is described formally by the so-called *zero-velocity Lieb-Robinson bound* [HSS12]

$$||[A, B(t)]|| \lesssim \min(|t|, 1) e^{-\eta d(A,B)}. \tag{4.1}$$

This inequality states that the degree of noncommutativity between the local observable A and time-evolved observable $B(t) \equiv U^\dagger B U$ initially separated by lattice

distance $d(A, B) > 0$, such that $[A, B] = 0$, is exponentially decaying with decay constant $\eta > 0$. It gives an effective speed at which disturbances propagate [LR72, NS06, HK06, NS10], which goes to zero with increasing propagation time in localizing systems. Correlations between distant lattice sites take exponential time to develop [BHV06].

In the case where A and B are unitary, and the norm taken is the Frobenius norm $||O||^2 \equiv \mathrm{tr}\left(O^\dagger O\right)$, the left-hand side of (4.1) is related to the infinite-temperature out-of-time-ordered correlation function (OTO correlator, see Chapter 3). Without loss of generality, we will refer to this quantity as the OTO correlator by the relation, Eq. (3.7). This quantity has arisen as a useful diagnostic tool for studying scrambling in chaotic quantum chaotic systems [MSS16, RY17b, AFI16, YH17, CDP17], including black holes [SS14, Kit14, Kit15a, RSS15], and recently, for many-body localization [SC17, Che16, HZC17, HL17, FZSZ17a]. As a first result, we provide an analytic formula for this quantity when A and B are Pauli observables, and the time evolution is described by a matchgate circuit. This is surprising considering that the evolution itself cannot even be stored efficiently by a classical computer in general, and so it constitutes an exponential speedup over the brute-force method. We next show that this quantity bounds the average-case change in expectation-value magnitude from truncating the Heisenberg evolution of $B(t)$ to a subset of qubits and thus provides a measure of the expected error incurred by such truncation. Finally, we provide numerical analysis verifying the bound (4.1) for two natural models of time-dependent disorder and construct phase diagrams demonstrating their transitions to localizing dynamics and subsequent classical simulatability.

4.2 Background

Define a matchgate $G(V, W)$ to be the following 2-qubit unitary, written in the (ordered) computational basis $\{|00\rangle, |01\rangle, |10\rangle, |11\rangle\}$ as

$$G(V,W) = \begin{pmatrix} V_{00} & 0 & 0 & V_{01} \\ 0 & W_{00} & W_{01} & 0 \\ 0 & W_{10} & W_{11} & 0 \\ V_{10} & 0 & 0 & V_{11} \end{pmatrix}, \tag{4.2}$$

where $V, W \in \mathrm{SU}(2)$ are single-qubit unitaries (crucially, $\det V = \det W$). $G(V,W)$ preserves the eigenspaces of $Z \otimes Z$ and so may be written as $e^{i\mathcal{L}}$, where $\mathcal{L}$ is an element of the vector space spanned by $\{X \otimes X, X \otimes Y, Y \otimes X, Y \otimes Y, Z \otimes I, I \otimes Z\}$. When the 2 qubits on which $G(V,W)$ acts are a nearest-neighboring pair, $\mathcal{L}$ is an instance of the 2-qubit spin-1/2 XY model. Such a Hamiltonian on n qubits is quadratic in the $2n$ Majorana operators $\{c_\mu\}$, for $\mu \in \{1, \ldots, 2n\}$, given by the Jordan-Wigner transformation

$$\begin{cases} c_{2j-1} & = \bigotimes_{k=1}^{j-1} Z_k \otimes X_j \\ c_{2j} & = \bigotimes_{k=1}^{j-1} Z_k \otimes Y_j \end{cases} \tag{4.3}$$

where $c_\mu^2 = I$ and $c_\mu c_\nu = -c_\nu c_\mu$ for all $\mu \neq \nu \in \{1, \ldots, 2n\}$. It is straightforward to verify that any such unitaries U generated by quadratics in the Majorana modes form a group (see Chapter 2 for details), and that this group is exactly that of circuits composed of nearest-neighbor matchgates [JM08]. Furthermore, such U preserve the number of Majorana modes, as

$$U^\dagger c_\mu U = \sum_{\nu=1}^{2n} u_{\mu\nu} c_\nu, \tag{4.4}$$

where $\mathbf{u} \in \mathrm{SO}(2n)$ is a $2n \times 2n$ orthogonal matrix. We introduce a *Majorana configuration* as an ordered tuple of indices $\vec{\alpha} \equiv (\alpha_1, \alpha_2, \ldots, \alpha_k)$ of degree $|\vec{\alpha}| \equiv k$ with $\alpha_j \in \{1, \ldots, 2n\}$ and $\alpha_j < \alpha_{j+1}$ for all $j \in \{1, \ldots, k\}$. The corresponding *Majorana configuration operator* is the ordered product $C_{\vec{\alpha}} \equiv \prod_{j=1}^{|\vec{\alpha}|} c_{\alpha_j}$, with Majorana indices

ascending from left to right. Finally, denote by $\mathbf{u}_{\vec{\alpha}\vec{\beta}}$ the submatrix of $\mathbf{u}$ given by taking the rows indexed by $\vec{\alpha}$ and the columns indexed by $\vec{\beta}$, i.e. $(\mathbf{u}_{\vec{\alpha}\vec{\beta}})_{jk} \equiv u_{\alpha_j \beta_k}$.

Majorana configuration operators transform under matchgate evolution as

$$U^\dagger C_{\vec{\alpha}} U = \sum_{\{\vec{\beta} || \vec{\beta}| = |\vec{\alpha}|\}} \det\left(\mathbf{u}_{\vec{\alpha}\vec{\beta}}\right) C_{\vec{\beta}}. \tag{4.5}$$

That is, the degree of a Majorana configuration operator is preserved, and configuration transition amplitudes are given by determinants of the corresponding single-mode transition submatrices. We also note that

$$Z_k = -iC_{(2k-1,2k)} \tag{4.6}$$

$$X_k = (-i)^{k-1} C_{(1,\ldots,2k-1)}. \tag{4.7}$$

From Eq. (4.5), we see that the Heisenberg evolution of Z_k will always consist of $\binom{n}{2}$ terms, regardless of k. However, that of X_k will consist of $\binom{n}{2k-1}$ terms, which may scale exponentially with n if k also scales with n, such as for $X_{\lfloor n/2 \rfloor}$ in the center of the chain. This is reflected in the fact that $\langle U^\dagger Z_k U \rangle$ can always be computed efficiently by a classical computer when the expectation values $\langle C_{\vec{\beta}} \rangle$, for $|\vec{\beta}| = 2$, can be, such as for product input [JM08]. On the other hand, $U^\dagger X_k U$ cannot even be stored efficiently on a classical computer in the worst case, so the same strategy will not work[1]. Nevertheless, localization will provide a means to efficiently approximate this quantity, as we state formally below.

4.3 Analytic results

We are able to efficiently calculate the left-hand side of (4.1) in our setting by our first result

[1] Though the distribution of such a measurement can be sampled efficiently, a weaker form of simulation, by the method in Ref. [Bro16].

Theorem 1 *(Analytic OTO correlator) The OTO correlator for Pauli observables $A \equiv i^a C_{\vec{\eta}}$ and $B \equiv i^b C_{\vec{\alpha}}$ may be computed analytically as*

$$\frac{1}{2^{n+2}}|||[A, U^\dagger B U]|||^2 = \frac{1}{2}\left\{1 \pm \det[\mathbf{u}_{\vec{\alpha}[2n]}(\mathbf{I} - 2\mathbf{P}_{\vec{\eta}})\mathbf{u}^{\mathrm{T}}_{[2n]\vec{\alpha}}]\right\},$$

where $(\mathbf{P}_{\vec{\eta}})_{jk} = 0$ if $j \notin \vec{\eta}$ or $k \notin \vec{\eta}$, and $(\mathbf{P}_{\vec{\eta}})_{jk} = \delta_{jk}$ otherwise (i.e. $\mathbf{P}_{\vec{\eta}}$ is the projector onto the modes $\vec{\eta}$). The sign factor is simply $(-1)^{|\vec{\alpha}||\vec{\eta}|+1}$.

The result follows from the Cauchy-Binet formula (see Appendix A.1). In fact, it is possible to modify the Cauchy-Binet formula to obtain an analytic calculation of the OTO correlator when $A \equiv \boldsymbol{n}_s \cdot \boldsymbol{\sigma}_s$ is any single-site Pauli observable (Appendices A.2 - A.4). This allows us to regard the OTO correlator as a quadratic form $\mathbf{M}_s$, as

$$\frac{1}{2^{n+2}}|||[\mathbf{n}_s \cdot \boldsymbol{\sigma}_s, U^\dagger B U]|||^2 \equiv \mathbf{n}_s^* \cdot \mathbf{M}_s \cdot \mathbf{n}_s \tag{4.8}$$

When the bound (4.1) holds, we can efficiently approximate the evolution in Eq. (4.5) by truncating the sum to those $\vec{\beta}$ whose support lies strictly within a constant subset of qubits. We model this truncation by the action of a completely depolarizing channel

$$\mathcal{E}_s(O) = \frac{1}{4}\left(O + \sum_{k\in\{x,y,z\}} \sigma_s^k O \sigma_s^k\right), \tag{4.9}$$

which takes any single-qubit operator to its identity component. With our second result, we show that this truncation incurs a bounded error in the average case (see Appendix A.5):

Theorem 2 *(Average disturbance by truncation) Let $\mathcal{E}_s$ be the completely depolarizing channel on qubit s. The average change in expectation-value magnitude of $U^\dagger B U$ under depolarization on a set of qubits S is bounded by the OTO correlator as*

$$\overline{|\langle U^\dagger B U\rangle - \langle(\otimes_{s\in S}\mathcal{E}_s)[U^\dagger B U]\rangle|} \leq \sum_{s\in S}\sqrt{\mathbf{n}_s^*\cdot\mathbf{M}_s\cdot\mathbf{n}_s},$$

where $\overline{(\,\cdot\,)}$ *denotes an average over a product basis whose Bloch axes are orthogonal to the vectors* $\{\mathbf{n}_s\}_s$*, and* $\mathbf{M}_s$ *is as defined in Equation 4.8.*

4.4 Numerical example

Theorem 1 is valid for every unitary time-evolution satisfying (4.4). However, we will narrow the focus of our numerical analysis to two specific Hamiltonian models, each of the form:

$$H(t) = \sum_{j=1}^{n-1} 2\mu_j(t)\left(X_jX_{j+1} + Y_jY_{j+1}\right) + \sum_{j=1}^{n} 2\nu_j(t)Z_j \tag{4.10}$$

In Model 1, we allow the local disorder to fluctuate in time about some mean static disorder, and in Model 2, we allow interactions to fluctuate in space and time about mean translationally invariant interactions. The fluctuations are chosen as independent, identically distributed random samples taken from the interval $[-\Delta, \Delta]$ every period $\delta t = 0.25$. We vary the strength of the mean value and the fluctuation strength Δ for each model, keeping the remaining parameter fixed. This is intended to resemble a discrete-time control setup, wherein some of the parameters are constrained but others may be varied with some control strength. The static limit, for which $\Delta = 0$, is well-understood (see e.g. Ref. [BO07]) and will provide a convenient reference point. These models are summarized in Table 4.1.

As the Hamiltonian (4.10) is quadratic in the Majorana operators, its time-evolution operator may be expressed as a matchgate circuit [JM08] and so we may apply our Theorem 1. In Fig. 4.1, we plot representative profiles of the OTO correlator (hereafter referred to as "light cones") for $B = Z_{50}$ (left) and $B = X_{50}$ (right) for

Parent Hamiltonian (4.10) $H(t) = \sum_{j=1}^{n-1} 2\mu_j(t)\left(X_jX_{j+1} + Y_jY_{j+1}\right) + \sum_{j=1}^{n} 2\nu_j(t)Z_j$			
Model	Fluctuation	Fixed	Varying
1	$\nu_j(t) = \nu_j + (2/\delta t)\kappa_j(t)$	$\mu = 1$	ν, Δ
2	$\mu_j(t) = \mu + (2/\delta t)\kappa_j(t)$	$\nu = 1$	μ, Δ

Table 4.1: Summary of the time-dependent models considered in this work, corresponding to the numerical phase diagram shown in Fig. 4.2. $\nu_j \sim [-\nu, \nu]$ are chosen uniformly randomly, and the $\kappa_j(t) \sim [-\Delta, \Delta]$ are uniformly randomly sampled every $\delta t = 0.25$

.

$n = 100$ in Model 1 in its ballistic (top), diffusive (middle), and localized (bottom) phases. In the localized propagation, for which static disorder $\nu = 2$ and $\Delta = 0$, the bound (4.1) is satisfied, and the observable support remains confined. As we increase fluctuations relative to static disorder in the middle plots, for which $\nu = 0.75$ and $\Delta = 1$, we see that time-dependent fluctuations induce a transition to diffusive propagation.

We identify the propagation phase of each profile by taking the principal singular component of its light cone, treated as a numerical matrix (see Appendix A.6). We argue that this gives an operationally meaningful, robust, and numerically inexpensive means of extracting the envelope and decay profile.

We characterize the propagation phase by fitting the principal temporal component of each lightcone to a polynomial and extract the exponent of the leading-order term t^m. In Fig. 4.2, we plot m for Z_{50} and X_{50} for our two models for $n = 100$, as in Fig. 4.1, as phase diagrams. We identify the *ballistic* phase with regions where m is very nearly one, the *localized* phase with regions where m is very nearly zero, and the *diffusive* phase with regions where m is nearly 0.5. With this identification, we see that as $\Delta \to 0$, our results agree with the known limit of static local disorder in Model 1. Similarly, as Δ becomes large, we see the emergence of a diffusive phase, which is consistent with the results put forth in [BEO09]. Finally, we see that, for small $\Delta \neq 0$, the localized phase survives. This indicates the existence of new matchgate

circuits for which localization may be applied to classically simulate $\langle U^\dagger X_k U\rangle$ for arbitrary k in a general product state input.

4.5 Discussion

We have presented examples where localization may be applied as a tool for classically simulating quantum circuits which were a priori believed to be classically intractable. This is achieved by an analytic calculation of the OTO correlator (presented in Appendix A.4), followed by truncation to a subset of qubits for which this quantity falls below a certain threshold.

One advantage of our method is that it gives the *interior* of the light cone in addition to its envelope. In each phase, we see that the light cone interior for X_{50} generally has a higher value than that for Z_{50}. This is a consistent difference between the profiles of these operators, which may have important consequences for the complexity required to exactly simulate their expectation values, in a similar fashion with [RY17b]. We attribute the emergence of a near-ballistic region in the X phase diagram of Model 2, which is absent from the Z diagram, to this observation. Though some amplitude propagates ballistically for both observables in this region, this only manifests as a spreading of the exponential tails for Z. For X however, this is exhibited as a ballistic spreading of the high-amplitude region due to interference between its many constituent Majorana operators. This indicates that, at least in the presence of fluctuating interactions, propagation behavior between different local operators can be strikingly different.

We empirically observe, however, that the difference between X and Z observables only emerges at late times, in the saturation value of the OTO correlator for each of these operators. By examining the constant-position slices from the light cones in Fig. 4.1 as functions of time, we observe a characteristic exponential early-time behavior for these values, which is identical between X and Z propagation. Only as the growth of these operators saturate to roughly their constant values do the differences

emerge. This suggests that the evolution of low-degree Majorana configurations may be useful as a good heuristic to observe the lightcone envelope, in a similar spirit to the treatment given in Ref. [XS18c] for finding a low bond-dimension matrix product operator approximation to the evolution of such observables in interacting-fermion systems.

Although we chose here so-called matchgate circuits, related to the time evolution of free fermions, because of their correspondence to Anderson localization, our method is expected to have further applications and extensions. On the former, for example, one may apply it to other random-circuit ensembles, such as those with Haar random matchgates, as was studied in Ref. [SPH$^+$18]. A preliminary analysis indicates that propagation in this case scales logarithmically, rather than polynomially. On the latter, we can extend our method to analyze universal quantum computation by considering matchgate circuits acting on certain entangled input states, such as those of Ref. [Bra06], as the method given in this chapter is independent of the input. In a similar way as Anderson localization has been extended to many-body localization, certain perturbative analysis (in analogy to that performed in [BG16] for Clifford circuits) could probe possible dynamical localization in general quantum circuits as well as simulating interacting fermions.

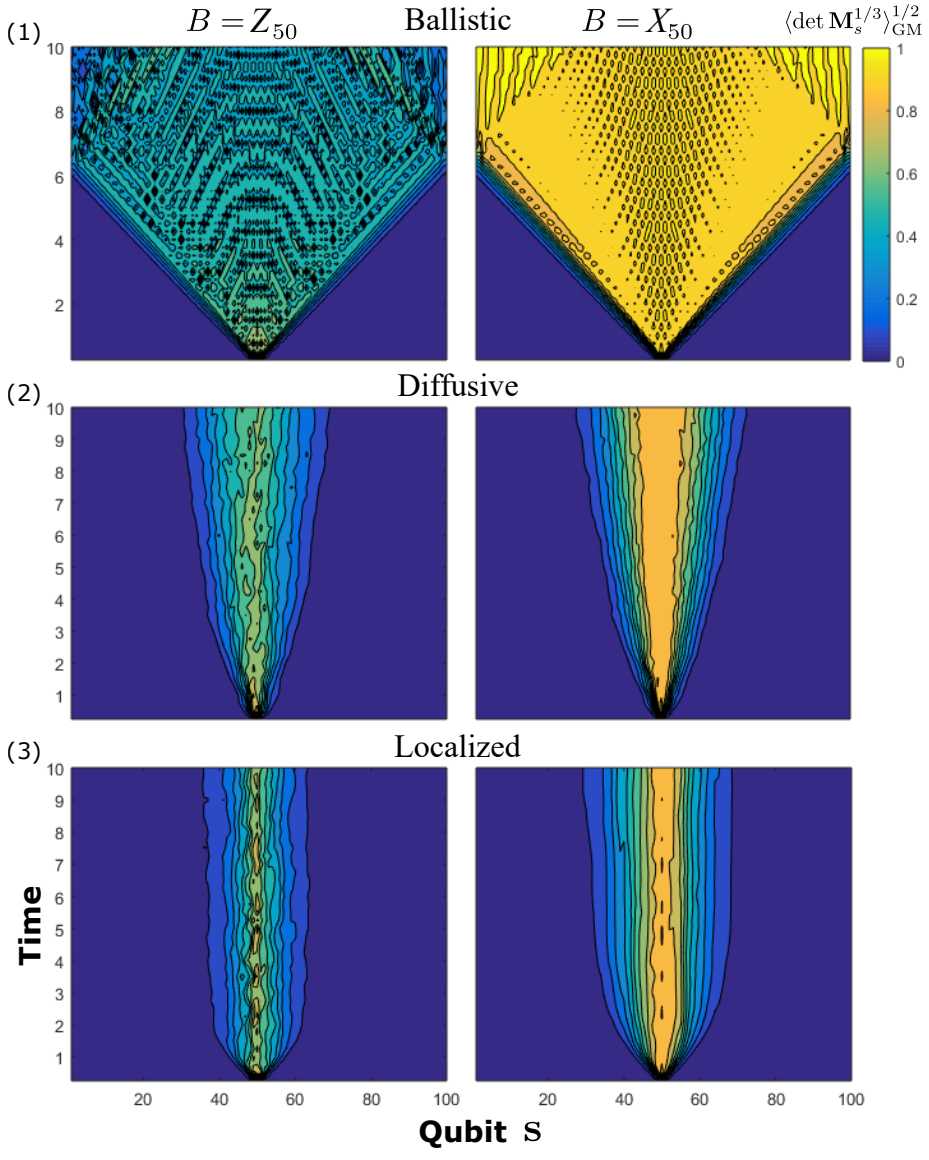

Figure 4.1: Typical light cones for Z_{50} (left) and X_{50} (right) propagating through the time-dependent disordered XY model (Model 1) with mean disorder strength ν and fluctuation strength Δ, for $n = 100$ qubits. Light cones are taken as the geometric mean of the determinant over 10 disorder realizations to preserve exponential decay. Representatives of the ballistic ($\nu = 0$, $\Delta = 0$, top), diffusive ($\nu = 0.75$, $\Delta = 1$, middle), and localized ($\nu = 2$, $\Delta = 0$, bottom) phases are shown. We note that, while the light cone envelopes for Z_{50} and X_{50} are always nearly the same, the interior of that for X_{50} generally has a higher value.

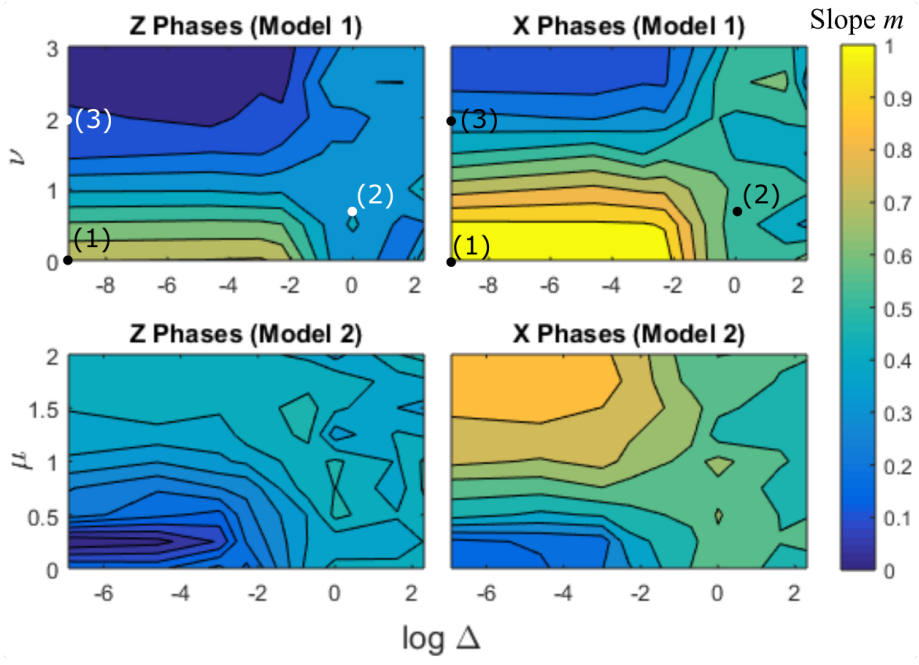

Figure 4.2: Phase diagrams for the propagation of Z (left) and X (right) in the presence of locally fluctuating disorder (top) and fluctuating interactions (bottom). These are given by taking the fitted slopes m of the light cone envelopes. Though this parameter is continuous, we see that several natural regions emerge: ballistic ($m \approx 1$), diffusive ($m \approx 0.5$), and localized ($m \approx 0$). Numbered points correspond to the corresponding light cones in Fig. 4.1, where points (1) and (3) on the y-axis meant to be located at $\Delta = 0$. The extended localized phase demonstrates that localization survives under weak fluctuations.

Chapter 5

Many-body-localization transition in universal quantum circuits

5.1 Introduction

By now it is well-understood that quantum effects play a prominent role for information propagation in many-body systems. Namely, the rate at which local disturbances propagate into nonlocal degrees of freedom — or scramble — under unitary dynamics is limited by the Lieb-Robinson bound [LR72]. This endows the system with an effective "speed of light," even without any invocation of relativity *a priori*. This uniquely quantum phenomenon follows from the locality structure of the Hamiltonian alone, and therefore is a ubiquitous property among quantum lattice systems.

A natural question, then, is how Lieb-Robinson-bounded propagation of quantum information will affect the performance of a quantum computer. As any practical realization of a quantum circuit will naturally possess some inherent notion of locality due to its connectivity structure, it seems obvious that there is a minimum circuit depth before the system will be able to access any given extensively nonlocal degree of freedom. This is simply the number of gate layers needed for the support of a local observable to interact with every qubit in the system. However, it may be

possible for a more stringent bound to hold due to the particular nature of the dynamics as well. An analogous situation can be seen in the *many-body-localized* regime for Hamiltonian dynamics in the presence of a disordered local field and perturbatively weak interactions [GMP05, BAA06, Imb16, SPacA13]. In such systems, the support of a disturbance will propagate logarithmically, rather than linearly, with time [HNO14, SC17, DLP$^+$17, NKH14]. The minimum time needed for the system to access extensively nonlocal degrees of freedom in this case is therefore exponential in the system size. Since strong quantum correlations cannot be built quickly, such systems admit many properties which are classically simulatable [BHV06, icvcvPPcv08, BPM12, KCA14, BnYC$^+$17]. We therefore ask whether a transition to many-body-localized behavior exists in quantum circuits. Such a transition would be tantamount to a *complexity transition*, for which a full understanding would be of great importance. Furthermore, the dynamics of quantum circuits is closely related to that of periodically-driven Floquet systems [CL15, KGRG16], where it has been shown that many-body-localized behavior indeed survives [ARH16, PPHA15, PCPA15, MGS17].

A recent tool developed for the purpose of accessing many-body-scrambling is the out-of-time-ordered (OTO) correlator, which was introduced by Kitaev to model the fast-scrambling behavior of black holes [Kit15b]. Since then, the OTO correlator has enjoyed success in describing the scrambling behavior of chaotic quantum systems. It has been used, for example, to study chaotic behavior in random quantum circuit models [GH18, ZN18, ZC18, JHN18, XS18b, SPH$^+$18, NVH18, vKRPS18] — including those with conservation laws [RPv17, KVH17] — and the related dynamics of random-matrix models [GHST18, KLP18, CZ18]. Conversely, it has been shown that the OTO correlator is effective at detecting the *absence of scrambling*, as seen in the many-body localized phase [FZSZ17b, HL17, Che16, XTAE, SBYX17]. In fact, it is argued in Ref. [HZC17] that the OTO correlator is uniquely-suited to this task. Such properties make the OTO correlator an ideal diagnostic for the many-body-localization transition in quantum circuits and ensembles thereof. Nevertheless, utilizing this quantity to detect localization without *a priori* knowledge of such behavior in the general, single-shot regime remains a challenge, since it would

in principle require full simulation over an exponentially large Hilbert space. In Ref.s [XS18a, SXS18], the authors utilize matrix product operators, truncated to low bond dimension, to approximate the Heisenberg operator time evolution and calculate the OTO correlator for scrambling and localizing systems. This method can be viewed as a generalization of performing gate cancellations outside of the trivial lightcone of a quantum circuit by taking the particular circuit dynamics into account, and approximating the circuit inside the "true lightcone" by one of low depth. In Ref. [SPH+18], the authors observe a many-body localization transition in a Floquet model with Haar random local unitaries together with disordered 2-qubit interactions, for which they employ a similarly clever tensor network contraction scheme to reduce the complexity of their quantity (which is not the OTO correlator) by an exponential factor, though it is still exponential overall. They also demonstrate localizing behavior in a Floquet circuit model of random Gaussian-fermionic circuits, which admits an efficient classical simulation.

In this chapter, we take advantage of the fact that any time evolution can be written in terms of dynamics of interacting fermions [BK02], so that the OTO correlator may be computed as a determinental formula as studied in our previous work for non-interacting fermions [CM18]. We first derive an exact formula for the OTO correlator for universal quantum circuits, expressed in terms of Gaussian-fermionic evolution together with fermionic "interaction" gates, as a superposition of exponentially many free-fermion trajectories. This formula is an alternating series of determinants of sub-matrices of an orthogonal, symmetric matrix, which reflects the fact that our fermionic interaction gates only permit transitions between certain configurations of fermions. In a similar spirit as light-front computational methods in quantum field theory, we restrict our formula to keep track of only the fastest traveling modes, allowing us to replicate the action of an interaction gate by that of a Gaussian-fermionic circuit coupling to a set of ancillary modes and approximate the time-evolution efficiently (i.e. in-terms of a single determinant). We apply our algorithm to a universal quantum circuit model consisting of alternating layers of non-interacting fermion evolution, and interaction gates coupling alternating subsets of

qubits, where we observe a transition to many-body-localized behavior as we increase the disorder strength. Though we consider an ensemble-averaged Floquet model for ease of presentation in this work, we emphasize that neither of these is necessary for our algorithm. Our algorithm can be applied for any one-dimensional nearest-neighbor quantum circuit, without need to work in the perturbatively-interacting regime, and without the need for super-computing resources.

5.2 Background

5.2.1 Out-of-Time-Ordered Correlator

Our figure of interest is the infinite-temperature out-of-time-ordered (OTO) correlator, defined between two observables A and $B(t) \equiv UBU^\dagger$ for a system of Hilbert-space dimension d and unitary time evolution U as

$$\mathcal{C}_{AB}(t) \equiv (4d)^{-1/2} |||[A, B(t)]|||_F, \tag{5.1}$$

where $||A||_F \equiv \sqrt{\mathrm{tr}(A^\dagger A)}$ is the Frobenius norm. When A and B are Hermitian and unitary operators (e.g. qubit Pauli observables), we have the relation

$$\mathcal{C}_{AB}(t)^2 = \frac{1}{2}\left\{1 - d^{-1}\,\mathrm{tr}\left[AB(t)AB(t)\right]\right\}. \tag{5.2}$$

Here, we will choose $A = X_{\lfloor n/2 \rfloor}$ and $B = Z_s$ for qubit $s \in \{1, 2, \ldots, n\}$. "Infinite temperature" refers to the fact that the trace in Eq. (5.2) is the trace inner product between $AB(t)AB(t)$ and the infinite-temperature Gibbs state $d^{-1}I$. This trace term is sometimes referred to as the OTO correlator in the literature, and $\mathcal{C}_{AB}$ is called the OTO *commutator*. Here we will refer to either quantity as the OTO correlator, as our meaning will be clear from context. The normalization in Eq. (5.1) is such that

$\mathcal{C}_{AB} \in [0,1]$. $\mathcal{C}_{AB}$ is further bounded by the conventional Lieb-Robinson commutator norm by the operator-norm inequality $||A||_F \leq \sqrt{d}||A||_2$, as

$$\mathcal{C}_{AB}(t) \leq \frac{1}{2}||[A, B(t)]||_2 \lesssim ||A||_2||B||_2 e^{-\eta(d_{AB}-vt)}, \tag{5.3}$$

where d_{AB} is the initial lattice distance between A and B ($d_{AB} = |\lfloor n/2 \rfloor - s|$ for our choices of A and B), and the second inequality is the Lieb-Robinson bound [LR72]. This bound confines the support of $B(t)$ to within an effective "lightcone" of speed v, outside of which the amplitudes of $B(t)$ in a local operator basis decay exponentially.

As stated above, a more stringent bound than Eq. (5.3) holds for many-body-localized systems. Namely, support in such systems is confined to within a *logarithmic lightcone*

$$\mathcal{C}_{AB}(t) \lesssim ||A||_2||B||_2 e^{-\eta(d_{AB}-v\ln t)}. \tag{5.4}$$

That is, disturbances take exponential time to propagate a given distance. This behavior is intimately related to a logarithmic spreading of entanglement [FZSZ17b], which is a signature of many-body localization [SBYX17, SC17, KCA14, BPM12, icvcvPPcv08, SPacA13, BnYC+17, DLP+17, Imb16] (further, it has been shown to be distinct from the Anderson-localized phase [HL17, Che16], in which the lightcone width is constant in time [And58]).

Though Eq. (5.3) is an upper bound, we expect $\mathcal{C}_{AB}(t)$ to give a good heuristic for the lightcone, and in fact it was shown in Ref. [HZC17] that the OTO correlator can detect the logarithmic lightcone where more conventional, two-point correlators cannot. Averages of the OTO correlator are also useful, since they are be related to the more familiar second Rényi entanglement entropy

$$S_M^{(2)} \equiv -\log \mathrm{tr}_M \left(\mathrm{tr}_{\overline{M}} \rho\right)^2, \tag{5.5}$$

with respect to a subsystem M for ρ an infinite-temperature Gibbs state quenched to the eigenbasis of an operator A. This relation is the so-called "OTOC-RE" theorem [FZSZ17b]

$$\exp\left[-S_M^{(2)}(t)\right] = \sum_{B\in\overline{M}} \mathrm{tr}\left[B(t)\Pi_A B(t)\Pi_A\right], \tag{5.6}$$

where Π_A is the trace-normalized projector onto the eigenbasis of A, the sum is taken over a local operator basis on $\overline{M}$, and normalization is chosen such that $\sum_{B\in\overline{M}} B_{ij}B_{lm} = \delta_{im}\delta_{lj}$, $\mathrm{tr}\,\Pi_A = 1$. This connection was extended to operator entanglement in Ref. [XS18a], building off of the work in [HQRY16], through the bound

$$S_M^{(2)}(t) \leq -\log\left(1 - \frac{1}{2}\sum_{\{P_j|j\in M\}} \mathcal{C}^2_{AP_j}(t)\right), \tag{5.7}$$

where here, the operator entanglement is that of the state related to the original operator by contracting the operator on one side, say, subsystem r of the infinite-temperature n-qubit thermofield double state

$$|\Phi\rangle = 2^{-n/2} \sum_{j\in\{0,1\}^{\times n}} |j\rangle_r \otimes |j\rangle_{\tilde{r}} \tag{5.8}$$

and the sum taken in Eq. (5.7) is over all single-qubit Pauli operators $\{I, X, Y, Z\}$ supported on M. Though a bounded second Rényi entropy does not guarantee a low-bond-dimension matrix product operator approximation, it is argued in Ref.s [XS18a, SXS18] that the lightcone envelope can be well-approximated using such a technique, since any disturbance due to truncating the matrix product operator to limited bond dimension cannot itself propagate outside of the lightcone. See also Ref.s [HQRY16, CHJLY17], where the averaged OTO correlator has been related to the tripartite second Rényi mutual information and the spectral form factor, respectively.

5.2.2 Gaussian Fermionic Evolution

We next give a brief review of Gaussian fermionic evolution (also known as matchgate circuits, see Ref.s [Kni01, TD02, BK02, Bra06, JM08, dMT13, BC14] for further details), which we define in terms of the Jordan-Wigner transformation from Pauli observables on n qubits to *Majorana operators* on $2n$ fermionic modes, as

$$c_{2j-1} = Z^{\otimes(j-1)} X_j \qquad c_{2j} = Z^{\otimes(j-1)} Y_j. \tag{5.9}$$

These operators satisfy the canonical anticommutation relations $\{c_\mu, c_\nu\} = 2\delta_{\mu,\nu} I$, where $\delta_{\mu,\nu}$ is the Kronecker delta. Gaussian fermionic unitaries are those of the form $U_g = \exp\left(\mathbf{c}^{\mathrm{T}} \cdot \mathbf{h} \cdot \mathbf{c}\right)$, where $\mathbf{c}$ is the column vector of Majorana operators. Unitarity and the canonical anticommutation relations restrict $\mathbf{h}$ to be a real, antisymmetric matrix without loss of generality.

Majorana operators are preserved under commutation with quadratic terms, as

$$[\mathbf{c}^{\mathrm{T}} \cdot \mathbf{h} \cdot \mathbf{c}, c_\mu] = (-4\mathbf{h} \cdot \mathbf{c})_\mu. \tag{5.10}$$

This implies that, under Gaussian evolution, we have

$$U_g^\dagger c_\mu U_g = \left(e^{-4\mathbf{h}} \cdot \mathbf{c}\right)_\mu. \tag{5.11}$$

As $\mathbf{h}$ is an antisymmetric matrix, $\mathbf{u} \equiv e^{-4\mathbf{h}} \in \mathrm{SO}(2n)$, and so Majorana operators form a representation of the group $\mathrm{SO}(2n)$ under Gaussian fermionic evolution. Additional representations can be constructed from ordered products of the Majorana operators — called *Majorana configuration operators* — which we define as

$$C_{\vec{\alpha}} \equiv c_{\alpha_1} c_{\alpha_2} \ldots c_{\alpha_k}, \tag{5.12}$$

where $\vec{\alpha}$ is an *ordered k-tuple*, for which $1 \leq \alpha_1 < \alpha_2 < \cdots < \alpha_k \leq 2n$. Under Gaussian fermionic evolution, the Majorana configuration operators transform as

$$U_g^\dagger C_{\vec{\alpha}} U_g = \sum_{\vec{\beta}} \det\left(\mathbf{u}_{\vec{\alpha}\vec{\beta}}\right) C_{\vec{\beta}}, \tag{5.13}$$

where $\mathbf{u}_{\vec{\alpha}\vec{\beta}}$ is the submatrix of $\mathbf{u}$ given by taking the rows indexed by $\vec{\alpha}$ and the columns indexed by $\vec{\beta}$. Matrices of amplitudes $\{\det\left(\mathbf{u}_{\vec{\alpha}\vec{\beta}}\right)\}_{\vec{\alpha}\vec{\beta}}$, whose elements are indexed by k-tuples, form a homomorphism of SO($2n$) by the *Cauchy-Binet formula*

$$\sum_{\vec{\beta}} \det\left[(\mathbf{u}_1)_{\vec{\alpha}\vec{\beta}}\right] \det\left[(\mathbf{u}_2)_{\vec{\beta}\vec{\gamma}}\right] = \det\left[(\mathbf{u}_1\mathbf{u}_2)_{\vec{\alpha}\vec{\gamma}}\right]. \tag{5.14}$$

Eq. (5.14) will prove useful for calculating operator amplitudes for arbitrary Pauli operators under Gaussian fermionic evolution, in addition to the Majorana operators, for which $k = 1$.

Finally, it will be convenient to define the following Gaussian operation, which exchanges pairs of fermionic modes between qubits j and k

$$S_{jk} = \frac{1}{2}\left(X_j Z^{\otimes(k-j)-1} X_k + Y_j Z^{\otimes(k-j)-1} Y_k + Z_j + Z_k\right) \tag{5.15}$$

$$= \frac{-i}{2}\left(c_{2j}c_{2k-1} - c_{2j-1}c_{2k} + c_{2j-1}c_{2j} + c_{2k-1}c_{2k}\right) \tag{5.16}$$

$$S_{jk} = -i\exp\left[\frac{\pi}{4}\left(c_{2j}c_{2k-1} - c_{2j-1}c_{2k} + c_{2j-1}c_{2j} + c_{2k-1}c_{2k}\right)\right] \tag{5.17}$$

This operation effects $c_{2j-1} \overset{S}{\leftrightarrow} c_{2k-1}$ and $c_{2j} \overset{S}{\leftrightarrow} c_{2k}$ by conjugation.

It was shown, surprisingly, in Ref. [JM08], that Gaussian fermionic operations, together with 2-qubit nearest-neighbor SWAP operations, are universal for quantum computation. SWAP has a similar form to Eq. (5.16), with the important distinction of a *quartic* term in the Majorana operators

$$\mathrm{SWAP}_{j,j+1} = \frac{1}{2}\left(I + X_j X_{j+1} + Y_j Y_{j+1} + Z_j Z_{j+1}\right) \tag{5.18}$$

$$\mathrm{SWAP}_{j,j+1} = \frac{1}{2}\left(I - ic_{2j}c_{2j+1} + ic_{2j-1}c_{2(j+1)} - c_{2j-1}c_{2j}c_{2j+1}c_{2(j+1)}\right). \tag{5.19}$$

In contrast to Eq. (5.10), the quartic term maps between Majorana configuration operators of different degree under commutation, e.g.

$$[Z_j Z_{j+1}, c_{2j-1}] = -2c_{2j}c_{2j+1}c_{2(j+1)}, \tag{5.20}$$

and in general

$$[Z_j Z_{j+1}, C_{\vec{\alpha}}] = \begin{cases} 2(Z_j Z_{j+1})C_{\vec{\alpha}} & |\vec{\alpha} \cap \vec{q}_j| \text{ odd} \\ 0 & |\vec{\alpha} \cap \vec{q}_j| \text{ even} \end{cases}, \tag{5.21}$$

where $\vec{q}_j \equiv (2j-1, 2j, 2j+1, 2j+2)$. For $\vec{\alpha} \subseteq \vec{q}_j$, $(Z_j Z_{j+1})C_{\vec{\alpha}} = \pm C_{\vec{q}_j/\vec{\alpha}}$, and $[Z_j Z_{j+1}, c_k] = 0$ for $k \notin \vec{q}$. Since Eq. (5.20) is analogous to a pair-production process for Majorana operators, we will refer to it as an "interaction" between modes.

Finally, in Ref. [CM18], it was shown that the infinite-temperature OTO correlator has an analytic closed-form expression when the unitary evolution is a Gaussian fermionic operation and $A \equiv i^a C_{\vec{\eta}}$ and $B \equiv i^b C_{\vec{\eta}}$ are Pauli operators (for integer a and b), as

$$\mathcal{C}^2_{AB}(t) = \frac{1}{2}\left\{1 \pm \det\left[\mathbf{u}_{\vec{\alpha}[2n]}\left(\mathbf{I} - 2\mathbf{P}_{\vec{\eta}}\right)\mathbf{u}^{\mathrm{T}}_{[2n]\vec{\alpha}}\right]\right\}, \tag{5.22}$$

where the sign factor is simply $(-1)^{|\vec{\alpha}||\vec{\eta}|+1}$, and $\mathbf{P}_{\vec{\eta}}$ is the projector onto the modes $\vec{\eta}$ (i.e. it is diagonal with ones on the diagonal for modes in $\vec{\eta}$ and zeroes elsewhere). In the following sections, we demonstrate a similar approach to that of Ref.s [XS18a,

SXS18] to approximate the OTO correlator by considering interactions acting on only the fastest-traveling Majorana modes, near the lightcone edge, where we can effect the action of an interaction by an equivalent Gaussian fermionic transformation and apply Eq. (5.22).

5.3 Results

5.3.1 A. Universal Circuit Model

Our universal circuit model is shown in Fig. 5.1. It consists of alternating layers between disordered Gaussian fermionic evolution and products of quartic fermion gates. The Gaussian fermionic evolution is given by

$$H_{XY}(\{\nu_j\}) = \sum_{j=1}^{n-1} \left(X_j X_{j+1} + Y_j Y_{j+1}\right) + \sum_{j=1}^{n} \nu_j Z_j \tag{5.23}$$

$$H_{XY}(\{\nu_j\}) = -i \sum_{j=1}^{n-1} \left(c_{2j} c_{2j+1} - c_{2j-1} c_{2(j+1)}\right) - i \sum_{j=1}^{n} \nu_j c_{2j-1} c_{2j} \tag{5.24}$$

with the $\{\nu_j\}$ a random local potential, chosen uniformly from the interval $[-\nu, \nu]$. We will demonstrate the existence of a many-body-localization transition to logarithmic scrambling at a disorder value of $\nu_c \sim 0.8$. When interactions are absent, however, propagation in this model is Anderson-localized for any nonzero disorder.

The quartic fermion "interaction" gates are of the form

$$\exp(-\frac{i\pi}{4} Z_j Z_{j+1}) = \frac{1}{\sqrt{2}}(I - i Z_j Z_{j+1}) \tag{5.25}$$

For $\vec{\alpha} \subseteq \vec{q}_j$, we have

$$e^{\frac{i\pi}{4} Z_j Z_{j+1}} C_{\vec{\alpha}} e^{-\frac{i\pi}{4} Z_j Z_{j+1}} = (i Z_j Z_{j+1})^{(|\vec{\alpha}| \bmod 2)} C_{\vec{\alpha}}. \tag{5.26}$$

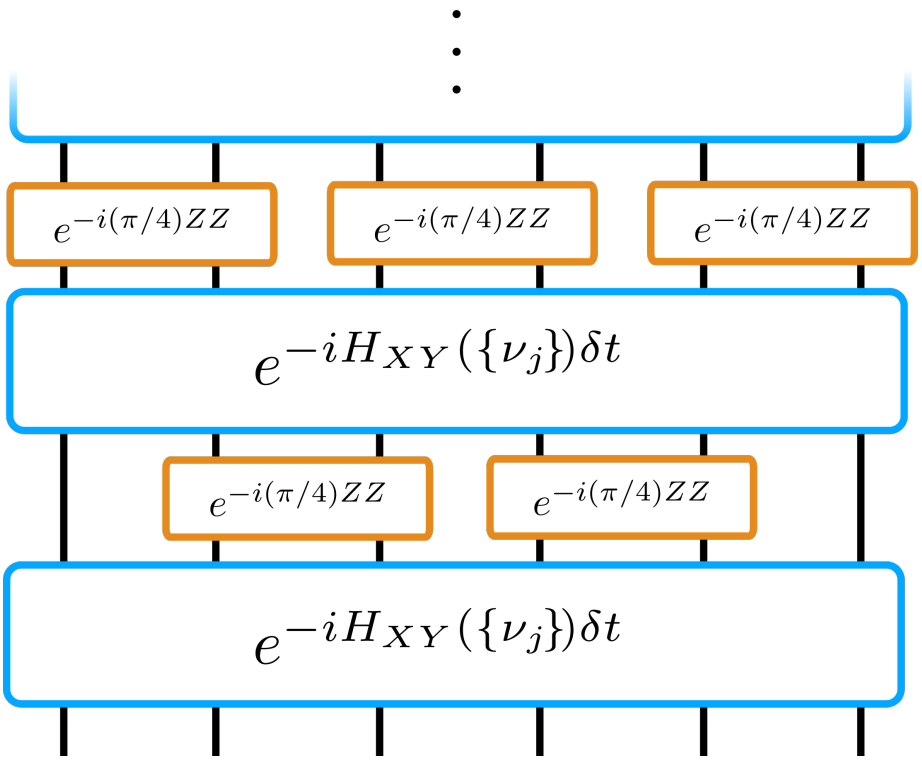

Figure 5.1: (Color online) Our alternating circuit model of-interest, consisting of repeated layers of the form shown above. Global layers are periods of localizing Gaussian fermionic dynamics, with local disorder configuration $\{\nu_j\}$ and duration δt. Local gate layers consist of "interaction gates, which are non-Gaussian. The positions of these layers are alternated between qubits 1 and 2 being the left-most qubits to interact.

It is crucial to our approximation that this gate be a Clifford operation (i.e. it preserves the set of Majorana configuration operators). This gate is equivalent to SWAP gate up to Gaussian fermionic gates, as

$$e^{\frac{i\pi}{4}}\text{SWAP} = \exp\left(-\frac{i\pi}{4}Z_jZ_{j+1}\right)\exp\left[\frac{5i\pi}{4}\left(Z_j+Z_{j+1}\right)\right]S_{j,j+1}. \tag{5.27}$$

Thus, the inclusion of these gates extends Gaussian fermionic operations to computationally universal quantum circuits.

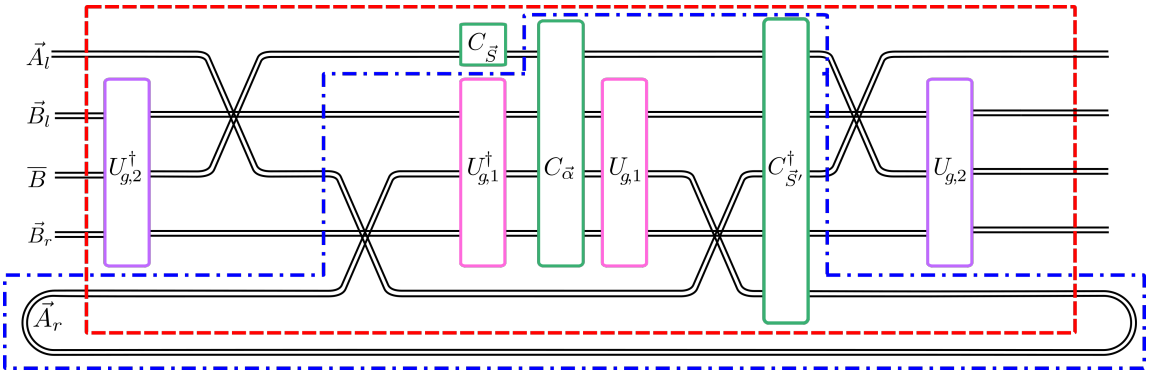

Figure 5.2: (Color online) A Gaussian fermionic circuit whose evaluation is used to prove Eq. (5.28). The circuit is depicted in the qubit picture, with pairs of circuit wires representing collections of arbitrarily many qubits. As such, all Majorana configuration operators ($C_{\vec{\alpha}}$, $C_{\vec{S}}$, and $C_{\vec{S}'}^\dagger$) are drawn with support all the way up to the top qubit, since there may in principle be a string of Pauli-Z operators up to this qubit if the number of Majorana operators in the configuration is odd. Nevertheless, we do assume that $\vec{S}' \subseteq \vec{A}_r$. That is, if $|\vec{S}'|$ is odd, then $C_{\vec{S}'}^\dagger$ only acts as a string of Z operators on the qubits corresponding to modes $(\vec{A}_l, \vec{B}_l, \overline{B}, \vec{B}_r)$, and so all Gaussian fermionic gates commute with $C_{\vec{S}'}^\dagger$ on these qubits. Crossing lines represent the Gaussian fermionic operation of rearranging subsets of fermionic modes (i.e. products of $\{S_{jk}\}$ defined in the text) while preserving these subsets' internal ordering, but possibly applying phases. Similarly, $U_{g,1}$ and $U_{g,2}$ are Gaussian fermionic unitaries. The self-contracted wires at the bottom represent a partial trace over this subset of qubits (notice we can reliably trace over the last subset since no Majorana configurations will have support here). The dotted and dot-dashed boxes indicate which portion of the circuit to contract in one step during its evaluation, followed by the contraction over everything else in the second step. For example, the dot-dashed-box contraction consists of conjugating $C_{\vec{\alpha}}$ by $U_{g,1}$, exchanging modes $\overline{B}$ and $\vec{A}_r$, and tracing over $\vec{A}_r$ with respect to $C_{\vec{S}'}^\dagger$ in the first step. Next, the modes $\overline{B}$ and $\vec{A}_l$ are exchanged and $U_{g,2}$ is applied in the second step. This contraction partitioning corresponds to the left-hand-side of Eq. (5.28). The dotted box consists of applying all Gaussian fermionic unitaries in the first step, and then performing the partial trace with respect to $C_{\vec{S}'}^\dagger$ in the second step (remember, $C_{\vec{S}'}^\dagger$ commutes with Gaussian fermionic unitaries on modes outside of $\vec{A}_r$). This contraction partitioning corresponds to the right-hand-side of Eq. (5.28). As these two contractions must evaluate to the same operator, their equivalence implies the equality.

5.3.2 Exact Formula

In Appendices B.1 and B.2, we prove an exact formula for a general quantum circuit expressed as a product of Gaussian fermionic evolution and interaction gates. This formula follows from a modification to the Cauchy-Binet formula (5.14):

$$\begin{aligned}&\sum_{\vec{\beta}\subseteq\vec{B}\equiv\left(\vec{B}_l,\vec{B}_r\right)} \det\left[(\mathbf{u}_1)_{\vec{\alpha},\vec{\beta}\cup\vec{S}'}\right]\det\left[(\mathbf{u}_2)_{\vec{\beta}\cup\vec{S},\vec{\gamma}}\right]\\ &\quad=(-1)^{|\vec{S}||\vec{S}'|}\det\begin{bmatrix}\mathbf{0}_{|\vec{S}|\times|\vec{S}'|} & (\mathbf{u}_2)_{\vec{S}\vec{\gamma}}\\ (\mathbf{u}_1)_{\vec{\alpha}\vec{S}'} & (\mathbf{u}_1)_{\vec{\alpha}\vec{B}}\,(\widetilde{\mathbf{u}}_2)_{\vec{B}\vec{\gamma}}\end{bmatrix}.\end{aligned} \tag{5.28}$$

Letting $\overline{B}$ be the set-complement of $\left(\vec{A}_l,\vec{B}_l,\vec{B}_r,\vec{A}_r\right)$ in the set of all modes (see Fig. 5.2), $\vec{S}$, $\vec{S}'\subseteq\overline{B}$ are fixed sets of modes which are not summed over. $\vec{B}_l$ is a contiguous subset of modes to the "left" of and disjoint from $\overline{B}$, and $\vec{B}_r$ is a contiguous subset of modes to the "right" of and disjoint from $\overline{B}$. Furthermore,

$$\widetilde{\mathbf{u}}_2\equiv\left(\mathbf{I}-2\delta_{|\vec{S}|+|\vec{S}'|=1(\mathrm{mod}\ 2)}\mathbf{P}_{\vec{B}_l}\right)\mathbf{u}_2. \tag{5.29}$$

That is, $\widetilde{\mathbf{u}}_2=\mathbf{u}_2$ unless $|\vec{S}|$ and $|\vec{S}'|$ have opposite parity, in which case the rows of $\mathbf{u}_2$ corresponding to the modes $\vec{B}_l$ are multiplied by (-1) to obtain $\widetilde{\mathbf{u}}_2$. Eq. (5.28) was proved for the special case where $\vec{S}=\vec{S}'$ in Ref. [CM18].

Though we prove Eq. (5.28) rigorously in Appendix B.2 using properties of determinants, a simple pictorial proof can be seen in Fig. 5.2 (for details of this version of the proof, see Appendix B.1). This figure depicts a circuit consisting of fixed evolution by Gaussian fermionic unitaries $U_{g,1}$, $U_{g,2}$, and rearrangements of fermionic modes (the crossing wires, which are products of the $\{S_{jk}\}$) with the ancillary modes ($\vec{A}_l$, $\vec{A}_r$). The self-contracted wires at the bottom represent a partial trace taken on the last subset of qubits. The modified Cauchy-Binet formula, Eq. (5.28), follows from considering the two equivalent ways we can choose to evaluate this circuit: either

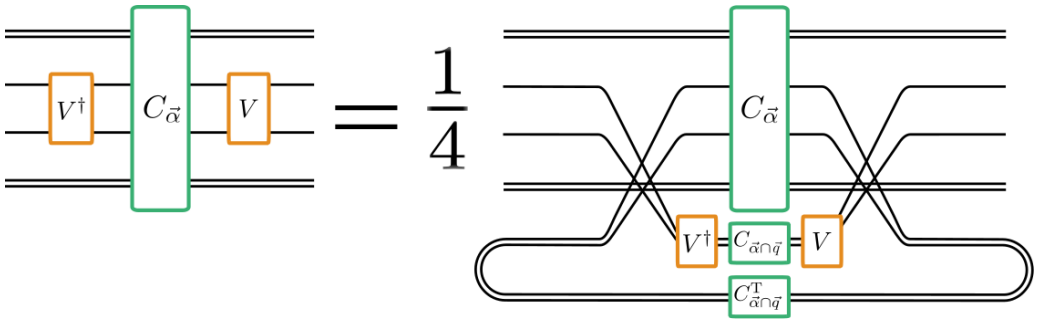

Figure 5.3: (Color online) The action of an interaction gate $V \equiv e^{-i(\pi/4)ZZ}$, acting on the modes $\vec{q}$ can be reproduced by exchanging the modes $\vec{q}$ with an ancilla occupied by $V^\dagger C_{\vec{\alpha}\cap\vec{q}} V$, and taking the partial trace with respect to $C_{\vec{\alpha}\cap\vec{q}}$. Note that, since $C^{\mathrm{T}}_{\vec{\alpha}\cap\vec{q}}$ potentially only differs from $C_{\vec{\alpha}\cap\vec{q}}$ by a sign, the product $V^\dagger C_{\vec{\alpha}\cap\vec{q}} V C^{\mathrm{T}}_{\vec{\alpha}\cap\vec{q}}$ does not have support on the qubits above it due to the parity-preserving property of V. Choosing the dotted contraction-ordering in Fig. 5.2 above, whereby the partial trace is taken at the very end, we can iterate the application of this identity and compute the OTO correlator as the single trace of a Majorana configuration under Gaussian fermionic evolution, with respect to the appropriate Majorana configuration output by the interaction gates.

we contract everything in the dotted box and perform the partial trace afterward, or we contract everything in the dot-dashed box (including taking the partial trace) and perform the remainder of the Gaussian fermionic evolution afterward. These two different contraction orderings yield the same operator (since they are the same circuit), yet the former evaluates to the right-hand-side of Eq. (5.28), and the latter evaluates to the left-hand-side. See the caption under Fig. 5.2 or Appendix B.2 for details.

We construct an exact formula for the OTO correlator of universal quantum circuit dynamics by iteratively applying Eq. (5.28). Since our interaction gate is parity-preserving, Eq. (5.28) can be realized as the identity shown in Fig. 5.3, whereby the input modes to the interaction are exchanged with the appropriate output modes on an ancilla, and the ancilla is traced over. Choosing the contraction corresponding to the dotted box in Fig. 5.2 (i.e. performing all traces at the end) we can calculate the OTO correlator as a series of terms of a similar form to Eq. (5.22), summed over all exponentially-many inputs to each interaction gate. Each such input configuration

can be thought of as a particular "computational path" in the operator space of Majorana configurations, and the OTO correlator is realized as a superposition over all of these paths, which will interfere in general. Our algorithm for exactly calculating the OTO correlator then proceeds as follows:

Exact series for the OTO correlator:

Given:

1. Universal quantum circuit $U \equiv U_1 U_2 \dots U_N$ on n qubits with g interaction gates.

2. Pauli observables $A \equiv i^a C_{\vec{\eta}}$ and $B \equiv i^b C_{\vec{\alpha}}$, for integers a and b.

Construct: An orthogonal, symmetric matrix $\mathbf{K}$ from which the infinite-temperature OTO correlator $\mathcal{C}_{AB}(t)^2$ can be calculated as a sum of minors from $\mathbf{K}$, as

$$1 - 2\mathcal{C}_{AB}(t)^2$$

$$= \sum_{\substack{\vec{B}=\bigcup_{i=1}^{g} \vec{\beta}_i \subseteq \vec{A}_{(N)} \\ \vec{B}'=\bigcup_{i=1}^{g} \vec{\beta}'_i \subseteq \vec{A}'_{(N)}}} (-1)^{f(\vec{B},\vec{B}')} \det\left[\mathbf{K}_{\left[\vec{B}',\mathcal{V}(\vec{B}),\vec{\alpha}\right]\left[\vec{B},\mathcal{V}(\vec{B}'),\vec{\alpha}\right]}\right] \tag{5.30}$$

for ancillary modes, $\vec{A}_{(N)}$, $\vec{A}'_{(N)}$, integers $\{f(\vec{B},\vec{B}')\}$, and $\mathcal{V}$ the map relating the Majorana configuration-tuple input to a set of interaction gates $V^{\otimes g}$ to the configuration-tuple of the output.

1. Let $\mathbf{u}_{(0)} \equiv \mathbf{I}_{2n}$, the $2n \times 2n$ identity matrix, and $\vec{A}_{(0)} \equiv ()$, the empty tuple.

2. For $j \in (1, \dots, N)$:

(a) If U_j is Gaussian fermionic, corresponding to $\mathbf{u} \in \mathrm{SO}(2n)$

i. $\mathbf{u}_{(j)} \equiv \mathbf{u}_{(j-1)} \left(\mathbf{I}_{\vec{A}_{(j-1)}} \oplus \mathbf{u} \right)$

ii. $\vec{A}_{(j)} \equiv \vec{A}_{(j-1)}$

(b) If $U_j = \exp\left(-\frac{i\pi}{4} Z_{i_j} Z_{i_j+1}\right)$, an interaction gate between qubits (i_j, i_j+1), on modes $\vec{q}_j \equiv \left(2i_j - 1, 2i_j, 2i_j+1, 2i_j+2\right)$

i. Let $\vec{B} \equiv \left(\vec{A}_{(j-1)}, [2n] + |\vec{A}_{(j-1)}|\right)$, where addition indicates adding a fixed value to every index of the set. Let $\widetilde{q}_j \equiv \vec{q}_j + |\vec{A}_{(j-1)}|$ and $\overline{q}_j \equiv \vec{B}/\widetilde{q}_j$

ii. $\mathbf{u}_{(j)} \equiv \begin{bmatrix} \mathbf{0}_{4\times 4} & \mathbf{I}_{\widetilde{q}_j \vec{B}} \\ \left(\mathbf{u}_{(j-1)}\right)_{\vec{B},\widetilde{q}_j} & \left(\mathbf{u}_{(j-1)}\right)_{\vec{B},\overline{B}} \mathbf{I}_{\overline{B},\vec{B}} \end{bmatrix}$

iii. $\vec{A}_{(j)} \equiv ([4], \vec{A}_{(j-1)} + 4)$

3. (a) Let $\vec{p} \equiv [2n] + |\vec{A}_{(j)}|$, $\vec{B} \equiv \left(\vec{A}_{(j)}, \vec{p}\right)$

(b) Let $\mathbf{R} \equiv (-1)^{|\vec{\eta}|} \left(\mathbf{I}_{2n} - 2\mathbf{P}_{\vec{\eta}}\right)$, a $2n \times 2n$ diagonal matrix whose diagonal elements are $(-1)^{|\vec{\eta}|+1}$ for modes in $\vec{\eta}$ and $(-1)^{|\vec{\eta}|}$ otherwise.

(c) $\mathbf{K} \equiv \begin{bmatrix} \mathbf{0}_{|\vec{A}_{(j)}|\times|\vec{A}_{(j)}|} & \left(\mathbf{u}_{(j)}^{\mathrm{T}}\right)_{\vec{A}_{(j)},\vec{B}} \\ \left(\mathbf{u}_{(j)}\right)_{\vec{B},\vec{A}_{(j)}} & \left(\mathbf{u}_{(j)}\right)_{\vec{B},\vec{p}} \mathbf{R} \left(\mathbf{u}_{(j)}^{\mathrm{T}}\right)_{\vec{p},\vec{B}} \end{bmatrix}$

The phases $(-1)^{f(\vec{B},\vec{B}')}$ are calculated by iterated application of Eq. (5.28) every time an interaction is applied in step 2(b) and are calculated explicitly in Appendix B.3.

5.3.3 Approximative method

Though our formula in Eq. (5.30) is exact, the number of terms in the sum scales exponentially in the number g of interaction gates (though each term can be evaluated using only polynomial resources in the number of qubits). We therefore make the physical restriction to the fastest traveling modes, which allows us to approximate the lightcone envelope by a series truncated to a single determinant corresponding to an

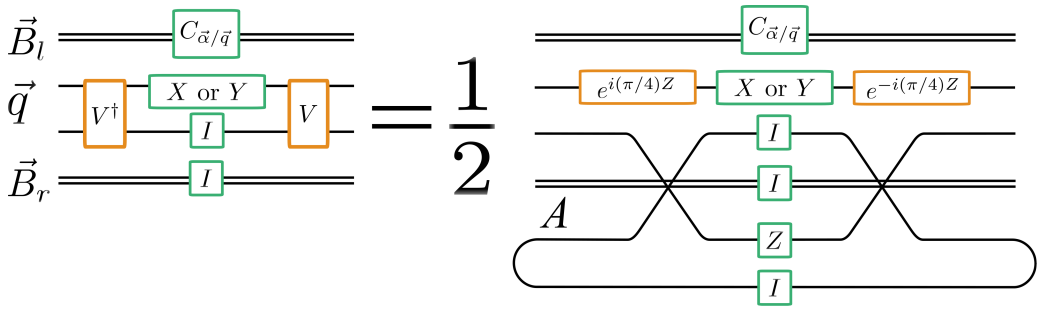

Figure 5.4: (Color online) We approximate the action of an interaction gate on the lightcone using the identity shown above (a similar identity holds when the identity input is replaced with a Z). Namely, the effect of conjugating an interaction gate on a single Pauli X or Y is equivalent (up to normalization) to performing a local Z rotation on that qubit, together with exchanging (via a Gaussian operation S_{jk}) a Pauli Z with an ancilla A, which is then traced over.

effective Gaussian fermionic evolution. Our workhorse identity is shown graphically in Fig. 5.4 and given by:

Conditional Gaussian evolution: For a Majorana operator c_μ, with $\mu \in (2j-1, 2j)$, we have

$$e^{\frac{i\pi}{4}Z_jZ_{j+1}}c_\mu e^{\frac{-i\pi}{4}Z_jZ_{j+1}} = \frac{1}{2}\,\mathrm{tr}_A\left[\left(e^{\frac{i\pi}{4}Z_j}c_\mu e^{\frac{-i\pi}{4}Z_j}\right)\left(S^\dagger_{j+1,A}Z_AS_{j+1,A}\right)\right], \tag{5.31}$$

$$e^{\frac{i\pi}{4}Z_jZ_{j+1}}\left(c_\mu Z_{j+1}\right)e^{\frac{-i\pi}{4}Z_jZ_{j+1}} = \frac{1}{2}\,\mathrm{tr}_A\left[\left(e^{\frac{i\pi}{4}Z_j}c_\mu e^{\frac{-i\pi}{4}Z_j}\right)\left(S^\dagger_{j+1,A}Z_{j+1}S_{j+1,A}\right)Z_A\right] \tag{5.32}$$

Similar identities hold for $\mu \in (2j+1, 2j+2)$.

The identities above relate the action of an interaction gate on an operator at the lightcone edge to that of a corresponding equivalent Gaussian fermionic gate, allowing us to approximately simulate it classically. By similar logic to that argued in Ref.s [XS18a, SXS18], we expect the propagation of any error introduced in this approximation to be bounded by the speed of light of the underlying dynamics. Such error results from terms in the operator expansion of $B(t)$ which are not of the form shown in Eq.s (5.31) or (5.32) (or the corresponding form for $\mu \in (2j+1, 2j+2)$). We

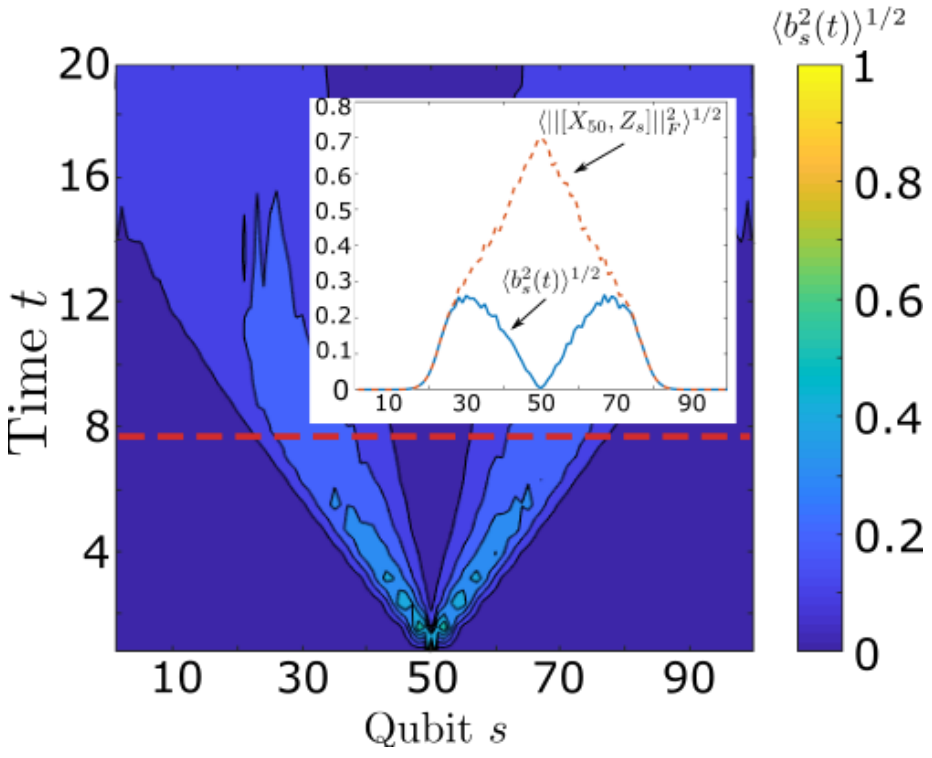

Figure 5.5: (Color online) The lightcone boundary as calculated by Eq. (5.33) for Gaussian fermionic evolution (no interaction gates) on $n = 100$ qubits and disorder strength $\nu = 1$, averaged over 25 disorder realizations, with $\delta t = \pi/4$. We see that the boundary spreads, leaving a depletion region in the center, and becomes wider with time. (Inset) The boundary at the time slice indicated by the dotted line, at $t = \frac{5\pi}{2}$, together with $\mathcal{C}_{XZ}$ at the same time. We see clearly a region where the lightcone has very nearly the exact value of the boundary, indicating that our approximate method becomes exact in this region, since the underlying assumption to the approximation is perfectly satisfied here.

calculate the weight of the assumption-satisfying terms using the modified Cauchy-Binet formula (5.14). Let

$$(-i)^b B(t) = \sum_{\vec{\beta}} \det\left(\mathbf{u}_{\vec{\alpha}\vec{\beta}}\right) C_{\vec{\beta}} \tag{5.33}$$

That is, assume $B = i^b C_{\vec{\alpha}}$ and that the evolution up to time t is described by a Gaussian fermionic operation as in Eq. (5.13). Additionally, let

$$b_s^2(t) \equiv \begin{cases} \sum_{\substack{\vec{\beta} \text{ with } X_s I^{\otimes(n-s)} \\ \text{or } Y_s I^{\otimes(n-s)} \text{ present}}} \det\left(\mathbf{u}_{\vec{\alpha}\vec{\beta}}\right)^2 & (s \geq \lfloor n/2 \rfloor) \\ \sum_{\substack{\vec{\beta} \text{ with } I^{\otimes(s-1)} X_s \\ \text{or } I^{\otimes(s-1)} Y_s \text{ present}}} \det\left(\mathbf{u}_{\vec{\alpha}\vec{\beta}}\right)^2 & (s \leq \lfloor n/2 \rfloor) \end{cases}. \tag{5.34}$$

This is the total weight of the terms which do not commute with $\exp\left(\frac{i\pi}{4} Z_s Z_{s\pm 1}\right)$ and which correspond to the right or left lightcone edge being found at qubit s. The condition in the upper sum (for which $s \geq \lfloor n/2 \rfloor$) will only be met if there exists a tuple $\vec{\beta}'$ for which $\vec{\beta} = (\vec{\beta}', 2s-1)$ or $\vec{\beta} = (\vec{\beta}', 2s)$. Similarly, for $B \equiv X_{\lfloor n/2 \rfloor}$, the condition in the lower sum (for which $s \leq \lfloor n/2 \rfloor$) will only be met if there exists a tuple $\vec{\beta}'$ for which $\vec{\beta} = ([2s-2], 2s-1, \vec{\beta}')$ or $\vec{\beta} = ([2s-2], 2s, \vec{\beta}')$, where $[2s-2] = (1, 2, \ldots, 2s-2)$ (since we know the total number of modes in $\vec{\beta}$ must be odd for $B = X_{\lfloor n/2 \rfloor}$). We therefore apply the modified Cauchy-Binet formula, Eq. (5.28), to calculate this quantity exactly (see Appendix B.4 for the full expression). For an illustration of the efficacy of this measure for the boundary, see Fig. 5.5.

We utilize this quantity $b_s(t)$, together with our conditional Gaussian evolution identities Eq.s (5.31), (5.32) in our approximation algorithm for the OTO correlator, which proceeds as follows:

Approximation to Interaction by Conditional Gaussian Evolution:

Given: $B(t-\delta t)$, described by an orthogonal matrix $\mathbf{u}$ as in Eq. (5.33) and a global tolerance ε

Approximate: $V_j B(t-\delta t) V_j^\dagger$ for $V_j = \exp\left(-\frac{i\pi}{4} Z_j Z_{j+1}\right)$

1. Calculate $b_s(t)$ for all $s \in (1, \ldots, 2n)$.

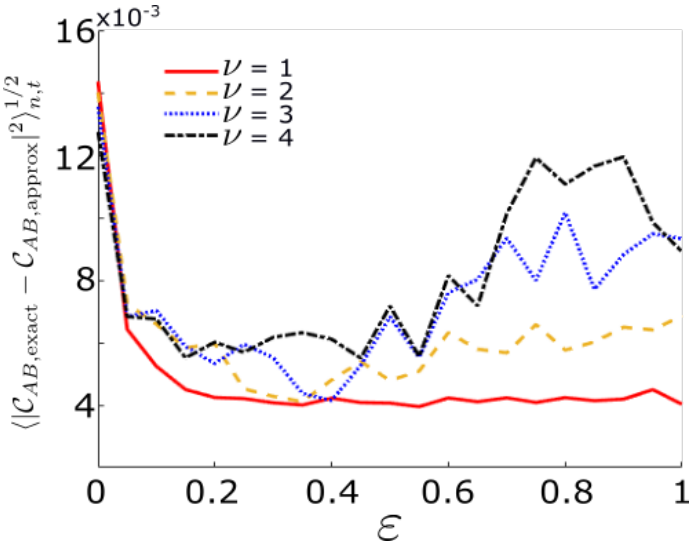

Figure 5.6: (Color online) Average (per pixel) Frobenius-norm error between the exact and approximate lightcones on 6 qubits for disorder values $\nu \in \{1, 2, 3, 4\}$ (see Fig. 5.7 for an example at disorder $\nu = 10$) as a function of the variationally optimized free parameter ε, averaged over 25 samples. We see the clear emergence of a local minimum at $\varepsilon \in [0.2, 0.4]$ as the disorder is increased above $\nu \sim 1$. This is due to the fact that, when the Gaussian fermionic evolution is nearly delocalized, the decision of whether to keep an interaction gate makes negligible difference for small system size, since interaction gates cannot extend the lightcone beyond a ballistic profile.

2. For $s \in (1, \ldots, 2n)$, *if* $b_s(t) \geq \varepsilon$:

   If $s \geq \lfloor n/2 \rfloor$ and $j = s$,
   or $s \leq \lfloor n/2 \rfloor$ and $j = s - 1$:

   Replace V_j with a Gaussian operation by Eq. (5.31) for $\mu \in (2s - 1, 2s)$.

Each approximation step introduces an extra ancillary qubit (see Fig. 5.4), but once again, we can perform the trace over the entire ancillary system as one with the trace in Eq. (5.2) (notice that the normalization is kept consistent as we add each ancillary qubit). This allows us to straightforwardly apply Eq. (5.22) to calculate the OTO correlator.

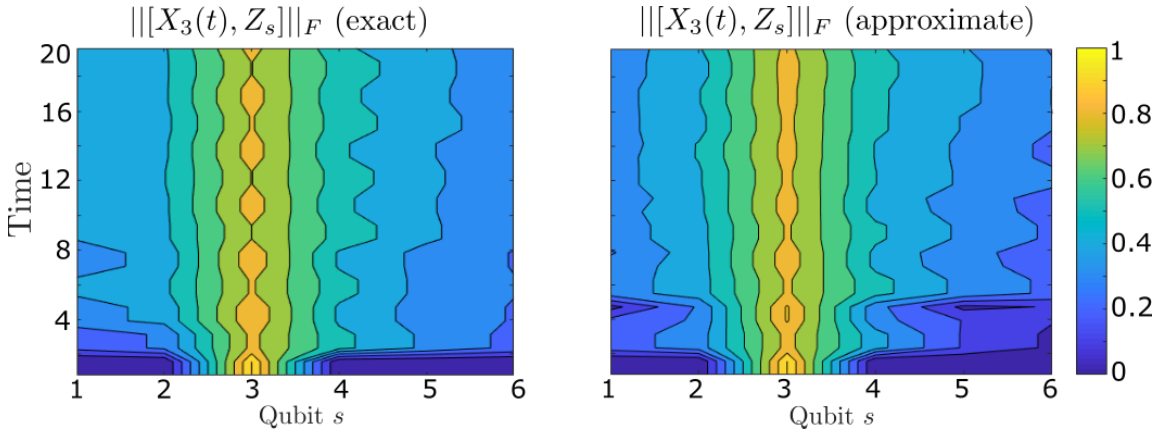

Figure 5.7: (Color online) A comparison between the output of our algorithm and a brute-force calculation done on $n = 6$ qubits with disorder $\nu = 10$, $\varepsilon = 0.2$, $\delta t = \pi/4$, averaged over 50 disorder realizations. We see good agreement at the interior of the lightcone, though edge fluctuations become more prominent under the approximation.

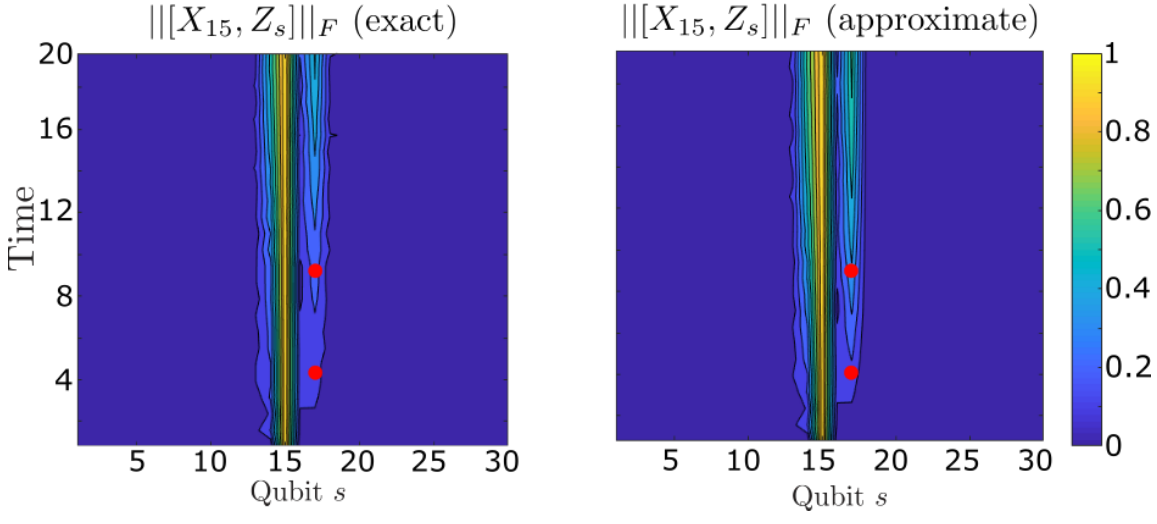

Figure 5.8: (Color online) A comparison between the output of our algorithm and an exact calculation, which scales exponentially in the number of interaction gates, but efficiently in the number of qubits, for disorder value $\nu = 10$, $\delta t = \pi/4$, and two interaction gates at qubits $(17, 18)$ at times $t = \frac{3\pi}{2}$, 3π (red circles). We consider only a single disorder instance here, so edge fluctuations are more pronounced. We nevertheless observe good agreement between the envelopes of the two lightcones at the optimized value $\varepsilon = 0.2$.

5.3.4 Variational Optimization of the Free Parameter

The free parameter ε in our algorithm effectively decides where we would like to truncate the free-particle lightcone. Since the lightcone edge will actually have some finite width (related to the decay length η in the bounds Eq.s (5.3) and (5.4)), this free parameter is necessary. A key assumption of our algorithm is that errors introduced *inside* the lightcone envelope will not change the propagation of the envelope itself, since such errors cannot travel faster than the speed of light. It is therefore important that we capture this lightcone edge precisely, without applying our approximation to interactions that fall outside of the lightcone of the exact dynamics. We are able to remove the free parameter by variationally optimizing the Frobenius norm of our approximate lightcone relative to the exact, brute-force calculation for small system size. In Fig. 5.6, we demonstrate the emergence of a local minimum in the average-case Frobenius norm error between our approximation at given ε and the brute-force calculation for $n = 6$ qubits, as a function of ε, as we tune the disorder strength from $\nu = 1$ to $\nu = 4$. We attribute this the appearance of this local minimum to the fact that, at low disorder, we expect the decision of whether to keep a given interaction gate to be less important, since an interaction cannot extend the lightcone beyond a ballistic one. The appearance of a local minimum is therefore consistent with the emergence of a genuine many-body-localization transition. In Fig. 5.7, we compare the output of our algorithm to that of a brute-force calculation at $\varepsilon = 0.2$, the optimal value, for $n = 6$, averaged over 50 disorder realizations of strength $\nu = 10$, where we observe good agreement (we choose high disorder here so that features of the lightcone can be seen within a region 6 qubits wide). In Fig. 5.8, we examine the correctness of our algorithm in the opposite extreme, where the number of qubits is large ($n = 30$) and the number of interaction gates is limited to two (at the red circles), using our exact formula Eq. (5.30). We see excellent agreement between the lightcone envelopes at disorder strength $\nu = 10$, again at the optimized value of $\varepsilon = 0.2$.

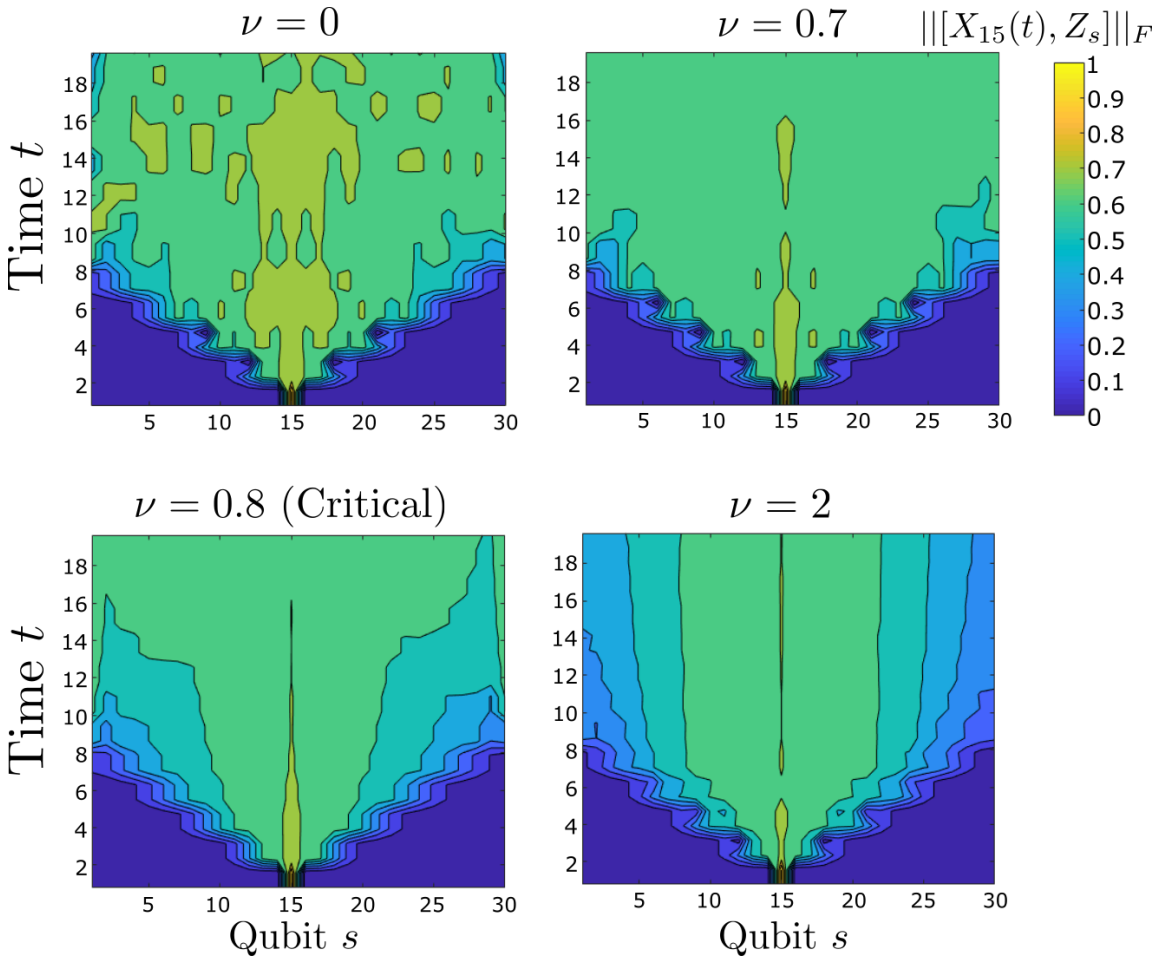

Figure 5.9: (Color online) Lightcone transition from ballistic propagation at low disorder ($\nu < \nu_c \approx 0.8$) to logarithmically localized propagation at high disorder ($\nu > \nu_c$), averaged over 10^3 disorder realizations. A characteristic feature of the localized phase is a region where the OTO correlator is maximized (> 0.6) about the location of the initial excitation.

5.4 Many-body location transition

Our main numerical result is shown in Fig.s 5.9 and 5.10, where we demonstrate that our universal circuit model, consisting of alternating disordered Gaussian fermionic evolution and interaction gates as in Fig. 5.1, exhibits a many-body-localization transition in $\mathcal{C}_{XZ}(t)$ as we tune the disorder strength across a critical value $\nu_c \approx 0.8$. In Fig. 5.9, we plot the lightcone propagation for disorder values $\nu \in \{0, 0.7, 0.8, 2\}$ across the critical disorder strength for 10^3 samples of the disorder. We note a clear

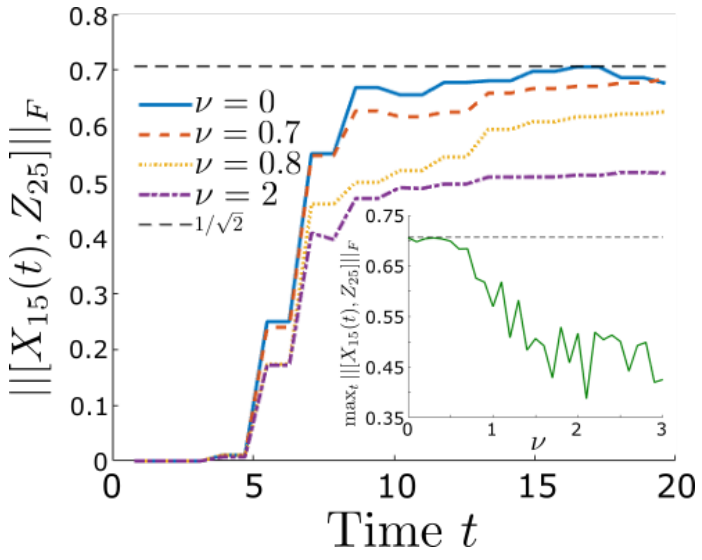

Figure 5.10: (Color online) The OTO correlator value at a fixed qubit ($s = 25$) for the four disorder values shown in Fig. 5.9. We see that below the critical value, the OTO correlator approaches a limiting value of $1/\sqrt{2}$, the Page scrambled value (see main text), and a lower limiting value in the localized regime. We plot this limiting value as a function of disorder strength (inset), where we see a clear deviation from Page scrambling for disorder values $\nu \geq \nu_c \approx 0.8$.

emergence of a highly localized region of maximal value ($\mathcal{C}_{XZ} \approx 0.7$), which persists for all time in this figure when the disorder strength is greater than ν_c. This is approximately the operator Page-scrambled value of $\frac{1}{\sqrt{2}}$ [SS08], where the operator $X_{15}(t)$ has equal weight for all four possible Pauli operators $\{I_s, X_s, Y_s, Z_s\}$ at a given site s. That is, contracting $X_{15}(t)$ on one side of the thermofield double state Eq. (5.8) and tracing over all but qubit s and s' on subsystems r and $\tilde{r}$, respectively, would give the 2-qubit maximally mixed state $\frac{1}{4}I$. Commutation with Z_s keeps only the weights on $\{X_s, Y_s\}$, each of which are $\frac{1}{4}$. Adding these and taking the square root gives the value of $\mathcal{C}_{XZ}$ to be approximately $\frac{1}{\sqrt{2}}$. Our numerics are therefore consistent with the fact that, within the localized region, the operator X_s is approximately Page scrambled. Since this property is preserved under Clifford-gate evolution, such as by our interaction gate, the existence of this Page-scrambled region justifies our approximation to neglect the action of such gates acting *inside* the lightcone, since they would have negligible effect on the lightcone interior.

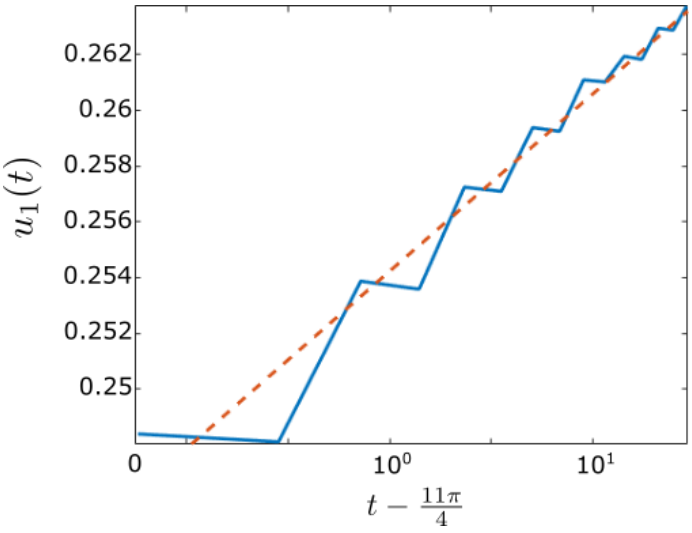

Figure 5.11: (Color online) The principal singular vector, $u_1(t)$, of the lightcone in Fig. 5.9 for $\nu = 2$, treated as a numerical matrix, and plotted on a logarithmic (base 10) x-axis. Logarithmic scrambling is observed by this method for $t \geq \frac{11\pi}{4}$, as prior to this, the principal-singular-vector behavior is dominated by a ballistically-spreading low-amplitude component.

In Fig. 5.10, we plot a spatial slice of each of the lightcones in Fig. 5.9 at $s = 25$. We see that below the critical value of $\nu_c = 0.8$, the limiting value is very nearly the Page value $1/\sqrt{2}$, while above the critical value, it begins to decrease with ν. In the inset, we plot the limiting value (which we take as the maximum) as a function of disorder strength, where we see that it clearly begins to deviate strongly from the Page value as we increase the disorder past the critical value. In Fig. 5.11, we plot the principal temporal singular vector of the $\nu = 2$ lightcone in Fig. 5.9, treated as a numerical matrix, against a logarithmic x-axis for $t \geq \frac{11\pi}{4}$. The principal singular component of this matrix is the closest product approximation to the lightcone in Frobenius norm, and so this provides a robust, numerically inexpensive means of analyzing the dynamical phase (see Appendix A.6 for details). Prior to $t = \frac{11\pi}{4}$, this principal vector is dominated by a ballistically-spreading low-amplitude component (see Fig. 5.9), but for $t \geq \frac{11\pi}{4}$, we see the OTO correlator growth is linear on this semi-logarithmic plot, indicating that the lightcone is logarithmic after this time. We choose to neglect this early-time behavior since we are primarily interested in the

long-time asymptotic growth of the OTO correlator for our model.

5.5 Discussion

We have demonstrated a transition to many-body localizing behavior in a universal circuit model composed of Gaussian fermionic evolution and fermionic interaction gates. This behavior is demonstrated by the transition to a logarithmic lightcone, seen clearly in Fig. 5.9 when the disorder is greater than the empirically observed value $\nu_c \sim 0.8$. Though we choose a specific model of alternating interactions and disordered free-fermionic evolution for clarity of presentation, we emphasize that our algorithm is completely general beyond this setting, since any universal quantum circuit can be decomposed as a product of Gaussian fermionic evolution and interaction gates, and does not require an ensemble average in principle.

For example, it would be interesting to see how the algorithm does to examine the performance of actual near-term quantum algorithms, such as a quantum adiabatic optimization algorithm (QAOA) [FGG14], which are characterized by a quantum circuit of the repeating structure seen in Fig. 5.1, variationally optimized over some parameterization of the repeated unit cell. As our algorithm is naturally suited to such a structure, we therefore expect it to reveal new classes of systems which exhibit localization in this setting as well.

Chapter 6

Autonomous quantum-correlated Maxwell demon

6.1 Introduction

With the discovery of his famous gedanken experiment, James Clerk Maxwell started physics on the long road to the unification of thermodynamics with information theory [MNV09, Jar13, PHS15]. Nearly 200 years later, with the ever-advancing miniaturization of devices [BdLS$^+$12, CL01, GLW$^+$02, HCR$^+$07, MHG$^+$12], the idea that one could exploit detailed knowledge of a system's microstate as a thermodynamic resource no longer seems like a mere idealization [VdBKL12, MQJ13, HBS14, SSBJ14, SIKS15, Hor15, BS14]. To the contrary, we hope to someday soon push our technology to the regime where quantum effects become relevant [RÅR$^+$11, DJ13, Jac12, Cav90, Scu01, HHH$^+$05, HSAL11, Zur03, OHHH02, Seg08, LJR15, GHR$^+$16]. Since there are more delicate constraints on correlations in the quantum world, like strong subadditivity of von Neumann entropy, as well as a variety of monogamy relations (exclusive tradeoffs) among different kinds of correlations, it is timely to consider a question unforeseen in Maxwell's time: *how can correlations be harnessed for the performance of these devices in the fully general quantum setting?*

This significant question has been studied extensively from different perspectives, and it has been mentioned that correlations can yield an advantage in performing certain thermodynamic tasks, such as work extraction [PLHH$^+$15, dRHRW16, FWU13, OHHH02, RASK$^+$14, BHL$^+$14, DL09, GKNBK15, HPLHA13]. In this chapter, we focus on two key challenges: (i) accounting for the contribution of correlations to the second law of thermodynamics, and (ii) comparing quantum and classical correlations as thermodynamic resources on the same footing. Regarding (i), it is important to notice that the system is coupled to external degrees of freedom in quantum open-system dynamics, and the resulting correlations can be utilized, in principle, by an external, *classical* agent to "measure" the system and gain knowledge in the framework of feedback control [SIKS15]. However, this utilization of correlations should be distinguished from the way an internal agent like a quantum Maxwell demon, or a part of the quantum system, handles correlations, since the latter is the scenario we are interested in here. Regarding (ii), the majority of prior works [RÅR$^+$11, Zur03, Cav90, Llo97, Jac12, PLHH$^+$15, Def13] defines quantum and classical Maxwell demons in such a manner that the classical version is treated as a limiting case (typically with a fixed basis). This obviously makes the classical demon at most as powerful as the quantum one, but it may not immediately imply that classical correlations are at most as useful as quantum correlations for the demon who can handle both kinds.

To address the point (i), we study a quantum system which exhibits an information-work tradeoff independently of any external agent. Following a pioneering work of the classical autonomous Maxwell demon studied in Ref. [MQJ13], we consider a scenario in which a qubit, in contact with two heat reservoirs of different temperatures, accesses sequentially many memory qubits, and analyze their correlations in the fully quantum regime. We think this to be among the simplest models to exhibit the thermodynamic features akin to a quantum Maxwell demon. For the point (ii), as defined formally in the next section, we stress that our demon is *identical* regardless of the nature of information in its memory. This allows us to unambiguously define work performed by the demon, since there has otherwise been difficulty in doing so

due to the intrinsic "uncertainty" of quantum systems [GEW16, GA15, Åbe13, BT06, GH13, HO13, SM10, SSP13, DRRV11, WNW15].

Here, we discover a new nonequilibrium phase of our demon: refrigeration against a thermal gradient coincident with memory erasure at the expense of correlations. We find that correlations enable our demon to exploit quantum coherence to realize an advantage over its classical counterpart. To handle the complexity of correlations, we apply a tool from condensed matter physics — the matrix product density operator formalism — which makes tractable our calculations in the fully quantum-correlated regime. This technique exploits the fact that correlations built under local interactions change locally [VGRC04, ZV04, Eis13, Or14]. It thus gives a powerful tool for treating correlations in the thermodynamic framework, a task which has otherwise remained formidable. We expect our proof-of-principle to inspire a cross-fertilization of quantum many-body physics and quantum information with quantum thermodynamics.

Section 6.2 is an introduction and overview of the autonomous quantum demon. In section 6.3.1, we apply techniques from quantum information theory to derive its effective second law constraint. We give an analytic solution using our matrix product density operator formalism in section 6.3.2. In section 6.3.3, we demonstrate the existence of a phase of simultaneous refrigeration and erasure in the presence of correlations, and in section 6.3.4, we demonstrate the quantum advantage. Finally, we close with a discussion in section 6.4.

6.2 Overview of the Model

Our autonomous Maxwell demon (Fig. 6.2) is a generalization of the model proposed in Ref. [MQJ13]. The "demon" D is a qubit spanned by orthonormal basis states $|g\rangle$ and $|e\rangle$ with energy gap $E_e - E_g = \Delta$. It interacts sequentially with qubits in an infinitely long one-dimensional array $\mathbb{M}$, called the memory. The qubits in $\mathbb{M}$ are energetically degenerate and may be initially correlated, though they are noninteracting amongst themselves. The memory thus acts only as an informational,

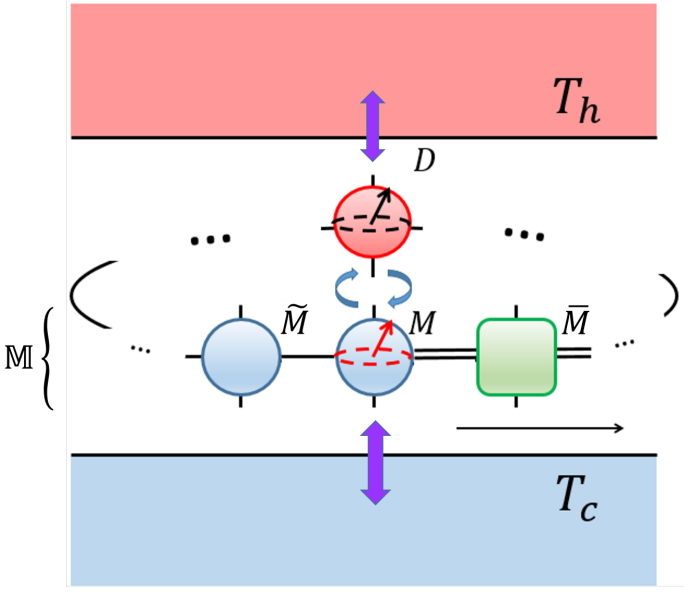

Figure 6.1: A snapshot of our quantum Maxwell demon. The demon qubit D interacts sequentially with each qubit in a memory $\mathbb{M}$ via an open-system process in contact with two thermal reservoirs of different temperatures. For a given interaction, M is the currently interacting qubit, $\bar{M}$ the subsystem of previously interacting qubits, and $\tilde{M}$ that of qubits yet to interact. The joint state of $D\mathbb{M}$ is described by a matrix product density operator with periodic boundary conditions, though we take sufficiently many interactions that the system has reached a periodic steady state. Interaction with the shared system D allows the possibility to build further correlations within $\bar{M}$, hence the double-line.

and not an energy, resource. When discussing a given interaction, we will refer to the interacting memory qubit simply as M, the system of memory qubits which have previously interacted as $\bar{M}$, and that of those which are yet to interact as $\tilde{M}$. For each such qubit, we define a "classical basis" $\{|0\rangle, |1\rangle\}$. In what follows, we choose the qubit Pauli-z operator of D, Z_D, to be diagonal in its energy eigenbasis and that of M, Z_M to be diagonal in its classical basis. We are free to choose a phase convention, which we keep fixed, in defining the Pauli-x and -y operators, X and Y respectively, of these systems. We will also need

$$2\sigma^0 = I + Z \qquad 2\sigma^+ = X + iY \tag{6.1}$$

$$2\sigma^- = X - iY \qquad 2\sigma^1 = I - Z \tag{6.2}$$

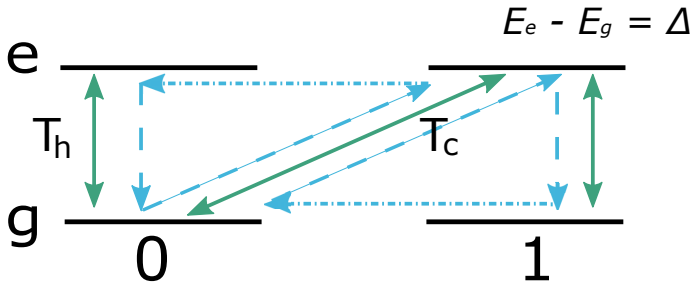

Figure 6.2: The transition diagram of an individual interaction between the demon qubit and a memory qubit. Solid arrows represent possible stochastic transitions, allowed by exchanging a unit Δ of energy with the associated reservoir, with transition rates satisfying the detailed balance condition. For example, intrinsic transitions coupled with the thermal reservoir of temperature T_h change only the state of the demon, whereas cooperative transitions coupled with that of $T_c(< T_h)$ change the joint state of the demon and the memory qubit, leaving a record on the memory. The dashed arrows indicate the cyclic processes which refrigerate (pump energy against the gradient), with the horizontal dot-dashed transitions provided by the memory shift. Note both refrigerative processes result in a net flip of the memory qubit from "0" to "1".

on these systems as well. Finally, we will use

$$\zeta \equiv \langle \sigma_M^0 \rangle - \langle \sigma_M^1 \rangle = \langle Z_M \rangle \tag{6.3}$$

as a shorthand for the population bias of M in its z basis.

The device operates cyclically; D interacts with M for an interaction time τ before $\mathbb{M}$ moves by one site to the right, and the sequence repeats. Each interaction consists of two simultaneous processes, each in contact with a different thermal reservoir. In the first, the demon undergoes *intrinsic transitions*, wherein it exchanges a unit Δ of energy with a "hot" reservoir at temperature T_h. In the second, the joint system DM undergoes *cooperative transitions*, wherein the demon exchanges Δ of energy with a "cold" reservoir at temperature $T_c < T_h$, and the interacting qubit is flipped. Intrinsic transitions occur with rates $\Gamma_{g\to e}$ and $\Gamma_{g\leftarrow e}$, and cooperative transitions with rates $\Gamma_{g0\to e1}$ and $\Gamma_{g0\leftarrow e1}$. These rates are chosen so as to satisfy detailed balance

$$\frac{\Gamma_{g\to e}}{\Gamma_{g\leftarrow e}} = e^{-\beta_h \Delta} \tag{6.4}$$

$$\frac{\Gamma_{g0\to e1}}{\Gamma_{g0\leftarrow e1}} = e^{-\beta_c \Delta}, \tag{6.5}$$

where the $\beta_i = 1/T_i$ are the inverse temperatures, and we have chosen units such that the Boltzmann factor is one. We thus describe each transition by a Lindblad jump operator

$$L_{g\to e} = \sqrt{\Gamma_{g\to e}}\sigma_D^- \otimes I_M \qquad L_{g0\to e1} = \sqrt{\Gamma_{g0\to e1}}\sigma_D^- \otimes \sigma_M^- \tag{6.6}$$

$$L_{g\leftarrow e} = \sqrt{\Gamma_{g\leftarrow e}}\sigma_D^+ \otimes I_M \qquad L_{g0\leftarrow e1} = \sqrt{\Gamma_{g0\leftarrow e1}}\sigma_D^+ \otimes \sigma_M^+. \tag{6.7}$$

Finally, we define

$$\varepsilon \equiv \tanh\left[\frac{(\beta_c - \beta_h)\,\Delta}{2}\right] \tag{6.8}$$

as a parameter quantifying the magnitude of the thermal gradient.

Formally, our interaction sequence is generated by the time-dependent Lindbladian

$$\mathcal{L}_{D\mathbb{M}}(t) = \sum_{j=1}^{\infty} \mathcal{L}_{DM}^{(j)} \Theta(j\tau - t)\Theta\left[t - (j-1)\tau\right], \tag{6.9}$$

where $\mathcal{L}_{DM}^{(j)}$ is the time-independent interaction Lindbladian between D and the jth qubit in $\mathbb{M}$, described by the aforementioned Lindblad jump operators (see Appendix C.1 for details). Θ is the Heaviside theta function, and so these factors "switch on" the interaction $\mathcal{L}_{DM}^{(j)}$ for $t \in [(j-1)\tau, j\tau)$. In the limit of many interactions, the system reaches a periodic steady state $\rho_{D\mathbb{M}}^{(\mathrm{ss})}$, for which

$$\rho_{D\mathbb{M}}^{(\mathrm{ss})} = \rho_{D\mathbb{M}}\left(n\tau\right) = \rho_{D\mathbb{M}}\left[(n+1)\tau\right], \tag{6.10}$$

where

$$\rho_{D\mathbb{M}}(t) \equiv \Phi_t \left[\rho_{D\mathbb{M}}(0)\right] = e^{\int_0^t \mathcal{L}_{D\mathbb{M}}(s)ds} \left[\rho_{D\mathbb{M}}(0)\right] \tag{6.11}$$

is the state of the full system at time t, and $n \in \mathbb{Z}^+$ is a sufficiently large positive integer. In what follows, we will only be interested in the performance of the device over a single interaction in periodic steady state. We therefore omit the explicit time dependence where appropriate and denote quantities corresponding to the outgoing qubit in the interaction as primed and those to the incoming as unprimed (e.g. $\rho_M \equiv \rho_M(n\tau)$ and $\rho'_M \equiv \rho_M\left[(n+1)\tau\right]$). Similarly, we will refer to the corresponding interaction Lindbladian simply as $\mathcal{L}_{DM}$, dropping the qubit label for convenience.

There are two special cases of this model which are of interest to us. The first is the *classical* case, in which the evolution during each interaction is constrained to population dynamics in the eigenbasis of $Z_D \otimes Z_M$. The interaction $\mathcal{L}_{DM}$ is "classical" in the sense that, if the initial state of DM is diagonal in this basis, then the evolution will remain so throughout. That is to say that the evolution does not mix together populations and coherences in this basis. Additionally, it drives the state of DM to a unique fixed point $\rho_{DM}^{(\mathrm{fp})} = \rho_D^{(\mathrm{fp})} \otimes \rho_M^{(\mathrm{fp})}$, which is a product of classical states of D and M.

The second special case is the *uncorrelated* case, in which the state of $\mathbb{M}$ is initially a product, and we neglect any correlations that are built over repeated interactions with the demon. Though the full dynamics, generated by $\mathcal{L}_{D\mathbb{M}}(t)$, is a sequence of local quantum operations, it may either build or consume correlations in the full state, since there is a common degree of freedom, D, between all of them. In general, one or both of these special cases may hold.

Figure 6.2 shows two cyclic processes over which energy is pumped against the thermal gradient (dashed arrows). The horizontal bit-flip transitions (dot-dashed arrows), which complete each cycle, are provided by the translation of the memory. If the sum of the probabilities of these processes is greater than that for the reverse

processes, then there is a net flow of energy against the gradient, and we say the system is *refrigerating*. Note that both processes flip the qubit from the $|0\rangle$ state to the $|1\rangle$ state, so a record of the refrigeration is left on the memory. We thus define

$$Q_{h\to c} \equiv \frac{\Delta}{2}\left(\zeta' - \zeta\right) \tag{6.12}$$

as the heat flow from the hot reservoir to the cold reservoir during the interaction, which is negative when the system is refrigerating. Note that this property of the model removes any ambiguity in our definition of work. We also define

$$\Delta S_M \equiv S(\rho'_M) - S(\rho_M), \tag{6.13}$$

where

$$S(\rho) \equiv -\operatorname{tr}\left(\rho \log \rho\right) \tag{6.14}$$

is the von Neumann entropy. The change ΔS_M represents the entropy dumped onto the memory. When $\Delta S_M < 0$, the memory is being *erased*.

In the uncorrelated classical regime, our model reduces to that of Ref. [MQJ13], where it was first introduced. There, it was shown that

$$Q_{h\to c}(\beta_c - \beta_h) + \Delta S_M \geq 0, \tag{6.15}$$

in this regime. We refer to Eq. (6.15) as the *local Clausius inequality*. It represents a strict tradeoff between the refrigeration ($Q_{h\to c} < 0$) and erasure ($\Delta S_M < 0$) phases of the device. This tradeoff can be understood geometrically. In the absence of

correlations or quantum coherence, the interacting qubit is driven monotonically along the z-axis of the Bloch sphere to its fixed point, $\rho_M^{(\mathrm{fp})}$, which has positive bias $\zeta^{(\mathrm{fp})} = \varepsilon > 0$. Erasure and refrigeration correspond to approaching this fixed point from $\zeta < \varepsilon$ and $\zeta > \varepsilon$, respectively. So long as this evolution is monotonic, the tradeoff is necessarily strict.

It is noted in Ref. [MQJ13] that when correlations cannot be neglected, this result generalizes to

$$Q_{h\to c}(\beta_c - \beta_h) + \Delta S_M \geq \Delta I_{D:M}, \tag{6.16}$$

where

$$\Delta I_{A:B} = I(A:B)' - I(A:B) \tag{6.17}$$

is the change in the quantum mutual information

$$I(A:B) \equiv S(\rho_A) + S(\rho_B) - S(\rho_{AB}). \tag{6.18}$$

$\Delta I_{D:M}$ can be either positive or negative in general, so the tradeoff in Eq. (6.15) becomes no longer strict. This suggests the possibility of a third thermodynamically nontrivial phase, in which the device is refrigerating and erasing simultaneously. We expect this to occur when correlations between D and M induce non-monotonic evolution on M alone. However, Eq. (6.16) is inconvenient in that it does not involve only terms that can be calculated from the evolution on the memory alone and so requires knowledge of the periodic steady state Eq. (6.10). One of our contributions is to provide a constraint free of this limitation, which is also strict in the presence of correlations and makes their utility as a thermodynamic resource manifest.

6.3 Main Results

6.3.1 Global Clausius Inequality

Our first result is to recover the Second Law in terms of the relevant thermodynamic variables in the fully quantum correlated case. This is the *global Clausius inequality*, which we state as a theorem

Theorem 3 *The global Clausius inequality,*

$$Q_{h\to c}(\beta_c - \beta_h) + \Delta S_M - \Delta I_{M:\tilde{M}} \geq 0, \tag{6.19}$$

which represents an information-work tradeoff of the thermodynamic quantities defined above, holds for a periodic steady state in the fully quantum correlated regime. Accordingly, simultaneous refrigeration and erasure is possible only if it is attended by the consumption of correlations.

Eq. (6.19) represents a strict three-way tradeoff between refrigeration, erasure, and the generation of correlations $\Delta I_{M:\tilde{M}}$, all of which may be calculated from knowledge of the initial and final states of the memory alone. The minus sign on $\Delta I_{M:\tilde{M}}$ places consumption of correlations as a resource; the more negative this term, the more negative the local terms can be.

To provide a sketch of the proof of Theorem 3 (full details can be found in Appendix C.2), we first note

$$Q_{h\to c}(\beta_c - \beta_h) + \Delta S_{M\tilde{M}} \geq \Delta I_{D:M\tilde{M}}, \tag{6.20}$$

which follows in the same manner as Eq. (6.16) from monotonic evolution to the fixed point $\rho_{DM}^{(\mathrm{fp})}$, but including the system $\tilde{M}$ as an ancilla. Next, we have

$$\Delta I_{D:M\tilde{M}} = I(D:M\tilde{M})' - I(D:M\tilde{M}) \tag{6.21}$$

$$\geq I(D:\tilde{M})' - I(D:M\tilde{M}) \tag{6.22}$$

$$\Delta I_{D:M\tilde{M}} \geq I(D:M\tilde{M}) - I(D:M\tilde{M}) = 0. \tag{6.23}$$

The first inequality follows from strong subaddivity: mutual information is nonincreasing under partial trace. The last step follows from the periodic steady state condition, Eq. (6.10). That is, the mutual information between D and the qubits yet to interact — $M\tilde{M}$ before the interaction and $\tilde{M}$ after the interaction — is a constant across interactions in steady state. Thus

$$Q_{h\to c}(\beta_c - \beta_h) + \Delta S_{M\tilde{M}} \geq 0, \tag{6.24}$$

and using

$$\Delta S_{M\tilde{M}} = \Delta S_M + \Delta S_{\tilde{M}} - \Delta I_{M:\tilde{M}}, \tag{6.25}$$

where $\Delta S_{\tilde{M}} = 0$ due to the fact that $\tilde{M}$ does not participate in the interaction, therefore gives the result.

We see that simultaneous refrigeration and local erasure is not forbidden by Eq. (6.19) so long as correlations are consumed, but it remains to be seen that our model actually exhibits such behavior. We address this in the following sections.

6.3.2 Matrix Product Density Operator Solution

The matrix product state formalism has been very successful as an efficient representation of the quantum correlations present in a one-dimensional spin-chain [FNW92, Vid03, PGVWC07]. Because dynamics in contact with a thermal bath are

dissipative, we need a generalization of this formalism to mixed states and classical correlations. This is the *matrix product density operator* (MPDO) formalism, introduced in Ref.'s [VGRC04, ZV04], and further developed in Ref.'s [BL14, WJS+16, CCBn15]. The MPDO description of a mixed state of N d-dimensional spins with periodic boundary conditions is given by

$$\rho_{\text{MPDO}} = \sum_{\vec{i}} \text{tr}\left(\mathcal{P}\prod_{j=1}^{N} A^{i_j}\right)\bigotimes_{j=1}^{N}\sigma^{i_j}, \tag{6.26}$$

where the $i_j \in \{0, 1, +, -\}$, and the A^{i_j} are $\chi_{j-1} \times \chi_j$ matrices corresponding to the spin at site j. $\mathcal{P}$ is the path-ordering operator, which places operators of higher j to the left in the product. It was shown in Ref. [VGRC04] that the description Eq. (6.26) can be obtained from a corresponding pure matrix product state by tracing out ancillary degrees of freedom on each of the spins. It thus reduces to those for pure matrix product states and classically correlated distributions as special cases. Because we are interested in the periodic steady state behavior of our model, we restrict ourselves to the single-site *translationally invariant* case where the A^{i_j} are independent of the site label j. We thus have that the $\chi_j = \chi$ are all equal. This quantity is known as the *bond dimension* of the MPDO, which quantifies the degree to which the state is correlated. Note that, in this representation, the state is specified by $d^2\chi^2$ complex parameters, an exponential improvement — when bond dimension is polynomial in N — over the $O(d^N)$ complex parameters required to specify each of the matrix elements of ρ_{MPDO} individually.

In our model, we let $\rho_{\mathbb{M}}(0) = \rho_{\text{MPDO}}$ be the parameterization of the initial quantum correlated state of the memory $\mathbb{M}$, which is uncorrelated with the initial state of D. We first solve the Lindblad master equation for an individual interaction

$$\frac{d\rho_{DM}}{dt} = \mathcal{L}_{DM}\left(\rho_{DM}\right) \tag{6.27}$$

analytically in Mathematica, obtaining an expression for the quantum operation

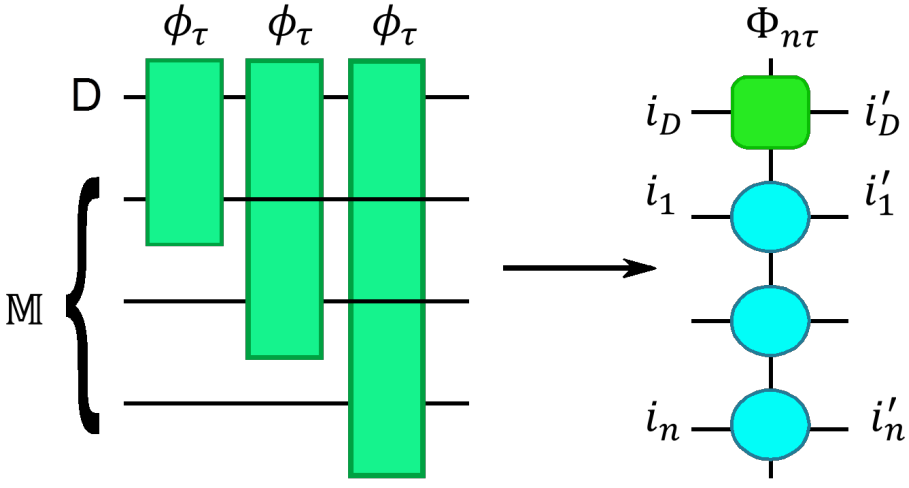

Figure 6.3: A pictorial representation of our time evolution method, which relies on a matrix product density operator (MPDO) description, for $n = 3$. On the left is a schematic depiction of our interaction sequence, with quantum operations vectorized so as to let us represent the sequence as a quantum circuit. The shared degree of freedom is the demon qubit D, and the remaining degrees of freedom are the memory $\mathbb{M}$. We indicate that a particular qubit is not acted upon by a given quantum operation by drawing the qubit's line *over* the quantum operation's box. We parameterize the sequence as a matrix product operator (MPO), shown on the right, with physical indices labeled according to the corresponding qubit degrees of freedom.

$$\phi_\tau \equiv e^{\mathcal{L}_{DM}\tau}. \tag{6.28}$$

We then update our initial state $\rho_{D\mathbb{M}}(0)$ to $\rho_{D\mathbb{M}}(n\tau) \approx \rho_{D\mathbb{M}}^{(\mathrm{ss})}$ according to the sequential evolution, Eq. (6.11), using the method schematically depicted in Fig.s 6.3 and 6.4. Here, we have vectorized the Hilbert space so as to represent quantum operations as matrices and density matrices as vectors (see Ref. [ZV04] for details). In Fig. 6.3, we apply a generalization of the result from Ref. [SSV+05] to parameterize our series of sequential quantum operations as a matrix product operator (MPO). Fig. 6.4 shows the update, which is performed by simply multiplying the initial MPDO, $\rho_{D\mathbb{M}}(0)$, by the MPO, $\Phi_{n\tau}$. This scheme permits us to only store $3 \times 4D_{(\mathrm{b})}^2$ parameters: the tensor corresponding to $M\tilde{M}$, that to $\bar{M}$, and a boundary tensor to D. The full details are given in Appendix C.3.

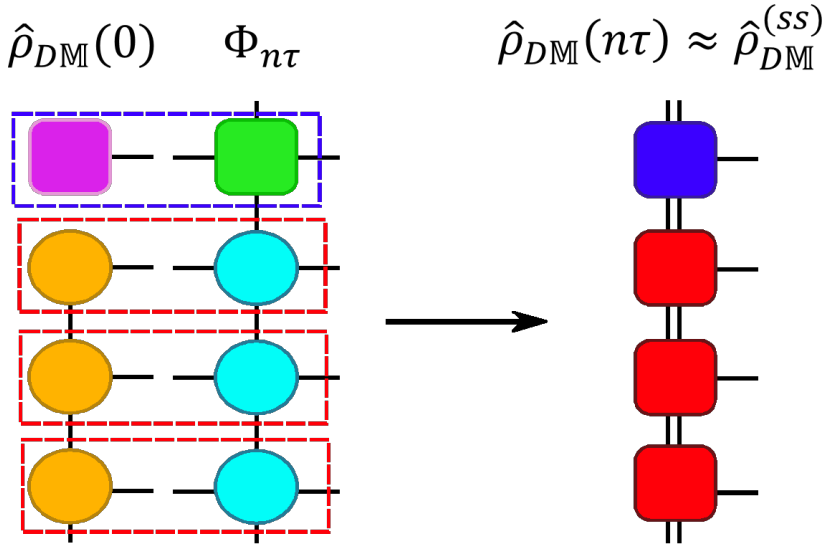

Figure 6.4: We multiply our initial MPDO, for which the state of $\mathbb{M}$ is translationally invariant and uncorrelated with that of D, by the MPO describing our interaction sequence to obtain an approximation to the steady state. This is done by performing a sequence of index contractions, shown on the left as dotted boxes. The approximation to the steady state, which is valid for sufficiently large n, is shown as the resulting MPDO on the right. All boundary conditions are taken to be periodic.

We next apply the classicality of our interaction, ϕ_τ, to simplify our MPDO description for $\rho_{DM\tilde{M}}^{(\mathrm{ss})}$ in terms of operationally-defined quantities as our second main result

Theorem 4 *The periodic steady state of $DM\tilde{M}$ prior to the interaction on M may be expressed as*

$$\rho_{DM\tilde{M}}^{(\mathrm{ss})} = \sum_{\vec{k}} p_{\vec{k}} \rho_D^{(\vec{k})} \otimes \rho_{M\tilde{M}}^{(\vec{k})}, \tag{6.29}$$

where the $\vec{k} \in \{0,1\}^n$ are classical bit strings of length n, which correspond to classical records on the memory subsystem $\bar{M}$. $p_{\vec{k}}$ is the probability of the record $\vec{k}$ ($\sum_{\vec{k}} p_{\vec{k}} = 1$), and $\rho_{M\tilde{M}}^{(\vec{k})}$ is the reduced state of $M\tilde{M}$ conditioned upon that record. $\rho_D^{(\vec{k})}$ is the reduced

state of D upon interacting with the string of uncorrelated classical pure qubits specified by $\vec{k}$, which is classical.

The proof and formal expressions for $p_{\vec{k}}$, $\rho_D^{(\vec{k})}$, and $\rho_{M\tilde{M}}^{(\vec{k})}$ can be found in Appendix C.3. Theorem 4 says that the steady state is always separable and given by a convex combination over all possible classical histories of the memory. Note that the memory part $\rho_{M\tilde{M}}^{(\vec{k})}$ could contain quantum coherence. It is convenient in that it expresses the steady state $\rho_{DM\tilde{M}}^{(\mathrm{ss})}$ in terms of the input (the $p_{\vec{k}}$ and the $\rho_{M\tilde{M}}^{(\vec{k})}$) and the interaction (the $\rho_D^{(\vec{k})}$) separately. This will allow us to engineer states of $\mathbb{M}$ so as to achieve a desired thermodynamic behavior. It is also a useful analytic tool when it is tractable (i.e. there are relatively few terms in the sum). We further demonstrate its utility by using it to prove that the demon's performance in steady state is invariant under local phase rotations on the memory, which we state formally in the following corollary

The Clausius terms, $Q_{h\to c}$, ΔS_M, and $\Delta I_{M:\tilde{M}}$, take the same values for the input states $\rho_{\mathbb{M}}(0)$ and $\mathcal{U}_{\mathbb{M}}^{z,\varphi}\left[\rho_{\mathbb{M}}(0)\right]$ in steady state, where

$$\mathcal{U}_{\mathbb{M}}^{z,\varphi}\left(\rho_{\mathbb{M}}\right) = \left(e^{-i(\varphi/2)Z}\right)^{\otimes n} \rho_{\mathbb{M}} \left(e^{i(\varphi/2)Z}\right)^{\otimes n} \tag{6.30}$$

constitutes an individual rotation about the z axis applied transversally to every qubit in $\mathbb{M}$.

To see this, we first note that we calculate $\rho_{DM\tilde{M}}^{(\mathrm{ss})}$ for $\mathcal{U}_{\mathbb{M}}^{z,\varphi}\left[\rho_{\mathbb{M}}(0)\right]$ by making the replacement

$$\rho_{M\tilde{M}}^{(\vec{k})} \mapsto \mathcal{U}_{M\tilde{M}}^{z,\varphi}\left(\rho_{M\tilde{M}}^{(\vec{k})}\right) \tag{6.31}$$

in Eq. (6.29). This is because transversal phase rotations do not affect the probabilities of classical measurements $p_{\vec{k}}$, nor the states $\rho_D^{(\vec{k})}$ by their definition. Furthermore, the states $\rho_D^{(\vec{k})}$ are classical and so invariant under phase rotation. We thus have

$$\sum_{\vec{k}} p_{\vec{k}} \rho_D^{(\vec{k})} \otimes \mathcal{U}_{M\tilde{M}}^{z,\varphi} \left(\rho_{M\tilde{M}}^{(\vec{k})} \right) = \sum_{\vec{k}} p_{\vec{k}} \, \mathcal{U}_{DM\tilde{M}}^{z,\varphi} \left(\rho_D^{(\vec{k})} \otimes \rho_{M\tilde{M}}^{(\vec{k})} \right) \tag{6.32}$$

$$\sum_{\vec{k}} p_{\vec{k}} \rho_D^{(\vec{k})} \otimes \mathcal{U}_{M\tilde{M}}^{z,\varphi} \left(\rho_{M\tilde{M}}^{(\vec{k})} \right) = \mathcal{U}_{DM\tilde{M}}^{z,\varphi} \left(\rho_{DM\tilde{M}} \right). \tag{6.33}$$

That is

$$(\mathcal{I}_D \otimes \mathcal{U}_M^{z,\varphi})(\rho_{DM}^{(\mathrm{ss})}) = \mathcal{U}_{DM}^{z,\varphi}(\rho_{DM}^{(\mathrm{ss})}), \tag{6.34}$$

where $\mathcal{I}$ is the identity superoperator. We see from Eq. (6.34) that $\mathcal{L}_{DM}$ commutes with $\mathcal{U}_M^{z,\varphi}$ on $\rho_{DM}^{(\mathrm{ss})}$, as the cooperative transition term commutes with $\mathcal{U}_{DM}^{z,\varphi}$, and the intrinsic transition and Hamiltonian terms commute with $\mathcal{U}_M^{z,\varphi}$ (Appendix C.1). Corollary 6.3.2 therefore follows from the fact that all of the terms in Eq. (6.19) are invariant under transversal phase rotations on $\rho_{M\tilde{M}}$ and $\rho'_{M\tilde{M}}$.

6.3.3 Simultaneous Refrigeration and Erasure

We first examine a special case, which is simple enough that the calculation of Eq. (6.29) is analytically tractable but also correlated enough to reveal nontrivial thermodynamic behavior.

Consider the family of Greenberger-Horne-Zeilinger (GHZ)-correlated states parametrized by a bias ζ,

$$|\psi\rangle_{\mathbb{M}} = \frac{1}{\sqrt{2}} \left(\sqrt{1+\zeta}|0\rangle^{\otimes N} + \sqrt{1-\zeta}|1\rangle^{\otimes N} \right), \tag{6.35}$$

with N sufficiently large to allow the system to reach a periodic steady state. There exists a non-equilibrium phase of simultaneous refrigeration ($Q_{h\to c} < 0$) and erasure

of memory ($\Delta S_M < 0$), when the memory is initially prepared to be the quantum entangled state $|\psi\rangle_{\mathbb{M}}$ with a bias ζ and a temperature gradient ε in the region illustrated in Fig. 6.5. We see that the reduced state on each qubit for any state in the family Eq. (6.35) is *locally classical* with bias ζ, and that for $\zeta = \pm 1$, $|\psi\rangle_{\mathbb{M}}$ is a product. For $\zeta \in (-1, 1)$ however, the state is entangled, with maximal entanglement at $\zeta = 0$.

For this family, we calculate the Clausius terms in Eq. (6.19) analytically by letting the system undergo n interactions — so that it reaches periodic steady state — and tracing out $\bar{M}$. In Eq. (6.29), only two classical histories appear in the sum, and we have

$$\rho_{M\tilde{M}} = \sum_{k\in\{0,1\}} \left[\frac{1+(-1)^k\zeta}{2}\right] \left(\sigma^k\right)^{\otimes(N-n)}, \tag{6.36}$$

and

$$\rho'_{M\tilde{M}} = \sum_{k\in\{0,1\}} \left[\frac{1+(-1)^k\zeta}{2}\right] \rho'^{(k)}_M \otimes \left(\sigma^k\right)^{\otimes(N-n-1)}, \tag{6.37}$$

where

$$\rho'^{(k)}_M = \mathrm{tr}_{D\bar{M}} \left\{ \Phi_{(n+1)\tau} \left[\rho_D(0) \otimes \sigma^k_M \otimes \left(\sigma^k\right)^{\otimes n}_{\bar{M}} \right] \right\} \tag{6.38}$$

is the state of M following its interaction for an uncorrelated tape of pure qubits in state $|k\rangle$, in periodic steady state. The global entropy change $\Delta S_{M\tilde{M}}$ then takes the particularly simple form

$$\Delta S_{M\tilde{M}} = \frac{1}{2}\left[(1+\zeta)S(\rho'^{(0)}_M) + (1-\zeta)S(\rho'^{(1)}_M)\right], \tag{6.39}$$

Note that this quantity is always nonnegative. By comparison, the local quantities

$$\Delta S_M = S\left[\left(\frac{1+\zeta}{2}\right)\rho_M'^{(0)} + \left(\frac{1-\zeta}{2}\right)\rho_M'^{(1)}\right] - S\left[\frac{1}{2}\left(I+\zeta Z\right)\right] \tag{6.40}$$

and

$$Q_{h\to c} = \frac{\Delta}{2}\left[\left(\frac{1+\zeta}{2}\right)\zeta'^{(0)} + \left(\frac{1-\zeta}{2}\right)\zeta'^{(1)} - \zeta\right], \tag{6.41}$$

where $\zeta'^{(i)} = \mathrm{tr}\left(Z_M \rho_M'^{(i)}\right)$, may be either positive or negative. Using the expressions for the $\zeta'^{(i)}$ given in Ref. [MQJ13], we analytically construct an analogous nonequilibrium phase diagram, Fig. 6.5, for $\tau = 0.3$ (in units of $1/\Delta$, where we have set $\hbar = 1$). We see that the effect of the correlation is to introduce a region of simultaneous refrigeration and erasure near the uncorrelated phase transition triple point at $\varepsilon = \zeta = 0$. ζ thus decreases below zero over the interaction in this region, indicating a deviation from monotonicity in the reduced evolution of M. This is the primary role of correlations in our thermodynamic model: in periodic steady state, initial correlations in $\mathbb{M}$ induce classical correlations between D and M to prior to their interaction, allowing ρ^M to pass through hitherto inaccessible regions of the Hilbert space in its evolution.

We examine this more closely in Fig. 6.6, where we plot the quantities in the local Clausius inequality, Eq. (6.15), for the input given in Eq. (6.35) as a function of τ for $\varepsilon = 0.01$ and $\zeta = 0$ as compared to the corresponding terms for product input with the same reduced state on every qubit. In Fig. 6.7, we plot the generation of correlations $\Delta I_{M:\tilde{M}} = \Delta S_M - \Delta S_{M\tilde{M}}$. We first note that, though correlations are always being consumed, the demon is not always able to use this to its advantage. This is as we expect, since the behavior must approach that of the uncorrelated case as $\tau \to \infty$. For $\tau \lesssim 0.54$, we see increasing simultaneous refrigeration and erasure with additional interaction time. Past $\tau \approx 0.54$, additional interaction time does not afford better thermodynamic performance, and eventually, we see that correlations

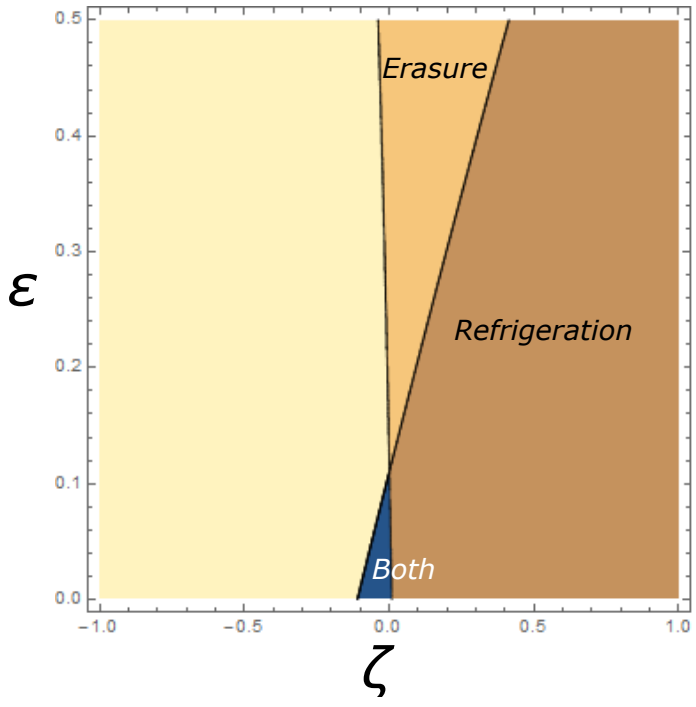

Figure 6.5: The nonequilibrium phase diagram for input states from the GHZ-correlated family described in Observation 6.3.3, analogous to Fig. 2 in Ref. [MQJ13], for $\tau = 0.3$ (units of $1/\Delta$ for $\hbar = 1$). For $\zeta = \pm 1$, the input is a product, and it is entangled for $\zeta \in (-1, 1)$, with the strongest correlations at $\zeta = 0$, for which it is the GHZ state. Note that, for every state in this family, the reduced state of any qubit is diagonal in the z basis. We see that correlations shift the phase boundaries so as to induce a region of simultaneous refrigeration and erasure near the uncorrelated phase transition triple point ($\varepsilon = \zeta = 0$).

actually begin to hinder the demon's erasure at $\tau \approx 1.6$. Finally, we see that the demon's behavior approaches that of the uncorrelated case as τ becomes large, as we expect.

We see from the diagonal form of $\rho_{M\tilde{M}}$ that we would have had the same effect if the input had been prepared in the equivalent classically correlated (i.e. diagonal in the computational basis) state

$$\rho_{\mathbb{M}}^{(\mathrm{c})} = \frac{1}{2}\left[(1+\zeta)\left(\sigma^0\right)^{\otimes N} + (1-\zeta)\left(\sigma^1\right)^{\otimes N}\right]. \tag{6.42}$$

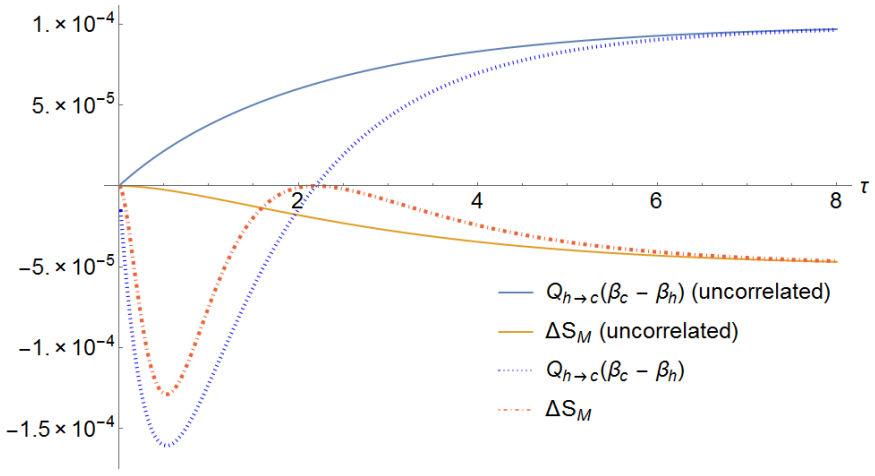

Figure 6.6: Dependence of the Clausius terms, $Q_{h\to c}(\beta_c - \beta_h)$ and ΔS_M, on the interaction time, τ when $\varepsilon = 0.01$ in comparing the GHZ-state ($\zeta = 0$) to its un-correlated counterpart (the product of its single-qubit reduced states, which are all maximally mixed). The reduced evolution of the interacting memory qubit is monotonic when there is a strict tradeoff of refrigeration and erasure; both cannot be simultaneously negative. This is obeyed by the uncorrelated input, but the correlated input shows a departure from monotonicity for $\tau \lesssim 2.2$. For long enough interaction times, the effect of correlations is "washed out" as the terms for correlated input approach the values for their uncorrelated-input counterparts.

We are then led to ask: is there anything to be said for the role of quantumness in this model? To address this, we consider another example, which will give our final result.

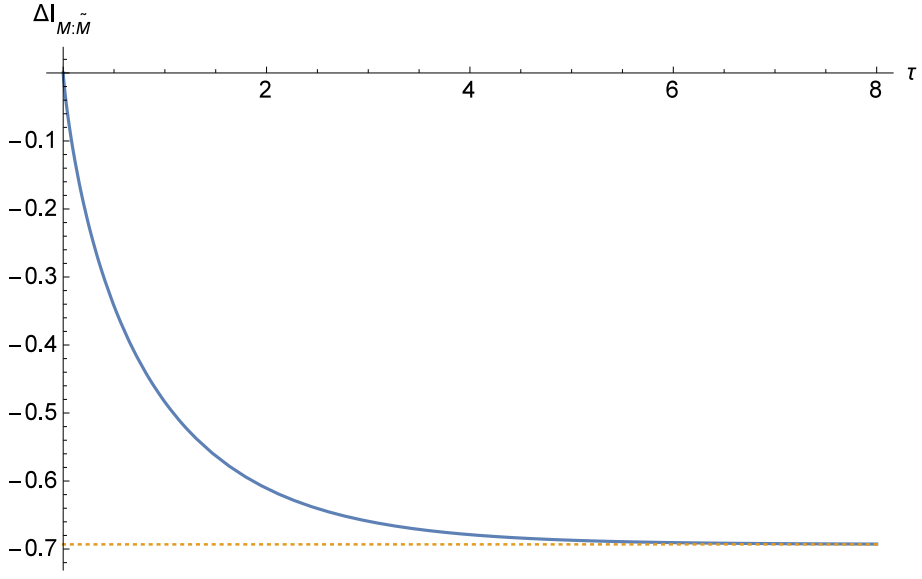

Figure 6.7: Generation of correlations $\Delta I_{M:\tilde{M}}$ between the interacting qubit M and the qubits $\tilde{M}$ yet to interact, as a function of the interaction time τ, for the GHZ input of Fig. 6.6. τ is in units of $1/\Delta$ for $\hbar = 1$, and $\varepsilon = 0.01$. Correlations are always being consumed, and so this term offsets the others in the Clausius inequality such that simultaneous refrigeration and erasure does not violate the second law for this input family. The dotted line is at $\Delta I_{M:\tilde{M}} = -\ln 2$ and is meant to provide a visual aid, as it represents the maximal possible consumption of correlations for this state.

6.3.4 Quantum Thermodynamic Advantage

As a final result, we observe that correlations can enable our model to exploit quantum coherence to gain a thermodynamic advantage. Using an arbitrary orthonormal $\vec{n}$ basis,

$$|+\vec{n}\rangle = \cos(\theta/2)\,|0\rangle + e^{i\phi}\sin(\theta/2)\,|1\rangle, \tag{6.43}$$

$$|-\vec{n}\rangle = \sin(\theta/2)\,|0\rangle - e^{i\phi}\cos(\theta/2)\,|1\rangle, \tag{6.44}$$

with $\theta \in [0, \pi]$, and $\phi \in [0, 2\pi)$, we define two states: (i) the GHZ-correlated input

family in an $\vec{n}$ basis $\rho^{(\mathrm{q})}_{\mathbb{M}} = |\psi\rangle\langle\psi|_{\mathbb{M}}$ such that

$$|\psi\rangle_{\mathbb{M}} = \frac{1}{\sqrt{2}}\left(\sqrt{1+\zeta_{\vec{n}}}|+\vec{n}\rangle^{\otimes N} + \sqrt{1-\zeta_{\vec{n}}}|-\vec{n}\rangle^{\otimes N}\right), \tag{6.45}$$

with N sufficiently large to allow the system to reach steady state, and (ii) its corresponding classically-correlated family,

$$\rho^{(\mathrm{c})}_{\mathbb{M}} = \sum_{\vec{k}} \left(\bigotimes_{j=1}^{N} \sigma^{k_j}\right) \rho^{(\mathrm{q})}_{\mathbb{M}} \left(\bigotimes_{j=1}^{N} \sigma^{k_j}\right) \tag{6.46}$$

with the $k_j \in \{0, 1\}$, obtained by eliminating all off-diagonal matrix elements from $\rho^{(\mathrm{q})}_{\mathbb{M}}$ in the z basis. The quantum entangled state $\rho^{(\mathrm{q})}_{\mathbb{M}}$ is advantageous in memory erasure over the classically-correlated mixed state $\rho^{(\mathrm{c})}_{\mathbb{M}}$, whose bias for every single-qubit reduced state is identical to that of $\rho^{(\mathrm{q})}_{\mathbb{M}}$.

This comparison might correspond to the scenario where the experimenter only has the ability to prepare correlations in a fixed basis, versus that where the experimenter has this ability in addition to the ability to perform phase rotations in an orthogonal basis. Thanks to Corollary 6.3.2, we know that this second ability is the only addition over the first needed to observe the full range of thermodynamic performance. Because the states $\rho^{(\mathrm{q})}_{\mathbb{M}}$ and $\rho^{(\mathrm{c})}_{\mathbb{M}}$ allow for all possible classical histories with some probability, the demon's performance cannot be easily calculated with Eq. (6.29) as with Eq. (6.35). We thus obtain our results numerically using the MPDO description.

In Fig. 6.9, we plot the exact region for which the advantage exists (i.e. $\Delta S^{(\mathrm{q})} < \Delta S^{(\mathrm{c})}$ and $\Delta S^{(\mathrm{q})} < 0$). We see here clearly the azimuthal symmetry of Corollary 6.3.2 and that this advantage sharply disappears as $\theta \to 0$. In Fig. 6.9 for $\varepsilon = 0.01$, we show the difference in erasures between the quantum and classical inputs as a function of τ. The quantum coherent state $\rho^{(\mathrm{q})}_{\mathbb{M}}$ has an advantage when this quantity is negative. This plot bears some resemblance to Fig. 6.6. This is no coincidence. In the same way as classical correlations in DM can allow the Bloch vector of M to momentarily move away from its fixed point along the z-axis, they can also allow it to do so in the

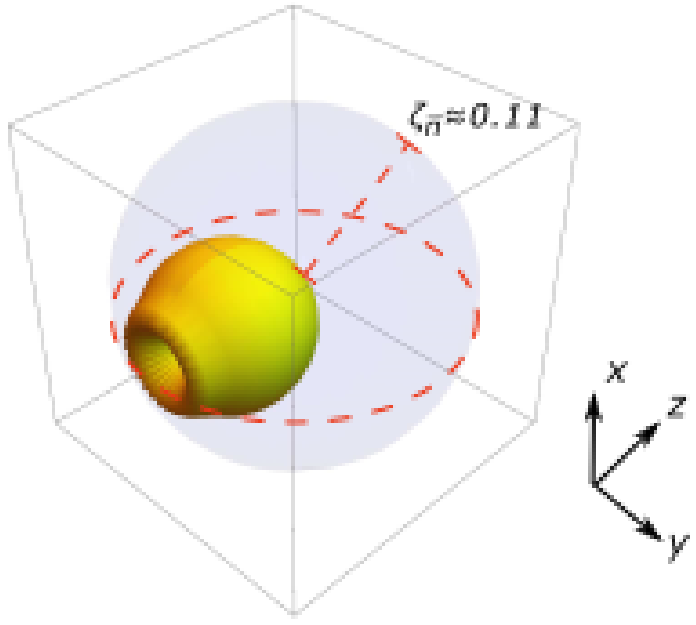

Figure 6.8: The 3-dimensional surface whose enclosure is the set of local Bloch vectors for which the locally coherent GHZ-correlated family attains a quantum erasure advantage over its corresponding classically correlated family, whose off-diagonal elements in the z basis have been projected out. Here, $\tau = 0.3$ and $\varepsilon = 0.01$. We see clearly the predicted azimuthal symmetry about the z-axis, and the advantage vanishes along this axis as we expect, since two inputs are the same in this case.

x-y plane, though the effect is smaller by several orders of magnitude. This deviation from monotonicity appears as an erasure advantage since our interaction ϕ_τ treats the classical and coherent components of the evolution separately. The refrigerative performances of the two inputs are thus identical as we expect.

What is remarkable is that even though both $\rho_{\mathbb{M}}^{(\mathrm{q})}$ and $\rho_{\mathbb{M}}^{(\mathrm{c})}$ share the same classical histories in Eq. (6.29), the small amount of coherence on the reduced state $\rho_M^{(\mathrm{q})}$ seems to be able to seed the production of more coherence. This is especially surprising given the fact that our dynamics ϕ_τ also has many classical features. The explanation is that the coherences on the conditional states of M for each classical history *interfere* such that there is more coherence on ρ_M after the evolution than before.

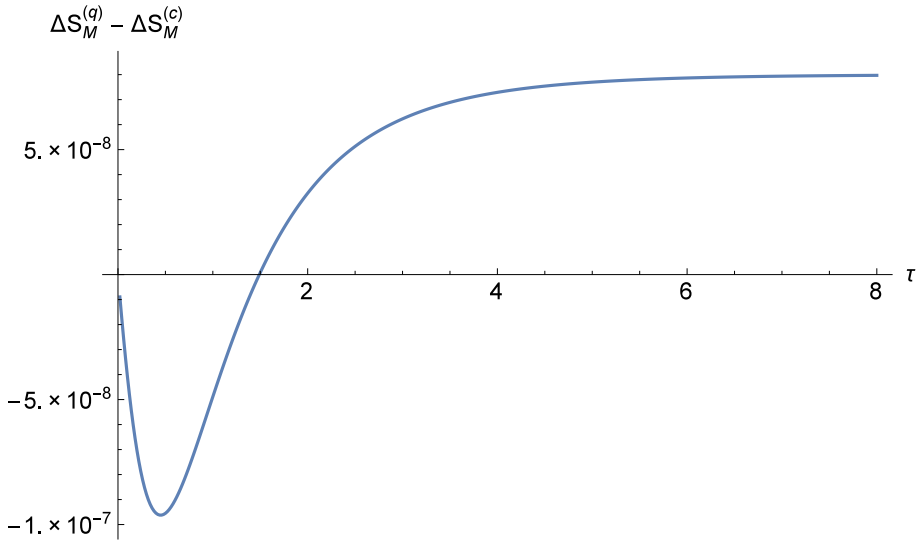

Figure 6.9: The difference between the erasure performance for the quantum correlated locally coherent input state and that of its decohered counterpart for $\varepsilon = 0.01$, $\phi = \pi/2$, $\theta = 0.01$, and $\zeta_{\vec{n}} = -0.02$ as a function of the interaction time τ. A quantum advantage is demonstrated when this quantity is negative. We see that the advantage is several orders of magnitude smaller and lost much faster than the advantage afforded by classical correlations of Fig. 6.5

6.4 Conclusion

We have shown that our model of an autonomous Maxwell demon can utilize correlations in its memory to gain a thermodynamic advantage over its uncorrelated counterpart. That is, as predicted by the global Clausius inequality, it performs simultaneous refrigeration and erasure, which is impossible without correlations, and exploits quantum coherence to enhance the performance of memory erasure. This work represents a proof-of-principle, and we hope that it paves the way to invent a quantum thermodynamic device which is more well-suited to utilizing correlations.

There are two concluding discussions. First, in this work, entanglement did not demonstrate a genuine advantage over classical correlations. This is because of the long-range nature of GHZ correlations. Namely, tracing out a distant subsystem gives a classically correlated state, but does not affect the thermodynamic performance, which is determined by the local interaction between the demon qubit and one of

memory qubits. However, as long as we explored shortly, short-range correlated states appear to lose the simultaneous refrigeration-erasure phase. So more demanding numerical calculation seems to be needed to generalize beyond these simple initial states, to address the question about strict supremacy of entanglement.

Second, thanks to the simplicity of our model, it could provide a feasible experimental test of quantum coherence as a thermodynamic resource. The autonomy of the model is convenient to brings it closer to the realm of quantum heat engines [SZAW03, GEV02, LPS10, CRVdB12, EKLVdB12, GKAK13, VFG13, BR13, CPAA13, CPAA14, Ali14, LBA15], and in particular those considered in Refs. [SGKA13, VW09, VSHW11]. These experiments relate to a two-level system (TLS) in a cavity with a buffer gas, driven by a laser field. The demon in this case is the TLS, while the two thermal reservoirs are the buffer gas and electromagnetic modes of the cavity. The memory is realized by the laser. Our work demonstrates that even classical correlations in the laser could provide an advantage in refrigerating the cavity, as would correlated coherences in the energy eigenbasis of the TLS. Thus, this model might represent a promising step in designing small heat engines which take advantage of correlations.

Chapter 7

Summary and Outlook

We have shown in this thesis how an understanding of propagation in quantum many-body systems is essential to the design and implementation of a quantum computation. With our first two main results, we demonstrated an application of the many-body-localization transition of condensed matter physics to the performance of a quantum computer. The essential idea behind this thesis is that, when the dynamics of a quantum computation are too disordered, propagation in the quantum system is limited to a regime where it can be simulated classically. In Chapter 4, we demonstrated how this could be done for computations which are simulated by noninteracting particles, and we extended to the interacting regime in Chapter 5. A key feature of many-body localization in the latter example is localization at a critical, nonzero value of the disorder. Finally, in Chapter 6, we, with the aid of matrix product density operators, were able to demonstrate how the presence of quantum correlations can enhance the performance of an autonomous quantum Maxwell demon.

One relevant question for future work is how localization affects other quantum computational tasks, and the first that comes to mind is error-correction. In quantum error-correction, the quantum information of interest is actually encoded in degrees of freedom which are inaccessible to natural decoherence processes, and so it is protected from the errors caused by these processes. A notable class of examples is the ground states of topologically ordered systems, such as the Kitaev toric code, which are

highly entangled. It would of-course be useful if the collective many-body dynamics of such systems also forced these error processes to localize, allowing us to quickly correct them before they could corrupt our logical quantum information.

Another clear application that we touched on in Chapter 5 is that of quantum adiabatic optimization algorithms (QAOA). These algorithms are generated by repetitions of a unit-cell unitary, which is then optimized to solve a particular computational task. It has been shown, even for low-depth instances, that these algorithms possess an advantage over classical computers for some problems. Naturally, we expect localization to hinder the performance of these algorithms, since that would generally render them classically simulatable. Nevertheless, it would be interesting to connect a transition in *classical complexity* to the many-body localization transition exhibited by such algorithms, as localizing QAOA circuits could reveal easy instances of classical problems that we were hitherto unaware of.

Appendix A

"Classical simulation of quantum circuits by dynamical localization"

A.1 Proof of Theorem 4.1

For convenience, we begin by first quickly re-deriving Eq. (3.7) here. Let A and B be two Pauli operators (i.e. $A^\dagger = A$, $B^\dagger = B$, and $A^2 = B^2 = I$) and U be a matchgate unitary, then we have

$$||[A, U^\dagger BU]||_F^2 = \mathrm{tr}\{[A, U^\dagger BU]^\dagger [A, U^\dagger BU]\} \tag{A.1}$$

$$= -\,\mathrm{tr}\{[A, U^\dagger BU]^2\} \tag{A.2}$$

$$= -\,\mathrm{tr}\Big[A\left(U^\dagger BU\right)A\left(U^\dagger BU\right) - A\left(U^\dagger BU\right)\left(U^\dagger BU\right)A - \left(U^\dagger BU\right)AA\left(U^\dagger BU\right) + \left(U^\dagger BU\right)A\left(U^\dagger BU\right)A\Big] \tag{A.3}$$

$$= \mathrm{tr}\Big[2I - 2A\left(U^\dagger BU\right)A\left(U^\dagger BU\right)\Big] \tag{A.4}$$

$$||[A, U^\dagger BU]||_F^2 = 2\left\{2^n - \mathrm{tr}\Big[A\left(U^\dagger BU\right)A\left(U^\dagger BU\right)\Big]\right\} \tag{A.5}$$

From Eq. (A.2) to Eq. (A.3), we used Hermiticity of A and B, and we expanded

the expresion in Eq. (A.4). From this equation to Eq. (A.5), we used $A^2 = B^2 = I$, and from the fourth to the fifth line, we used $\mathrm{tr}(I) = 2^n$ on n qubits. Dividing by a normalization of 2^{n+2} on both sides, we have

$$\frac{1}{2^{n+2}}|||[A, U^\dagger BU]|||_F^2 = \frac{1}{2}\left\{1 - \frac{1}{2^n}\,\mathrm{tr}\left[A\left(U^\dagger BU\right)A\left(U^\dagger BU\right)\right]\right\} \tag{A.6}$$

Next, we assume $A = i^a C_{\vec{\eta}}$ and $B = i^b C_{\vec{\alpha}}$ for some integers a and b, such that i^a and i^b ensure that A and B are Hermitian, respectively. E.g., for A, this implies

$$A^\dagger = (-i)^a C_{\vec{\eta}}^\dagger \tag{A.7}$$

$$A^\dagger = (-i)^a (-1)^{\frac{1}{2}|\vec{\eta}|(|\vec{\eta}|-1)} C_{\vec{\eta}}, \tag{A.8}$$

where $C_{\vec{\eta}}^\dagger = (-1)^{\frac{1}{2}|\vec{\eta}|(|\vec{\eta}|-1)} C_{\vec{\eta}}$, since the individual Majorana modes are Hermitian and we need $\frac{1}{2}|\vec{\eta}|(|\vec{\eta}|-1)$ anticommutations between individual distinct modes to reverse the order of $|\vec{\eta}|$ modes. Since $A^\dagger = A$, Eq. (A.8) implies

$$i^a C_{\vec{\eta}} \;\; = (-i)^a (-1)^{\frac{1}{2}|\vec{\eta}|(|\vec{\eta}|-1)} C_{\vec{\eta}}, \tag{A.9}$$

and multiplying both sides of this equation by $i^a C_{\vec{\eta}}^\dagger$ gives

$$i^{2a} I \;\; = (-1)^{\frac{1}{2}|\vec{\eta}|(|\vec{\eta}|-1)} I. \tag{A.10}$$

Thus, $i^{2a} = (-1)^{\frac{1}{2}|\vec{\eta}|(|\vec{\eta}|-1)}$, and similarly, $i^{2b} = (-1)^{\frac{1}{2}|\vec{\alpha}|(|\vec{\alpha}|-1)}$. Continuing from the dynamical term in Eq. (A.6), we have

$$\frac{1}{2^n}(-1)^{\frac{1}{2}[|\vec{\alpha}|(|\vec{\alpha}|-1)+|\vec{\eta}|(|\vec{\eta}|-1)]}\,\mathrm{tr}\left[A\left(U^\dagger BU\right)A\left(U^\dagger BU\right)\right]$$

$$= \frac{1}{2^n}\,\mathrm{tr}\left[C_{\vec{\eta}}\left(U^\dagger C_{\vec{\alpha}}U\right)C_{\vec{\eta}}\left(U^\dagger C_{\vec{\alpha}}U\right)\right] \tag{A.11}$$

$$= \frac{1}{2^n}\sum_{\{\vec{\beta},\vec{\beta}'||\vec{\beta}|=|\vec{\beta}'|=|\vec{\alpha}|\}}\det\left(\mathbf{u}_{\vec{\alpha}\vec{\beta}}\right)\det\left(\mathbf{u}_{\vec{\alpha}\vec{\beta}'}\right)\mathrm{tr}\left(C_{\vec{\eta}}C_{\vec{\beta}}C_{\vec{\eta}}C_{\vec{\beta}'}\right) \tag{A.12}$$

$$= \frac{1}{2^n}(-1)^{|\vec{\alpha}||\vec{\eta}|+\frac{1}{2}|\vec{\eta}|(|\vec{\eta}|-1)}\sum_{\{\vec{\beta},\vec{\beta}'||\vec{\beta}|=|\vec{\beta}'|=|\vec{\alpha}|\}}(-1)^{|\vec{\eta}\cap\vec{\beta}|}\det\left(\mathbf{u}_{\vec{\alpha}\vec{\beta}}\right)$$
$$\times\det\left(\mathbf{u}_{\vec{\alpha}\vec{\beta}'}\right)\mathrm{tr}\left(C_{\vec{\beta}}C_{\vec{\beta}'}\right) \tag{A.13}$$

$$= (-1)^{|\vec{\alpha}||\vec{\eta}|+\frac{1}{2}[|\vec{\alpha}|(|\vec{\alpha}|-1)+|\vec{\eta}|(|\vec{\eta}|-1)]}\sum_{\{\vec{\beta},\vec{\beta}'||\vec{\beta}|=|\vec{\beta}'|=|\vec{\alpha}|\}}(-1)^{|\vec{\eta}\cap\vec{\beta}|}$$
$$\times\det\left(\mathbf{u}_{\vec{\alpha}\vec{\beta}}\right)\det\left(\mathbf{u}_{\vec{\alpha}\vec{\beta}'}\right)\delta_{\vec{\beta}\vec{\beta}'} \tag{A.14}$$

$$\frac{1}{2^n}\,\mathrm{tr}\left[A\left(U^\dagger BU\right)A\left(U^\dagger BU\right)\right] = (-1)^{|\vec{\alpha}||\vec{\eta}|}\sum_{\{\vec{\beta},\vec{\beta}'||\vec{\beta}|=|\vec{\beta}'|=|\vec{\alpha}|\}}(-1)^{|\vec{\eta}\cap\vec{\beta}|}$$
$$\times\det\left(\mathbf{u}_{\vec{\alpha}\vec{\beta}}\right)\det\left(\mathbf{u}_{\vec{\alpha}\vec{\beta}'}\right)\delta_{\vec{\beta}\vec{\beta}'} \tag{A.15}$$

From Eq. (A.12) to Eq. (A.13), we used

$$C_{\vec{\eta}}C_{\vec{\beta}} = (-1)^{|\vec{\beta}||\vec{\eta}|+|\vec{\eta}\cap\vec{\beta}|}C_{\vec{\beta}}C_{\vec{\eta}} \tag{A.16}$$

$$C_{\vec{\eta}}^2 = (-1)^{\frac{1}{2}|\vec{\eta}|(|\vec{\eta}|-1)}I \tag{A.17}$$

and similarly from Eq. (A.13) to the Eq. (A.14), as well as the fact that $|\vec{\beta}| = |\vec{\alpha}|$. We recognize that

$$\det\left[(\mathbf{I}-2\mathbf{P}_{\vec{\eta}})_{\vec{\beta}\vec{\beta}'}\right] = (-1)^{|\vec{\eta}\cap\vec{\beta}|}\delta_{\vec{\beta}\vec{\beta}'} \tag{A.18}$$

where $\mathbf{P}_{\vec{\eta}}$ is the projector onto modes $\vec{\eta}$. We therefore have

$$\frac{1}{2^n}\,\mathrm{tr}\left[A\left(U^\dagger BU\right)A\left(U^\dagger BU\right)\right]$$
$$= (-1)^{|\vec{\alpha}||\vec{\eta}|}\sum_{\{\vec{\beta},\vec{\beta}'||\vec{\beta}|=|\vec{\beta}'|=|\vec{\alpha}|\}}\det\left(\mathbf{u}_{\vec{\alpha}\vec{\beta}}\right)\det\left[(\mathbf{I}-2\mathbf{P}_{\vec{\eta}})_{\vec{\beta}\vec{\beta}'}\right]\det\left(\mathbf{u}_{\vec{\alpha}\vec{\beta}'}\right) \tag{A.19}$$

$$= (-1)^{|\vec{\alpha}||\vec{\eta}|}\det[\mathbf{u}_{\vec{\alpha}[2n]}(\mathbf{I}-2\mathbf{P}_{\vec{\eta}})\mathbf{u}^{\mathrm{T}}_{[2n]\vec{\alpha}}], \tag{A.20}$$

which follows from the Cauchy-Binet formula. This therefore proves the theorem

$$\frac{1}{2^{n+2}}|||[A,U^\dagger BU]|||^2 = \frac{1}{2}\left\{1-(-1)^{|\vec{\alpha}||\vec{\eta}|}\det[\mathbf{u}_{\vec{\alpha}[2n]}(\mathbf{I}-2\mathbf{P}_{\vec{\eta}})\mathbf{u}^{\mathrm{T}}_{[2n]\vec{\alpha}}]\right\} \tag{A.21}$$

A.2 Modified Cauchy-Binet Formula

Here we prove

$$\sum_{\{\vec{\beta}\subset\vec{B}||\vec{\beta}|=|\vec{\alpha}|-|\vec{S}|\}}\det\left(\mathbf{u}_{\vec{\alpha},\vec{\beta}\cup\vec{S}}\right)\det\left(\mathbf{v}_{\vec{\alpha},\vec{\beta}\cup\vec{S}}\right) = (-1)^{|\vec{S}|}\det\begin{pmatrix}\mathbf{0}_{|\vec{S}|\times|\vec{S}|} & \mathbf{v}^{\mathrm{T}}_{\vec{S}\vec{\alpha}}\\ \mathbf{u}_{\vec{\alpha}\vec{S}} & \mathbf{u}_{\vec{\alpha}\vec{B}}\mathbf{v}^{\mathrm{T}}_{\vec{B}\vec{\alpha}}\end{pmatrix} \tag{A.22}$$

for $\vec{S}$ disjoint from $\vec{B}$. We first rearrange rows and columns inside the matrices $\mathbf{u}$ and $\mathbf{v}$ in the l.h.s. of (A.22) to bring each of them to a fiducial form, $\mathbf{u}'$ and $\mathbf{v}'$, respectively. These are such that $\mathbf{u}'_{\vec{\alpha}'\vec{S}'} = \mathbf{u}_{\vec{\alpha}\vec{S}}$ and $\mathbf{u}'_{\vec{\alpha}'\vec{B}'} = \mathbf{u}_{\vec{\alpha}\vec{B}}$ (and similarly for $\mathbf{v}'$), for $\vec{\alpha}' \equiv [|\vec{\alpha}|]$ and $\vec{S}' \equiv [|\vec{S}|]$. That is, we bring the rows $\vec{\alpha}$ to the top and the columns $\vec{S}$ to the left inside the matrices $\mathbf{u}$ and $\mathbf{v}$ without changing the internal ordering of these tuples, nor the ordering of $\vec{B}$. This is done purely for convenience of presentation and will not affect the argument, as we will undo the rearrangement in the end. We will continue to refer to the numbers of elements in these rearranged tuples by those of their unprimed counterparts (i.e. using $|\vec{S}|$ instead of $|\vec{S}'|$), as they

are equal. Since this rearrangement is done for both $\mathbf{u}$ and $\mathbf{v}$, any resulting sign factor acquired due to the alternating sign property of the determinant will cancel in the product, and we have

$$\begin{aligned}
&\sum_{\{\vec{\beta}\subset\vec{B}||\vec{\beta}|=|\vec{\alpha}|-|\vec{S}|\}} \det\left(\mathbf{u}_{\vec{\alpha},\vec{\beta}\cup\vec{S}}\right)\det\left(\mathbf{v}_{\vec{\alpha},\vec{\beta}\cup\vec{S}}\right) \\
&\quad= \sum_{\{\vec{\beta}\subset\vec{B}'||\vec{\beta}|=|\vec{\alpha}|-|\vec{S}|\}} \det\left[\mathbf{u}'_{\vec{\alpha}'(\vec{S}',\vec{\beta})}\right]\det\left[\mathbf{v}'_{\vec{\alpha}'(\vec{S}',\vec{\beta})}\right],
\end{aligned} \tag{A.23}$$

We will next need the Laplace "expansion by complimentary minors" formula

$$\det(\mathbf{u}) = \sum_{\{\vec{H}||\vec{H}|=k\}} \varepsilon^{\vec{H},\vec{L}}\det(\mathbf{u}_{\vec{H}\vec{L}})\det(\mathbf{u}_{\bar{H}\bar{L}}), \tag{A.24}$$

where $\varepsilon^{\vec{H},\vec{L}} = (-1)^{\sum_{j=1}^{k}\left(H_j+L_j\right)}$, $\vec{L}$ is a fixed subset of the columns of $\mathbf{u}$ of size k, the sum is over all subsets $\vec{H}$ of rows of $\mathbf{u}$ of size k, and $\overline{L}$ and $\overline{H}$ are the set-complements of $\vec{L}$ and $\vec{H}$ in the sets of all columns and rows of $\mathbf{u}$, respectively. This is the analogous formula to expanding the determinant by minors of a fixed column, generalized to a subset of columns $\vec{L}$. Applying Eq. (A.24) to the columns $\vec{S}'$ of $\mathbf{u}'$ and $\mathbf{v}'$ on the r.h.s. of (A.23) gives

$$\begin{aligned}
&\sum_{\{\vec{\beta}\subset\vec{B}||\vec{\beta}|=|\vec{\alpha}|-|\vec{S}|\}} \det\left(\mathbf{u}_{\vec{\alpha},\vec{\beta}\cup\vec{S}}\right)\det\left(\mathbf{v}_{\vec{\alpha},\vec{\beta}\cup\vec{S}}\right) \\
&\quad= \sum_{\{\vec{\beta}\subset\vec{B}'||\vec{\beta}|=|\vec{\alpha}|-|\vec{S}|\}} \left[\sum_{\{\vec{H}\subset\vec{\alpha}'||\vec{H}|=|\vec{S}|\}} \varepsilon^{\vec{H},\vec{S}'}\det\left(\mathbf{u}'_{\vec{H}\vec{S}'}\right)\det\left(\mathbf{u}'_{\vec{\alpha}'\setminus\vec{H},\vec{\beta}}\right)\right] \\
&\qquad\times\left[\sum_{\{\vec{L}\subset\vec{\alpha}'||\vec{L}|=|\vec{S}|\}} \varepsilon^{\vec{L},\vec{S}'}\det\left(\mathbf{v}'_{\vec{L}\vec{S}'}\right)\det\left(\mathbf{v}'_{\vec{\alpha}'\setminus\vec{L},\vec{\beta}}\right)\right] \\
&\quad= \sum_{\substack{\{\vec{H}\subset\vec{\alpha}'||\vec{H}|=|\vec{S}|\}\\ \{\vec{L}\subset\vec{\alpha}'||\vec{L}|=|\vec{S}|\}}} \varepsilon^{\vec{H},\vec{S}'}\varepsilon^{\vec{L},\vec{S}'}\det\left(\mathbf{u}'_{\vec{H}\vec{S}'}\right)\det\left(\mathbf{v}'_{\vec{L}\vec{S}'}\right)
\end{aligned} \tag{A.25}$$

$$\times \left[\sum_{\{\vec{\beta}\subset\vec{B}'||\vec{\beta}|=|\vec{\alpha}|-|\vec{S}|\}} \det\left(\mathbf{u}'_{\vec{\alpha}'\setminus\vec{H},\vec{\beta}}\right) \det\left(\mathbf{v}'_{\vec{\alpha}'\setminus\vec{L},\vec{\beta}}\right) \right]. \tag{A.26}$$

We next apply the Cauchy-Binet formula to the sum in square brackets, as

$$\sum_{\{\vec{\beta}\subset\vec{B}'||\vec{\beta}|=|\vec{\alpha}|-|\vec{S}|\}} \det\left(\mathbf{u}'_{\vec{\alpha}'\setminus\vec{H},\vec{\beta}}\right) \det\left(\mathbf{v}'_{\vec{\alpha}'\setminus\vec{L},\vec{\beta}}\right) = \det\left(\mathbf{u}'_{\vec{\alpha}'\setminus\vec{H},\vec{B}'}\mathbf{v}'^{\mathrm{T}}_{\vec{B}',\vec{\alpha}'\setminus\vec{L}}\right). \tag{A.27}$$

Notice that the matrix in the determinant of the r.h.s. above is simply $\mathbf{u}'_{\vec{\alpha}'\vec{B}'}\mathbf{v}'^{\mathrm{T}}_{\vec{B}'\vec{\alpha}'}$ with the rows $\vec{H}$ and columns $\vec{L}$ removed (i.e. instead of removing the rows and columns and then multiplying, we can multiply and then remove rows and columns from the product). This gives

$$\begin{aligned}
&\sum_{\{\vec{\beta}\subset\vec{B}||\vec{\beta}|=|\vec{\alpha}|-|\vec{S}|\}} \det\left(\mathbf{u}_{\vec{\alpha},\vec{\beta}\cup\vec{S}}\right) \det\left(\mathbf{v}_{\vec{\alpha},\vec{\beta}\cup\vec{S}}\right) \\
&\quad = \sum_{\substack{\{\vec{H}\subset\vec{\alpha}'||\vec{H}|=|\vec{S}|\} \\ \{\vec{L}\subset\vec{\alpha}'||\vec{L}|=|\vec{S}|\}}} \varepsilon^{\vec{H},\vec{S}'}\varepsilon^{\vec{L},\vec{S}'} \det\left(\mathbf{u}'_{\vec{H}\vec{S}'}\right) \det\left(\mathbf{v}'_{\vec{L}\vec{S}'}\right) \det\left[\left(\mathbf{u}'_{\vec{\alpha}'\vec{B}'}\mathbf{v}'^{\mathrm{T}}_{\vec{B}'\vec{\alpha}'}\right)_{\vec{\alpha}'\setminus\vec{H},\vec{\alpha}'\setminus\vec{L}}\right].
\end{aligned} \tag{A.28}$$

The next step is to "put back in" the rows $\vec{H}$ and columns $\vec{L}$. We do this by treating (A.28) as an expansion of the determinant of a larger matrix by complimentary minors of rows $\mathbf{v}'^{\mathrm{T}}_{\vec{S}'\vec{\alpha}'}$ and then columns $\mathbf{u}'_{\vec{\alpha}'\vec{S}'}$. Working backwards, we see that the sum over $\vec{H}$ in Eq. (A.28) evaluates to

$$\begin{aligned}
&\sum_{\{\vec{H}\subset\vec{\alpha}'||\vec{H}|=|\vec{S}|\}} \varepsilon^{\vec{H},\vec{S}'} \det\left(\mathbf{u}'_{\vec{H}\vec{S}'}\right) \det\left[\left(\mathbf{u}'_{\vec{\alpha}'\vec{B}'}\mathbf{v}'^{\mathrm{T}}_{\vec{B}'\vec{\alpha}'}\right)_{\vec{\alpha}'\setminus\vec{H},\vec{\alpha}'\setminus\vec{L}}\right] \\
&\qquad = \det\left[\begin{pmatrix} \mathbf{u}'_{\vec{\alpha}'\vec{S}'} & \left(\mathbf{u}'_{\vec{\alpha}'\vec{B}'}\mathbf{v}'^{\mathrm{T}}_{\vec{B}'\vec{\alpha}'}\right)_{\vec{\alpha}',\vec{\alpha}'\setminus\vec{L}} \end{pmatrix}\right]
\end{aligned} \tag{A.29}$$

To put the rows back in, we note that

$$\det\left(\mathbf{v}'_{\vec{L}\vec{S}'}\right) = \det\left(\mathbf{v}'^{\mathrm{T}}_{\vec{S}'\vec{L}}\right) = (-1)^{|\vec{S}|}\det\left[\begin{pmatrix} \mathbf{0}_{|\vec{S}|\times|\vec{S}|} & \mathbf{v}'^{\mathrm{T}}_{\vec{S}'\vec{\alpha}'} \end{pmatrix}_{\vec{S}'\vec{L}'}\right], \tag{A.30}$$

where $\vec{L}'$ is related to $\vec{L}$ by $L'_j = L_j + |\vec{S}|$ for all $j \in \{1, 2, \ldots, |\vec{L}| = |\vec{S}|\}$. Shifting the columns over by $|\vec{S}|$ inside the determinant gives the overall factor of $(-1)^{|\vec{S}|}$. Thus, the sum over $\vec{L}$ in Eq. (A.28) evaluates to

$$\begin{aligned}
&\sum_{\{\vec{L}\subset\vec{\alpha}'||\vec{L}|=|\vec{S}|\}} \varepsilon^{\vec{L},\vec{S}'}\det\left(\mathbf{v}'_{\vec{L}\vec{S}'}\right)\det\left[\begin{pmatrix} \mathbf{u}'_{\vec{\alpha}'\vec{S}'} & \left(\mathbf{u}'_{\vec{\alpha}'\vec{B}'}\mathbf{v}'^{\mathrm{T}}_{\vec{B}'\vec{\alpha}'}\right)_{\vec{\alpha}',\vec{\alpha}'\setminus\vec{L}} \end{pmatrix}\right] \\
&\quad = (-1)^{|\vec{S}|}\sum_{\{\vec{L}\subset\left[|\vec{\alpha}|+|\vec{S}|\right]||\vec{L}|=|\vec{S}|\}} \varepsilon^{\vec{L},\vec{S}'}\det\left[\begin{pmatrix} \mathbf{0}_{|\vec{S}|\times|\vec{S}|} & \mathbf{v}'^{\mathrm{T}}_{\vec{S}'\vec{\alpha}'} \end{pmatrix}_{\vec{S}'\vec{L}}\right] \\
&\qquad\qquad \times\det\left[\begin{pmatrix} \mathbf{u}'_{\vec{\alpha}'\vec{S}'} & \mathbf{u}'_{\vec{\alpha}'\vec{B}'}\mathbf{v}'^{\mathrm{T}}_{\vec{B}'\vec{\alpha}'} \end{pmatrix}_{\vec{\alpha}',\vec{\alpha}'\setminus\vec{L}}\right] \qquad (A.31) \\
&\quad = (-1)^{|\vec{S}|}\det\begin{pmatrix} \mathbf{0}_{|\vec{S}|\times|\vec{S}|} & \mathbf{v}^{\mathrm{T}}_{\vec{S}\vec{\alpha}} \\ \mathbf{u}_{\vec{\alpha}\vec{S}} & \mathbf{u}_{\vec{\alpha}\vec{B}}\mathbf{v}^{\mathrm{T}}_{\vec{B}\vec{\alpha}} \end{pmatrix}. \qquad (A.32)
\end{aligned}$$

In the first equality, we apply Eq. (A.30) together with the fact that, for each term in the sum for which $\vec{L}$ contains any of the first $|\vec{S}|$ columns, the matrix in the first determinant factor of that term contains at least one column of all zeros, and so the term evaluates to zero. This brings the second line to a form which we recognize to be an expansion by complementary minors of the rows $\vec{S}'$ in the larger matrix in the third line. Finally, we use $\mathbf{u}'_{\vec{\alpha}'\vec{S}'} = \mathbf{u}_{\vec{\alpha}\vec{S}}$ (and similarly for the other submatrices) to undo our initial row and column rearrangements and therefore obtain the formula, Eq. (A.22).

A.3 Fixed-Parity Sum

Here we prove

$$\sum_{\substack{\{\vec{\beta}_l \subset \vec{B}_l, \vec{\beta}_r \subset \vec{B}_r || \vec{\beta}_l| + |\vec{\beta}_r| = |\vec{\alpha}| - |\vec{S}|, \\ |\vec{\beta}_r| \bmod 2 = p\}}} \det\left[\mathbf{u}_{\vec{\alpha},(\vec{\beta}_l,\vec{S},\vec{\beta}_r)}\right] \det\left[\mathbf{v}_{\vec{\alpha},(\vec{\beta}_l,\vec{S},\vec{\beta}_r)}\right]$$

$$= \frac{(-1)^{|\vec{S}|}}{2}\left[\det\begin{pmatrix} \mathbf{0}_{|\vec{S}|\times|\vec{S}|} & \mathbf{v}^{\mathrm{T}}_{\vec{S}\vec{\alpha}} \\ \mathbf{u}_{\vec{\alpha}\vec{S}} & \mathbf{u}_{\vec{\alpha}\vec{B}}\mathbf{v}^{\mathrm{T}}_{\vec{B}\vec{\alpha}} \end{pmatrix} + (-1)^p \det\begin{pmatrix} \mathbf{0}_{|\vec{S}|\times|\vec{S}|} & \mathbf{v}^{\mathrm{T}}_{\vec{S}\vec{\alpha}} \\ \mathbf{u}_{\vec{\alpha}\vec{S}} & \mathbf{u}_{\vec{\alpha}\vec{B}}\left(\mathbf{I} - 2\mathbf{P}_{\vec{B}_r}\right)_{\vec{B}\vec{B}}\mathbf{v}^{\mathrm{T}}_{\vec{B}\vec{\alpha}} \end{pmatrix}\right], \tag{A.33}$$

where $\vec{S}$ is disjoint from $\vec{B} \equiv (\vec{B}_l, \vec{B}_r)$. The statement follows simply from

$$\left(\sum_{\substack{\{\vec{\beta}_l \subset \vec{B}_l, \vec{\beta}_r \subset \vec{B}_r || \vec{\beta}_l| + |\vec{\beta}_r| = |\vec{\alpha}| - |\vec{S}|, \\ |\vec{\beta}_r| \text{ even}\}}} - \sum_{\substack{\{\vec{\beta}_l \subset \vec{B}_l, \vec{\beta}_r \subset \vec{B}_r || \vec{\beta}_l| + |\vec{\beta}_r| = |\vec{\alpha}| - |\vec{S}|, \\ |\vec{\beta}_r| \text{ odd}\}}}\right) \times \det\left[\mathbf{u}_{\vec{\alpha},(\vec{\beta}_l,\vec{S},\vec{\beta}_r)}\right] \det\left[\mathbf{v}_{\vec{\alpha},(\vec{\beta}_l,\vec{S},\vec{\beta}_r)}\right]$$

$$= \left[\sum_{\substack{\{\vec{\beta}_l \subset \vec{B}_l, \vec{\beta}_r \subset \vec{B}_r || \vec{\beta}_l| + |\vec{\beta}_r| = |\vec{\alpha}| - |\vec{S}|, \\ |\vec{\beta}_r| \text{ even}\}}} (-1)^{|\vec{\beta}_r|} + \sum_{\substack{\{\vec{\beta}_l \subset \vec{B}_l, \vec{\beta}_r \subset \vec{B}_r || \vec{\beta}_l| + |\vec{\beta}_r| = |\vec{\alpha}| - |\vec{S}|, \\ |\vec{\beta}_r| \text{ odd}\}}} (-1)^{|\vec{\beta}_r|}\right] \times \det\left[\mathbf{u}_{\vec{\alpha},(\vec{\beta}_l,\vec{S},\vec{\beta}_r)}\right] \det\left[\mathbf{v}_{\vec{\alpha},(\vec{\beta}_l,\vec{S},\vec{\beta}_r)}\right] \tag{A.34}$$

$$= \sum_{\{(\vec{\beta}_l,\vec{\beta}_r) \subset \vec{B} || \vec{\beta}_l| + |\vec{\beta}_r| = |\vec{\alpha}| - |\vec{S}|\}} (-1)^{|\vec{\beta}_r|} \det\left[\mathbf{u}_{\vec{\alpha},(\vec{\beta}_l,\vec{S},\vec{\beta}_r)}\right] \det\left[\mathbf{v}_{\vec{\alpha},(\vec{\beta}_l,\vec{S},\vec{\beta}_r)}\right] \tag{A.35}$$

In Eq. (A.34), we used the fact that $(-1)^{|\vec{\beta}_r|} = 1$ in the former sum, and $(-1)^{|\vec{\beta}_r|} = -1$ in the latter. In Eq. (A.34), we simply combined the sums over all even-sized $\vec{\beta}_r$ and all odd-sized $\vec{\beta}_r$ with the same summand into the sum over all $(\vec{\beta}_l, \vec{\beta}_r)$. We next apply the steps we used to prove the modified Cauchy-Binet formula, except now applying

$$\det\left[\left(\mathbf{I} - 2\mathbf{P}_{\vec{B}_r}\right)_{(\vec{\beta}_l,\vec{\beta}_r)(\vec{\beta}'_l,\vec{\beta}'_r)}\right] = (-1)^{|\vec{\beta}_r|}\delta_{\vec{\beta}_l\vec{\beta}'_l}\delta_{\vec{\beta}_r\vec{\beta}'_r} \tag{A.36}$$

to evaluate the sum with the sign factor $(-1)^{|\vec{\beta}_r|}$ which appears in the place of Eq. (A.27). This gives

$$\begin{aligned}
&\left(\sum_{\substack{\{\vec{\beta}_l \subset \vec{B}_l, \vec{\beta}_r \subset \vec{B}_r || \vec{\beta}_l| + |\vec{\beta}_r| = |\vec{\alpha}| - |\vec{S}|, \\ |\vec{\beta}_r| \text{ even}\}}} - \sum_{\substack{\{\vec{\beta}_l \subset \vec{B}_l, \vec{\beta}_r \subset \vec{B}_r || \vec{\beta}_l| + |\vec{\beta}_r| = |\vec{\alpha}| - |\vec{S}|, \\ |\vec{\beta}_r| \text{ odd}\}}} \right) \\
&\qquad \times \det \left[\mathbf{u}_{\vec{\alpha},(\vec{\beta}_l,\vec{S},\vec{\beta}_r)} \right] \det \left[\mathbf{v}_{\vec{\alpha},(\vec{\beta}_l,\vec{S},\vec{\beta}_r)} \right] \\
&\qquad = (-1)^{|\vec{S}|} \det \begin{pmatrix} \mathbf{0}_{|\vec{S}| \times |\vec{S}|} & \mathbf{v}^{\mathrm{T}}_{\vec{S}\vec{\alpha}} \\ \mathbf{u}_{\vec{\alpha}\vec{S}} & \mathbf{u}_{\vec{\alpha}\vec{B}} (\mathbf{I} - 2\mathbf{P}_{\vec{B}_r})_{\vec{B}\vec{B}} \mathbf{v}^{\mathrm{T}}_{\vec{B}\vec{\alpha}} \end{pmatrix},
\end{aligned} \tag{A.37}$$

from Eq. (A.22). Applying this, together with

$$\begin{aligned}
&\left(\sum_{\substack{\{\vec{\beta}_l \subset \vec{B}_l, \vec{\beta}_r \subset \vec{B}_r || \vec{\beta}_l| + |\vec{\beta}_r| = |\vec{\alpha}| - |\vec{S}|, \\ |\vec{\beta}_r| \text{ even}\}}} + \sum_{\substack{\{\vec{\beta}_l \subset \vec{B}_l, \vec{\beta}_r \subset \vec{B}_r || \vec{\beta}_l| + |\vec{\beta}_r| = |\vec{\alpha}| - |\vec{S}|, \\ |\vec{\beta}_r| \text{ odd}\}}} \right) \\
&\qquad \times \det \left[\mathbf{u}_{\vec{\alpha},(\vec{\beta}_l,\vec{S},\vec{\beta}_r)} \right] \det \left[\mathbf{v}_{\vec{\alpha},(\vec{\beta}_l,\vec{S},\vec{\beta}_r)} \right] \\
&\qquad = (-1)^{|\vec{S}|} \det \begin{pmatrix} \mathbf{0}_{|\vec{S}| \times |\vec{S}|} & \mathbf{v}^{\mathrm{T}}_{\vec{S}\vec{\alpha}} \\ \mathbf{u}_{\vec{\alpha}\vec{S}} & \mathbf{u}_{\vec{\alpha}\vec{B}} \mathbf{v}^{\mathrm{T}}_{\vec{B}\vec{\alpha}} \end{pmatrix}
\end{aligned} \tag{A.38}$$

we solve for the sums over even $|\vec{\beta}_r|$ and odd $|\vec{\beta}_r|$ individually to obtain Eq. (A.33) above.

A.4 Exact Calculation of the OTO Correlator

Here we give an explicit calculation of the matrix $\mathbf{M}_s$, defined implicitly by

$$\frac{1}{2^{n+2}} ||[\mathbf{n}_s \cdot \boldsymbol{\sigma}_s, U^\dagger C_{\vec{\alpha}} U]||_F^2 \equiv \mathbf{n}_s^* \cdot \mathbf{M}_s \cdot \mathbf{n}_s \tag{A.39}$$

for some single-spin operator $\mathbf{n}_s \cdot \boldsymbol{\sigma}_s$ acting on qubit s, matchgate unitary U, and Majorana configuration $C_{\vec{\alpha}}$, where $||A||^2 \equiv \mathrm{tr}\left(A^\dagger A\right)$. Since we are only considering a single spin s, we drop the spin labels on $\mathbf{n} \equiv \mathbf{n}_s$ and $\mathbf{M} \equiv \mathbf{M}_s$ in this section for convenience, choosing to label the components of these objects by subscripts instead. We begin by expanding the r.h.s., using this definition and Eq. (2.77)

$$\begin{aligned}
&\frac{1}{2^{n+2}}|||[\mathbf{n}\cdot\boldsymbol{\sigma}_s, U^\dagger C_{\vec{\alpha}} U]|||_F^2 \\
&\quad= \frac{1}{2^{n+2}}\,\mathrm{tr}\left\{\left[\sum_{k\in\{x,y,z\}} n_k \sigma_s^k, \sum_{\{\vec{\beta}||\vec{\beta}|=|\vec{\alpha}|\}} \det\left(\mathbf{u}_{\vec{\alpha}\vec{\beta}}\right) C_{\vec{\beta}}\right]^\dagger \right. \\
&\qquad\qquad \left. \times \left[\sum_{k'\in\{x,y,z\}} n_{k'} \sigma_s^{k'}, \sum_{\{\vec{\beta}'||\vec{\beta}'|=|\vec{\alpha}|\}} \det\left(\mathbf{u}_{\vec{\alpha}\vec{\beta}'}\right) C_{\vec{\beta}'}\right]\right\} \qquad \text{(A.40)} \\
&\quad= \frac{1}{2^{n+2}} \sum_{k,k'\in\{x,y,z\}} n_k^* n_{k'} \\
&\qquad\qquad \times \sum_{\substack{\{\vec{\beta}||\vec{\beta}|=|\vec{\alpha}|\} \\ \{\vec{\beta}'||\vec{\beta}'|=|\vec{\alpha}|\}}} \det\left(\mathbf{u}_{\vec{\alpha}\vec{\beta}}\right) \det\left(\mathbf{u}_{\vec{\alpha}\vec{\beta}'}\right) \mathrm{tr}\left\{\left[\sigma_s^k, C_{\vec{\beta}}\right]^\dagger \left[\sigma_s^{k'}, C_{\vec{\beta}'}\right]\right\}
\end{aligned}$$

(A.41)

Thus

$$M_{kk'} \equiv \frac{1}{2^{n+2}} \sum_{\substack{\{\vec{\beta}||\vec{\beta}|=|\vec{\alpha}|\} \\ \{\vec{\beta}'||\vec{\beta}'|=|\vec{\alpha}|\}}} \det\left(\mathbf{u}_{\vec{\alpha}\vec{\beta}}\right) \det\left(\mathbf{u}_{\vec{\alpha}\vec{\beta}'}\right) \mathrm{tr}\left\{\left[\sigma_s^k, C_{\vec{\beta}}\right]^\dagger \left[\sigma_s^{k'}, C_{\vec{\beta}'}\right]\right\} \qquad \text{(A.42)}$$

We can obtain the diagonal elements of $\mathbf{M}$, for which $k = k'$, from Theorem 1. It remains, then, to calculate the off-diagonal elements of $\mathbf{M}$. Clearly, $\mathbf{M} = \mathbf{M}^{\mathrm{T}}$ by the cyclic property of the trace and the fact that the sum over $\vec{\beta}$ and $\vec{\beta}'$ is symmetric in these indices. Furthermore, we must have $M_{xz} = M_{yz} = 0$ since there are no $\vec{\beta}$ and $\vec{\beta}'$ for which $|\vec{\beta}| = |\vec{\beta}'|$ and which describe the same Pauli string on every spin except

s, with a X_s (or Y_s) present on one and a Z_s present on the other. This is because the former are always described by exactly one Majorana operator and the latter by either two or zero Majorana operators. Therefore, we are only left to calculate M_{xy}. In this case, we have

$$M_{xy} = \frac{1}{2^{n+2}} \sum_{\substack{\{\vec{\beta}||\vec{\beta}|=|\vec{\alpha}|\} \\ \{\vec{\beta}'||\vec{\beta}'|=|\vec{\alpha}|\}}} \det\left(\mathbf{u}_{\vec{\alpha}\vec{\beta}}\right) \det\left(\mathbf{u}_{\vec{\alpha}\vec{\beta}'}\right) \operatorname{tr}\left\{\left[X_s, C_{\vec{\beta}}\right]^\dagger \left[Y_s, C_{\vec{\beta}'}\right]\right\} \tag{A.43}$$

The only nonvanishing terms will be those for which $\vec{\beta}$ and $\vec{\beta}'$ describe the same Pauli string on every spin except for s and for which there is a Y_s present for $C_{\vec{\beta}}$ and an X_s present for $C_{\vec{\beta}'}$. We examine the conditions under which an operator $\sigma_s^{k'}$ will be present in $C_{\vec{\beta}}$. Let $\vec{\beta} = \left(\vec{\beta}_l, \vec{\beta}_s, \vec{\beta}_r\right)$, where $\vec{\beta}_l \subset [2(s-1)]$ consists of all indices less than $2s-1$, and $\vec{\beta}_r \subset \overline{[2s]}$ consists of all indices greater than $2s$ (corresponding to the spins to the left and right of s, respectively). We have

$$\begin{aligned}
X_s \text{ present only if either : } \vec{\beta}_s &= \begin{cases} (2s-1) & \text{and } |\vec{\beta}_r| \text{ even} \\ (2s) & \text{and } |\vec{\beta}_r| \text{ odd} \end{cases} \\
Y_s \text{ present only if either : } \vec{\beta}_s &= \begin{cases} (2s) & \text{and } |\vec{\beta}_r| \text{ even} \\ (2s-1) & \text{and } |\vec{\beta}_r| \text{ odd} \end{cases} \\
Z_s \text{ present only if either : } \vec{\beta}_s &= \begin{cases} (2s-1, 2s) & \text{and } |\vec{\beta}_r| \text{ even} \\ () & \text{and } |\vec{\beta}_r| \text{ odd} \end{cases}
\end{aligned} \tag{A.44}$$

When $|\vec{\beta}_r|$ is odd, then $C_{\vec{\beta}}$ and $C_{\vec{\beta}'}$ will have a relative phase of -1 between them since $X_s Z_s = -iY_s$, but $Y_s Z_s = iX_s$. Additionally taking into account the fact that $[X_s, Y_s] = -[Y_s, X_s]$ gives

$$M_{xy} = \left(\sum_{\substack{\{(\vec{\beta}_l,\vec{\beta}_r)||\vec{\beta}_l|+|\vec{\beta}_r|+1=|\vec{\alpha}|,\\ |\vec{\beta}_r| \text{ odd}\}}} - \sum_{\substack{\{(\vec{\beta}_l,\vec{\beta}_r)||\vec{\beta}_l|+|\vec{\beta}_r|+1=|\vec{\alpha}|,\\ |\vec{\beta}_r| \text{ even}\}}} \right) \times \det\left[\mathbf{u}_{\vec{\alpha}(\vec{\beta}_l,2s-1,\vec{\beta}_r)}\right] \det\left[\mathbf{u}_{\vec{\alpha}(\vec{\beta}_l,2s,\vec{\beta}_r)}\right] \tag{A.45}$$

$$M_{xy} = \det \begin{pmatrix} 0 & \mathbf{u}^{\mathrm{T}}_{(2s)\vec{\alpha}} \\ \mathbf{u}_{\vec{\alpha}(2s-1)} & \mathbf{u}_{\vec{\alpha}\overline{(2s-1,2s)}} \left(\mathbf{I} - 2\mathbf{P}_{\overline{[2s]}}\right)_{\overline{(2s-1,2s)}(2s-1,2s)} \mathbf{u}^{\mathrm{T}}_{\overline{(2s-1,2s)}\vec{\alpha}} \end{pmatrix}, \tag{A.46}$$

therefore completing the calculation. For completeness, we list the elements of $\mathbf{M}$, once again, below

$$M_{xx} = \frac{1}{2}\left\{1 - (-1)^{|\vec{\alpha}|} \det[\mathbf{u}_{\vec{\alpha}[2n]}(\mathbf{I} - 2\mathbf{P}_{[2s-1]})\mathbf{u}^{\mathrm{T}}_{[2n]\vec{\alpha}}]\right\} \tag{A.47}$$

$$M_{yy} = \frac{1}{2}\left\{1 - (-1)^{|\vec{\alpha}|} \det[\mathbf{u}_{\vec{\alpha}[2n]}(\mathbf{I} - 2\mathbf{P}_{[2(s-1)]\cup(2s)})\mathbf{u}^{\mathrm{T}}_{[2n]\vec{\alpha}}]\right\} \tag{A.48}$$

$$M_{zz} = \frac{1}{2}\left\{1 - \det[\mathbf{u}_{\vec{\alpha}[2n]}(\mathbf{I} - 2\mathbf{P}_{(2s-1,2s)})\mathbf{u}^{\mathrm{T}}_{[2n]\vec{\alpha}}]\right\} \tag{A.49}$$

$$M_{xy} = M_{yx} = \det \begin{pmatrix} 0 & \mathbf{u}^{\mathrm{T}}_{(2s)\vec{\alpha}} \\ \mathbf{u}_{\vec{\alpha}(2s-1)} & \mathbf{u}_{\vec{\alpha}\overline{(2s-1,2s)}} \left(\mathbf{I} - 2\mathbf{P}_{\overline{[2s]}}\right)_{\overline{(2s-1,2s)}(2s-1,2s)} \mathbf{u}^{\mathrm{T}}_{\overline{(2s-1,2s)}\vec{\alpha}} \end{pmatrix} \tag{A.50}$$

$$M_{xz} = M_{zx} = M_{yz} = M_{zy} = 0 \tag{A.51}$$

A.5 Proof of Theorem 4.2

Here we prove the statement

$$\overline{|\langle O\rangle - \langle(\otimes_{s\in S}\mathcal{E}_s)(O)\rangle|} \leq \frac{1}{\sqrt{2^{n+2}}} \sum_{s\in S} ||[\mathbf{n}_s\cdot\boldsymbol{\sigma}_s, O]|| \equiv \sum_{s\in S} \sqrt{\mathbf{n}_s^*\cdot\mathbf{M}_s\cdot\mathbf{n}_s}, \tag{A.52}$$

where the average $\overline{(\cdot)}$ is taken over a product basis $\{\otimes_{j=1}^{n}|(-1)^{\ell_j}\mathbf{n}_j^{\perp}\rangle\}_{\boldsymbol{\ell}\in\{0,1\}^{\times n}}$ whose Bloch axes are orthogonal to the $\{\mathbf{n}_s\}_s$, and $\mathcal{E}_s$ is the depolarizing channel on qubit s, given by

$$\mathcal{E}_s(O) = \frac{1}{4}\left(O + \sum_{k\in\{x,y,z\}} \sigma_s^k O \sigma_s^k\right). \tag{A.53}$$

This channel has the effect of projecting O onto its component which acts only as the identity on site s. We further assume that O is a traceless Hermitian operator. We first show that the left-hand side of Eq. (A.52) is bounded by the trace norm for any averaging orthonormal basis set $\{|j\rangle\}_j$ and Hermitian operator A, as

$$\overline{|\langle A\rangle|} \equiv \frac{1}{2^n}\sum_{j=1}^{2^n}|\langle j|A|j\rangle| \tag{A.54}$$

$$= \frac{1}{2^n}\sum_{j=1}^{2^n}|\sum_{k=1}^{2^n}U_{kj}^* d_k U_{kj}| \tag{A.55}$$

$$\leq \frac{1}{2^n}\sum_{j,k=1}^{2^n}|d_k||U_{kj}|^2 \tag{A.56}$$

$$= \frac{1}{2^n}\sum_{k=1}^{2^n}|d_k| \tag{A.57}$$

$$\overline{|\langle A\rangle|} \leq \frac{1}{2^n}\operatorname{tr}|A| \tag{A.58}$$

From the first to the second line, we used the fact that we assume A to be a Hermitian operator, and so can be diagonalized as $A = U^\dagger D U$, for D a diagonal matrix. From the second to the third line, we applied the triangle inequality, and from the third to the fourth line, we rearranged sums and used the fact that $\sum_{j=1}^{2^n}|U_{kj}|^2 = 1$. The resulting quantity is the trace norm.

Without loss of generality, let $S = \{1, 2, \ldots, |S|\}$. Then we have, for any input state

$$|\langle O\rangle - \langle(\otimes_{s\in S}\mathcal{E}_s)(O)\rangle| = |\langle O\rangle + \sum_{k=1}^{|S|-1}\left[\langle\left(\otimes_{j=1}^{k}\mathcal{E}_j\right)(O)\rangle - \langle\left(\otimes_{j=1}^{k}\mathcal{E}_j\right)(O)\rangle\right] - \langle(\otimes_{s\in S}\mathcal{E}_s)(O)\rangle| \tag{A.59}$$

$$= |\sum_{k=1}^{|S|}\left\{\langle\left(\otimes_{j=1}^{k-1}\mathcal{E}_j\right)(O)\rangle - \langle\left(\otimes_{j=1}^{k-1}\mathcal{E}_j\right)[\mathcal{E}_k(O)]\rangle\right\}| \tag{A.60}$$

$$|\langle O\rangle - \langle(\otimes_{j\in S}\mathcal{E}_j)(O)\rangle| \leq \sum_{k=1}^{|S|}|\langle\left(\otimes_{j=1}^{k-1}\mathcal{E}_j\right)(O)\rangle - \langle\left(\otimes_{j=1}^{k-1}\mathcal{E}_j\right)[\mathcal{E}_k(O)]\rangle|, \tag{A.61}$$

where, from the first to the second line, we expressed the difference as a telescoping sum (let $\otimes_{j=1}^{0}\mathcal{E}_j(O) \equiv O$) and applied the triangle inequality in the third line. Next, we use the fact that, for any single-spin input $|\mathbf{n}^{\perp}\rangle$, the depolarized operator expectation value is the same as that of the dephased operator in any basis orthogonal to the input. That is, let $(\mathbf{n}\cdot\boldsymbol{\sigma})\,|\mathbf{n}^{\perp}\rangle = e^{i\phi}|-\mathbf{n}^{\perp}\rangle$ for some phase ϕ, and we have

$$|\langle O\rangle - \langle\mathcal{E}_s(O)\rangle| = |\langle O\rangle - \langle\frac{1}{2}\left[O + (\mathbf{n}\cdot\boldsymbol{\sigma}_s)\,O\,(\mathbf{n}\cdot\boldsymbol{\sigma}_s)\right]\rangle| \tag{A.62}$$

$$|\langle O\rangle - \langle\mathcal{E}_s(O)\rangle| = \frac{1}{2}|\langle O\rangle - \langle(\mathbf{n}\cdot\boldsymbol{\sigma}_s)\,O\,(\mathbf{n}\cdot\boldsymbol{\sigma}_s)\rangle| \tag{A.63}$$

on input state $|\mathbf{n}^{\perp}\rangle$ on qubit s. Furthermore, taking the same quantity for input state $|-\mathbf{n}^{\perp}\rangle$ has the effect of exchanging O and $(\mathbf{n}\cdot\boldsymbol{\sigma}_s)\,O\,(\mathbf{n}\cdot\boldsymbol{\sigma}_s)$ inside the absolute value, leaving it unchanged. Thus, we average over a product basis of $\{\otimes_{j=1}^{n}|(-1)^{\ell_j}\mathbf{n}_j^{\perp}\rangle\}_{\boldsymbol{\ell}\in\{0,1\}^{\times n}}$ on both sides of Eq. (A.61) and apply Eq. (A.63) to obtain

$$\overline{|\langle O\rangle - \langle(\otimes_{s\in S}\mathcal{E}_s)(O)\rangle|} \leq \frac{1}{2^{n+1}}\sum_{k=1}^{|S|}\mathrm{tr}\,|\left(\otimes_{j=1}^{k-1}\mathcal{E}_j\right)(O) - \left(\otimes_{j=1}^{k-1}\mathcal{E}_j\right)\left[(\mathbf{n}_k\cdot\boldsymbol{\sigma}_k)\,O\,(\mathbf{n}_k\cdot\boldsymbol{\sigma}_k)\right]| \tag{A.64}$$

$$\overline{|\langle O\rangle - \langle(\otimes_{s\in S}\mathcal{E}_s)(O)\rangle|} \leq \frac{1}{2^{n+1}}\sum_{k=1}^{|S|}\mathrm{tr}\,|O - (\mathbf{n}_k\cdot\boldsymbol{\sigma}_k)\,O\,(\mathbf{n}_k\cdot\boldsymbol{\sigma}_k)\,|, \tag{A.65}$$

using the bound (A.58) in the second line and the fact that the depolarizing channel cannot increase the trace distance between operators in the third. Finally, we apply the operator norm inequality

$$\operatorname{tr}|A| \equiv \operatorname{tr}\sqrt{A^\dagger A} \leq \sqrt{r \operatorname{tr} A^\dagger A} \leq \sqrt{2^n \operatorname{tr} A^\dagger A}, \tag{A.66}$$

where $r \leq 2^n$ is the rank of A, together with the fact that

$$\begin{aligned} \operatorname{tr}\left\{ \left[O - (\mathbf{n}_k \cdot \boldsymbol{\sigma}_k)\, O\, (\mathbf{n}_k \cdot \boldsymbol{\sigma}_k)\right]^\dagger \left[O - (\mathbf{n}_k \cdot \boldsymbol{\sigma}_k)\, O\, (\mathbf{n}_k \cdot \boldsymbol{\sigma}_k)\right] \right\} \\ = ||[\mathbf{n}_k \cdot \boldsymbol{\sigma}_k, O]||_F^2, \end{aligned} \tag{A.67}$$

for $||\cdot||_F$ the Frobenius norm, to arrive at our result

$$\overline{|\langle O\rangle - \langle(\otimes_{s\in S}\mathcal{E}_s)(O)\rangle|} \leq \frac{1}{2^{n+1}} \sum_{s\in S} \operatorname{tr}|O - (\mathbf{n}_s \cdot \boldsymbol{\sigma}_s)\, O\, (\mathbf{n}_s \cdot \boldsymbol{\sigma}_s)\,| \tag{A.68}$$

$$\leq \frac{\sqrt{2^n}}{2^{n+1}} \sum_{s\in S} ||[\mathbf{n}_s \cdot \boldsymbol{\sigma}_s, O]||_F \tag{A.69}$$

$$\overline{|\langle O\rangle - \langle(\otimes_{s\in S}\mathcal{E}_s)(O)\rangle|} \leq \frac{1}{\sqrt{2^{n+2}}} \sum_{s\in S} ||[\mathbf{n}_s \cdot \boldsymbol{\sigma}_s, O]||_F \equiv \sum_{s\in S} \sqrt{\mathbf{n}_s^* \cdot \mathbf{M}_s \cdot \mathbf{n}_s}. \tag{A.70}$$

We remark that the bound is a sum of terms which are always between zero and one, and by Markov's inequality, we can use this result to bound the fraction of these basis states for which the change in expectation value exceeds some threshold δ

$$\mu\left[|\langle O\rangle - \langle(\otimes_{s\in S}\mathcal{E}_s)(O)\rangle| \geq \delta\right] \leq \frac{1}{\delta} \sum_{s\in S} \sqrt{\mathbf{n}_s^* \cdot \mathbf{M}_s \cdot \mathbf{n}_s}. \tag{A.71}$$

Since we expect each of these terms to be exponentially decaying outside of the lightcone, depolarizing in this region should only induce a change in expectation value greater than the threshold for some exponentially small set of input states. This affords us exponential precision so long as we are willing to tolerate a fixed fraction of these "pathological" states. Finally, since we had a freedom in choosing which basis over which to depolarize in Eq. (A.63), we may optimize each of the $\{\mathbf{n}_s\}_s$ over the subspace for which they are orthogonal to the Bloch axes of the input to make this bound as restrictive as possible.

A.6 Numerical Analysis

We characterize the propagation of $B(t)$ by taking the singular value decomposition in discrete time

$$|||[\mathbf{n}_s \cdot \boldsymbol{\sigma}_s, B(t_k)]|||_F = \sum_j \lambda_j u_j(t_k) v_j(s), \tag{A.72}$$

where $t_k \equiv k\delta t$, and $\lambda_1 > \lambda_2 > \ldots$ for the singular values λ_j. We take the function $u_1(t)$ to represent the light cone envelope and $v_1(s)$ the decay profile of $|||[\mathbf{n}_s \cdot \boldsymbol{\sigma}_s, B(t)]|||_F$ outside of this envelope. This method has several advantages: (i) the principal singular value component is the closest *product* approximation to the light cone, and so has the form of the right-hand-side of Eq. (4.1) in the main text; (ii) the singular values themselves give the error incurred in the approximation; and (iii) the principal singular value component is robust to fluctuations from specific disorder realizations, greatly reducing the number of samples needed. It therefore gives an operationally meaningful, robust, and numerically inexpensive means of extracting the envelope and decay profile, which is completely general beyond the setting of matchgate circuits considered here.

In Fig. A.1, we plot the results of our analysis for the X-light cones of Fig. 4.1 in the main text. We see that the envelopes (linear scale on top left, and log-log scale

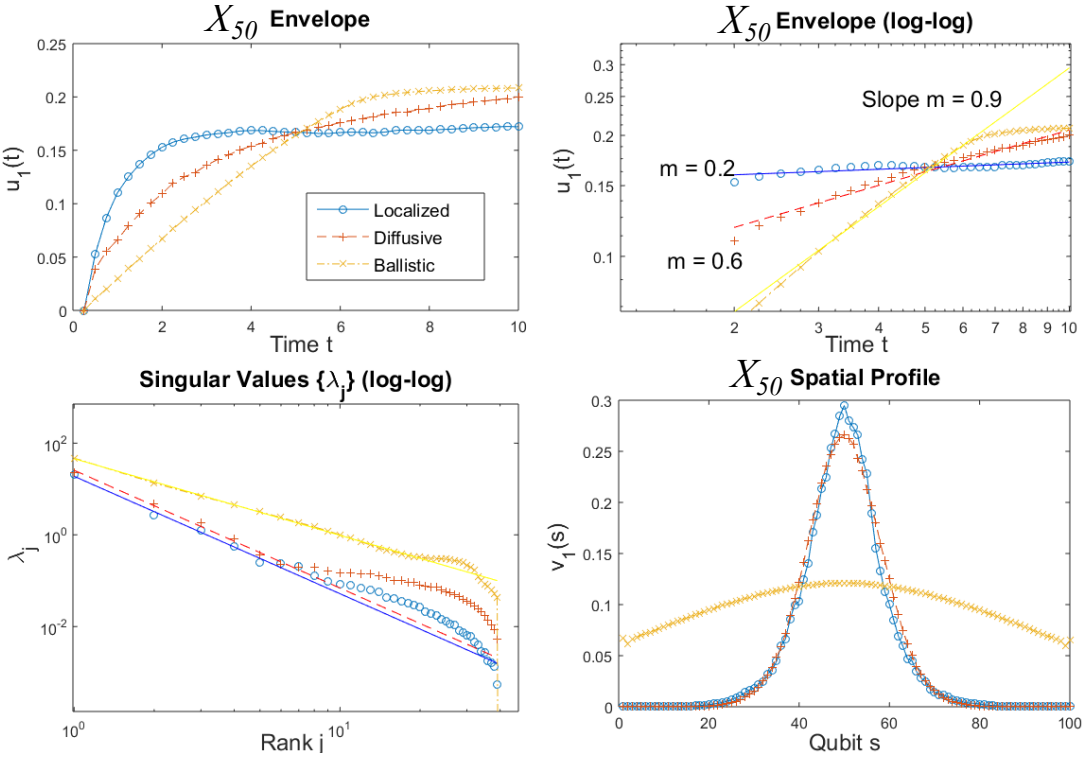

Figure A.1: (Color online) (Top, left) Envelopes of the X-light cones in Fig. 1 in the main text, given by the principal temporal components of their singular value decompositions. (Top, right) Envelopes on a log-log plot, with fitted slopes displayed. Note the saturation of the ballistic case around $t \simeq 6$ is a boundary effect; otherwise, it is expected to be a straight slope. (Bottom, left) Singular values in these decompositions on log-log scale, which demonstrate the error in truncating to a product function; we see that these decay by several orders of magnitude over the first ten. (Bottom, right) Light cone decay profiles, given by the principal spatial vectors; these profiles are very nearly Gaussian, rather than exponential.

on top right) $u_1(t)$ propagate as polynomials with different exponents m, which we take to be indicative of the dynamical phases of these profiles.

Appendix B

"Many-body-localization transition in universal quantum circuits"

B.1 Modified Cauchy-Binet Formula with Different Background Sets – Diagrammatic Proof

Here, we prove Eq. (5.28) using the diagrammatic proof shown in Fig. 5.2. This figure depicts a particular quantum circuit composed of general Gaussian fermionic evolution on modes $(\vec{B}_l, \overline{B}, \vec{B}_r)$, rearrangements between these modes and the ancillary mode-sets $\vec{A}_l$ and $\vec{A}_r$, and a partial trace over the qubits corresponding to the ancillary modes $\vec{A}_r$. As stated in the main text, the equivalence between two different ways of evaluating this circuit implies the identity. This equivalence is given by the operator equality

$$\begin{aligned}\left(F_{\overline{B}\vec{A}_l}U_{g,2}\right)^\dagger \left\{C_{\vec{S}}\,\mathrm{tr}_{\vec{A}_r}\left[\left(U_{g,1}F_{\overline{B}\vec{A}_r}\right)^\dagger C_{\vec{\alpha}}\left(U_{g,1}F_{\overline{B}\vec{A}_r}\right)C_{\vec{S}'}^\dagger\right]\right\}\left(F_{\overline{B}\vec{A}_l}U_{g,2}\right)\\ = \mathrm{tr}_{\vec{A}_r}\left[\left(U_{g,1}F_{\overline{B}\vec{A}_r}F_{\overline{B},\vec{A}_l}U_{g,2}\right)^\dagger C_{\vec{S}}C_{\vec{\alpha}}\left(U_{g,1}F_{\overline{B}\vec{A}_r}F_{\overline{B}\vec{A}_l}U_{g,2}\right)C_{\vec{S}'}^\dagger\right]\end{aligned} \tag{B.1}$$

where the operators $F_{\overline{B}\vec{A}_r}$ and $F_{\overline{B}\vec{A}_l}$ are rearrangements of fermionic modes. We choose these operators to have corresponding single-particle transition matrices

$$\mathbf{f}_{\overline{B}\vec{A}_l} = \begin{pmatrix} \mathbf{0} & \mathbf{0} & \mathbf{I} & \mathbf{0} & \mathbf{0} \\ \mathbf{0} & (-1)^{|\vec{S}|+|\vec{S}'|}\mathbf{I} & \mathbf{0} & \mathbf{0} & \mathbf{0} \\ \mathbf{I} & \mathbf{0} & \mathbf{0} & \mathbf{0} & \mathbf{0} \\ \mathbf{0} & \mathbf{0} & \mathbf{0} & \mathbf{I} & \mathbf{0} \\ \mathbf{0} & \mathbf{0} & \mathbf{0} & \mathbf{0} & \mathbf{I} \end{pmatrix} \tag{B.2}$$

$$\mathbf{f}_{\overline{B}\vec{A}_r} = \begin{pmatrix} \mathbf{I} & \mathbf{0} & \mathbf{0} & \mathbf{0} & \mathbf{0} \\ \mathbf{0} & \mathbf{I} & \mathbf{0} & \mathbf{0} & \mathbf{0} \\ \mathbf{0} & \mathbf{0} & \mathbf{0} & \mathbf{0} & \mathbf{I} \\ \mathbf{0} & \mathbf{0} & \mathbf{0} & \mathbf{I} & \mathbf{0} \\ \mathbf{0} & \mathbf{0} & \mathbf{I} & \mathbf{0} & \mathbf{0} \end{pmatrix} \tag{B.3}$$

where $F^{\dagger}_{\overline{B}\vec{A}_l} c_\mu F_{\overline{B},\vec{A}_l} \equiv \left(\mathbf{f}_{\overline{B}\vec{A}_l} \cdot \mathbf{c}\right)_\mu$, and similarly for $\mathbf{f}_{\overline{B}\vec{A}_r}$. The blocks in the matrices above act on modes $\vec{A}_l$, $\vec{B}_l$, $\overline{B}$, $\vec{B}_r$, $\vec{A}_r$, respectively. In Eq. (B.1), we made use of the fact that $\vec{S}' \subseteq \vec{A}_r$, so $C_{\vec{S}'}$ commutes with $\left(F_{\overline{B}\vec{A}_l} U_{g,2}\right)$, which acts as the identity on these modes. The right-hand-side of this equation corresponds to the dot-dashed contraction ordering in Fig. 5.2, and the left-hand-side corresponds to the dotted contraction ordering. Labeling the indices of our block matrices in the same way as in Eq.s (B.2) and (B.3), we thus have

$$\mathbf{u}_1 \mathbf{f}_{\overline{B}\vec{A}_r} = \begin{bmatrix} \mathbf{I} & \mathbf{0} & \mathbf{0} & \mathbf{0} & \mathbf{0} \\ \mathbf{0} & (\mathbf{u}_1)_{\vec{B}_l\vec{B}_l} & \mathbf{0} & (\mathbf{u}_1)_{\vec{B}_l\vec{B}_r} & (\mathbf{u}_1)_{\vec{B}_l\overline{B}} \\ \mathbf{0} & (\mathbf{u}_1)_{\overline{B}\vec{B}_l} & \mathbf{0} & (\mathbf{u}_1)_{\overline{B}\vec{B}_r} & (\mathbf{u}_1)_{\overline{BB}} \\ \mathbf{0} & (\mathbf{u}_1)_{\vec{B}_r\vec{B}_l} & \mathbf{0} & (\mathbf{u}_1)_{\vec{B}_r\vec{B}_r} & (\mathbf{u}_1)_{\vec{B}_r\overline{B}} \\ \mathbf{0} & \mathbf{0} & \mathbf{I} & \mathbf{0} & \mathbf{0} \end{bmatrix} \tag{B.4}$$

and similarly

$$\mathbf{f}_{\overline{B}\vec{A}_l}\mathbf{u}_2 = \begin{bmatrix} \mathbf{0} & (\widetilde{\mathbf{u}}_2)_{\overline{B}\vec{B}_l} & (\widetilde{\mathbf{u}}_2)_{\overline{B}\overline{B}} & (\widetilde{\mathbf{u}}_2)_{\overline{B}\vec{B}_r} & \mathbf{0} \\ \mathbf{0} & (\widetilde{\mathbf{u}}_2)_{\vec{B}_l\vec{B}_l} & (\widetilde{\mathbf{u}}_2)_{\vec{B}_l\overline{B}} & (\widetilde{\mathbf{u}}_2)_{\vec{B}_l\vec{B}_r} & \mathbf{0} \\ \mathbf{I} & \mathbf{0} & \mathbf{0} & \mathbf{0} & \mathbf{0} \\ \mathbf{0} & (\widetilde{\mathbf{u}}_2)_{\vec{B}_r\vec{B}_l} & (\widetilde{\mathbf{u}}_2)_{\vec{B}_r\overline{B}} & (\widetilde{\mathbf{u}}_2)_{\vec{B}_r\vec{B}_r} & \mathbf{0} \\ \mathbf{0} & \mathbf{0} & \mathbf{0} & \mathbf{0} & \mathbf{I} \end{bmatrix}, \tag{B.5}$$

where $\widetilde{\mathbf{u}}_2$ is as defined in Eq. (5.29) This gives, from the left-hand-side (dot-dashed contraction ordering) of Eq. (B.1)

$$\begin{aligned}
&\left(F_{\overline{B}\vec{A}_l}U_{g,2}\right)^\dagger \left\{C_{\vec{S}}\,\mathrm{tr}_{\vec{A}_r}\left[\left(U_{g,1}F_{\overline{B}\vec{A}_r}\right)^\dagger C_{\vec{\alpha}}\left(U_{g,1}F_{\overline{B}\vec{A}_r}\right)C^\dagger_{\vec{S}'}\right]\right\}\left(F_{\overline{B}\vec{A}_l}U_{g,2}\right) \\
&\quad = 2^{|\vec{A}_r|/2}\sum_{\vec{\beta}}\det\left[\left(\mathbf{u}_1\mathbf{f}_{\overline{B}\vec{A}_r}\right)_{\vec{\alpha},(\vec{\beta},\vec{S}')}\right]\left(F_{\overline{B}\vec{A}_l}U_{g,2}\right)^\dagger C_{\vec{S}}C_{\vec{\beta}}\left(F_{\overline{B}\vec{A}_l}U_{g,2}\right) &\text{(B.6)}\\
&\quad = 2^{|\vec{A}_r|/2}\sum_{\vec{\gamma}}\left\{\sum_{\vec{\beta}}\det\left[\left(\mathbf{u}_1\mathbf{f}_{\overline{B}\vec{A}_r}\right)_{\vec{\alpha},(\vec{\beta},\vec{S}')}\right]\det\left[\left(\mathbf{f}_{\overline{B}\vec{A}_l}\mathbf{u}_2\right)_{(\vec{S},\vec{\beta}),\vec{\gamma}}\right]\right\}C_{\vec{\gamma}} &\text{(B.7)}\\
&\quad = 2^{|\vec{A}_r|/2}\sum_{\vec{\gamma}}\left\{\sum_{\vec{\beta}=(\vec{\beta}_l,\vec{\beta}_r)}(-1)^{(|\vec{S}|+|\vec{S}'|)|\vec{\beta}_l|}\det\left[(\mathbf{u}_1)_{\vec{\alpha},(\vec{\beta}_l,\vec{\beta}_r,\vec{S}')}\right]\right. \\
&\qquad\left.\times\det\left[(\mathbf{u}_2)_{(\vec{S},\vec{\beta}_l,\vec{\beta}_r),\vec{\gamma}}\right]\right\}C_{\vec{\gamma}} &\text{(B.8)}\\
&\quad = 2^{|\vec{A}_r|/2}\sum_{\vec{\gamma}}\left\{\sum_{\vec{\beta}=(\vec{\beta}_l,\vec{\beta}_r)}(-1)^{(|\vec{S}|+|\vec{S}'|)|\vec{\beta}_l|+|\vec{S}'||\vec{\beta}_r|+|\vec{S}||\vec{\beta}_l|}\right. \\
&\qquad\left.\times\det\left[(\mathbf{u}_1)_{\vec{\alpha},(\vec{\beta}_l,\vec{S}',\vec{\beta}_r)}\right]\det\left[(\mathbf{u}_2)_{(\vec{\beta}_l,\vec{S},\vec{\beta}_r),\vec{\gamma}}\right]\right\}C_{\vec{\gamma}} &\text{(B.9)}\\
&\quad = 2^{|\vec{A}_r|/2}\sum_{\vec{\gamma}}(-1)^{|\vec{S}'|(|\vec{S}|-|\vec{\gamma}|)} \\
&\qquad\times\left\{\sum_{\vec{\beta}=(\vec{\beta}_l,\vec{\beta}_r)}\det\left[(\mathbf{u}_1)_{\vec{\alpha},(\vec{\beta}_l,\vec{S}',\vec{\beta}_r)}\right]\det\left[(\mathbf{u}_2)_{(\vec{\beta}_l,\vec{S},\vec{\beta}_r),\vec{\gamma}}\right]\right\}C_{\vec{\gamma}}. &\text{(B.10)}
\end{aligned}$$

To obtain Eq. (B.7), we expanded the Gaussian fermionic evolution of the Majorana configuration by Eq. (5.13) (since we take $\vec{A}_r$ to correspond to the fermionic modes

on a collection of qubits, $|\vec{A}_r|$ must be even). From Eq. (B.7) to Eq. (B.8), we used the block-matrix forms in Eq.s (B.4) and (B.5) to re-ëxpress the series in terms of minors of $\mathbf{u}_1$ and $\mathbf{u}_2$ only. To obtain Eq. (B.9), we rearranged rows and columns in $\mathbf{u}_1$ and $\mathbf{u}_2$, acquiring a phase. To obtain Eq. (B.10), we simplified the phase using the relation $|\vec{\beta}_l| + |\vec{\beta}_r| = |\vec{\gamma}| - |\vec{S}|$ (since the sub-matrix of $\mathbf{u}_2$ must be square). Similarly, we have

$$\mathbf{u}_1\mathbf{f}_{\overline{B}\vec{A}_r}\mathbf{f}_{\overline{B}\vec{A}_l}\mathbf{u}_2 = \begin{bmatrix} \mathbf{0} & (\widetilde{\mathbf{u}}_2)_{\overline{B}\vec{B}_l} & (\widetilde{\mathbf{u}}_2)_{\overline{B}\overline{B}} & (\widetilde{\mathbf{u}}_2)_{\overline{B}\vec{B}_r} & \mathbf{0} \\ \mathbf{0} & (\mathbf{u}_1)_{\vec{B}_l\vec{B}}\,(\widetilde{\mathbf{u}}_2)_{\vec{B}\vec{B}_l} & (\mathbf{u}_1)_{\vec{B}_l\vec{B}}\,(\widetilde{\mathbf{u}}_2)_{\vec{B}\overline{B}} & (\mathbf{u}_1)_{\vec{B}_l\vec{B}}\,(\widetilde{\mathbf{u}}_2)_{\vec{B}\vec{B}_r} & (\mathbf{u}_1)_{\vec{B}_l\overline{B}} \\ \mathbf{0} & (\mathbf{u}_1)_{\overline{B}\vec{B}}\,(\widetilde{\mathbf{u}}_2)_{\vec{B}\vec{B}_l} & (\mathbf{u}_1)_{\overline{B}\vec{B}}\,(\widetilde{\mathbf{u}}_2)_{\vec{B}\overline{B}} & (\mathbf{u}_1)_{\overline{B}\vec{B}}\,(\widetilde{\mathbf{u}}_2)_{\vec{B}\vec{B}_r} & (\mathbf{u}_1)_{\overline{B}\overline{B}} \\ \mathbf{0} & (\mathbf{u}_1)_{\vec{B}_r\vec{B}}\,(\widetilde{\mathbf{u}}_2)_{\vec{B}\vec{B}_l} & (\mathbf{u}_1)_{\vec{B}_r\vec{B}}\,(\widetilde{\mathbf{u}}_2)_{\vec{B}\overline{B}} & (\mathbf{u}_1)_{\vec{B}_r\vec{B}}\,(\widetilde{\mathbf{u}}_2)_{\vec{B}\vec{B}_r} & (\mathbf{u}_1)_{\vec{B}_r\overline{B}} \\ \mathbf{I} & \mathbf{0} & \mathbf{0} & \mathbf{0} & \mathbf{0} \end{bmatrix} \tag{B.11}$$

Thus, the right-hand-side (dotted contraction ordering) of Eq. (B.1) gives

$$\begin{aligned} &\mathrm{tr}_{\vec{A}_r}\left[\left(U_{g,1}F_{\overline{B}\vec{A}_r}F_{\overline{B}\vec{A}_l}U_{g,2}\right)^\dagger C_{\vec{S}}C_{\vec{\alpha}}\left(U_{g,1}F_{\overline{B}\vec{A}_r}F_{\overline{B}\vec{A}_l}U_{g,2}\right)C^\dagger_{\vec{S}'}\right] \\ &\quad= 2^{|\vec{A}_r|/2}\sum_{\vec{\gamma}}\det\left[\left(\mathbf{u}_1\mathbf{f}_{\overline{B}\vec{A}_r}\mathbf{f}_{\overline{B}\vec{A}_l}\mathbf{u}_2\right)_{(\vec{S},\vec{\alpha})(\vec{\gamma},\vec{S}')}\right]C_{\vec{\gamma}} &\text{(B.12)} \\ &\quad= 2^{|\vec{A}_r|/2}\sum_{\vec{\gamma}}\det\begin{bmatrix}(\widetilde{\mathbf{u}}_2)_{\vec{S}\vec{\gamma}} & \mathbf{0}_{|\vec{S}|\times|\vec{S}'|} \\ (\mathbf{u}_1)_{\vec{\alpha}\vec{B}}\,(\widetilde{\mathbf{u}}_2)_{\vec{B}\vec{\gamma}} & (\mathbf{u}_1)_{\vec{\alpha}\vec{S}'}\end{bmatrix}C_{\vec{\gamma}} &\text{(B.13)} \\ &\quad= 2^{|\vec{A}_r|/2}\sum_{\vec{\gamma}}(-1)^{|\vec{S}'||\vec{\gamma}|}\det\begin{bmatrix}\mathbf{0}_{|\vec{S}|\times|\vec{S}'|} & (\mathbf{u}_2)_{\vec{S}\vec{\gamma}} \\ (\mathbf{u}_1)_{\vec{\alpha}\vec{S}'} & (\mathbf{u}_1)_{\vec{\alpha}\vec{B}}\,(\widetilde{\mathbf{u}}_2)_{\vec{B}\vec{\gamma}}\end{bmatrix}C_{\vec{\gamma}}, &\text{(B.14)} \end{aligned}$$

where $\vec{B} \equiv (\vec{B}_l, \vec{B}_r)$. From Eq. (B.12) to Eq. (B.13), we similarly used the block-matrix form of Eq. (B.11) to re-ëxpress the minor in Eq. (B.12) in-terms of minors of $\mathbf{u}_1$ and $\widetilde{\mathbf{u}}_2$ only. From Eq. (B.13) to Eq. (B.14), we again rearranged columns in the matrix determinant, acquiring a phase, and used the fact that $(\widetilde{\mathbf{u}}_2)_{\vec{S}\vec{\gamma}} = (\mathbf{u}_2)_{\vec{S}\vec{\gamma}}$, since $\vec{S}$ is disjoint from $\vec{B}_l$.

Setting Eq.s (B.14) and (B.10) equal by Eq. (B.1), canceling corresponding factors of $2^{|\vec{A}_r|/2}$, and using linear independence of the $\{C_{\vec{\gamma}}\}$ gives

$$(-1)^{|\vec{S}'|(|\vec{S}|-|\vec{\gamma}|)} \sum_{\vec{\beta}=\left(\vec{\beta}_l,\vec{\beta}_r\right)} \det\left[(\mathbf{u}_1)_{\vec{\alpha},\left(\vec{\beta}_l,\vec{S}',\vec{\beta}_r\right)}\right] \det\left[(\mathbf{u}_2)_{\left(\vec{\beta}_l,\vec{S},\vec{\beta}_r\right),\vec{\gamma}}\right]$$

$$= (-1)^{|\vec{S}'||\vec{\gamma}|} \det \begin{bmatrix} \mathbf{0}_{|\vec{S}|\times|\vec{S}'|} & (\mathbf{u}_2)_{\vec{S}\vec{\gamma}} \\ (\mathbf{u}_1)_{\vec{\alpha}\vec{S}'} & (\mathbf{u}_1)_{\vec{\alpha}\vec{B}} (\widetilde{\mathbf{u}}_2)_{\vec{B}\vec{\gamma}} \end{bmatrix} \tag{B.15}$$

$$= (-1)^{|\vec{S}'||\vec{S}|} \det \begin{bmatrix} \mathbf{0}_{|\vec{S}|\times|\vec{S}'|} & (\mathbf{u}_2)_{\vec{S}\vec{\gamma}} \\ (\mathbf{u}_1)_{\vec{\alpha}\vec{S}'} & (\mathbf{u}_1)_{\vec{\alpha}\vec{B}} (\widetilde{\mathbf{u}}_2)_{\vec{B}\vec{\gamma}} \end{bmatrix} \tag{B.16}$$

B.2 Modified Cauchy-Binet Formula with Different Background Sets – Determinental Proof

Here we prove Eq. (5.28) using determinental identities. Let $\mathbf{u}_1$ and $\mathbf{u}_2$ be orthogonal matrices, and let $\vec{\alpha}$, $\vec{\beta}$, $\vec{\gamma}$, $\vec{S}$, $\vec{S}'$ be tuples, for which

$$|\vec{\beta}| = |\vec{\alpha}| - |\vec{S}'| = |\vec{\gamma}| - |\vec{S}|, \tag{B.17}$$

and

$$\begin{cases} \vec{S},\, \vec{S}' \subseteq \overline{B} \\ \vec{B} \equiv \left(\vec{B}_l, \vec{B}_r\right) \\ \vec{\beta} = \left(\vec{\beta}_l, \vec{\beta}_r\right) \quad \text{where } \vec{\beta}_l \subseteq \vec{B}_l \text{ and } \vec{\beta}_r \subseteq \vec{B}_r \end{cases} \tag{B.18}$$

for $\vec{B}$ a contiguous set of indices and $\vec{B}_l$, $\vec{B}_r$, and $\overline{B}$ all disjoint. We will show

$$\sum_{\vec{\beta}} \det\left[(\mathbf{u}_1)_{\vec{\alpha}\left(\vec{\beta}_l,\vec{S}',\vec{\beta}_r\right)}\right] \det\left[(\mathbf{u}_2)_{\left(\vec{\beta}_l,\vec{S},\vec{\beta}_r\right)\vec{\gamma}}\right]$$

$$= (-1)^{|\vec{S}||\vec{S}'|} \det \begin{bmatrix} \mathbf{0}_{|\vec{S}|\times|\vec{S}'|} & (\mathbf{u}_2)_{\vec{S}\vec{\gamma}} \\ (\mathbf{u}_1)_{\vec{\alpha}\vec{S}'} & (\mathbf{u}_1)_{\vec{\alpha}\vec{B}} (\widetilde{\mathbf{u}}_2)_{\vec{B}\vec{\gamma}} \end{bmatrix}, \tag{B.19}$$

where the sum is over all tuples $\vec{\beta}$ consistent with the constraints. We first rearrange columns in $\mathbf{u}_1$ and $\mathbf{u}_2$ such that the first $\vec{B}$ constitutes the first $|\vec{B}|$ columns, as

$$\begin{aligned} &\sum_{\vec{\beta}} \det\left[(\mathbf{u}_1)_{\vec{\alpha}(\vec{\beta}_l,\vec{S}',\vec{\beta}_r)}\right] \det\left[(\mathbf{u}_2)_{(\vec{\beta}_l,\vec{S},\vec{\beta}_r)\vec{\gamma}}\right] \\ &\quad = \sum_{\vec{\beta}} (-1)^{|\vec{\beta}_l|(|\vec{S}|+|\vec{S}'|)} \det\left[\left(\mathbf{u}_1'\right)_{\vec{\alpha}\left(\vec{S}',\vec{\beta}\right)}\right] \det\left[\left(\mathbf{u}_2'\right)_{\left(\vec{S},\vec{\beta}\right)\vec{\gamma}}\right] \end{aligned} \tag{B.20}$$

where $\mathbf{u}_1'$ and $\mathbf{u}_2'$ are the rearranged matrices. If $|\vec{S}|$ and $|\vec{S}'|$ have the same parity, then the sign factor inside the sum is 1. Otherwise, it evaluates to $(-1)^{|\vec{\beta}_l|}$, which we absorb onto $\mathbf{u}_2'$ by multiplying its columns in $\vec{B}_l$ by (-1) to obtain $\widetilde{\mathbf{u}}_2'$. This gives

$$\begin{aligned} &\sum_{\vec{\beta}} \det\left[\left(\mathbf{u}_1'\right)_{\vec{\alpha}\left(\vec{S}',\vec{\beta}\right)}\right] \det\left[\left(\widetilde{\mathbf{u}}_2'\right)_{\left(\vec{S},\vec{\beta}\right)\vec{\gamma}}\right] \\ &\quad = \sum_{\vec{\beta}} \left\{ \sum_{\vec{H}} \varepsilon^{\vec{H}\vec{S}'} \det\left[\left(\mathbf{u}_1'\right)_{\vec{H}\vec{S}'}\right] \det\left[\left(\mathbf{u}_1'\right)_{\vec{\alpha}/\vec{H},\vec{\beta}}\right] \right\} \\ &\qquad \times \left\{ \sum_{\vec{L}} \varepsilon^{\vec{L}\vec{S}} \det\left[\left(\widetilde{\mathbf{u}}_2'\right)_{\vec{S}\vec{L}}\right] \det\left[\left(\widetilde{\mathbf{u}}_2'\right)_{\vec{\beta},\vec{\gamma}/\vec{L}}\right] \right\} \end{aligned} \tag{B.21}$$

$$\begin{aligned} &= \sum_{\vec{H},\vec{L}} \varepsilon^{\vec{H}\vec{S}'} \varepsilon^{\vec{L}\vec{S}} \det\left[\left(\mathbf{u}_1'\right)_{\vec{H}\vec{S}'}\right] \det\left[\left(\widetilde{\mathbf{u}}_2'\right)_{\vec{S}\vec{L}}\right] \\ &\qquad \times \left\{ \sum_{\vec{\beta}} \det\left[\left(\mathbf{u}_1'\right)_{\vec{\alpha}/\vec{H},\vec{\beta}}\right] \det\left[\left(\widetilde{\mathbf{u}}_2'\right)_{\vec{\beta},\vec{\gamma}/\vec{L}}\right] \right\} \end{aligned} \tag{B.22}$$

$$= \sum_{\vec{H},\vec{L}} \varepsilon^{\vec{H}\vec{S}'} \varepsilon^{\vec{L}\vec{S}} \det\left[\left(\mathbf{u}_1'\right)_{\vec{H}\vec{S}'}\right] \det\left[\left(\widetilde{\mathbf{u}}_2'\right)_{\vec{S}\vec{L}}\right] \det\left[\left(\mathbf{u}_1'\right)_{\vec{\alpha}/\vec{H},\left(\vec{B}_l,\vec{B}_r\right)} \left(\widetilde{\mathbf{u}}_2'\right)_{\left(\vec{B}_l,\vec{B}_r\right),\vec{\gamma}/\vec{L}}\right] \tag{B.23}$$

$$= \sum_{\vec{L}} \varepsilon^{\vec{L}\vec{S}} \det\left[\left(\widetilde{\mathbf{u}}_2'\right)_{\vec{S}\vec{L}}\right] \det\begin{bmatrix} \left(\mathbf{u}_1'\right)_{\vec{\alpha}\vec{S}'} & \left(\mathbf{u}_1'\right)_{\vec{\alpha},\left(\vec{B}_l,\vec{B}_r\right)} \end{bmatrix} \left(\widetilde{\mathbf{u}}_2'\right)_{\left(\vec{B}_l,\vec{B}_r\right),\vec{\gamma}/\vec{L}} \tag{B.24}$$

$$= \sum_{\vec{L}} \varepsilon^{\vec{L}\vec{S}} \det\left[\mathbf{0}_{|\vec{S}|\times|\vec{S}'|} \quad \left(\widetilde{\mathbf{u}}_2'\right)_{\vec{S}\vec{L}}\right] \det\left[\left(\mathbf{u}_1'\right)_{\vec{\alpha}\vec{S}'} \quad \left(\mathbf{u}_1'\right)_{\vec{\alpha},\left(\vec{B}_l,\vec{B}_r\right)} \left(\widetilde{\mathbf{u}}_2'\right)_{\left(\vec{B}_l,\vec{B}_r\right),\vec{\gamma}/\vec{L}}\right] \tag{B.25}$$

$$= (-1)^{|\vec{S}'||\vec{S}|} \det \begin{bmatrix} \mathbf{0}_{|\vec{S}|\times|\vec{S}'|} & \left(\widetilde{\mathbf{u}}_2'\right)_{\vec{S}\vec{\gamma}} \\ \left(\mathbf{u}_1'\right)_{\vec{\alpha}\vec{S}'} & \left(\mathbf{u}_1'\right)_{\vec{\alpha}\left(\vec{B}_l,\vec{B}_r\right)} \left(\widetilde{\mathbf{u}}_2'\right)_{\left(\vec{B}_l,\vec{B}_r\right)\vec{\gamma}} \end{bmatrix} \tag{B.26}$$

From Eq. (B.21) to Eq. (B.22), we used the Laplace expansion by complementary minors formula, where $\varepsilon^{\vec{H}\vec{L}} = (-1)^{\sum_{i=1}^{|\vec{H}|} H_i + \sum_{i=1}^{|\vec{L}|} L_i}$. From Eq. (B.22) to Eq. (B.23), we used the Cauchy-Binet formula for the sum on $\vec{\beta}$. From Eq. (B.23) to Eq. (B.24), we identify the sum on $\vec{H}$ with the Laplace expansion by complementary minors. From Eq. (B.24) to Eq. (B.25), we include a block of zeroes in $\widetilde{\mathbf{u}}_2'$ so as to identify the sum on $\vec{L}$ as a second Laplace expansion by complementary minors from Eq. (B.25) to Eq. (B.26). However, since including this block of zeroes shifts the indices of $\vec{L}$ by $|\vec{S}'|$, this incurs an additional factor of $(-1)^{|\vec{S}||\vec{S}'|}$ from $\varepsilon^{\vec{L}\vec{S}}$.

Finally, we may rearrange columns and use the fact that $(\widetilde{\mathbf{u}}_2)_{\vec{S}\vec{\gamma}} = (\mathbf{u}_2)_{\vec{S}\vec{\gamma}}$ to recover the formula

$$\sum_{\vec{\beta}} \det\left[(\mathbf{u}_1)_{\vec{\alpha}\left(\vec{\beta}_l,\vec{S}',\vec{\beta}_r\right)}\right] \det\left[(\mathbf{u}_2)_{\left(\vec{\beta}_l,\vec{S},\vec{\beta}_r\right)\vec{\gamma}}\right]$$
$$= (-1)^{|\vec{S}||\vec{S}'|} \det \begin{bmatrix} \mathbf{0}_{|\vec{S}|\times|\vec{S}'|} & (\mathbf{u}_2)_{\vec{S}\vec{\gamma}} \\ (\mathbf{u}_1)_{\vec{\alpha}\vec{S}'} & (\mathbf{u}_1)_{\vec{\alpha}\vec{B}} (\widetilde{\mathbf{u}}_2)_{\vec{B}\vec{\gamma}} \end{bmatrix}. \tag{B.27}$$

B.3 Exact Formula for the OTO Commutator

Let a unitary consisting of one interaction gate with two periods of Gaussian fermionic be given by $U = U_{g,1} V_j U_{g,2}$, for Gaussian fermionic operations $U_{g,\{1,2\}}$ and $V_j = \exp\left(-\frac{i\pi}{4} Z_j Z_{j+1}\right) \equiv V$. As in the main text, let $\vec{q}_j = (2j-1, 2j, 2j+1, 2(j+1)) \equiv \vec{q}$ (since the index j can be seen from context). From Eq. (5.2), we see that it suffices to calculate

$$d^{-1}\,\mathrm{tr}\left[AB(t)AB(t)\right] = d^{-1}(-1)^{\frac{1}{2}[|\vec{\alpha}|(|\vec{\alpha}|-1)+|\vec{\eta}|(|\vec{\eta}|-1)]} \times \mathrm{tr}\left[C_{\vec{\eta}}\left(U_{g,1}V_jU_{g,2}\right)^\dagger C_{\vec{\alpha}}\left(U_{g,1}V_jU_{g,2}\right) C_{\vec{\eta}}\left(U_{g,1}V_jU_{g,2}\right)^\dagger C_{\vec{\alpha}}\left(U_{g,1}V_jU_{g,2}\right)\right], \tag{B.28}$$

where $A = i^a C_{\vec{\eta}}$ and $B = i^b C_{\vec{\alpha}}$ for integers a and b, and for which $i^{2a} = (-1)^{\frac{1}{2}|\vec{\alpha}|(|\vec{\alpha}|-1)}$ and $i^{2b} = (-1)^{\frac{1}{2}|\vec{\eta}|(|\vec{\eta}|-1)}$ from the relations $A^2 = B^2 = I$ (we have assumed A and B to be Hermitian and unitary). From Eq. (5.13), we have

$$U_{g,1}^\dagger C_{\vec{\alpha}} U_{g,1} = \sum_{\vec{\beta}} \det\left[(\mathbf{u}_1)_{\vec{\alpha}\vec{\beta}}\right] C_{\vec{\beta}} \tag{B.29}$$

Let $\vec{\beta} = (\vec{\beta}_q \cup \vec{\beta}_{\overline{q}})$, where $\vec{\beta}_q = \vec{\beta} \cap \vec{q}$ and $\vec{\beta}_{\overline{q}} = \vec{\beta} \cap \overline{q}$, for $\overline{q}$ the complement of $\vec{q}$ in $[2n] \equiv (1, 2, \ldots, 2n)$, the full set of modes. Since $\vec{q}$ is contiguous, we can apply Eq. (B.27) to obtain

$$\left(U_{g,1}VU_{g,2}\right)^\dagger C_{\vec{\alpha}}\left(U_{g,1}VU_{g,2}\right) = \sum_{\vec{\beta}} \det\left[(\mathbf{u}_1)_{\vec{\alpha}\vec{\beta}}\right]\left(VU_{g,2}\right)^\dagger C_{\vec{\beta}}\left(VU_{g,2}\right) \tag{B.30}$$

$$= \sum_{k=0}^{\min(|\vec{q}|,|\vec{\alpha}|)} \sum_{\{\vec{\beta}_q||\vec{\beta}_q|=k\}} \sum_{\vec{\beta}_{\overline{q}}} \det\left[(\mathbf{u}_1)_{\vec{\alpha},\left(\vec{\beta}_q\cup\vec{\beta}_{\overline{q}}\right)}\right]\left(VU_{g,2}\right)^\dagger C_{\left(\vec{\beta}_q\cup\vec{\beta}_{\overline{q}}\right)}\left(VU_{g,2}\right) \tag{B.31}$$

$$= \sum_{k=0}^{\min(|\vec{q}|,|\vec{\alpha}|)} \sum_{\{\vec{\beta}_q||\vec{\beta}_q|=k\}} i^{\varphi(\vec{\beta}_q)} \sum_{\vec{\beta}_{\overline{q}}} \det\left[(\mathbf{u}_1)_{\vec{\alpha},\left(\vec{\beta}_q\cup\vec{\beta}_{\overline{q}}\right)}\right] U_{g,2}^\dagger C_{\left(\mathcal{V}(\vec{\beta}_q)\cup\vec{\beta}_{\overline{q}}\right)} U_{g,2} \tag{B.32}$$

$$= \sum_{k=0}^{\min(|\vec{q}|,|\vec{\alpha}|)} \sum_{\{\vec{\beta}_q||\vec{\beta}_q|=k\}} i^{\varphi(\vec{\beta}_q)} \sum_{\vec{\beta}_{\overline{q}}} \det\left[(\mathbf{u}_1)_{\vec{\alpha},\left(\vec{\beta}_q\cup\vec{\beta}_{\overline{q}}\right)}\right] \times \sum_{\vec{\gamma}} \det\left[(\mathbf{u}_2)_{\left(\mathcal{V}(\vec{\beta}_q)\cup\vec{\beta}_{\overline{q}}\right),\vec{\gamma}}\right] C_{\vec{\gamma}} \tag{B.33}$$

$$= \sum_{k=0}^{\min(|\vec{q}|,|\vec{\alpha}|)} \sum_{\{\vec{\beta}_q||\vec{\beta}_q|=k\}} i^{\varphi(\vec{\beta}_q)}$$

$$\times \sum_{\vec{\gamma}} \left\{ \sum_{\vec{\beta}_{\overline{q}}} \det\left[(\mathbf{u}_1)_{\vec{\alpha},\left(\vec{\beta}_q \cup \vec{\beta}_{\overline{q}}\right)}\right] \det\left[(\mathbf{u}_2)_{\left(\mathcal{V}(\vec{\beta}_q)\cup\vec{\beta}_{\overline{q}}\right),\vec{\gamma}}\right] \right\} C_{\vec{\gamma}} \tag{B.34}$$

$$= \sum_{\vec{\gamma}} \left\{ \sum_{\{\left(k,\vec{\beta}_q\right)||\vec{\beta}_q|=k\}} i^{\varphi(\vec{\beta}_q)}(-1)^{|\vec{\beta}_q||\mathcal{V}(\vec{\beta}_q)|} \det \begin{bmatrix} \mathbf{0}_{|\mathcal{V}(\vec{\beta}_q)|\times|\vec{\beta}_q|} & (\mathbf{u}_2)_{\mathcal{V}(\vec{\beta}_q)\vec{\gamma}} \\ (\mathbf{u}_1)_{\vec{\alpha}\vec{\beta}_q} & (\mathbf{u}_1)_{\vec{\alpha}\overline{q}}\,(\mathbf{u}_2)_{\overline{q}\vec{\gamma}} \end{bmatrix} \right\} C_{\vec{\gamma}} \tag{B.35}$$

$$\equiv \sum_{\vec{\gamma}} \left(\sum_{\{\left(k,\vec{\beta}_q\right)||\vec{\beta}_q|=k\}} i^{\varphi(\vec{\beta}_q)}(-1)^{|\vec{\beta}_q||\mathcal{V}(\vec{\beta}_q)|} \det\left\{ \left[\mathbf{u}_{(1,2)}\right]_{\left[\mathcal{V}(\vec{\beta}_q),\vec{\alpha}\right],\left[\vec{\beta}_q,\vec{\gamma}\right]} \right\} \right) C_{\vec{\gamma}}. \tag{B.36}$$

In Eq. (B.31), we split the sum into sums over $\vec{\beta}_q$, $\vec{\beta}_{\overline{q}}$. In Eq. (B.32), we let

$$V^\dagger C_{\vec{\beta}_q} V = i^{\varphi\left(\vec{\beta}_q\right)} C_{\mathcal{V}(\vec{\beta}_q)}. \tag{B.37}$$

using the fact that V commutes with any modes not in $\vec{q}$, and that the set $\vec{q}$ is contiguous. From Eq.s (B.32)-(B.35), we applied Eq. (B.27) (ang grouped sums for notational convenience). In Eq. (B.36), we defined

$$\mathbf{u}_{(1,2)} \equiv \begin{bmatrix} \mathbf{0}_{|\vec{q}|\times|\vec{q}|} & (\mathbf{u}_2)_{\vec{q}[2n]} \\ (\mathbf{u}_1)_{[2n]\vec{q}} & (\mathbf{u}_1)_{[2n]\overline{q}}\,(\mathbf{u}_2)_{\overline{q}[2n]} \end{bmatrix}. \tag{B.38}$$

It is straightforward to show that $\mathbf{u}_{(1,2)}$ is itself orthogonal for orthogonal $\mathbf{u}_{\{1,2\}}$, as

$$\mathbf{u}_{(1,2)}\mathbf{u}_{(1,2)}^{\mathrm{T}} = \begin{bmatrix} \mathbf{0}_{|\vec{q}|\times|\vec{q}|} & (\mathbf{u}_2)_{\vec{q}[2n]} \\ (\mathbf{u}_1)_{[2n]\vec{q}} & (\mathbf{u}_1)_{[2n]\overline{q}}\,(\mathbf{u}_2)_{\overline{q}[2n]} \end{bmatrix} \begin{bmatrix} \mathbf{0}_{|\vec{q}|\times|\vec{q}|} & \left(\mathbf{u}_1^{\mathrm{T}}\right)_{\vec{q}[2n]} \\ \left(\mathbf{u}_2^{\mathrm{T}}\right)_{[2n]\vec{q}} & \left(\mathbf{u}_2^{\mathrm{T}}\right)_{[2n]\overline{q}}\left(\mathbf{u}_1^{\mathrm{T}}\right)_{\overline{q}[2n]} \end{bmatrix} \tag{B.39}$$

$$= \begin{bmatrix} \mathbf{I}_{\vec{q}\vec{q}} & \mathbf{I}_{\vec{q}\overline{q}}\left(\mathbf{u}_1^{\mathrm{T}}\right)_{\overline{q}[2n]} \\ (\mathbf{u}_1)_{[2n]\overline{q}}\,\mathbf{I}_{\overline{q}\vec{q}} & (\mathbf{u}_1)_{[2n]\vec{q}}\left(\mathbf{u}_1^{\mathrm{T}}\right)_{\vec{q}[2n]} + (\mathbf{u}_1)_{[2n]\overline{q}}\left(\mathbf{u}_1^{\mathrm{T}}\right)_{\overline{q}[2n]} \end{bmatrix} \tag{B.40}$$

$$= \begin{pmatrix} \mathbf{I}_{\vec{q}\vec{q}} & \mathbf{0}_{\vec{q}[2n]} \\ \mathbf{0}_{[2n]\vec{q}} & \mathbf{I}_{[2n][2n]} \end{pmatrix} \tag{B.41}$$

$$\mathbf{u}_{(1,2)}\mathbf{u}_{(1,2)}^{\mathrm{T}} = \mathbf{I} \tag{B.42}$$

In Eq. (B.40), we applied the orthogonality of $\mathbf{u}_{\{1,2\}}$ when contracted along the indices $[2n]$. From Eq. (B.40) to Eq. (B.41), we used the facts

$$\begin{cases} \mathbf{I}_{\vec{q}\bar{q}} = \mathbf{0}_{\vec{q}\bar{q}} \\ (\mathbf{u}_1)_{[2n]\vec{q}} \left(\mathbf{u}_1^{\mathrm{T}}\right)_{\vec{q}[2n]} + (\mathbf{u}_1)_{[2n]\bar{q}} \left(\mathbf{u}_1^{\mathrm{T}}\right)_{\bar{q}[2n]} = \mathbf{u}_1\mathbf{u}_1^{\mathrm{T}} = \mathbf{I} \end{cases} \tag{B.43}$$

It is straightforward to show that $\mathbf{u}_{(1,2)}^{\mathrm{T}}\mathbf{u}_{(1,2)} = \mathbf{I}$ as well. We can therefore iterate this procedure for conjugation by an additional interaction gate, V', acting on the subset of qubits $\vec{q}'$, as

$$U^{\dagger} C_{\vec{\alpha}} U \equiv \left(U_{g,1} V U_{g,2} V' U_{g,3}\right)^{\dagger} C_{\vec{\alpha}} \left(U_{g,1} V U_{g,2} V' U_{g,3}\right) \tag{B.44}$$

$$= \sum_{\vec{\lambda}} \left[\sum_{\substack{\left\{\left(k,\vec{\beta}_q\right)||\vec{\beta}_q|=k\right\} \\ \left\{\left(k',\vec{\gamma}_{q'}\right)||\vec{\gamma}_{q'}|=k'\right\}}} i^{\varphi\left(\vec{\beta}_q\right)+\varphi\left(\vec{\gamma}_{q'}\right)} (-1)^{|\vec{\beta}_q||\mathcal{V}(\vec{\beta}_q)|} \right. \tag{B.45}$$
$$\left. \times \left(\sum_{\vec{\gamma}} \det\left\{ \left[\mathbf{u}_{(1,2)}\right]_{\left[\mathcal{V}\left(\vec{\beta}_q\right),\vec{\alpha}\right]\left[\vec{\beta}_q,\left(\vec{\gamma}\cup\vec{\gamma}_{q'}\right)\right]} \right\} \det\left[(\mathbf{u}_3)_{\left[\vec{\gamma}\cup\mathcal{V}\left(\vec{\gamma}_{q'}\right)\right]\vec{\lambda}} \right] \right) \right] C_{\vec{\lambda}}$$

$$= \sum_{\vec{\lambda}} \left\{ \sum_{\substack{\left\{\left(k,\vec{\beta}_q\right)||\vec{\beta}_q|=k\right\} \\ \left\{\left(k',\vec{\gamma}_{q'}\right)||\vec{\gamma}_{q'}|=k'\right\}}} i^{\varphi\left(\vec{\beta}_q\right)+\varphi\left(\vec{\gamma}_{q'}\right)} (-1)^{|\vec{\beta}_q||\mathcal{V}\left(\vec{\beta}_q\right)|+\left(|\vec{\beta}_q|+|\vec{\gamma}_{q'}|\right)|\mathcal{V}\left(\vec{\gamma}_{q'}\right)|} \right. \tag{B.46}$$
$$\left. \times \det \begin{pmatrix} \mathbf{0}_{|\mathcal{V}\left(\vec{\gamma}_{q'}\right)|\times\left(|\vec{\beta}_q|+|\vec{\gamma}_{q'}|\right)} & (\mathbf{u}_3)_{\mathcal{V}\left(\vec{\gamma}_{q'}\right)\vec{\lambda}} \\ \left[\mathbf{u}_{(1,2)}\right]_{\left[\mathcal{V}\left(\vec{\beta}_q\right),\vec{\alpha}\right]\left(\vec{\beta}_q,\vec{\gamma}_{q'}\right)} & \left[\mathbf{u}_{(1,2)}\right]_{\left[\mathcal{V}\left(\vec{\beta}_q\right),\vec{\alpha}\right]\bar{q}'} (\mathbf{u}_3)_{\bar{q}'\vec{\lambda}} \end{pmatrix} \right\} C_{\vec{\lambda}}$$

$$= \sum_{\vec{\lambda}} \sum_{\substack{\left\{\left(k,\vec{\beta}_q\right)||\vec{\beta}_q|=k\right\} \\ \left\{\left(k',\vec{\gamma}_{q'}\right)||\vec{\gamma}_{q'}|=k'\right\}}} i^{\varphi\left(\vec{\beta}_q\right)+\varphi\left(\vec{\gamma}_{q'}\right)} (-1)^{|\vec{\beta}_q||\mathcal{V}\left(\vec{\beta}_q\right)|+|\vec{\gamma}_{q'}||\mathcal{V}\left(\vec{\gamma}_{q'}\right)|} \times \det\left\{ \left[\mathbf{u}_{(1,2,3)}\right]_{\left[\mathcal{V}\left(\vec{\gamma}_{q'}\right),\mathcal{V}\left(\vec{\beta}_q\right),\vec{\alpha}\right]\left[\vec{\gamma}_{q'},\vec{\beta}_q,\vec{\lambda}\right]} \right\} C_{\vec{\lambda}}, \tag{B.47}$$

where

$$\mathbf{u}_{(1,2,3)} \equiv \begin{bmatrix} \mathbf{0}_{|\vec{q}'|\times|\vec{q}'|} & \mathbf{0}_{|\vec{q}'|\times|\vec{q}|} & (\mathbf{u}_3)_{\vec{q}'[2n]} \\ (\mathbf{u}_2)_{\vec{q}\vec{q}'} & \mathbf{0}_{|\vec{q}|\times|\vec{q}|} & (\mathbf{u}_2)_{\vec{q}\vec{q}'}\,(\mathbf{u}_3)_{\vec{q}'[2n]} \\ (\mathbf{u}_1)_{[2n]\vec{q}}\,(\mathbf{u}_2)_{\vec{q}\vec{q}} & (\mathbf{u}_1)_{[2n]\vec{q}} & (\mathbf{u}_1)_{[2n]\vec{q}}\,(\mathbf{u}_2)_{\vec{q}\vec{q}'}\,(\mathbf{u}_3)_{\vec{q}'[2n]}\,. \end{bmatrix} \tag{B.48}$$

From Eq. (B.46) to Eq. (B.47), we cancelled a phase of $(-1)^{|\vec{\beta}_q||\mathcal{V}(\vec{\gamma}_{q'})|}$ by exchanging columns $\vec{\beta}_q \leftrightarrow \vec{\gamma}_{q'}$ inside the determinant to yield a phase of $(-1)^{|\vec{\beta}_q||\vec{\gamma}_{q'}|}$ and used the fact that $(-1)^{|\vec{\beta}_q|\left(|\vec{\gamma}_{q'}|+|\mathcal{V}\left(\vec{\gamma}_{q'}\right)|\right)} = 1$ by the parity-preserving property of V. It is clear that $\mathbf{u}_{(1,2,3)}$ is orthogonal by the orthogonality property of $\mathbf{u}_{(1,2)}$. We can continue to iterate this process, g times for g interaction gates present, incurring an ancillary set of modes $\vec{q}_i$ for every iteration $i \in \{1, 2, \ldots, g\}$. Let $\vec{B} = \bigcup_{i=1}^{g} \vec{\beta}_i$ for $\vec{\beta}_i \subseteq \vec{q}_i$, and let $\mathbf{M}$ be the orthogonal matrix obtained as the result of these iterations. We have

$$\begin{aligned} &\left(U_{g,1}V_1U_{g,2}\ldots V_nU_{g,n+1}\right)^{\dagger} C_{\vec{\alpha}} \left(U_{g,1}V_1U_{g,2}\ldots V_nU_{g,n+1}\right) \\ &\quad = \sum_{\vec{B}\subseteq\bigcup_{i=1}^{g}\vec{q}_i} i^{\sum_{i=1}^{g}\varphi\left(\vec{\beta}_i\right)} (-1)^{\sum_{i=1}^{g}|\vec{\beta}_i||\mathcal{V}\left(\vec{\beta}_i\right)|} \sum_{\vec{\gamma}} \det\left\{ \mathbf{M}_{\left[\mathcal{V}^{\times g}(\vec{B}),\vec{\alpha}\right]\left[\vec{B},\vec{\gamma}\right]} \right\} C_{\vec{\gamma}}, \end{aligned} \tag{B.49}$$

where the $\vec{\beta}_i \subseteq \vec{B}$ are ordered in descending order of i when indexing the rows and columns of $\mathbf{M}$ inside the determinant, and the length $|\vec{\gamma}|$ of the tuple $\vec{\gamma}$ is such that the determinant inside the matrix is square.

We next calculate the OTO correlator as

$$\operatorname{tr}\left[C_{\vec{\eta}}\left(U^{\dagger}C_{\vec{\alpha}}U\right)C_{\vec{\eta}}\left(U^{\dagger}C_{\vec{\alpha}}U\right)\right]=\sum_{\vec{B},\vec{B}'\subseteq\bigcup_{i=1}^{g}\vec{q}_i} i^{\sum_{i=1}^{g}\left[\varphi\left(\vec{\beta}_i\right)+\varphi\left(\vec{\beta}'_i\right)\right]} \tag{B.50}$$
$$\times(-1)^{\sum_{i=1}^{g}\left[|\vec{\beta}_i|\mathcal{V}\left(\vec{\beta}_i\right)|+|\vec{\beta}'_i|\mathcal{V}\left(\vec{\beta}'_i\right)|\right]}\sum_{\vec{\gamma},\vec{\gamma}'}\det\left\{\mathbf{M}_{\left[\mathcal{V}^{\times g}\left(\vec{B}\right),\vec{\alpha}\right]\left[\vec{B},\vec{\gamma}\right]}\right\}$$
$$\times\det\left\{\mathbf{M}_{\left[\mathcal{V}^{\times g}\left(\vec{B}'\right),\vec{\alpha}\right]\left[\vec{B}',\vec{\gamma}'\right]}\right\}\operatorname{tr}\left(C_{\vec{\eta}}C_{\vec{\gamma}}C_{\vec{\eta}}C_{\vec{\gamma}'}\right)$$

$$\frac{1}{2^n}(-1)^{\frac{1}{2}|\vec{\eta}|(\vec{\eta}-1)}\operatorname{tr}\left[C_{\vec{\eta}}\left(U^{\dagger}C_{\vec{\alpha}}U\right)C_{\vec{\eta}}\left(U^{\dagger}C_{\vec{\alpha}}U\right)\right]=\sum_{\vec{B},\vec{B}'\subseteq\bigcup_{i=1}^{g}\vec{q}_i} i^{\sum_{i=1}^{g}\left[\varphi\left(\vec{\beta}_i\right)+\varphi\left(\vec{\beta}'_i\right)\right]} \tag{B.51}$$
$$\times(-1)^{\sum_{i=1}^{g}\left[|\vec{\beta}_i|\mathcal{V}\left(\vec{\beta}_i\right)|+|\vec{\beta}'_i|\mathcal{V}\left(\vec{\beta}'_i\right)|\right]}\sum_{\vec{\gamma},\vec{\gamma}'}(-1)^{\frac{1}{2}|\vec{\gamma}|(|\vec{\gamma}|-1)+|\vec{\eta}||\vec{\gamma}|+|\vec{\eta}\cap\vec{\gamma}|}$$
$$\times\det\left\{\mathbf{M}_{\left[\mathcal{V}^{\times g}\left(\vec{B}\right),\vec{\alpha}\right]\left[\vec{B},\vec{\gamma}\right]}\right\}\det\left\{\mathbf{M}_{\left[\mathcal{V}^{\times g}\left(\vec{B}'\right),\vec{\alpha}\right]\left[\vec{B}',\vec{\gamma}'\right]}\right\}\delta_{\vec{\gamma}\vec{\gamma}'}$$

$$\frac{1}{2^n}(-1)^{\frac{1}{2}[|\vec{\eta}|(\vec{\eta}-1)+|\vec{\alpha}|(\vec{\alpha}-1)]}\operatorname{tr}\left[C_{\vec{\eta}}\left(U^{\dagger}C_{\vec{\alpha}}U\right)C_{\vec{\eta}}\left(U^{\dagger}C_{\vec{\alpha}}U\right)\right]$$
$$=\sum_{\vec{B},\vec{B}'\subseteq\bigcup_{i=1}^{g}\vec{q}_i} i^{\sum_{i=1}^{g}\left[\varphi\left(\vec{\beta}_i\right)+\varphi\left(\vec{\beta}'_i\right)\right]}(-1)^{|\vec{B}|+|\vec{B}'|+\frac{1}{2}\sum_{i=1}^{g}\left[|\mathcal{V}\left(\vec{\beta}_i\right)|-|\vec{\beta}_i|\right]} \tag{B.52}$$
$$\times\sum_{\vec{\gamma},\vec{\gamma}'}\det\left\{\mathbf{M}_{\left[\mathcal{V}^{\times g}\left(\vec{B}\right),\vec{\alpha}\right]\left[\vec{B},\vec{\gamma}\right]}\right\}\det\left[(-1)^{|\vec{\eta}|}\left(\mathbf{I}-2\mathbf{P}_{\vec{\eta}}\right)_{\vec{\gamma}\vec{\gamma}'}\right]$$
$$\times\det\left\{\mathbf{M}_{\left[\mathcal{V}^{\times g}\left(\vec{B}'\right),\vec{\alpha}\right]\left[\vec{B}',\vec{\gamma}'\right]}\right\}$$

$$\frac{1}{2^n}(-1)^{\frac{1}{2}[|\vec{\eta}|(\vec{\eta}-1)+|\vec{\alpha}|(\vec{\alpha}-1)]}\operatorname{tr}\left[C_{\vec{\eta}}\left(U^{\dagger}C_{\vec{\alpha}}U\right)C_{\vec{\eta}}\left(U^{\dagger}C_{\vec{\alpha}}U\right)\right]$$
$$=\sum_{\vec{B},\vec{B}'\subseteq\bigcup_{i=1}^{g}\vec{q}_i} i^{\sum_{i=1}^{g}\left[\varphi\left(\vec{\beta}_i\right)+\varphi\left(\vec{\beta}'_i\right)\right]}(-1)^{|\vec{B}|+|\vec{B}'|+|\vec{B}||\vec{B}'|+\frac{1}{2}\sum_{i=1}^{g}\left[|\mathcal{V}\left(\vec{\beta}_i\right)|-|\vec{\beta}_i|\right]} \tag{B.53}$$
$$\times\det\begin{pmatrix}\mathbf{0}_{|\vec{B}'|\times|\vec{B}|} & \mathbf{M}^{\mathrm{T}}_{\vec{B}'\left[\mathcal{V}^{\times g}\left(\vec{B}'\right),\vec{\alpha}\right]}\\ \mathbf{M}_{\left[\mathcal{V}^{\times g}\left(\vec{B}\right),\vec{\alpha}\right]\vec{B}} & (-1)^{|\vec{\eta}|}\mathbf{M}_{\left[\mathcal{V}^{\times g}\left(\vec{B}\right),\vec{\alpha}\right][2n]}\left(\mathbf{I}-2\mathbf{P}_{\vec{\eta}}\right)\mathbf{M}^{\mathrm{T}}_{[2n]\left[\mathcal{V}^{\times g}\left(\vec{B}'\right),\vec{\alpha}\right]}\end{pmatrix} \tag{B.54}$$

$$\frac{1}{2^n}(-1)^{\frac{1}{2}[|\vec{\eta}|(\vec{\eta}-1)+|\vec{\alpha}|(\vec{\alpha}-1)]}\operatorname{tr}\left[C_{\vec{\eta}}\left(U^{\dagger}C_{\vec{\alpha}}U\right)C_{\vec{\eta}}\left(U^{\dagger}C_{\vec{\alpha}}U\right)\right]$$
$$=\sum_{\vec{B},\vec{B}'\subseteq\bigcup_{i=1}^{g}\vec{q}_i}(-1)^{|\vec{B}|+|\vec{B}'|+|\vec{B}||\vec{B}'|+\sum_{i=1}^{g}\left[|\vec{\beta}_i|\left(\sum_{j\in\vec{\beta}_i}j\right)+|\vec{\beta}'_i|\left(\sum_{j\in\vec{\beta}'_i}j\right)+\delta_{|\vec{\beta}_i|,3}+\delta_{|\vec{\beta}'_i|,3}\right]}$$
$$\times\det\left[\mathbf{K}\left(\vec{\eta}\right)_{\left[\vec{B}',\mathcal{V}^{\times g}\left(\vec{B}\right),\vec{\alpha}\right]\left[\vec{B},\mathcal{V}^{\times g}\left(\vec{B}'\right),\vec{\alpha}\right]}\right], \tag{B.55}$$

where, letting $\vec{Q} = \bigcup_{i=1}^{g} \vec{q}_i$,

$$\mathbf{K}\left(\vec{\eta}\right) = \begin{pmatrix} \mathbf{0}_{|\vec{Q}|\times|\vec{Q}|} & \mathbf{M}^{\mathrm{T}}_{\vec{Q}\left[\vec{Q},[2n]\right]} \\ \mathbf{M}_{\left[\vec{Q},[2n]\right]\vec{Q}} & (-1)^{|\vec{\eta}|}\mathbf{M}_{\left[\vec{Q},[2n]\right][2n]}\left(\mathbf{I}-2\mathbf{P}_{\vec{\eta}}\right)\mathbf{M}^{\mathrm{T}}_{[2n]\left[\vec{Q},[2n]\right]} \end{pmatrix}. \tag{B.56}$$

From Eq. (B.51) to Eq. (B.52), we use the fact that

$$(-1)^{\frac{1}{2}(|\vec{\alpha}|+2k)(|\vec{\alpha}|+2k-1)} = (-1)^{\frac{1}{2}|\vec{\alpha}|(|\vec{\alpha}|-1)+k(2|\vec{\alpha}|-1)+2k^2} \tag{B.57}$$

$$(-1)^{\frac{1}{2}(|\vec{\alpha}|+2k)(|\vec{\alpha}|+2k-1)} = (-1)^{\frac{1}{2}|\vec{\alpha}|(|\vec{\alpha}|-1)}(-1)^{k} \tag{B.58}$$

for $|\vec{\gamma}| = |\vec{\alpha}| + 2k$ and $2k = |\mathcal{V}\left(\vec{B}\right)| - |\vec{B}|$. The latter quantity is guaranteed to be even by the parity-preserving property of $\mathcal{V}$. By the same property, we have

$$(-1)^{\sum_{i=1}^{g}\left(|\vec{\beta}_i||\mathcal{V}\left(\vec{\beta}_i\right)|+|\vec{\beta}'_i||\mathcal{V}\left(\vec{\beta}'_i\right)|\right)} = (-1)^{\sum_{i=1}^{g}\left(|\vec{\beta}_i|+|\vec{\beta}'_i|\right)} \tag{B.59}$$

$$(-1)^{\sum_{i=1}^{g}\left(|\vec{\beta}_i||\mathcal{V}\left(\vec{\beta}_i\right)|+|\vec{\beta}'_i||\mathcal{V}\left(\vec{\beta}'_i\right)|\right)} = (-1)^{|\vec{B}|+|\vec{B}'|} \tag{B.60}$$

From Eq. (B.54) to Eq. (B.55), we used the particular form for the function $\varphi(\vec{\beta}_j)$, from

$$V_i^{\dagger} C_{\vec{\beta}_i} V_i = \begin{cases} C_{\vec{\beta}_i} & |\vec{\beta}_i| \text{ even} \\ (-i)(-1)^{\sum_{j\in\vec{\beta}_i} j} C_{\overline{\beta}_i} & |\vec{\beta}_i| \text{ odd} \end{cases}, \tag{B.61}$$

where $\overline{\beta}_i = \vec{q}_i/\vec{\beta}_i$, and the phase comes from the fact that $Z_j Z_{j+1} = -C_{\vec{q}_j}$ and $C_{\vec{q}_j} c_k = (-1)^{|\vec{q}_j|-k} C_{\vec{q}_j/k}$ for $|\vec{q}_j| = 4$. We see there is a factor of $-i$ for every $\vec{\beta}_i$ for which $|\vec{\beta}_i|$ is odd. Since the sub-matrix inside the determinant of Eq. (B.55) must be square, we must have

$$|\vec{B}'| + |\mathcal{V}^{\times g}\left(\vec{B}\right)| + |\vec{\alpha}| = |\vec{B}| + |\mathcal{V}^{\times g}\left(\vec{B}'\right)| + |\vec{\alpha}| \tag{B.62}$$

$$|\mathcal{V}^{\times g}\left(\vec{B}\right)| - |\vec{B}| = |\mathcal{V}^{\times g}\left(\vec{B}'\right)| - |\vec{B}'| \tag{B.63}$$

$$\frac{1}{2}\sum_{i=1}^{g}\left[|\mathcal{V}^{\times g}\left(\vec{\beta}_i\right)| - |\vec{\beta}_i|\right] = \frac{1}{2}\sum_{i=1}^{g}\left[|\mathcal{V}^{\times g}\left(\vec{\beta}'_i\right)| - |\vec{\beta}'_i|\right], \tag{B.64}$$

and thus

$$(-1)^{\frac{1}{2}\sum_{i=1}^{g}\left[|\mathcal{V}^{\times g}\left(\vec{\beta}_i\right)|-|\vec{\beta}_i|\right]} = i^{\frac{1}{2}\sum_{i=1}^{g}\left\{\left[|\mathcal{V}^{\times g}\left(\vec{\beta}_i\right)|-|\vec{\beta}_i|\right]+\left[|\mathcal{V}^{\times g}\left(\vec{\beta}'_i\right)|-|\vec{\beta}'_i|\right]\right\}} \tag{B.65}$$

$$(-1)^{\frac{1}{2}\sum_{i=1}^{g}\left[|\mathcal{V}^{\times g}\left(\vec{\beta}_i\right)|-|\vec{\beta}_i|\right]} = (-1)^{\sum_{i=1}^{g}\left(\delta_{|\vec{\beta}_i|,3}+\delta_{|\vec{\beta}'_i|,3}\right)} i^{\frac{1}{2}\sum_{i=1}^{g}\left[||\mathcal{V}^{\times g}\left(\vec{\beta}_i\right)|-|\vec{\beta}_i||+||\mathcal{V}^{\times g}\left(\vec{\beta}'_i\right)|-|\vec{\beta}'_i||\right]}, \tag{B.66}$$

and the exponent on the factor of i is the number of $\vec{\beta}_i$ for which $|\vec{\beta}_i|$ is odd, which cancels the corresponding factor of $-i$ from Eq. (B.61).

B.4 Exact formula for Lightcone Boundary

We want to calculate

$$b_s^2(t) \equiv \begin{cases} \sum_{\substack{\vec{\beta} \text{ with } X_s I^{\otimes(n-s)} \\ \text{or } Y_s I^{\otimes(n-s)} \text{ present}}} \det\left(\mathbf{u}_{\vec{\alpha}\vec{\beta}}\right)^2 & (s \geq \lfloor n/2 \rfloor) \\ \sum_{\substack{\vec{\beta} \text{ with } I^{\otimes(s-1)} X_s \\ \text{or } I^{\otimes(s-1)} Y_s \text{ present}}} \det\left(\mathbf{u}_{\vec{\alpha}\vec{\beta}}\right)^2 & (s \leq \lfloor n/2 \rfloor) \end{cases}. \tag{B.67}$$

As stated in the main text, we can apply the Jordan-Wigner transformation on the strings satisfying the condition in each sum to obtain

$$b_s^2(t) = \begin{cases} \sum_{\vec{\beta}'} \left\{ \det\left[\mathbf{u}_{\vec{\alpha}\left(\vec{\beta}', 2s-1\right)}\right]^2 + \det\left[\mathbf{u}_{\vec{\alpha}\left(\vec{\beta}', 2s\right)}\right]^2 \right\} & (s \geq \lfloor n/2 \rfloor) \\ \sum_{\vec{\beta}'} \left\{ \det\left[\mathbf{u}_{\vec{\alpha}\left([2s-2], 2s-1, \vec{\beta}'\right)}\right]^2 + \det\left[\mathbf{u}_{\vec{\alpha}\left([2s-2], 2s, \vec{\beta}'\right)}\right]^2 \right\} & (s \leq \lfloor n/2 \rfloor) \end{cases}. \tag{B.68}$$

Each of these sums is of the form in Eq. (5.28), which we can evaluate to obtain

$$-b_s^2(t) = \begin{cases} \det\begin{pmatrix} 0 & \mathbf{u}_{2s-1,\vec{\alpha}}^{\mathrm{T}} \\ \mathbf{u}_{\vec{\alpha},2s-1} & \mathbf{u}_{\vec{\alpha}[2(s-1)]}\mathbf{u}_{[2(s-1)]\vec{\alpha}}^{\mathrm{T}} \end{pmatrix} & (s \geq \lfloor n/2 \rfloor) \\ \quad + \det\begin{pmatrix} 0 & \mathbf{u}_{2s,\vec{\alpha}}^{\mathrm{T}} \\ \mathbf{u}_{\vec{\alpha},2s} & \mathbf{u}_{\vec{\alpha}[2(s-1)]}\mathbf{u}_{[2(s-1)]\vec{\alpha}}^{\mathrm{T}} \end{pmatrix} & \\ \det\begin{pmatrix} \mathbf{0}_{(2s-1)\times(2s-1)} & \mathbf{u}_{([2(s-1)],2s-1),\vec{\alpha}}^{\mathrm{T}} \\ \mathbf{u}_{\vec{\alpha},([2(s-1)],2s-1)} & \mathbf{u}_{\vec{\alpha}\overline{[2s]}}\mathbf{u}_{\overline{[2s]}\vec{\alpha}}^{\mathrm{T}} \end{pmatrix} & (s \leq \lfloor n/2 \rfloor) \\ \quad + \det\begin{pmatrix} \mathbf{0}_{(2s-1)\times(2s-1)} & \mathbf{u}_{([2(s-1)],2s),\vec{\alpha}}^{\mathrm{T}} \\ \mathbf{u}_{\vec{\alpha},([2(s-1)],2s)} & \mathbf{u}_{\vec{\alpha}\overline{[2s]}}\mathbf{u}_{\overline{[2s]}\vec{\alpha}}^{\mathrm{T}} \end{pmatrix} & \end{cases}. \tag{B.69}$$

We see that $b_s^2(t)$ can therefore be evaluated efficiently as the sum of only two determinants of polynomially-sized matrices.

Appendix C

"Autonomous quantum Maxwell demon"

C.1 Exposition of the Interaction Lindbladian

Here we give the details of our interaction Lindbladian $\mathcal{L}_{DM}$. As mentioned in the main text, the intrinsic and cooperative transitions are characterized by the Lindblad jump operators

$$L_{g\to e} = \sqrt{\Gamma_{g\to e}}\sigma_D^- \otimes \mathbb{1}_M \tag{C.1}$$

$$L_{g\leftarrow e} = \sqrt{\Gamma_{g\leftarrow e}}\sigma_D^+ \otimes \mathbb{1}_M \tag{C.2}$$

for the intrinsic transitions, and

$$L_{g0\to e1} = \sqrt{\Gamma_{g0\to e1}}\sigma_D^- \otimes \sigma_M^- \tag{C.3}$$

$$L_{g0\leftarrow e1} = \sqrt{\Gamma_{g0\leftarrow e1}}\sigma_D^+ \otimes \sigma_M^+ \tag{C.4}$$

for the cooperative transitions. Here, $\sigma^{\pm} = \frac{1}{2}(X \pm iY)$ are the qubit ladder operators, and $\sigma^{\{x,y\}}$ are qubit Pauli-x and -y operators. Once again, the transition rates are chosen to satisfy detailed balance

$$\frac{\Gamma_{g\to e}}{\Gamma_{g\leftarrow e}} = e^{-\beta_h \Delta} \qquad \frac{\Gamma_{g0\to e1}}{\Gamma_{g0\leftarrow e1}} = e^{-\beta_c \Delta}. \tag{C.5}$$

Finally, the demon has an intrinsic Hamiltonian

$$\hat{H}_D = \Delta |e\rangle\langle e| = \frac{\Delta}{2}(\mathbb{1}_D - Z_D), \tag{C.6}$$

and so the full dynamics of the interaction are generated by the Lindbladian

$$\mathcal{L}_{DM}(\rho_{DM}) = -i[\hat{H}_D \otimes \mathbb{1}_M, \rho_{DM}] + \sum_i \mathcal{L}_i(\rho_{DM}), \tag{C.7}$$

where

$$\mathcal{L}_i(\rho_{DM}) \;\; = L_i \rho_{DM} L_i^\dagger - \tfrac{1}{2}\{L_i^\dagger L_i, \rho_{DM}\}, \tag{C.8}$$

is the term corresponding to a particular jump operator. $[.,.]$ and $\{.,.\}$ are the commutator and anticommutator, respectively, and we have chosen units such that $\hbar = 1$. As mentioned in the main text, $\mathcal{L}_{g0\to e1}$ and $\mathcal{L}_{g0\leftarrow e1}$ commute with $\mathcal{U}_{DM}^{z,\varphi}$ as defined in Corollary 6.3.2, due to the fact that $\sigma_D^z \otimes \sigma_M^z$ commutes with $\sigma_D^i \otimes \sigma_M^j$ for $i, j \in \{x, y\}$. Clearly $\mathcal{L}_{g\to e}$, $\mathcal{L}_{g\leftarrow e}$, and the Hamiltonian terms commute with $\mathcal{U}_M^{z,\varphi}$.

$\mathcal{L}_{DM}$ has a fixed point $\rho_{DM}^{(\mathrm{fp})}$, for which

$$\mathcal{L}_{DM}\left(\rho_{DM}^{(\mathrm{fp})}\right) = \rho_{DM}^{(\mathrm{fp})} \tag{C.9}$$

and given by a product

$$\rho_{DM}^{(\mathrm{fp})} = \rho_{D}^{(\mathrm{fp})} \otimes \rho_{M}^{(\mathrm{fp})}, \tag{C.10}$$

where

$$\rho_{D}^{(fp)} = \frac{1}{1+e^{\beta_h \Delta}} \begin{pmatrix} 1 & 0 \\ 0 & e^{\beta_h \Delta} \end{pmatrix} \tag{C.11}$$

in the energy eigenbasis, and

$$\rho_{M}^{(fp)} = \frac{1}{1+e^{(\beta_h-\beta_c)\Delta}} \begin{pmatrix} 1 & 0 \\ 0 & e^{(\beta_h-\beta_c)\Delta} \end{pmatrix} \tag{C.12}$$

in the z basis. The form of this fixed point will be important for the following proofs.

C.2 Generalized Clausius Inequality

Here we give a proof of Eq.s (6.15, 6.16, 6.20). As stated in the main text, we have monotonic evolution to the fixed point in a single interaction ($\phi_\tau \otimes \mathcal{I}_{\tilde{M}}$)

$$D(\rho_{DM\tilde{M}}||\rho_{DM}^{(\mathrm{fp})} \otimes \rho_{\tilde{M}}) - D(\rho'_{DM\tilde{M}}||\rho_{DM}^{(\mathrm{fp})} \otimes \rho_{\tilde{M}}) \geq 0 \tag{C.13}$$

where

$$D(\rho||\sigma) = -S(\rho) - \mathrm{tr}\,(\rho \ln \sigma) \tag{C.14}$$

is the quantum relative entropy. Using

$$\ln(\rho_A \otimes \rho_B) = \ln \rho_A \otimes \mathbb{1}_B + \mathbb{1}_A \otimes \ln \rho_B \tag{C.15}$$

$$\mathrm{tr}\left[\rho_{AB}\left(\hat{O}_A \otimes \mathbb{1}_B\right)\right] = \mathrm{tr}\left(\rho_A \hat{O}_A\right) \equiv \left\langle \hat{O}_A \right\rangle \tag{C.16}$$

and

$$\mathrm{tr}\left[\left(\rho'_D - \rho_D\right) \ln \rho_D^{(\mathrm{fp})}\right] \ = 0, \tag{C.17}$$

from the periodic steady state condition on D, additionally with the fact that the interaction acts as the identity on $\tilde{M}$, Eq. (C.13) reduces to

$$\Delta S_{DM\tilde{M}} + \mathrm{tr}\left[\left(\rho'_M - \rho_M\right) \ln \rho_M^{(\mathrm{fp})}\right] \geq 0 \tag{C.18}$$

Next, we note that

$$\left\langle \ln \rho_M^{(\mathrm{fp})} \right\rangle \ = \tfrac{\Delta}{2}(\beta_h - \beta_c)\,(1 - \zeta) - \ln\left[1 + e^{(\beta_h - \beta_c)\Delta}\right] \tag{C.19}$$

All of the constant terms cancel in the difference, and so we are left with

$$\mathrm{tr}\left[\left(\rho'_M - \rho_M\right)\ln \rho_M^{(fp)}\right] = \frac{\Delta}{2}(\zeta' - \zeta)(\beta_c - \beta_h) \tag{C.20}$$

Defining $Q_{h\to c} \equiv \frac{\Delta}{2}(\zeta' - \zeta)$, Eq. (C.18) gives

$$Q_{h\to c}(\beta_c - \beta_h) + \Delta S_{DM\tilde{M}} \geq 0 \tag{C.21}$$

Finally, we use the definition of quantum mutual information

$$S(\rho_{DM\tilde{M}}) \quad = S(\rho_D) + S(\rho_{M\tilde{M}}) - I(D : M\tilde{M}) \tag{C.22}$$

and the fact that $\Delta S_D = 0$, again from the periodic steady state condition on D, in Eq. (C.21) to obtain Eq. (6.20)

$$Q_{h\to c}(\beta_c - \beta_h) + \Delta S_{M\tilde{M}} \geq \Delta I_{D:M\tilde{M}} \tag{C.23}$$

Eq. (6.16) follows in the same manner, but without including $\tilde{M}$, and Eq. (6.15) requires neglecting correlations ($\Delta I_{D:M} \approx 0$).

C.3 Matrix Product Density Operator Update Method

We describe our matrix product quantum operation shown in Fig. 6.3 by its action on the product basis elements in Eq. (6.26). Using a generalization of the result in

Ref. [SSV+05] from vectors to operators as in Ref. [ZV04], we update each element by n sequential interactions, $\Phi_{n\tau}$, as

$$\Phi_{n\tau}\left(\sigma_D^{i_D}\bigotimes_{j=1}^{n}\sigma^{i_j}\right)=\sum_{i_D',\vec{i}'}\mathrm{tr}\left(B^{i_D}\mathcal{P}\prod_{j=1}^{n}C^{i_j'i_j}\right)\sigma_D^{i_D'}\bigotimes_{j=1}^{n}\sigma^{i_j'}, \tag{C.24}$$

where

$$\left(C^{i'i}\right)_{\alpha\beta}=\mathrm{tr}\left[\left(\sigma_D^{\alpha}\otimes\sigma_M^{i'}\right)^{\dagger}\phi_\tau\left(\sigma_D^{\beta}\otimes\sigma_M^{i}\right)\right] \tag{C.25}$$

$$\left(B^{i_D}\right)_{\alpha\beta}=\mathrm{tr}\left[\left(\sigma_D^{\alpha}\right)^{\dagger}\rho_D(0)\right]\delta_{i_D\beta}, \tag{C.26}$$

$\delta_{i_D\beta}$ is the Kronecker delta, and the σ^{i_D} are the basis elements for D. These expressions follow from completeness under the *trace inner product* for this operator basis

$$\langle A,B\rangle_{\mathrm{tr}}=\mathrm{tr}\,A^{\dagger}B \tag{C.27}$$

$$A=\sum_i\left\langle\sigma^i,A\right\rangle_{\mathrm{tr}}\sigma^i \tag{C.28}$$

Thus, after rearranging,

$$\begin{aligned}\rho_{D\mathbb{M}}(n\tau) \quad &= \textstyle\sum_{i_D,\vec{i}}\mathrm{tr}\Big[\left(B^{i_D}\otimes\mathbb{1}\right)\mathcal{P}\prod_{j=n+1}^{N}\left(\mathbb{1}\otimes A^{i_j}\right)\\ &\quad\times\mathcal{P}\textstyle\prod_{j=1}^{n}\left(\sum_k C^{i_jk}\otimes A^k\right)\Big]\sigma_D^{i_D}\bigotimes_{j=1}^{N}\sigma^{i_j},\end{aligned} \tag{C.29}$$

and in the next interaction, we make the replacement

$$\mathbb{1}\otimes A^{i_{n+1}}\mapsto\sum_k C^{i_{n+1}k}\otimes A^k. \tag{C.30}$$

We see that this leaves the description of Eq. (C.29) approximately unchanged for sufficiently large N, n. This is the aforementioned periodic steady state of the system.

Finally, we trace out all previously interacted degrees of freedom to obtain

$$\rho_{DM\tilde{M}} = \sum_{i_D,\vec{i}} \mathrm{tr}\Big[\left(B^{i_D} \otimes \mathbb{1}\right) \mathcal{P} \prod_{j=n+1}^{N} \left(\mathbb{1} \otimes A^{i_j}\right) \times \left(\sum_k D^k \otimes A^k\right)^n \Big] \sigma^{i_D} \bigotimes_{j=n+1}^{N} \sigma^{i_j}, \tag{C.31}$$

where

$$D^k = \sum_l C^{lk} \,\mathrm{tr}\, \sigma^l. \tag{C.32}$$

After the next interaction, we have

$$\rho'_{DM\tilde{M}} = \sum_{i_D,\vec{i}} \mathrm{tr}\Big[\left(B^{i_D} \otimes \mathbb{1}\right) \mathcal{P} \prod_{j=n+2}^{N} \left(1 \otimes A^{i_j}\right) \times \left(\sum_k C^{i_{n+1}k} \otimes A^{i_{n+1}}\right) \left(\sum_k D^k \otimes A^k\right)^n \Big] \sigma^{i_D} \bigotimes_{j=n+1}^{N} \sigma^{i_j}. \tag{C.33}$$

We now simplify Eq. (C.31) using is the classicality of our interaction, ϕ_τ, which implies $D^{\pm} = 0$. Rearranging, and making the identifications

$$\rho_D^{(\vec{k})} = \sum_{i_D} \mathrm{tr}\left[B^{i_D} \mathcal{P} \left(\prod_{j=1}^{n} D^{k_j}\right)\right] \sigma_D^{i_D}, \tag{C.34}$$

$$p_{\vec{k}} \rho_{M\tilde{M}}^{(\vec{k})} = \sum_{\vec{i}} \mathrm{tr}\left[\mathcal{P}\left(\prod_{j=n+1}^{N} A^{i_j}\right)\left(\prod_{j=1}^{n} A^{k_j}\right)\right] \bigotimes_{j=n+1}^{N} \sigma^{i_j}, \tag{C.35}$$

for $\vec{k} \in \{0,1\}^n$ gives our Theorem 4

$$\rho_{DM\tilde{M}} = \sum_{\vec{k}} p_{\vec{k}} \rho_D^{(\vec{k})} \otimes \rho_{M\tilde{M}}^{(\vec{k})}, \tag{C.36}$$

where

$$\rho_D^{(\vec{k})} = \mathcal{P} \prod_{j=1}^{n} \mathcal{T}^{k_j} \left[\rho_D(0)\right], \tag{C.37}$$

$$\rho_{M\tilde{M}}^{(\vec{k})} = \frac{1}{p_{\vec{k}}} \operatorname{tr}_{\bar{M}} \left[\left(\mathbb{1}_{M\tilde{M}} \bigotimes_{j=1}^{n} \sigma^{k_j} \right) \rho_{\mathbb{M}}(0) \right], \tag{C.38}$$

and

$$\mathcal{T}^{k_j}\left(\rho_D\right) \equiv \operatorname{tr}_M \phi_\tau \left(\rho_D \otimes \sigma_M^{k_j} \right), \tag{C.39}$$

$$p_{\vec{k}} = \operatorname{tr} \left[\left(\mathbb{1}_{M\tilde{M}} \bigotimes_{j=1}^{n} \sigma^{k_j} \right) \rho_{\mathbb{M}}(0) \right]. \tag{C.40}$$

The classicality of the $\rho_D^{(\vec{k})}$ follows from the uniqueness of the fixed point of the transfer operator $\mathcal{T}^k$, which is the periodic steady state of the demon upon interacting with a string of uncorrelated pure classical qubits, $|k\rangle^{\otimes n}$, and found in Ref. [MQJ13]. Because this fixed point is classical and unique, $\mathcal{T}^k$ must be dephasing in the energy eigenbasis, and so the $\rho_D^{(\vec{k})}$ are classical as well.

References

A

[Åbe13] J. Åberg. Truly work-like work extraction via a single-shot analysis. *Nature Communications*, 4:1925 EP –, 06 2013. 95

[Abr10] E. Abrahams. *50 Years of Anderson Localization*. World Scientific, Singapore, 2010. 55

[AFI16] I. L. Aleiner, L. Faoro, and L. B. Ioffe. Microscopic model of quantum butterfly effect: Out-of-time-order correlators and traveling combustion waves. *Annals of Physics*, 375:378 – 406, 2016. 57

[Ali14] R. Alicki. Quantum thermodynamics: An example of two-level quantum machine. *Open Systems & Information Dynamics*, 21(01n02):1440002, 2014. 117

[AMPS13] A. Almheiri, D. Marolf, J. Polchinski, and J. Sully. Black holes: complementarity or firewalls? *Journal of High Energy Physics*, 2013(2):62, Feb 2013. 34

[And58] P. W. Anderson. Absence of diffusion in certain random lattices. *Phys. Rev.*, 109:1492–1505, Mar 1958. 55, 71

[ARH16] D. A. Abanin, W. D. Roeck, and F. Huveneers. Theory of many-body localization in periodically driven systems. *Annals of Physics*, 372:1 – 11, 2016. 68

B

[BAA06] D. Basko, I. Aleiner, and B. Altshuler. Metalinsulator transition in a weakly interacting many-electron system with localized single-particle states. *Annals of Physics*, 321(5):1126 – 1205, 2006. 55, 68

[BC14] D. J. Brod and A. M. Childs. The computational power of matchgates and the xy interaction on arbitrary graphs. *Quantum Info. Comput.*, 14(11-12):901–916, September 2014. 7, 32, 56, 73

[BDEK04] C. W. J. Beenakker, D. P. DiVincenzo, C. Emary, and M. Kindermann. Charge detection enables free-electron quantum computation. *Phys. Rev. Lett.*, 93:020501, Jul 2004. 7

[BdLS+12] M. J. Burek, N. P. de Leon, B. J. Shields, B. J. M. Hausmann, Y. Chu, Q. Quan, A. S. Zibrov, H. Park, M. D. Lukin, and M. Lonar. Free-standing mechanical and photonic nanostructures in single-crystal diamond. *Nano Letters*, 12(12):6084–6089, 2012. PMID: 23163557. 93

[BEO09] C. K. Burrell, J. Eisert, and T. J. Osborne. Information propagation through quantum chains with fluctuating disorder. *Phys. Rev. A*, 80:052319, Nov 2009. 56, 62

[BG16] S. Bravyi and D. Gosset. Improved classical simulation of quantum circuits dominated by clifford gates. *Phys. Rev. Lett.*, 116:250501, Jun 2016. 64

[BGa11] D. J. Brod and E. F. Galvão. Extending matchgates into universal quantum computation. *Phys. Rev. A*, 84:022310, Aug 2011. 7, 32

[BHL+14] N. Brunner, M. Huber, N. Linden, S. Popescu, R. Silva, and P. Skrzypczyk. Entanglement enhances cooling in microscopic quantum refrigerators. *Phys. Rev. E*, 89:032115, Mar 2014. 94

[BHV06] S. Bravyi, M. B. Hastings, and F. Verstraete. Lieb-robinson bounds and the generation of correlations and topological quantum order. *Phys. Rev. Lett.*, 97:050401, Jul 2006. 57, 68

[BK02] S. B. Bravyi and A. Y. Kitaev. Fermionic quantum computation. *Annals of Physics*, 298(1):210 – 226, 2002. 56, 69, 73

[BL14] L. Bonnes and A. M. Läuchli. Superoperators vs. Trajectories for Matrix Product State Simulations of Open Quantum System: A Case Study. *ArXiv e-prints*, November 2014. arXiv:1411.4831 [cond-mat.quant-gas]. 104

[BLCR15] Y. Bar Lev, G. Cohen, and D. R. Reichman. Absence of diffusion in an interacting system of spinless fermions on a one-dimensional disordered lattice. *Phys. Rev. Lett.*, 114:100601, Mar 2015. 55

[BN13] B. Bauer and C. Nayak. Area laws in a many-body localized state and its implications for topological order. *Journal of Statistical Mechanics: Theory and Experiment*, 2013(09):P09005, 2013. 55

[BnYC+17] M. C. Bañuls, N. Y. Yao, S. Choi, M. D. Lukin, and J. I. Cirac. Dynamics of quantum information in many-body localized systems. *Phys. Rev. B*, 96:174201, Nov 2017. 68, 71

[BO07] C. K. Burrell and T. J. Osborne. Bounds on the speed of information propagation in disordered quantum spin chains. *Phys. Rev. Lett.*, 99:167201, Oct 2007. 55, 61

[BPM12] J. H. Bardarson, F. Pollmann, and J. E. Moore. Unbounded growth of entanglement in models of many-body localization. *Phys. Rev. Lett.*, 109:017202, Jul 2012. 68, 71

[BR13] E. Boukobza and H. Ritsch. Breaking the carnot limit without violating the second law: A thermodynamic analysis of off-resonant quantum light generation. *Phys. Rev. A*, 87:063845, Jun 2013. 117

[Bra] S. Bravyi. Contraction of matchgate tensor networks on non-planar graphs. *Contemporary Mathematics*, 482:179–211. 7

[Bra06] S. Bravyi. Universal quantum computation with the $\nu = 52$ fractional quantum hall state. *Phys. Rev. A*, 73:042313, Apr 2006. 7, 56, 64, 73

[Bro16] D. J. Brod. Efficient classical simulation of matchgate circuits with generalized inputs and measurements. *Phys. Rev. A*, 93:062332, Jun 2016. 31, 32, 59

[BS14] A. C. Barato and U. Seifert. Unifying three perspectives on information processing in stochastic thermodynamics. *Phys. Rev. Lett.*, 112:090601, Mar 2014. 93

[BSHMB15] S. Bera, H. Schomerus, F. Heidrich-Meisner, and J. H. Bardarson. Many-body localization characterized from a one-particle perspective. *Phys. Rev. Lett.*, 115:046603, Jul 2015. 55

[BT06] E. Boukobza and D. J. Tannor. Thermodynamics of bipartite systems: Application to light-matter interactions. *Phys. Rev. A*, 74:063823, Dec 2006. 95

C

[Cav90] C. M. Caves. Quantitative limits on the ability of a maxwell demon to extract work from heat. *Phys. Rev. Lett.*, 64:2111–2114, Apr 1990. 93, 94

[CCBn15] J. Cui, J. I. Cirac, and M. C. Bañuls. Variational matrix product operators for the steady state of dissipative quantum systems. *Phys. Rev. Lett.*, 114:220601, Jun 2015. 104

[CDP17] J. S. Cotler, D. Ding, and G. R. Penington. Out-of-time-order Operators and the Butterfly Effect. *ArXiv e-prints*, April 2017. arXiv:1704.02979 [quant-ph]. 35, 57

[Che16] Y. Chen. Universal Logarithmic Scrambling in Many Body Localization. *ArXiv e-prints*, August 2016. arXiv:1608.02765 [cond-mat.dis-nn]. 54, 57, 68, 71

[CHJLY17] J. Cotler, N. Hunter-Jones, J. Liu, and B. Yoshida. Chaos, complexity, and random matrices. *Journal of High Energy Physics*, 2017(11):48, Nov 2017. 72

[CL01] Y. Cui and C. M. Lieber. Functional nanoscale electronic devices assembled using silicon nanowire building blocks. *Science*, 291(5505):851–853, 2001. 93

[CL15] A. Chandran and C. R. Laumann. Semiclassical limit for the many-body localization transition. *Phys. Rev. B*, 92:024301, Jul 2015. 56, 68

[CM18] A. Chapman and A. Miyake. Classical simulation of quantum circuits by dynamical localization: Analytic results for pauli-observable scrambling in time-dependent disorder. *Phys. Rev. A*, 98:012309, Jul 2018. 69, 75, 79

[COR+13] A. Crespi, R. Osellame, R. Ramponi, V. Giovannetti, R. Fazio, L. Sansoni, F. D. Nicola, F. Sciarrino, , and P. Mataloni. Anderson localization of entangled photons in an integrated quantum qalk. *Nat. Photon.*, 7:322–328, Mar 2013. 55

[CPAA13] L. A. Correa, J. P. Palao, G. Adesso, and D. Alonso. Performance bound for quantum absorption refrigerators. *Phys. Rev. E*, 87:042131, Apr 2013. 117

[CPAA14] L. A. Correa, J. P. Palao, G. Adesso, and D. Alonso. Optimal performance of endoreversible quantum refrigerators. *Phys. Rev. E*, 90:062124, Dec 2014. 117

[CRVdB12] B. Cleuren, B. Rutten, and C. Van den Broeck. Cooling by heating: Refrigeration powered by photons. *Phys. Rev. Lett.*, 108:120603, Mar 2012. 117

[CZ18] X. Chen and T. Zhou. Operator scrambling and quantum chaos. *ArXiv e-prints*, April 2018. arXiv:1804.08655 [cond-mat.str-el]. 68

[CZZ17] Y. Chen, H. Zhai, and P. Zhang. Tunable quantum chaos in the sachdev-ye-kitaev model coupled to a thermal bath. *Journal of High Energy Physics*, 2017(7):150, Jul 2017. 36

D

[Def13] S. Deffner. Information-driven current in a quantum maxwell demon. *Phys. Rev. E*, 88:062128, Dec 2013. 94

[Deu91] J. M. Deutsch. Quantum statistical mechanics in a closed system. *Phys. Rev. A*, 43:2046–2049, Feb 1991. 55

[DFT+18] A. Deshpande, B. Fefferman, M. C. Tran, M. Foss-Feig, and A. V. Gorshkov. Dynamical phase transitions in sampling complexity. *Phys. Rev. Lett.*, 121:030501, Jul 2018. 56

[DJ13] S. Deffner and C. Jarzynski. Information processing and the second law of thermodynamics: An inclusive, hamiltonian approach. *Phys. Rev. X*, 3:041003, Oct 2013. 93

[DL09] R. Dillenschneider and E. Lutz. Energetics of quantum correlations. *EPL (Europhysics Letters)*, 88(5):50003, 2009. 94

[DLP+17] D.-L. Deng, X. Li, J. H. Pixley, Y.-L. Wu, and S. Das Sarma. Logarithmic entanglement lightcone in many-body localized systems. *Phys. Rev. B*, 95:024202, Jan 2017. 68, 71

[dMT13] F. de Melo, P. wikliski, and B. M. Terhal. The power of noisy fermionic quantum computation. *New Journal of Physics*, 15(1):013015, 2013. 56, 73

[dRHRW16] L. del Rio, A. Hutter, R. Renner, and S. Wehner. Relative thermalization. *Phys. Rev. E*, 94:022104, Aug 2016. 94

[DRRV11] O. C. O. Dahlsten, R. Renner, E. Rieper, and V. Vedral. Inadequacy of von neumann entropy for characterizing extractable work. *New Journal of Physics*, 13(5):053015, 2011. 95

E

[Eis13] J. Eisert. Entanglement and tensor network states. *ArXiv e-prints*, August 2013. arXiv:1308.3318 [quant-ph]. 95

[EKLVdB12] M. Esposito, N. Kumar, K. Lindenberg, and C. Van den Broeck. Stochastically driven single-level quantum dot: A nanoscale finite-time thermodynamic machine and its various operational modes. *Phys. Rev. E*, 85:031117, Mar 2012. 117

F

[FGG14] E. Farhi, J. Goldstone, and S. Gutmann. A Quantum Approximate Optimization Algorithm. *ArXiv e-prints*, November 2014. arXiv:1411.4028 [quant-ph]. 92

[FNW92] M. Fannes, B. Nachtergaele, and R. F. Werner. Finitely correlated states on quantum spin chains. *Communications in Mathematical Physics*, 144(3):443–490, Mar 1992. 103

[FWB+15] M. Friesdorf, A. H. Werner, W. Brown, V. B. Scholz, and J. Eisert. Many-body localization implies that eigenvectors are matrix-product states. *Phys. Rev. Lett.*, 114:170505, May 2015. 55

[FWU13] K. Funo, Y. Watanabe, and M. Ueda. Thermodynamic work gain from entanglement. *Phys. Rev. A*, 88:052319, Nov 2013. 94

[FZSZ17a] R. Fan, P. Zhang, H. Shen, and H. Zhai. Out-of-time-order correlation for many-body localization. *Science Bulletin*, 62(10):707 – 711, 2017. 40, 57

[FZSZ17b] R. Fan, P. Zhang, H. Shen, and H. Zhai. Out-of-time-order correlation for many-body localization. *Science Bulletin*, 62(10):707 – 711, 2017. 49, 53, 54, 68, 71, 72

G

[GA15] J. Gemmer and J. Anders. From single-shot towards general work extraction in a quantum thermodynamic framework. *New Journal of Physics*, 17(8):085006, 2015. 95

[GEV02] E. GEVA. On the irreversible performance of a quantum heat engine. *Journal of Modern Optics*, 49(3-4):635–644, 2002. 117

[GEW16] R. Gallego, J. Eisert, and H. Wilming. Thermodynamic work from operational principles. *New Journal of Physics*, 18(10):103017, 2016. 95

[GH13] H. P. Goswami and U. Harbola. Thermodynamics of quantum heat engines. *Phys. Rev. A*, 88:013842, Jul 2013. 95

[GH18] M. J. Gullans and D. A. Huse. Entanglement structure of current driven quantum many-body systems. *ArXiv e-prints*, March 2018. arXiv:1804.00010 [cond-mat.stat-mech]. 68

[GHR+16] J. Goold, M. Huber, A. Riera, L. del Rio, and P. Skrzypczyk. The role of quantum information in thermodynamicsa topical review. *Journal of Physics A: Mathematical and Theoretical*, 49(14):143001, 2016. 93

[GHST18] H. Gharibyan, M. Hanada, S. H. Shenker, and M. Tezuka. Onset of Random Matrix Behavior in Scrambling Systems. *ArXiv e-prints*, March 2018. arXiv:1803.08050 [hep-th]. 68

[GKAK13] D. Gelbwaser-Klimovsky, R. Alicki, and G. Kurizki. Minimal universal quantum heat machine. *Phys. Rev. E*, 87:012140, Jan 2013. 117

[GKNBK15] D. Gelbwaser-Klimovsky, W. Niedenzu, P. Brumer, and G. Kurizki. Power enhancement of heat engines via correlated thermalization in a three-level "working fluid". *Scientific Reports*, 5:14413 EP –, 09 2015. 94

[GLW+02] M. S. Gudiksen, L. J. Lauhon, J. Wang, D. C. Smith, and C. M. Lieber. Growth of nanowire superlattice structures for nanoscale photonics and electronics. *Nature*, 415:617 EP –, 02 2002. 93

[GMP05] I. V. Gornyi, A. D. Mirlin, and D. G. Polyakov. Interacting electrons in disordered wires: Anderson localization and low-t transport. *Phys. Rev. Lett.*, 95:206603, Nov 2005. 55, 68

H

[HBS14] D. Hartich, A. C. Barato, and U. Seifert. Stochastic thermodynamics of bipartite systems: transfer entropy inequalities and a maxwells demon interpretation. *Journal of Statistical Mechanics: Theory and Experiment*, 2014(2):P02016, 2014. 93

[HCR+07] Y. Hu, H. O. H. Churchill, D. J. Reilly, J. Xiang, C. M. Lieber, and C. M. Marcus. A ge/si heterostructure nanowire-based double quantum dot with integrated charge sensor. *Nature Nanotechnology*, 2:622 EP –, 09 2007. 93

[HHH+05] M. Horodecki, P. Horodecki, R. Horodecki, J. Oppenheim, A. Sen(De), U. Sen, and B. Synak-Radtke. Local versus nonlocal information in quantum-information theory: Formalism and phenomena. *Phys. Rev. A*, 71:062307, Jun 2005. 93

[HK06] M. B. Hastings and T. Koma. Spectral gap and exponential decay of correlations. *Communications in Mathematical Physics*, 265(3):781–804, Aug 2006. 40, 57

[HL17] R.-Q. He and Z.-Y. Lu. Characterizing many-body localization by out-of-time-ordered correlation. *Phys. Rev. B*, 95:054201, Feb 2017. 54, 57, 68, 71

[HNO+13] D. A. Huse, R. Nandkishore, V. Oganesyan, A. Pal, and S. L. Sondhi. Localization-protected quantum order. *Phys. Rev. B*, 88:014206, Jul 2013. 55

[HNO14] D. A. Huse, R. Nandkishore, and V. Oganesyan. Phenomenology of fully many-body-localized systems. *Phys. Rev. B*, 90:174202, Nov 2014. 53, 68

[HO13] M. Horodecki and J. Oppenheim. Fundamental limitations for quantum and nanoscale thermodynamics. *Nature Communications*, 4:2059 EP –, 06 2013. 95

[Hor15] J. M. Horowitz. Multipartite information flow for multiple maxwell demons. *Journal of Statistical Mechanics: Theory and Experiment*, 2015(3):P03006, 2015. 93

[HPLHA13] K. V. Hovhannisyan, M. Perarnau-Llobet, M. Huber, and A. Acín. Entanglement generation is not necessary for optimal work extraction. *Phys. Rev. Lett.*, 111:240401, Dec 2013. 94

[HQRY16] P. Hosur, X.-L. Qi, D. A. Roberts, and B. Yoshida. Chaos in quantum channels. *Journal of High Energy Physics*, 2016(2):4, Feb 2016. 50, 51, 72

[HSAL11] S. Hilt, S. Shabbir, J. Anders, and E. Lutz. Landauer's principle in the quantum regime. *Phys. Rev. E*, 83:030102, Mar 2011. 93

[HSS12] E. Hamza, R. Sims, and G. Stolz. Dynamical localization in disordered quantum spin systems. *Communications in Mathematical Physics*, 315(1):215–239, Oct 2012. 56

[Hua15] Y. Huang. Efficient simulation of many-body localized systems. , 2015. arXiv:1508.04756 [cond-mat.dis-nn]. 55

[HZC17] Y. Huang, Y.-L. Zhang, and X. Chen. Out-of-time-ordered correlators in many-body localized systems. *Annalen der Physik*, 529(7):1600318–n/a, 2017. 1600318. 40, 54, 57, 68, 71

I

[icvcvPPcv08] M. Žnidarič, T. c. v. Prosen, and P. Prelovšek. Many-body localization in the heisenberg xxz magnet in a random field. *Phys. Rev. B*, 77:064426, Feb 2008. 56, 68, 71

[Imb16] J. Z. Imbrie. On many-body localization for quantum spin chains. *Journal of Statistical Physics*, 163(5):998–1048, Jun 2016. 68, 71

J

[Jac66] N. Jacobson. *Lie Algebras*. John Wiley Sons Inc., Franklin Township, New Jersey, 1966. 14

[Jac12] K. Jacobs. Quantum measurement and the first law of thermodynamics: The energy cost of measurement is the work value of the acquired information. *Phys. Rev. E*, 86:040106, Oct 2012. 93, 94

[Jar13] C. Jarzynski. *Equalities and Inequalities: Irreversibility and the Second Law of Thermodynamics at the Nanoscale*, pages 145–172. Springer Basel, Basel, 2013. 93

[JHN18] C. Jonay, D. A. Huse, and A. Nahum. Coarse-grained dynamics of operator and state entanglement. *ArXiv e-prints*, February 2018. arXiv:1803.00089 [cond-mat.stat-mech]. 68

[JM08] R. Jozsa and A. Miyake. Matchgates and classical simulation of quantum circuits. *Proceedings of the Royal Society of London A: Mathematical, Physical and Engineering Sciences*, 464(2100):3089–3106, 2008. 7, 15, 16, 17, 29, 56, 58, 59, 61, 73, 74

[JMS15] R. Jozsa, A. Miyake, and S. Strelchuk. Jordan-wigner formalism for arbitrary 2-input 2-output matchgates and their classical simulation. *Quant. Inform. Comp.*, 15:0541–0556, 2015. 6, 18

K

[Kas61] P. W. Kasteleyn. The statistics of dimers on a lattice : I. The number of dimer arrangements on a quadratic lattice. *Physica*, 27:1209–1225, December 1961. 6

[KBP14] J. A. Kjäll, J. H. Bardarson, and F. Pollmann. Many-body localization in a disordered quantum ising chain. *Phys. Rev. Lett.*, 113:107204, Sep 2014. 55

[KCA14] I. H. Kim, A. Chandran, , and D. A. Abanin. Local integrals of motion and the logarithmic lightcone in many-body localized systems. , 2014. arXiv:1412.3073 [cond-mat.dis-nn]. 55, 68, 71

[KGRG16] A. C. Keser, S. Ganeshan, G. Refael, and V. Galitski. Dynamical many-body localization in an integrable model. *Phys. Rev. B*, 94:085120, Aug 2016. 68

[Kit14] A. Kitaev. Hidden correlations in the hawking radiation and thermal noise. Fundamental Physics Prize Symposium, 2014. 34, 57

[Kit15a] A. Kitaev. A simple model of quantum holography. KITP strings seminar and Entanglement 2015 program, 2015. 34, 57

[Kit15b] A. Kitaev. A simple model of quantum holography. KITP strings seminar and Entanglement 2015 program, 2015. 68

[KLP18] P. Kos, M. Ljubotina, and T. c. v. Prosen. Many-body quantum chaos: Analytic connection to random matrix theory. *Phys. Rev. X*, 8:021062, Jun 2018. 68

[Kni01] E. Knill. Fermionic linear optics and matchgates. *ArXiv e-prints*, 2001. arXiv:quant-ph/0108033. 7, 56, 73

[KVH17] V. Khemani, A. Vishwanath, and D. A. Huse. Operator spreading and the emergence of dissipation in unitary dynamics with conservation laws. *ArXiv e-prints*, October 2017. arXiv:1710.09835 [cond-mat.stat-mech]. 68

L

[Lan61] R. Landauer. Irreversibility and heat generation in the computing process. *IBM Journal of Research and Development*, 5(3):183?191, 1961. 2

[LBA15] B. Leggio, B. Bellomo, and M. Antezza. Quantum thermal machines with single nonequilibrium environments. *Phys. Rev. A*, 91:012117, Jan 2015. 117

[LBCS10] Y. Lahini, Y. Bromberg, D. N. Christodoulides, and Y. Silberberg. Quantum correlations in two-particle anderson localization. *Phys. Rev. Lett.*, 105:163–905, Oct 2010. 55

[LJR15] M. Lostaglio, D. Jennings, and T. Rudolph. Description of quantum coherence in thermodynamic processes requires constraints beyond free energy. *Nature Communications*, 6:6383 EP –, 03 2015. 93

[Llo97] S. Lloyd. Quantum-mechanical maxwell's demon. *Phys. Rev. A*, 56:3374–3382, Nov 1997. 94

[LPS10] N. Linden, S. Popescu, and P. Skrzypczyk. How small can thermal machines be? the smallest possible refrigerator. *Phys. Rev. Lett.*, 105:130401, Sep 2010. 117

[LR72] E. H. Lieb and D. W. Robinson. The finite group velocity of quantum spin systems. *Comm. Math. Phys.*, 28(3):251–257, 1972. 40, 57, 67, 71

M

[MGS17] M. Mierzejewski, K. Giergiel, and K. Sacha. Many-body localization caused by temporal disorder. *Phys. Rev. B*, 96:140201, Oct 2017. 68

[MHG+12] P. Maletinsky, S. Hong, M. S. Grinolds, B. Hausmann, M. D. Lukin, R. L. Walsworth, M. Loncar, and A. Yacoby. A robust scanning diamond sensor for nanoscale imaging with single nitrogen-vacancy centres. *Nature Nanotechnology*, 7:320 EP –, 04 2012. 93

[MNV09] K. Maruyama, F. Nori, and V. Vedral. Colloquium: The physics of maxwell's demon and information. *Rev. Mod. Phys.*, 81:1–23, Jan 2009. 93

[MQJ13] D. Mandal, H. T. Quan, and C. Jarzynski. Maxwell's refrigerator: An exactly solvable model. *Phys. Rev. Lett.*, 111:030602, Jul 2013. 93, 94, 95, 100, 101, 110, 111, 159

[MSS16] J. Maldacena, S. H. Shenker, and D. Stanford. A bound on chaos. *Journal of High Energy Physics*, 2016(8):106, Aug 2016. 35, 57

N

[NH15] R. Nandkishore and D. A. Huse. Many-body localization and thermalization in quantum statistical mechanics. *Annual Review of Condensed Matter Physics*, 6(1):15–38, 2015. 55

[NKH14] A. Nanduri, H. Kim, and D. A. Huse. Entanglement spreading in a many-body localized system. *Phys. Rev. B*, 90:064201, Aug 2014. 68

[NS06] B. Nachtergaele and R. Sims. Lieb-robinson bounds and the exponential clustering theorem. *Communications in Mathematical Physics*, 265(1):119–130, Jul 2006. 40, 57

[NS10] B. Nachtergaele and R. Sims. Lieb-robinson bounds in quantum many-body physics. *Contem. Math.*, 529:141–176, 2010. 40, 57

[NVH18] A. Nahum, S. Vijay, and J. Haah. Operator spreading in random unitary circuits. *Phys. Rev. X*, 8:021014, Apr 2018. 68

O

[OH07] V. Oganesyan and D. A. Huse. Localization of interacting fermions at high temperature. *Phys. Rev. B*, 75:155111, Apr 2007. 55

[OHHH02] J. Oppenheim, M. Horodecki, P. Horodecki, and R. Horodecki. Thermodynamical approach to quantifying quantum correlations. *Phys. Rev. Lett.*, 89:180402, Oct 2002. 93, 94

[Or14] R. Ors. A practical introduction to tensor networks: Matrix product states and projected entangled pair states. *Annals of Physics*, 349:117 – 158, 2014. 95

P

[Pal12] A. Pal. *Many-body localization*. PhD thesis, 2012. 55

[PCPA15] P. Ponte, A. Chandran, Z. Papi, and D. A. Abanin. Periodically driven ergodic and many-body localized quantum systems. *Annals of Physics*, 353:196 – 204, 2015. 68

[PGVWC07] D. Perez-Garcia, F. Verstraete, M. M. Wolf, and J. I. Cirac. Matrix product state representations. *Quantum Info. Comput.*, 7(5):401–430, July 2007. 103

[PH10] A. Pal and D. A. Huse. Many-body localization phase transition. *Phys. Rev. B*, 82:174411, Nov 2010. 55

[PHS15] J. M. R. Parrondo, J. M. Horowitz, and T. Sagawa. Thermodynamics of information. *Nature Physics*, 11:131 EP –, 02 2015. 93

[PKCS16] F. Pollmann, V. Khemani, J. I. Cirac, and S. L. Sondhi. Efficient variational diagonalization of fully many-body localized hamiltonians. *Phys. Rev. B*, 94:041116, Jul 2016. 55

[PLHH+15] M. Perarnau-Llobet, K. V. Hovhannisyan, M. Huber, P. Skrzypczyk, N. Brunner, and A. Acín. Extractable work from correlations. *Phys. Rev. X*, 5:041011, Oct 2015. 94

[PPHA15] P. Ponte, Z. Papić, F. Huveneers, and D. A. Abanin. Many-body localization in periodically driven systems. *Phys. Rev. Lett.*, 114:140401, Apr 2015. 68

R

[RÅR+11] L. d. Rio, J. Åberg, R. Renner, O. Dahlsten, and V. Vedral. The thermodynamic meaning of negative entropy. *Nature*, 474:61 EP –, 06 2011. 93, 94

[RASK+14] J. Roßnagel, O. Abah, F. Schmidt-Kaler, K. Singer, and E. Lutz. Nanoscale heat engine beyond the carnot limit. *Phys. Rev. Lett.*, 112:030602, Jan 2014. 94

[RPv17] T. Rakovszky, F. Pollmann, and C. W. von Keyserlingk. Diffusive hydrodynamics of out-of-time-ordered correlators with charge conservation. *ArXiv e-prints*, October 2017. arXiv:1710.09827 [cond-mat.stat-mech]. 68

[RSS15] D. A. Roberts, D. Stanford, and L. Susskind. Localized shocks. *Journal of High Energy Physics*, 2015(3):51, Mar 2015. 57

[RY17a] D. A. Roberts and B. Yoshida. Chaos and complexity by design. *Journal of High Energy Physics*, 2017(4):121, Apr 2017. 41, 46, 47, 48

[RY17b] D. A. Roberts and B. Yoshida. Chaos and complexity by design. *Journal of High Energy Physics*, 2017(4):121, Apr 2017. 57, 63

S

[SBYX17] K. Slagle, Z. Bi, Y.-Z. You, and C. Xu. Out-of-time-order correlation in marginal many-body localized systems. *Phys. Rev. B*, 95:165136, Apr 2017. 68, 71

[SC17] B. Swingle and D. Chowdhury. Slow scrambling in disordered quantum systems. *Phys. Rev. B*, 95:060201, Feb 2017. 57, 68, 71

[Scu01] M. O. Scully. Extracting work from a single thermal bath via quantum negentropy. *Phys. Rev. Lett.*, 87:220601, Nov 2001. 93

[SD16] K. Sacha and D. Delande. Anderson localization in the time domain. *Phys. Rev. A*, 94:023633, Aug 2016. 56

[Seg08] D. Segal. Stochastic pumping of heat: Approaching the carnot efficiency. *Phys. Rev. Lett.*, 101:260601, Dec 2008. 93

[SGKA13] K. Szczygielski, D. Gelbwaser-Klimovsky, and R. Alicki. Markovian master equation and thermodynamics of a two-level system in a strong laser field. *Phys. Rev. E*, 87:012120, Jan 2013. 117

[Sho97] P. Shor. Polynomial-time algorithms for prime factorization and discrete logarithms on a quantum computer. *SIAM Journal on Computing*, 26(5):1484–1509, 1997. 3

[SIKS15] N. Shiraishi, S. Ito, K. Kawaguchi, and T. Sagawa. Role of measurement-feedback separation in autonomous maxwell's demons. *New Journal of Physics*, 17(4):045012, 2015. 93, 94

[SM10] H. Schröder and G. Mahler. Work exchange between quantum systems: The spin-oscillator model. *Phys. Rev. E*, 81:021118, Feb 2010. 95

[SPacA13] M. Serbyn, Z. Papić, and D. A. Abanin. Local conservation laws and the structure of the many-body localized states. *Phys. Rev. Lett.*, 111:127201, Sep 2013. 53, 68, 71

[SPH+18] C. Sünderhauf, D. Pérez-García, D. A. Huse, N. Schuch, and J. I. Cirac. Localisation with random time-periodic quantum circuits. *ArXiv e-prints*, May 2018. arXiv:1805.08487 [cond-mat.stat-mech]. 64, 68, 69

[SRF+13] P. SILVI, D. ROSSINI, R. FAZIO, G. E. SANTORO, and V. GIOVANNETTI. Matrix product state representation for slater determinants and configuration interaction states. *International Journal of Modern Physics B*, 27(01n03):1345029, 2013. 33

[SS08] Y. Sekino and L. Susskind. Fast scramblers. *Journal of High Energy Physics*, 2008(10):065, 2008. 90

[SS14] S. H. Shenker and D. Stanford. Black holes and the butterfly effect. *Journal of High Energy Physics*, 2014(3):67, Mar 2014. 35, 57

[SSBJ14] P. Strasberg, G. Schaller, T. Brandes, and C. Jarzynski. Second laws for an information driven current through a spin valve. *Phys. Rev. E*, 90:062107, Dec 2014. 93

[SSP13] P. Skrzypczyk, A. J. Short, and S. Popescu. Extracting work from quantum systems. *ArXiv e-prints*, February 2013. arXiv:1302.2811 [quant-ph]. 95

[SSV+05] C. Schön, E. Solano, F. Verstraete, J. I. Cirac, and M. M. Wolf. Sequential generation of entangled multiqubit states. *Phys. Rev. Lett.*, 95:110503, Sep 2005. 105, 157

[SXS18] S. Sahu, S. Xu, and B. Swingle. Scrambling dynamics across a thermalization-localization quantum phase transition. , July 2018. arXiv:1807.06086 [cond-mat.str-el]. 69, 72, 76, 83

[SZAW03] M. O. Scully, M. S. Zubairy, G. S. Agarwal, and H. Walther. Extracting work from a single heat bath via vanishing quantum coherence. *Science*, 299(5608):862–864, 2003. 117

T

[TD02] B. M. Terhal and D. P. DiVincenzo. Classical simulation of noninteracting-fermion quantum circuits. *Phys. Rev. A*, 65:032325, Mar 2002. 7, 56, 73

[TF61] H. N. V. Temperley and M. E. Fisher. Dimer problem in statistical mechanics-an exact result. *The Philosophical Magazine: A Journal of Theoretical Experimental and Applied Physics*, 6(68):1061–1063, 1961. 6

V

[VA14] R. Vosk and E. Altman. Dynamical quantum phase transitions in random spin chains. *Phys. Rev. Lett.*, 112:217204, May 2014. 55

[Val02] L. Valiant. Quantum circuits that can be simulated classically in polynomial time. *SIAM J. Comput.*, 31:1229–1254, Nov 2002. 6

[VdBKL12] C. Van den Broeck, N. Kumar, and K. Lindenberg. Efficiency of isothermal molecular machines at maximum power. *Phys. Rev. Lett.*, 108:210602, May 2012. 93

[VdN11a] M. Van den Nest. Quantum matchgate computations and linear threshold gates. *Proceedings of the Royal Society of London A: Mathematical, Physical and Engineering Sciences*, 467(2127):821–840, 2011. 32

[VDN11b] M. Van Den Nest. Simulating quantum computers with probabilistic methods. *Quantum Info. Comput.*, 11(9-10):784–812, September 2011. 32

[VFG13] D. Venturelli, R. Fazio, and V. Giovannetti. Minimal self-contained quantum refrigeration machine based on four quantum dots. *Phys. Rev. Lett.*, 110:256801, Jun 2013. 117

[VGRC04] F. Verstraete, J. J. García-Ripoll, and J. I. Cirac. Matrix product density operators: Simulation of finite-temperature and dissipative systems. *Phys. Rev. Lett.*, 93:207204, Nov 2004. 95, 104

[Vid03] G. Vidal. Efficient classical simulation of slightly entangled quantum computations. *Phys. Rev. Lett.*, 91:147902, Oct 2003. 103

[vKRPS18] C. W. von Keyserlingk, T. Rakovszky, F. Pollmann, and S. L. Sondhi. Operator hydrodynamics, otocs, and entanglement growth in systems without conservation laws. *Phys. Rev. X*, 8:021013, Apr 2018. 68

[Vla01] A. Y. Vlasov. Clifford algebras and universal sets of quantum gates. *Phys. Rev. A*, 63:054302, Apr 2001. 14

[VSHW11] U. Vogl, A. Sa, S. Haelmann, and M. Weitz. Collisional redistribution laser cooling of a high-pressure atomic gas. *Journal of Modern Optics*, 58(15):1300–1309, 2011. 117

[VW09] U. Vogl and M. Weitz. Laser cooling by collisional redistribution of radiation. *Nature*, 461:70 EP –, 09 2009. 117

W

[WJS+16] A. H. Werner, D. Jaschke, P. Silvi, M. Kliesch, T. Calarco, J. Eisert, and S. Montangero. Positive tensor network approach for simulating open quantum many-body systems. *Phys. Rev. Lett.*, 116:237201, Jun 2016. 104

[WNW15] M. P. Woods, N. Ng, and S. Wehner. The maximum efficiency of nano heat engines depends on more than temperature. *ArXiv e-prints*, June 2015. arXiv:1506.02322 [quant-ph]. 95

X

[XS18a] S. Xu and B. Swingle. Accessing scrambling using matrix product operators. *ArXiv e-prints*, February 2018. arXiv:1802.00801 [quant-ph]. 33, 50, 51, 54, 69, 72, 75, 83

[XS18b] S. Xu and B. Swingle. Locality, Quantum Fluctuations, and Scrambling. *ArXiv e-prints*, May 2018. arXiv:1805.05376 [cond-mat.str-el]. 68

[XS18c] S. Xu and B. Swingle. Accessing scrambling using matrix product operators. *ArXiv e-prints*, 2018. arXiv:1802.00801 [quant-ph]. 64

[XTAE] C. Xiao, Z. Tianci, H. D. A., and F. Eduardo. Outoftimeorder correlations in manybody localized and thermal phases. *Annalen der Physik*, 529(7):1600332. 68

Y

[YH17] N. Yunger Halpern. Jarzynski-like equality for the out-of-time-ordered correlator. *Phys. Rev. A*, 95:012120, Jan 2017. 57

[YPC17] X. Yu, D. Pekker, and B. K. Clark. Finding matrix product state representations of highly excited eigenstates of many-body localized hamiltonians. *Phys. Rev. Lett.*, 118:017201, Jan 2017. 55

[YQX16] Y.-Z. You, X.-L. Qi, and C. Xu. Entanglement holographic mapping of many-body localized system by spectrum bifurcation renormalization group. *Phys. Rev. B*, 93:104205, Mar 2016. 55

Z

[ZC18] T. Zhou and X. Chen. Operator Dynamics in Brownian Quantum Circuit. *ArXiv e-prints*, May 2018. arXiv:1805.09307 [cond-mat.str-el]. 68

[ZN18] T. Zhou and A. Nahum. Emergent statistical mechanics of entanglement in random unitary circuits. *ArXiv e-prints*, April 2018. arXiv:1804.09737 [cond-mat.stat-mech]. 68

[Zur03] W. H. Zurek. Quantum discord and maxwell's demons. *Phys. Rev. A*, 67:012320, Jan 2003. 93, 94

[ZV04] M. Zwolak and G. Vidal. Mixed-state dynamics in one-dimensional quantum lattice systems: A time-dependent superoperator renormalization algorithm. *Phys. Rev. Lett.*, 93:207205, Nov 2004. 95, 104, 105, 157